frontiers | Research Topics

Advances in integrative medicine for neurodegenerative diseases: From basic research to clinical practice, 2nd Edition

Edited by
Shaonan Liu, Guo-qing Zheng, Hansen Chen, Guowei Li and Xinfeng Guo

Published in
Frontiers in Neurology
Frontiers in Neuroscience

ISSN 1664-8714
ISBN 978-2-8325-4579-9
DOI 10.3389/978-2-8325-4579-9

About Frontiers

Frontiers is more than just an open access publisher of scholarly articles: it is a pioneering approach to the world of academia, radically improving the way scholarly research is managed. The grand vision of Frontiers is a world where all people have an equal opportunity to seek, share and generate knowledge. Frontiers provides immediate and permanent online open access to all its publications, but this alone is not enough to realize our grand goals.

Frontiers journal series

The Frontiers journal series is a multi-tier and interdisciplinary set of open-access, online journals, promising a paradigm shift from the current review, selection and dissemination processes in academic publishing. All Frontiers journals are driven by researchers for researchers; therefore, they constitute a service to the scholarly community. At the same time, the *Frontiers journal series* operates on a revolutionary invention, the tiered publishing system, initially addressing specific communities of scholars, and gradually climbing up to broader public understanding, thus serving the interests of the lay society, too.

Dedication to quality

Each Frontiers article is a landmark of the highest quality, thanks to genuinely collaborative interactions between authors and review editors, who include some of the world's best academicians. Research must be certified by peers before entering a stream of knowledge that may eventually reach the public - and shape society; therefore, Frontiers only applies the most rigorous and unbiased reviews. Frontiers revolutionizes research publishing by freely delivering the most outstanding research, evaluated with no bias from both the academic and social point of view. By applying the most advanced information technologies, Frontiers is catapulting scholarly publishing into a new generation.

What are Frontiers Research Topics?

Frontiers Research Topics are very popular trademarks of the *Frontiers journals series*: they are collections of at least ten articles, all centered on a particular subject. With their unique mix of varied contributions from Original Research to Review Articles, Frontiers Research Topics unify the most influential researchers, the latest key findings and historical advances in a hot research area.

Find out more on how to host your own Frontiers Research Topic or contribute to one as an author by contacting the Frontiers editorial office: frontiersin.org/about/contact

Advances in integrative medicine for neurodegenerative diseases: From basic research to clinical practice, 2nd Edition

Topic editors

Shaonan Liu — Guangzhou University of Chinese Medicine, China
Guo-qing Zheng — Zhejiang Chinese Medical University, China
Hansen Chen — Stanford University, United States
Guowei Li — Guangdong Second Provincial General Hospital, China
Xinfeng Guo — Guangzhou University of Chinese Medicine, China

Citation

Liu, S., Zheng, G.-q., Chen, H., Li, G., Guo, X., eds. (2024). *Advances in integrative medicine for neurodegenerative diseases: From basic research to clinical practice, 2nd Edition*. Lausanne: Frontiers Media SA. doi: 10.3389/978-2-8325-4579-9

Publisher's note: This is a 2nd edition due to an article retraction.

Table of contents

frontiers | Frontiers in Neurology

TYPE Editorial
PUBLISHED 16 May 2023
DOI 10.3389/fneur.2023.1197641

OPEN ACCESS

EDITED BY
Bruce Miller,
University of California, San Francisco,
United States

REVIEWED BY
Elissaios Karageorgiou,
Independent Researcher, Athens, Greece
Allan Bregola,
Central London Community Healthcare NHS
Trust, United Kingdom

*CORRESPONDENCE
Shaonan Liu
✉ shaonanliu819@gzucm.edu.cn

RECEIVED 31 March 2023
ACCEPTED 02 May 2023
PUBLISHED 16 May 2023

CITATION
Liu S, Zheng G, Chen H, Li G and Guo X (2023) Editorial: Advances in integrative medicine for neurodegenerative diseases: from basic research to clinical practice.
Front. Neurol. 14:1197641.
doi: 10.3389/fneur.2023.1197641

Editorial: Advances in integrative medicine for neurodegenerative diseases: from basic research to clinical practice

Shaonan Liu[1]*, Guoqing Zheng[2], Hansen Chen[3], Guowei Li[4] and Xinfeng Guo[1]

[1]Guangdong Provincial Hospital of Chinese Medicine, Guangzhou University of Chinese Medicine, Guangzhou, China, [2]Department of Neurology, The First Affiliated Hospital of Zhejiang Chinese Medical University (Zhejiang Provincial Hospital of Chinese Medicine), Hangzhou, China, [3]Department of Neurosurgery, School of Medicine, Stanford University, Stanford, CA, United States, [4]Guangdong Second Provincial General Hospital, Guangzhou, China

KEYWORDS

integrative medicine, neurodegenerative disease, complementary and alternative medicine, preclinical and clinical study, Chinese medicine (CM)

Editorial on the Research Topic
Advances in integrative medicine for neurodegenerative diseases: from basic research to clinical practice

Neurodegenerative diseases (NDs) are disorders characterized by the progressive loss of neurons, which can result in motor dysfunctions and psychobehavioral manifestations such as ataxia and dementia (1). Alzheimer's disease (AD) as the most common NDs represents ~60%−70% of about 50 million people worldwide who suffer from dementia (2). The Research Topic aims to explore the therapeutic effect and mechanism action of integrative medicine of NDs for the improvement of patient healthcare, in order to stimulate further understanding and ultimately provide new methods for the prevention and treatment of NDs. For integrative medicine (IM), the topic mainly focuses on Chinese herbal medicine, acupuncture and related therapies, other Chinese medicine therapies based on modern clinical medicine. This collection spans different diseases such as AD and amyotrophic lateral sclerosis (ALS), and mainly focus on the mechanisms of neurodegeneration and treatment strategies.

In this volume, most studies focus on AD. Pathogenic mechanisms and new targeted drugs are still urgently needed although some progress has been made in this field. Zhang et al. performed an integrated analysis of the hub gene based on cuproptosis which is a copper-triggered modality of mitochondrial cell death by the bioinformatics approach for the diagnosis and treatment of AD. Seven hub genes including A4GALT, ALOX5AP, CLIC1, IFI30, LYZ, PLA1A, and PYGL were involved in phosphoribosyl pyrophosphate, lipid and glucose metabolism as revealed by GO analysis. Four of the seven cuproptosis genes (including IFI30, PLA1A, ALOX5AP, and A4GALT) can help with the clinical diagnosis of AD. These cuproptosis gene signatures may be an important diagnostic and prognostic indicator for AD. A similar bioinformatics analysis was conducted to explore the biomarkers and potential mechanisms that distinguish between Dementia with Lewy bodies (DLB) and Parkinson's disease dementia (PDD). Xu et al. identified seven upregulated genes, namely, SNAP25, GRIN2A, GABRG2, GABRA1, GRIA1, SLC17A6 and SYN1, which are

involved in the heterogeneous pathogenesis of PDD and DLB. Blood pressure variability (BPV) has emerged as a novel risk factor for Alzheimer's disease, Yu et al. investigated the association of night BPV with brain atrophy and cognitive function changes from Korean Genome Epidemiology Study (KoGES). The results showed that high night systolic BPV was associated with temporal gray matter atrophy and impaired visual memory and verbal fluency. Subcortical vascular mild cognitive impairment (svMCI) is one of the most treatable cognitive impairments. Wang et al. explored the spontaneous brain activities regarding Chinese medicine deficiency patterns (DPs) and excess patterns (EPs) of svMCI patients based on fMRI data. The results found that the right middle frontal gyrus might serve as a brain response to endogenic cognitive impairments of DPs in svMCI patients. In addition to mechanisms exploration, several studies investigated the potential therapeutic strategies. Liu et al. found that the Chinese formula Liuwei Dihuang decoction could ameliorate cognitive dysfunction and hippocampal synaptic ultrastructure damage in aging mice by regulating lipid metabolism and oxidative stress via the microbiota-gut-brain axis. The current evidence showed that deficits of adult hippocampal neurogenesis (AHN) were the main hallmark of psychiatric diseases and neurodegeneration. Sun et al. conducted a review and found that exercise may be the ideal option to improve mitochondrial functions and AHN due to the relatively few safety concerns. Cao et al. summarized the studies about Alzheimer's drug development by the clinical trial registry platform. Sixteen compounds of disease-modifying therapies and symptomatic therapies such as gantenerumab, aducanumab, and others, may change the situation in China where there is no alternative drug for the treatment AD.

Two studies focus on ALS. Gong et al. explored the correlation between cerebrospinal fluid (CSF) and serum tau (t-tau, p-tau) in patients with ALS. Results suggest that CSF P-tau may be recognized as a potential cognition impairment biomarker in ALS. Liao et al. conducted a systematic review to explore the efficacy and safety of Chinese herbal medicine for the treatment of ALS. The findings suggest that the adjunct use of CHM can improve the ALS functional rating scale when compared with placebo or riluzole alone.

The collection of articles on this topic provides molecular mechanisms and clinical insights into neurodegenerative diseases, as well as the potential application of integrative medicine for neurodegenerative diseases.

Author contributions

SL drafted the editorial. GZ, HC, GL, and XG reviewed the manuscript. All authors listed have made a substantial, direct, and intellectual contribution to the work and approved it for publication.

Funding

HC was funded by American Heart Association Postdoctoral Fellowship (916011).

Conflict of interest

The authors declare that the research was conducted in the absence of any commercial or financial relationships that could be construed as a potential conflict of interest.

Publisher's note

References

1. Gitler AD, Dhillon P, Shorter J. Neurodegenerative disease: models, mechanisms, and a new hope. *Dis Model Mech*. (2017) 10:499–502. doi: 10.1242/dmm.030205

2. Tanaka M, Toldi J, Vécsei L. Exploring the etiological links behind neurodegenerative diseases: inflammatory cytokines and bioactive kynurenines. *Int J Mol Sci*. (2020) 21:2431. doi: 10.3390/ijms21072431

frontiers | Frontiers in Neuroscience

ORIGINAL RESEARCH
published: 01 July 2022
doi: 10.3389/fnins.2022.949298

Liuwei Dihuang Decoction Alleviates Cognitive Dysfunction in Mice With D-Galactose-Induced Aging by Regulating Lipid Metabolism and Oxidative Stress *via* the Microbiota-Gut-Brain Axis

Baiyan Liu[1,2†], Bowei Chen[1†], Jian Yi[1,2†], Hongping Long[1], Huiqiao Wen[1], Fengming Tian[1], Yingfei Liu[1], Lan Xiao[3] and Lisong Li[4]*

[1] The First Affiliated Hospital, Hunan University of Chinese Medicine, Changsha, China, [2] Hunan Academy of Chinese Medicine, Changsha, China, [3] College of Pharmacy, Hunan University of Chinese Medicine, Changsha, China, [4] College of Information Science and Engineering, Hunan University of Chinese Medicine, Changsha, China

Background: Aging is an important cause of cognitive dysfunction. Liuwei Dihuang decoction (LW), a commonly applied Chinese medicine formula, is widely used for the treatment of aging-related diseases in China. Previously, LW was confirmed to be effective in prolonging life span and reducing oxidative stress in aged mice. Unfortunately, the underlying mechanism of LW remains unclear. The aim of this study was to interpret the mechanism by which LW alleviates cognitive dysfunction related to aging from the perspective of the microbiota-gut-brain axis.

Method: All C57BL/6 mice ($n = 60$) were randomly divided into five groups: the control, model, vitamin E (positive control group), low-dose LW and high-dose LW groups ($n = 12$ in each group). Except for those in the control group, D-galactose was subcutaneously injected into mice in the other groups to induce the aging model. The antiaging effect of LW was evaluated by the water maze test, electron microscopy, 16S rRNA sequencing, combined LC–MS and GC–MS metabolomics, and ELISA.

Results: Liuwei Dihuang decoction ameliorated cognitive dysfunction and hippocampal synaptic ultrastructure damage in aging mice. Moreover, LW decreased *Proteobacteria* abundance and increased gut microbiota diversity in aging mice. Metabolomic analysis showed that LW treatment was associated with the significantly differential abundance of 14 metabolites, which were mainly enriched in apelin signaling, sphingolipid metabolism, glycerophospholipid and other metabolic pathways. Additionally, LW affected lipid metabolism and oxidative stress in aging mice. Finally, we also found that LW-regulated

OPEN ACCESS

Edited by:
Guo-qing Zheng,
Zhejiang Chinese Medical University, China

Reviewed by:
Jia Liang,
Jinzhou Medical University, China
Weijun Peng,
Central South University, China

***Correspondence:**
Baiyan Liu
liubaiyan9657@163.com

† These authors have contributed equally to this work

Specialty section:
This article was submitted to Translational Neuroscience, a section of the journal Frontiers in Neuroscience

Received: *20 May 2022*
Accepted: *15 June 2022*
Published: *01 July 2022*

Citation:
Liu B, Chen B, Yi J, Long H, Wen H, Tian F, Liu Y, Xiao L and Li L (2022) Liuwei Dihuang Decoction Alleviates Cognitive Dysfunction in Mice With D-Galactose-Induced Aging by Regulating Lipid Metabolism and Oxidative Stress via the Microbiota-Gut-Brain Axis. Front. Neurosci. 16:949298. doi: 10.3389/fnins.2022.949298

microbial species such as *Proteobacteria* and *Fibrobacterota* had potential relationships with lipid metabolism, oxidative stress and hippocampal metabolites.

Conclusion: In brief, LW improved cognitive function in aging mice by regulating lipid metabolism and oxidative stress through restoration of the homeostasis of the microbiota-gut-brain axis.

Keywords: Liuwei Dihuang decoction, aging, cognitive function, microbiota-gut-brain axis, metabolomics, lipid metabolism, oxidative stress

INTRODUCTION

Currently, the proportion of the world's population that is elderly is growing rapidly. It is estimated that by 2050, the world's elderly population will increase from 841 million in 2013 to 2 billion, representing 21% of the world's population (Partridge et al., 2020). Cognitive impairment accompanies aging and becomes increasingly evident with age. At present, cognitive impairment has become a major problem that plagues the physical and mental health of elderly individuals. The hippocampus mainly regulates learning and memory, and the occurrence of cognitive impairment is closely related to functional changes in the hippocampus (Bettio et al., 2017; Solé et al., 2017). Maintaining the normal physiological function of the hippocampus can effectively alleviate the cognitive dysfunction caused by aging.

Liuwei Dihuang decoction (LW), a commonly applied traditional Chinese medicine formula, has been widely used for centuries in China for the treatment of aging-related diseases, and its efficacy has been validated by evidence-based medicine (Chen B. et al., 2019). Previous studies have found that LW can improve spatial learning ability by increasing neurogenesis in the dentate gyrus in rats (Lee et al., 2005). It also improves age-related learning and memory decline by inducing long-term potentiation (LTP) of hippocampal neurons (Huang et al., 2012). In addition, LW has been found to prolong the life span of elderly mice and reduce the oxidative stress state (Chen W. et al., 2019). Unfortunately, the mechanism of LW in the treatment of aging-related cognitive dysfunction remains unclear.

The gut is considered an important organ for regulating body function and promoting longevity due to its functions in immunity and nutrient intake (Qin et al., 2010). When the body enters the aging period, the intestinal barrier, absorption and immune function change, and various external factors can lead to the destruction of the intestinal microecological balance (Biagi et al., 2010). Studies have found that there are pathways connecting nerves in the gut and brain in the human body, which are closely related to gut microbes, and this connection is called the microbiota-gut-brain axis (Shabbir et al., 2021). The gut microbiota is an important player in bidirectional communication between the gut and the brain and can have a major impact on the body's neurological function, not only by neurotransmitter secretion but also by immune and metabolic regulation (Dinan and Cryan, 2017; Bambury et al., 2018; Osadchiy et al., 2019). Therefore, restoring intestinal homeostasis and delaying the aging process are of great significance for improving the quality of life of the elderly population.

Metabolomics is mainly the study of small molecule metabolites as substrates and products of various metabolic pathways and can comprehensively reveal the changes occurring in organisms during the treatment of diseases (Baker, 2011). However, due to technical limitations, there is currently no technology that can describe all possible compounds in the body. Liquid chromatography–mass spectrometry (LC–MS) has a wide molecular weight range, with high sensitivity and simple preprocessing methodology, and is suitable for the detection of compounds with poor volatility, medium or strong polarity, and large molecular weight. Gas chromatography-MS (GC–MS) is suitable for the detection of highly volatile, small molecular weight and polar compounds (Zeki et al., 2020).

In this study, a combined LC–MS and GC–MS whole-spectrum metabolomics method was used to analyze the effect of LW on the metabolic profile of the hippocampus of mice with D-galactose-induced aging, and 16S ribosomal RNA (16S rRNA) sequencing was used to interpret the mechanism by which LW improves age-related cognitive dysfunction from the perspective of the microbiota-gut-brain axis.

MATERIALS AND METHODS

Animals

Sixty male C57BL/6 mice with body weights of 18–22 g were purchased from Gempharmatech Co., Ltd. (Jiangsu, China) and housed in the specific pathogen-free (SPF) animal room of the First Affiliated Hospital of Hunan University of Chinese Medicine at a temperature of 22–26°C and a humidity of 45–55%. The animals were housed in groups of 5/cage. Distilled water and feed were freely provided, with natural light and bedding changed every other day. The Ethics Committee of Laboratory Animal Studies of the First Affiliated Hospital of Hunan University of Chinese Medicine approved all the experimental protocols (No. ZYFY20210710).

Preparation of Liuwei Dihuang Decoction

Liuwei Dihuang decoction is composed of six herbs (**Table 1**), all of which were purchased from the First Affiliated Hospital of Hunan University of Chinese Medicine and qualified by the herbal medicinal botanist Hongping Long.

As in a previous study (Chen W. et al., 2019), *Rehmannia glutinosa* (Gaertn.) DC., *Cornus officinalis* Siebold & Zucc., *Dioscorea oppositifolia* L., *Paeonia suffruticosa* Andr., *Alisma orientalis (*Sam.*)* Juzep. and *Wolfiporia extensa* (Peck) Ginns were

TABLE 1 | Components of the Liuwei Dihuang decoction (LW).

Scientific name	Chinese name	English name	Part used	Origin	Batch number	Weight
Rehmannia glutinosa (Gaertn.) DC.	Shu Di Huang	Radix Rehmanniae	Root	Henan	2009063	24 g
Cornus officinalis Siebold & Zucc.	Shan Zhu Yu	Comus Officinalis	fruit	Henan	TH20111101	12 g
Dioscorea oppositifolia L.	Shan Yao	Rhizoma Dioscoreae	Root	Henan	CK20113001	12 g
Paeonia suffruticosa Andr.	Dan Pi	Paeoniaceae	Root bark	AnHui	NG20121102	9 g
Alisma orientalis(Sam.)Juzep.	Ze Xie	Alismatis	Tuber	SiChuan	CK20121503	9 g
Wolfiporia extensa (Peck) Ginns	Fu Ling	Poria Cocos	Rhizome	Hunan	CK20120802	9 g

mixed at a ratio of 8:4:4:3:3:3. Distilled water at a 5× volume was then added for 1 h, after which the mixture was boiled for 2 h at 100°C and filtered with three layers of gauze. After washing with distilled water three times, the filtrate was extracted again by the same method. After combining the filtrate from the two extractions, the solution was concentrated to 2 g of crude drug/ml using a rotary evaporator.

Main Reagents

Vitamin E soft capsules (H20003539) were purchased from Zhejiang Pharmaceutical Co., Ltd. (Hangzhou, China); D-galactose (v900922) was purchased from Sigma–Aldrich (Shanghai, China); mouse adiponectin ELISA kit (EK0596) was purchased from Boster (Wuhan, China); mouse apolipoprotein E (ApoE) ELISA kit (ab215086) and mouse free fatty acid (FFA) assay kit (ab65341) were purchased from Abcam (Cambridge, United Kingdom); and superoxide dismutase (SOD) assay kit (20190412), glutathione peroxidase (GSH-Px) assay kit (20190309), and malondialdehyde (MDA) assay kit (20190315) were purchased from Jiancheng (Nanjing, China).

The UPLC-Q-TOF/MS for Quality Control of Liuwei Dihuang Decoction

As in our previous study (Chen et al., 2022), LW was analyzed by ultra-performance liquid chromatography coupled with quadrupole time-of-flight mass spectrometry (UPLC-Q-TOF/MS). In short, 10 mL of concentrated LW solution was placed in a 50 mL conical flask, and 30 mL of 70% methanol was added; LW was dissolved by ultrasonic vibration for 30 min. After standing, 2 mL of the solution was centrifuged at 8,000 r/min for 5 min, and then the supernatant was filtered through a 0.22 μm microporous membrane and placed in an injection bottle. The chromatography and MS conditions were the same as those previously reported (Chen et al., 2022).

Experiment Design

A total of 60 mice were randomly divided into five groups after adaptive feeding: the control group, model group, vitamin E (200 mg·kg^{-1}) group [positive control group, vitamin E has been used as a positive control in a large number of studies related to aging (Zeng et al., 2022)], low-dose LW (LW-L) (10 g·kg^{-1}) group and high-dose LW (LW-H) (20 g·kg^{-1}) group. Except for those in the control group, the mice in the other groups were subcutaneously injected with 100 mg·kg^{-1} D-galactose (Ali et al., 2015) once per day for 6 consecutive weeks, and subcutaneous injection of D-galactose is a commonly used method to replicate aging models (Huang X. et al., 2020). The control group mice were injected with the same volume of normal saline. After conducting the Morris water maze (MWM) test on the 6th week, we anesthetized all mice by intraperitoneal injection of 1% sodium pentobarbital. The eyeballs were removed, and the collected blood was centrifuged to obtain serum. Then, the contents of the cecum were collected under aseptic conditions, and the hippocampus of the mice was collected and placed on ice. All samples were stored at −80°C until further use. Eight mice from each group were randomly selected for 16S rRNA sequencing of cecal contents, metabolomics, and lipid metabolism and oxidative stress analysis, and the remaining four mice were analyzed by transmission electron microscopy (TEM), as shown in **Figure 1**.

Morris Water Maze Test

The MWM was used to detect the learning and memory ability of mice and evaluate their cognitive function. According to previous reports (Hui et al., 2017), a black circular pool (depth 60 cm, diameter 150 cm) was used, the platform was fixed in the second quadrant, tap water was added to the pool, the water level was 2 cm higher than the platform, and the water temperature was controlled at 22–24°C. Mice were placed with their head toward the wall of the pool, and water points were randomly selected, with a detection time of 60 s. The time required for mice to find the submerged platform time was recorded, and if the platform was found within 60 s, the animal was allowed to stay on the platform for 10 s to rest; if the platform was not found, the animal was guided to the platform and left for 10 s. Each animal was trained three times daily, with a 15–20 min interval between each session, for 5 days. A video tracking system recorded animal location, swimming distance and time. On the 6th day, the platform was removed, the animals were put into the water from the opposite side of the original platform quadrant, and the latency and times of animals crossing the original platform quadrant within 60 s were recorded.

Detection of the Synaptic Ultrastructure in the Hippocampus

Synaptic ultrastructure detection by TEM was performed as described previously (Sheng et al., 2020). Briefly, specimens that had been fixed for 48 h before TEM were postfixed in 1% osmic acid at room temperature for 2 h and dehydrated stepwise by an ethanol gradient and again by acetone. Tissues were first infiltrated overnight in solutions with different ratios of acetone to embedding medium, and then the tissues were

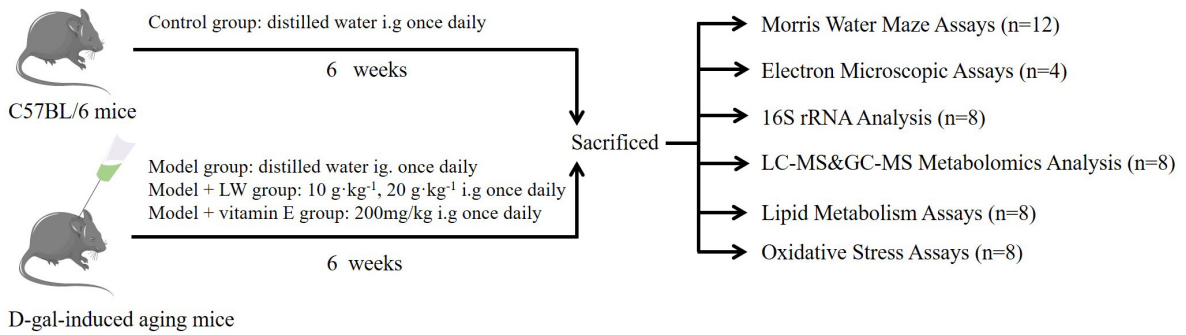

FIGURE 1 | Experimental design of intervention study of Liuwei Dihuang decoction (LW).

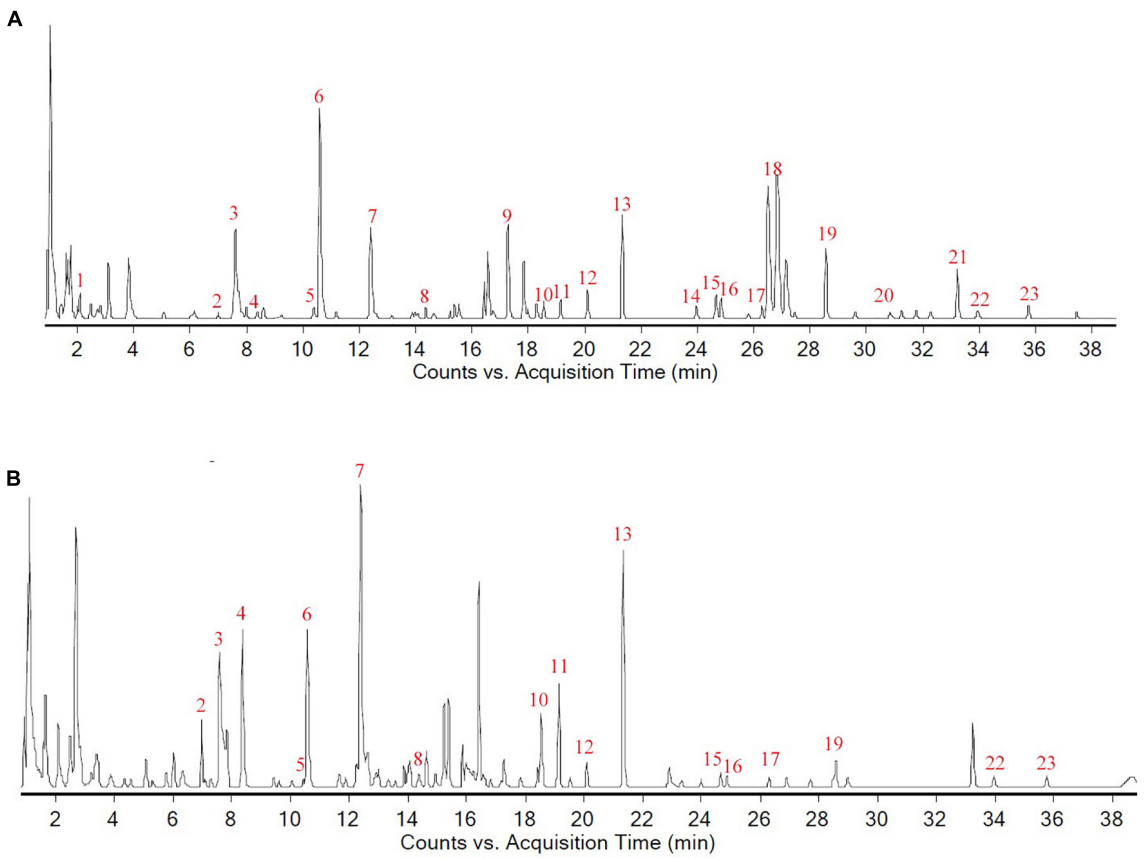

FIGURE 2 | Chemical composition analysis of Liuwei Dihuang decoction. **(A)** The total composition chromatogram (TCC) in positive ion mode; **(B)** The TCC in negative ion mode.

polymerized in pure embedding medium at 60°C for 48 h for embedding. The tissue was cut into 60–80 nm ultrathin sections, stained with uranium acetate and lead citrate, and dried overnight at room temperature. The presynaptic membrane, postsynaptic membrane and synaptic vesicles were observed by TEM.

16S rRNA Analysis

Total genomic DNA was extracted using DNA Extraction Kit following the manufacturer's instructions. The concentration of DNA was verified with a NanoDrop and agarose gel electrophoresis. The genomic DNA was used as a template for PCR amplification with barcoded primers and Tks Gflex DNA Polymerase (Takara). The primer sequences used to amplify the V3-V4 region were 343F: TACGGRAGGCAGCAG and 798R: AGGGTATCTAATCCT.

Then, the purified PCR products were quantified by a Qubit. The samples were mixed equally according to the concentration of PCR products and sequenced using an Illumina

NovaSeq6000. Microbial community structure was assessed by alpha diversity and beta diversity analyses. In addition, phylogenetic investigation of communities by reconstruction of unobserved states (PICRUSt), the Kyoto Encyclopedia of Genes and Genomes (KEGG), and other functional spectrum databases were used for functional group prediction based on the 16S rDNA gene sequence. Library sequencing and data processing were conducted by OE Biotech Co., Ltd. (Shanghai, China).

Metabolomics Analysis

LC-MS Analysis

First, 30 mg of hippocampal tissue was accurately weighed into a 1.5 ml EP tube with an internal standard (20 μl). Next, 600 μL of methanol-water (V:V = 4:1) was added. Then, two small steel beads were added and, after precooling in a −20°C freezer for 2 min, the sample was placed in a grinder for grinding (60 Hz, 2 min). Subsequently, the sample was submitted to ultrasonic extraction with an ice water bath for 10 min. Next, the sample was allowed to stand at −20°C for 2 h. Finally, the sample was centrifuged for 10 min (13,000 rpm, 4°C). Then, 150 μL of the supernatant was aspirated with a syringe, and the organic phase was filtered through a 0.22 μm pinhole filter, transferred to an LC injection vial, and stored at −80°C until LC–MS analysis was performed. The chromatography and MS analysis conditions and data processing methods are described in **Supplementary Material 1**.

GC-MS Analysis

Similar to the above steps, first, 30 mg of hippocampal tissue was accurately weighed into a 1.5 ml EP tube with an internal standard (20 μl). Then, 600 μL of methanol-water (V:V = 4:1) was added. Second, two small steel beads were added, and after precooling in a −20°C freezer for 2 min, the sample was placed in a grinder for grinding (60 Hz, 2 min). Third, 120 μL chloroform was added, and the sample was rotated for 2 min and then submitted to ultrasonic extraction in an ice water bath for 10 min. Fourth, the sample was allowed to stand at −20°C for 30 min. Subsequently, the sample was centrifuged at low temperature for 10 min (13,000 rpm, 4°C); 150 μL of supernatant was transferred into a standard glass flask. Next, the sample was dried with a centrifugal concentrator dryer. Then, 80 μL of methoxylamine hydrochloride pyridine solution (15 mg/mL) was added to the standard glass vials, and the vials were shaken for 2 min and then shaken in an incubator at 37°C for 90 min for the oxime reaction. After the samples were removed, 50 μL of bis(trimethylsilyl)trifluoroacetamide (BSTFA) (containing 1% chlorotrimethylsilane) derivatizing reagent and 20 μL of n-hexane were added, 10 kinds of internal standards (10 μL) were added, and the samples were shaken by vortexing for 2 min and reacted at 70°C for 60 min. After the samples were removed the heat block, they were placed at room temperature for 30 min for GC-MS analysis, and the data processing methods are shown in **Supplementary Material 2**. Both LC–MS and GC–MS analyses were performed by OE Biotech Co., Ltd. (Shanghai, China).

Lipid Metabolism Assays

Serum levels of adiponectin, ApoE and FFA were determined using commercial kits according to the manufacturer's instructions, and the absorbance was read at 450 nm (adiponectin and ApoE) and 570 nm (FFA).

Oxidative Stress Detection

The hippocampal tissue was removed from the refrigerator, rinsed with precooled normal saline, cut into pieces with sterile ophthalmic scissors and added to normal saline at a m (tissue): V (normal saline) ratio = 1 g:9 mL (the sample was maintained on ice for the whole time). The sample was homogenized by an automatic homogenizer (intermittently once every 3 s to prevent excessive heat generation) to make a 10% mass fraction of homogenate, which was centrifuged at 1,000 × *g* (4°C) for 15 min. The supernatant was collected, and an appropriate amount of physiological saline was added to dilute the sample to an appropriate concentration. The instructions of the kit were strictly followed to detect SOD and GSH-Px activity and MDA content in serum and brain tissue.

Statistical Analysis

GraphPad Prism 8.0.2 statistical analysis software was used for statistical analysis of the data. Metrology data are presented as the mean plus or minus the standard error ($\bar{x} \pm$ s). Multiple comparisons among experiments were performed by one-way analysis of variance (ANOVA) with the least significant difference (LSD) test for multiple comparisons, and $P < 0.05$ was considered to indicate statistical significance.

In the 16S rRNA analysis, the operational taxonomic units (OTUs) were subjected to alpha diversity and beta diversity analysis. Communities or species that significantly differentially affected sample division were estimated using linear discriminant analysis (LDA) (Wang et al., 2022). For metabolomic analysis, orthogonal partial least squares discriminant analysis (OPLS-DA) was used to screen differentially abundant metabolites. Variable importance of projection (VIP) > 1 and $P < 0.05$ were used as thresholds to identify differentially abundant metabolites. To prevent overfitting, we used sevenfold cross validation and 200-response permutation testing (RPT) to assess the quality of the model (Wang et al., 2022). Finally, association analysis was performed using the Spearman correlation analysis method (Lu et al., 2022).

RESULTS

Chemical Composition Analysis of Liuwei Dihuang Decoction

The retention time (RT) and mass spectrometric data of each chemical component in LW were obtained after UPLC-Q-TOF-MS detection, and 23 components, including morroniside, loganin and paeonol, were resolved from the collected data, as shown in **Figure 2** and **Supplementary Table 1**.

Effects of Liuwei Dihuang Decoction on Cognitive Function and Hippocampal Synaptic Ultrastructure in Aging Mice

In the navigation test, with the increase in training time and sessions, the time for mice in each group to find the platform tended to decrease. Compared with that of mice in the control group, the escape latency of mice in the model group was significantly prolonged ($P < 0.01$), and the latency of mice in the LW-L, LW-H, and vitamin E groups was significantly shortened compared with that of mice in the model group ($P < 0.01$, **Figure 3A**). The results of the spatial exploration test showed that compared with the control group mice, the model group mice also spent less time in the target quadrant ($P < 0.01$) and had significantly fewer platform crossings ($P < 0.05$), indicating that D-galactose injection induced cognitive dysfunction. Interestingly, LW improved D-galactose injection-induced cognitive impairment in a dose-dependent manner. Compared with those of mice in the model group, the time in the target quadrant ($P < 0.05$ or $P < 0.01$) and the number of platform crossings ($P < 0.05$ or $P < 0.01$) of mice in the LW-L, LW-H, and vitamin E groups were significantly increased (**Figures 3B–D**). These results suggest that LW can improve cognitive impairment in aging mice.

Transmission electron microscopy was used to assess the ultrastructure of hippocampal synapses. We found that the synaptic structure of the hippocampal neurons in the control group was intact, and the presynaptic membrane, synaptic cleft, postsynaptic membrane and postsynaptic dense material were clearly visible. Compared with those of the control group, the synaptic structure of the model group was blurred, the postsynaptic dense material was sparse, and the boundary between the anterior and posterior membranes was unclear. Compared with those of the model group, the synaptic structure of the LW-L, LW-H, and vitamin E groups was clearer, the boundaries of the anterior and posterior membranes were clear, and the postsynaptic dense matter increased, as shown in **Figure 3E**. It is suggested that LW can improve the damage to hippocampal synapses in aging mice.

Effects of Liuwei Dihuang Decoction on the Gut Microbiota of Aging Mice

Based on the above MWM test results, the control, model and LW-H groups were selected for subsequent 16S rRNA and metabolomics analyses. Analysis of the alpha diversity, calculated using the Chao 1 index and observed species index, showed that the number and diversity of microbiota constituents in the model group relative to those in the control group decreased ($P < 0.05$), as shown in **Figure 4A**. After treatment with LW administration, the number and diversity of intestinal microbiota returned to their normal levels ($P < 0.05$), as shown in **Figure 4B**. In addition, beta diversity analysis was also utilized to assess differences between microbial communities. Principal coordinate analysis (PCoA) based on the weighted UniFrac distance showed that the microbial composition and structure of the model group and the control group were significantly different, and the LW group had a similar trend to the control group, suggesting that LW could partially restore the gut microbial composition of aging mice, as shown in **Figure 4C**.

To understand the effect of LW on the gut microbiota, we analyzed the relative abundance of gut microbiota constituents in the different groups. At the phylum level, aging mice showed a decreased relative abundance of *Bacteroidota* and an increased abundance of *Firmicutes* and *Proteobacteria*. In contrast, LW reduced the levels of *Proteobacteria* in aging mice (**Figure 4D**). At the genus level, the abundances of *Muribaculaceae*, *Alloprevotella*, *Prevotellaceae_UCG-001*, *Bacteroides* and *Clostridia_UCG-014* were decreased, and the abundances of *Lachnospiraceae_NK4A136_group* and *Parabacteroides* were increased in aging mice. LW treatment significantly increased the abundances of *Alloprevotella*, *Prevotellaceae_UCG-001*, *Bacteroides*, and *Clostridia_UCG-014* and decreased the abundances of *Lachnospiraceae_NK4A136_group* and *Parabacteroides*, as shown in **Figure 4E**.

Linear discriminate analysis effect size (LEfSe) analysis was applied to identify key microbiota members differentially represented in LW-treated mice. The dominant flora constituents in the LW group were *Clostridiacea*e and *Lactobacillales* at the order level, *Oscillospiraceae* and *Clostridiaceae* at the class level, and *Alistipes* and *Roseburia* at the genus level, as shown in **Figures 4F,G**.

Finally, to determine whether taxonomic changes in the gut microbiota affected its function, we performed functional prediction based on representative sequences with PICRUSt2. Based on a comparison with the control group, there were significant differences ($P < 0.05$) in glycan biosynthesis and metabolism, lipid metabolism, metabolism of other amino acids, exogenous compound biodegradation and metabolism, transport and catabolism, and the nervous system. LW reversed the above changes in pathways ($P < 0.05$), as shown in **Figure 4H**.

Effects of Liuwei Dihuang Decoction on the Metabolic Profile of Hippocampal Tissue in Aging Mice

The effects of LW on the metabolites in the hippocampal tissue of aging mice were first analyzed by LC–MS. OPLS-DA was used to distinguish the overall differences in the metabolic profiles between the groups, as shown in **Figures 5A,B**. The differences among the control group, model group and LW group were obvious. In addition, to prevent model overfitting, 7-fold cross validation and 200-RPT methods were used to examine the quality of the model. The results showed that compared with the control group, the model group had $R2 = 0.737$ and $Q2 = -0.708$ (**Figure 5C**). Moreover, compared with the model group, the LW group had $R2 = 0.793$ and $Q2 = -0.471$ (**Figure 5D**), suggesting that the OPLS-DA model is stable and has good predictive ability. Finally, according to the screening thresholds of VIP > 1 and $p < 0.05$, the metabolites with differential abundances between different groups were determined. There were 47 metabolites with differential abundances between the model group and the control group and 30 metabolites with differential abundances between the LW group and the model group (**Supplementary Table 2**).

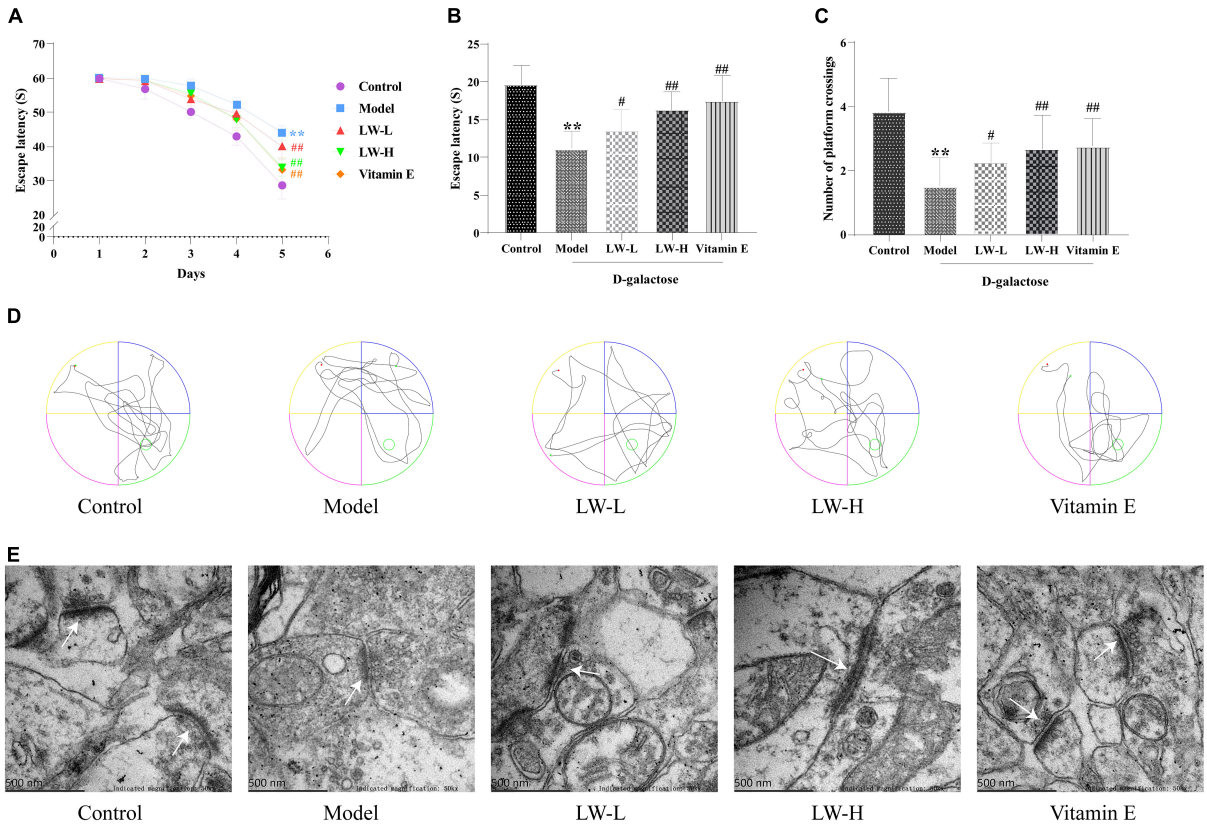

FIGURE 3 | Effects of Liuwei Dihuang decoction on cognitive function and hippocampal synaptic ultrastructure in aging mice. **(A)** Navigation test. **(B)** Spatial exploration. **(C)** Platform crossing. **(D)** MWM representative figures. **(E)** Ultrastructure of hippocampal synapses. $^{**}p < 0.01$ vs. Control group. $^{\#}p < 0.05$, $^{\#\#}p < 0.01$ vs. Model group.

Subsequently, we analyzed the effects of LW on the metabolites in the hippocampal tissue of aging mice by GC–MS. GC–MS is able to detect compounds with strong volatility, small molecular weight, and low polarity and can be used as a complement to LC–MS for identifying thermally stable compounds (Zeki et al., 2020). OPLS-DA was used to distinguish the overall differences in metabolic profiles among the groups, as shown in **Figures 5E,F**, which were obvious among the control, model and LW groups. Evaluation of the OPLS-DA model showed that the model group had R2 = 0.928 and Q2 = −0.264 compared with the control group (**Figure 5G**). Moreover, compared with the model group, the LW group had R2 = 0.952 and Q2 = −0.22 (**Figure 5H**), suggesting that the OPLS-DA model is stable and has good predictive ability. Finally, we found a total of 53 metabolites with differential abundances between the model group and the control group and 22 metabolites with differential abundances between the LW group and the model group, as shown in **Supplementary Table 3**.

By integrating data from the dual-platform metabolomic analysis, we found that LW reversed the changes in the levels of 14 differentially abundant metabolites in the model group, of which five metabolites were depleted in the model group and enriched in the LW group, and the other nine metabolites were enriched in the model group and depleted in the LW group, as shown in **Figure 5I** and **Table 2**. Using the KEGG database, we analyzed the metabolic pathways in which the above 14 metabolites were involved. Finally, we found that apelin signaling, calcium signaling, phospholipase D signaling, sphingolipid metabolism, neuroactive ligand–receptor interaction and glycerophospholipid metabolism were significantly enriched metabolic pathways ($p < 0.05$), as shown in **Figure 5J**. Excitingly, we found that as determined by metabolomics, the significant enrichment of sphingolipid metabolism and glycerophospholipid metabolism closely resembled the changes in metabolic pathways such as lipid metabolism in the gut microbiota that were predicted by PICRUSt based on 16S rRNA sequencing data. This alignment suggests that the effects of LW intervention on the gut microbiota and hippocampal metabolites may be related.

Effects of Liuwei Dihuang Decoction on Lipid Metabolism and Oxidative Stress in Aging Mice

The above results of 16S rRNA sequencing and metabolomic analysis of the hippocampus suggest that LW may play a therapeutic role by affecting lipid metabolism in aging mice. Therefore, we further studied the effect of LW on the lipid metabolism-related factors ApoE, adiponectin and FFA in the

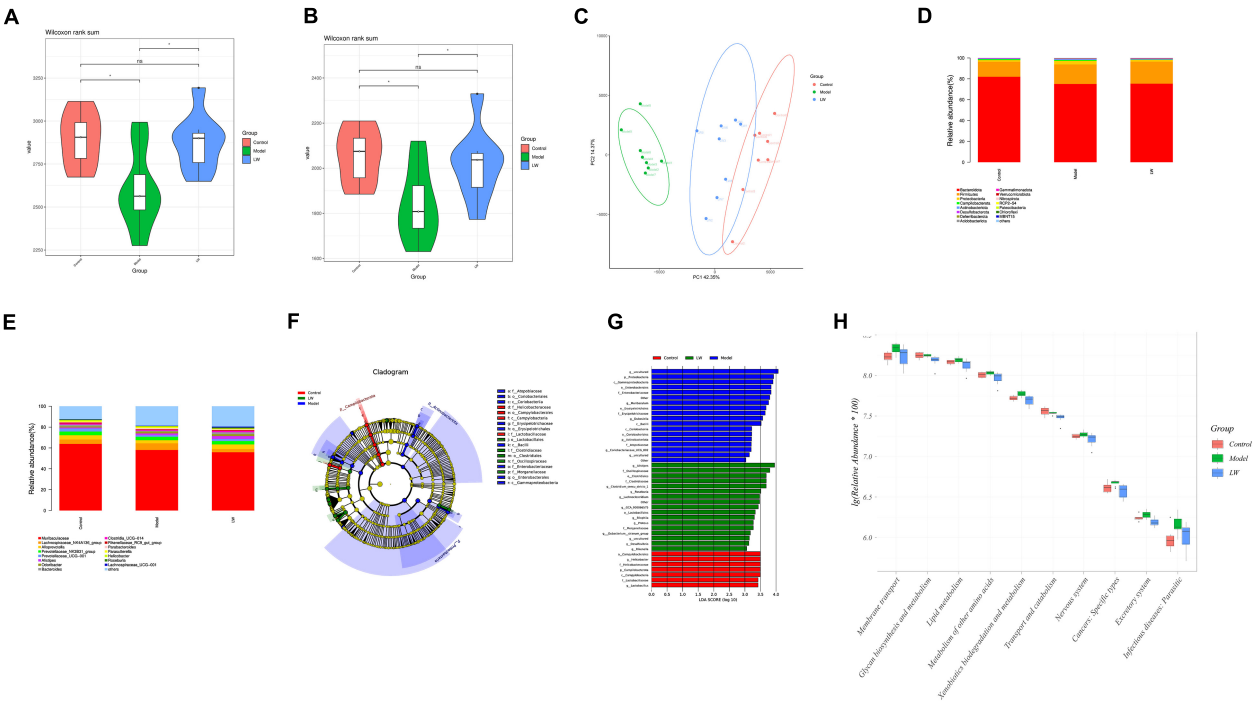

FIGURE 4 | Effects of Liuwei Dihuang decoction on the gut microbiota of aging Mice. **(A)** Chao 1 index. **(B)** Observed species index. **(C)** PCoA analysis. **(D)** Relative abundance of gut microbiota (phylum level). **(E)** Relative abundance of gut microbiota (genus level). **(F)** Cladogram of LEfSe analysis. **(G)** LDA of LEfSe analysis. **(H)** PICRUSt2 analysis.

serum of rapidly aging mice. As shown in **Figures 6A–C**, compared with those in the control group, the ApoE and adiponectin contents in the model group were significantly decreased ($p < 0.01$), and the FFA content was significantly increased ($p < 0.01$), while LW and vitamin E treatment reversed the levels of these factors ($p < 0.05$ or $p < 0.01$). This finding suggested that LW can affect lipid metabolism in aging mice.

Disturbances in lipid metabolism are often accompanied by oxidative stress, which is often also an important risk factor for aging and cognitive dysfunction (Morgan et al., 2016). Therefore, we examined the effects of LW on the activities of SOD, GSH-Px and MDA content in the serum and brain tissue of aging mice. As shown in **Figures 6D–I**, compared with the control group, the MDA content in the serum and brain tissue of the mice in the model group was significantly increased ($P < 0.05$), and the activities of SOD and GSH-Px were significantly decreased ($P < 0.01$), indicating that the antioxidant capacity of serum and brain tissue of D-galactose-induced aging mice was significantly reduced. LW and vitamin E reversed the above changes ($P < 0.05$ or $P < 0.01$), suggesting that LW could improve the antioxidant capacity of model mice.

Relationship Between Gut Microbes and Hippocampal Metabolites, Lipid Metabolism, and Oxidative Stress

Next, we analyzed the potential relationship between the differentially abundant gut microbiota constituents and differentially abundant metabolites in the hippocampus. As shown in **Figures 7A,B**, at the phylum level, *Proteobacteria* was positively correlated with oleic acid-2,6-diisopropylanilide, methacholine, PG [22:6(4Z,7Z,10Z,13Z,16Z,19Z)/0:0] and asparaginyl-methionine ($p < 0.05$). At the genus level, *Roseburia* and *Lachnoclostridium* were positively correlated with lipid metabolites such as sphingosine-1-phosphate and lysophosphatidylcholine lysoPC [20:2 (11z, 14z)] ($P < 0.05$), and *Muribaculum* was significantly negatively correlated with lipid metabolites such as sphingosine-1-phosphate, lysoPC (15:0) and lysoPC [20:2 (11z, 14z)] ($P < 0.05$, $P < 0.01$ or $P < 0.001$), as shown in **Figures 7C,D**.

Similarly, we analyzed the correlation of the microbiota with factors related to lipid metabolism and oxidative stress in serum. At the phylum level, *Proteobacteria* was positively correlated with FFA and MDA ($p < 0.05$ or $p < 0.01$), and negatively correlated with ApoE, GSH-Px, adiponectin, and SOD ($p < 0.05$); *Fibrobacterota* was positively correlated with ApoE, GSH-Px, adiponectin and SOD were positively correlated ($p < 0.05$), and negatively correlated with FFA and MDA ($p < 0.05$), as shown in **Figures 7E,F**. At the genus level, *Muribaculum* was positively correlated with FFA and MDA ($p < 0.01$ or $p < 0.001$), and negatively correlated with ApoE, GSH-Px, adiponectin, and SOD ($p < 0.01$ or $p < 0.001$); *Roseburia* was positively correlated with ApoE, GSH-Px, adiponectin and SOD were positively correlated ($p < 0.05$ or $p < 0.01$), and negatively correlated with FFA and MDA ($p < 0.05$ or $p < 0.01$), as shown in **Figures 7G,H**. Thus, these findings revealed potential

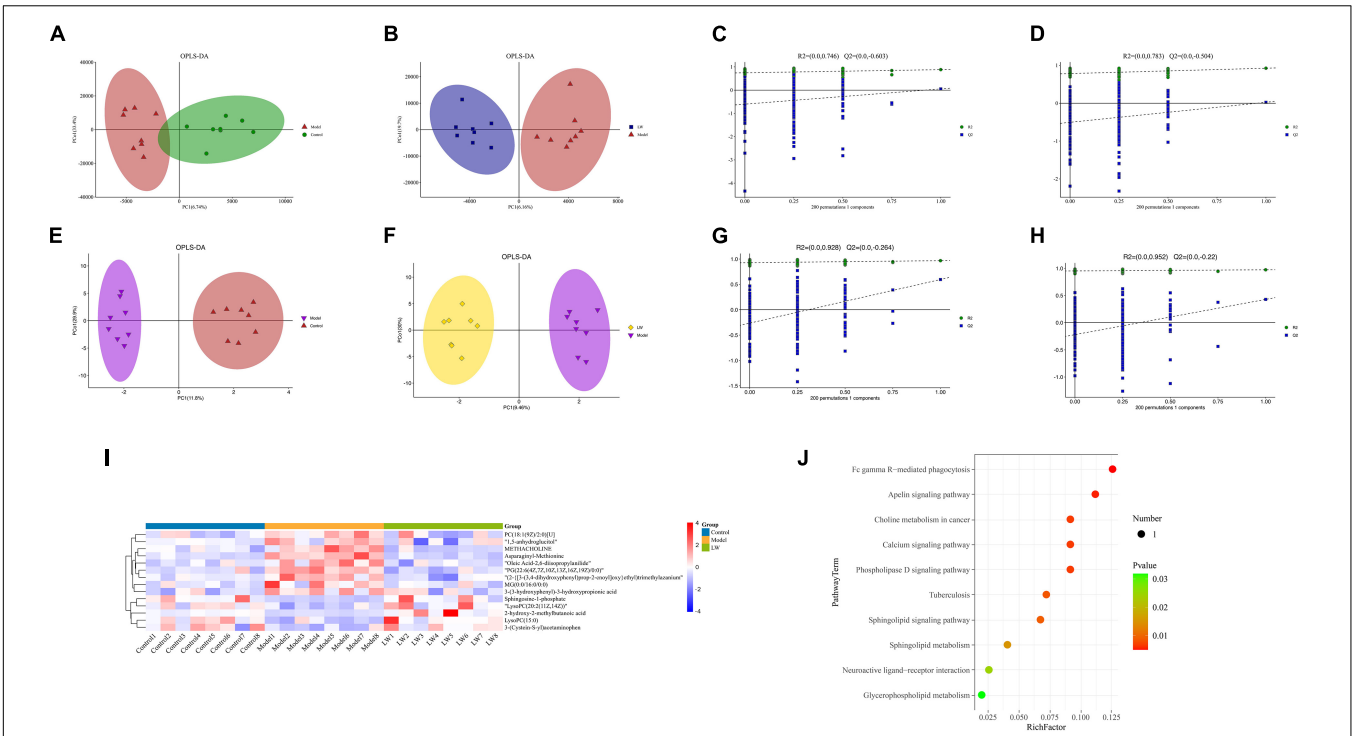

FIGURE 5 | Effects of LW on the metabolic profile of hippocampal tissue in aging mice. **(A)** OPLS-DA of LC-MS (Model vs. Control). **(B)** OPLS-DA of LC-MS (LW vs. Model). **(C)** Permutation of OPLS-DA model (Model vs. Control). **(D)** Permutation of OPLS-DA model (LW vs. Model). **(E)** OPLS-DA of GC-MS (Model vs. Control). **(F)** OPLS-DA of GC-MS (LW vs. Model). **(G)** Permutation of OPLS-DA model (Model vs. Control). **(H)** Permutation of OPLS-DA model (LW vs. Model). **(I)** Differentially abundant metabolites. **(J)** Analysis of metabolic pathway enrichment.

TABLE 2 | Identification and variation tendency of 14 differential metabolites by LC-MS & GC-MS.

Metabolites	Compound ID	Mode	Formula	Model vs. Control		LW vs. Model	
				VIP	*P*-value	VIP	*P*-value
LysoPC(20:2(11Z,14Z))	HMDB0010392	LC-MS	$C_{28}H_{54}NO_7P$	1.97653516	0.009151234	2.257710481	0.017475092
LysoPC(15:0)	HMDB0010381	LC-MS	$C_{23}H_{48}NO_7P$	1.072222462	0.006313074	1.190052623	0.034020136
3-(Cystein-S-yl)acetaminophen	HMDB0240217	LC-MS	$C_{11}H_{14}N_2O_4S$	1.007448543	0.03183613	1.207377077	0.009769263
2-hydroxy-2-methylbutanoic acid	HMDB0001987	GC-MS	/	1.792910311	6.49489E−06	2.572525386	0.040679786
3-(3-hydroxyphenyl)-3-hydroxypropionic acid	HMDB0002643	GC-MS	/	1.997405882	0.004959811	1.58286374	0.041028306
PC(18:1(9Z)/2:0)[U]	39642	LC-MS	$C_{28}H_{54}NO_8P$	1.273559624	0.009100443	1.174542693	0.040487874
(2-{[3-(3,4-dihydroxyphenyl)prop-2-enoyl]oxy}ethyl) trimethylazanium	HMDB0136312	LC-MS	$C_{14}H_{20}NO_4$	1.282963036	0.000837746	1.688485234	0.001014712
1,5-anhydroglucitol	HMDB0002712	GC-MS	/	1.316636006	0.012282553	2.310523814	0.049125615
PG(22:6(4Z,7Z,10Z,13Z,16Z,19Z)/0:0)	LMGP04050016	LC-MS	$C_{28}H_{45}O_9P$	2.006290372	0.000168751	2.574115085	2.89809E−05
METHACHOLINE	43545	LC-MS	$C_8H_{17}NO_2$	4.259755705	0.00245965	5.736589467	0.000250805
Sphingosine-1-phosphate	3891	LC-MS	$C_{18}H_{38}NO_5P$	1.64865281	0.047778962	1.663805976	0.048089092
Oleic Acid-2,6-diisopropylanilide	64645	LC-MS	$C_{30}H_{51}NO$	1.021481093	0.003157587	1.074957858	0.003608528
MG(0:0/16:0/0:0)	HMDB0011533	LC-MS	$C_{19}H_{38}O_4$	1.188356611	0.036927406	1.290358375	0.044092221
Asparaginyl-Methionine	HMDB0028737	LC-MS	$C_9H_{17}N_3O_4S$	1.800887048	1.06379E−05	2.219478238	5.13366E−06

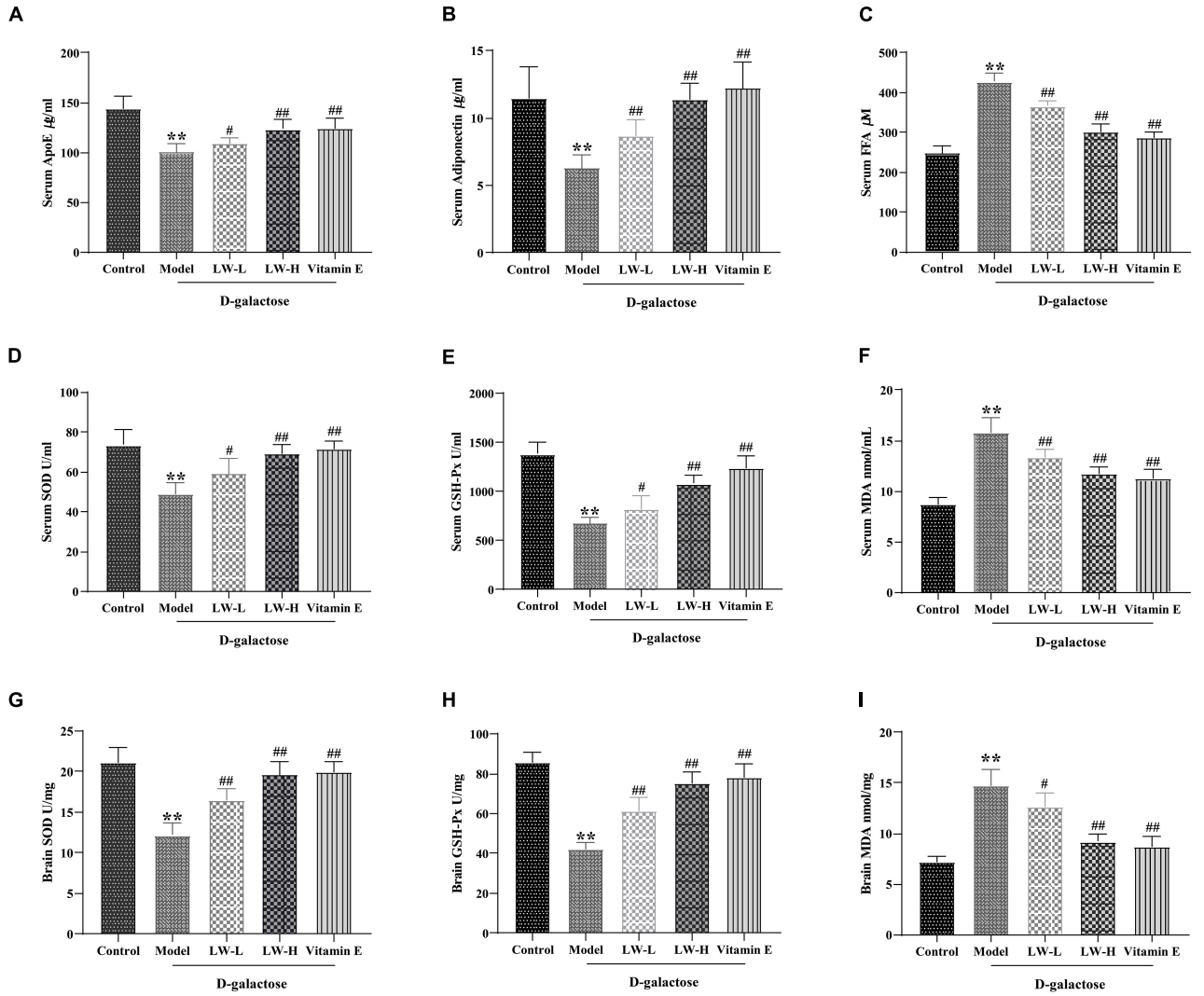

FIGURE 6 | Effects of Liuwei Dihuang decoction on lipid metabolism and oxidative stress in aging mice. **(A)** ApoE. **(B)** Adiponectin. **(C)** FFA. **(D)** SOD in serum. **(E)** GSH-Px in serum. **(F)** MDA in serum. **(G)** SOD in brain tissue. **(H)** GSH-Px in brain tissue. **(I)** MDA in brain tissue. $^{**}p < 0.01$ vs. Control group. $^{\#}p < 0.05$, $^{\#\#}p < 0.01$ vs. Model group.

interactions between LW-regulated microbial species and lipid metabolism and oxidative stress.

DISCUSSION

At present, the proportion of the elderly population in the world is growing rapidly, and the challenges associated with aging have become an international problem. Aging is an irreversible natural law, and researchers cannot prevent aging, although they can delay it. The multitarget and multilinking mechanism of traditional Chinese medicine is an important direction for aging delay therapeutic development. In this study, we found that LW can improve cognitive function in aging mice and improve the synaptic structure of the hippocampus. Subsequently, by 16S rRNA sequencing, we found that LW improved gut microbiota diversity in rapidly aging mice, and subsequent metabolomic analysis revealed that LW could alter the levels of endogenous metabolites in the hippocampus of aging mice. Notably, both 16S rRNA sequencing and metabolomic functional enrichment analyses identified lipid metabolism as a target of LW. In subsequent explorations, we confirmed that LW could affect lipid metabolism and oxidative stress in aging mice.

The gut microbiota is considered to be the host's "second genome," which plays important roles in maintaining the body's homeostasis and in the occurrence and development of cognitive dysfunction (Li et al., 2019; Liu et al., 2021b). Studies have shown that the gut microecological characteristics of elderly individuals include lower diversity (Bunker et al., 2019), depletion of *Bacteroidota*, and enrichment of *Proteobacteria* and *Firmicutes* (Luo et al., 2020). Other studies have pointed out that increased *gram-negative bacteria* in the intestinal flora can lead to increased

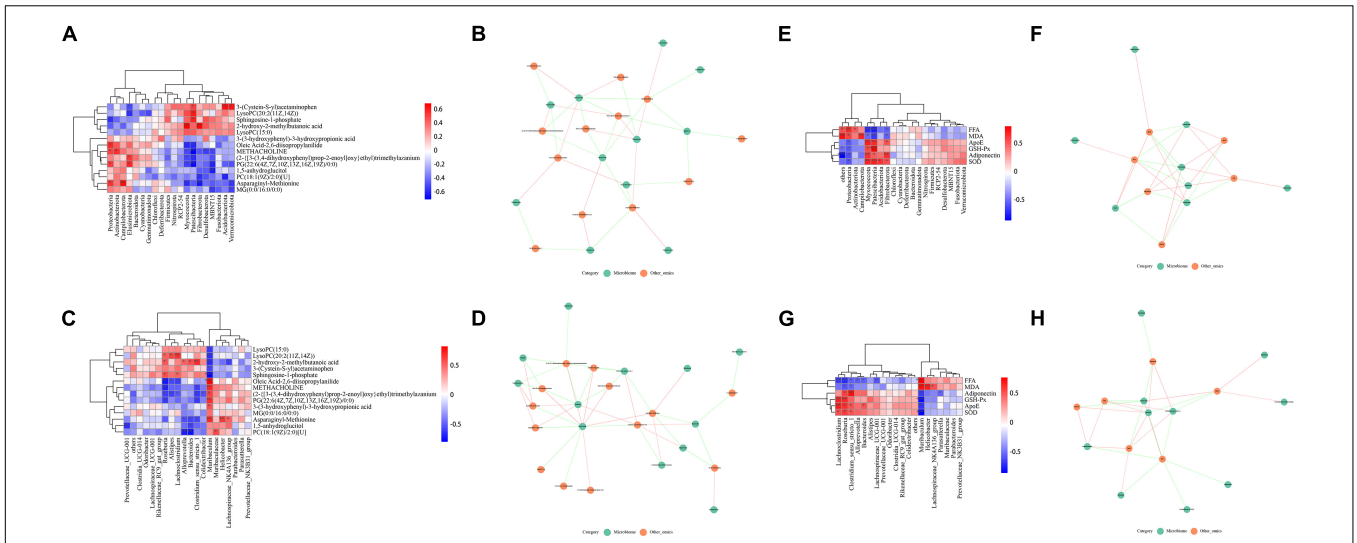

FIGURE 7 | Relationship between gut microbes and hippocampal metabolites, lipid metabolism and oxidative stress. **(A,B)** Correlation of microbiota related to differentially abundant metabolites (phylum level). **(C,D)** Correlation of microbiota related to differentially abundant metabolites (genus level). **(E,F)** Correlation of microbiota with factors related to lipid metabolism and oxidative stress (phylum level). **(G,H)** Correlation of microbiota with factors related to lipid metabolism and oxidative stress (genus level).

secretion of proinflammatory cytokines, and these products can reach the central nervous system (CNS) through the circulation to promote neuroinflammatory responses (Wang and Quinn, 2010). Moreover, signaling molecules secreted by the gut microbiota are transferred *via* the lymphatic and systemic circulation throughout the CNS where they then modulate brain plasticity and cognitive function (de Haas and van der Eijk, 2018). Our study showed that LW treatment was able to improve the alpha diversity index of the gut microbiota and reduce the levels of *Proteobacteria*. *Proteobacteria* is the largest phylum of bacteria and accounts for a small proportion in the healthy adult gut, and its enrichment is considered a marker of gut dysbiosis (Shin et al., 2015). Previous studies have shown that *Proteobacteria* is closely related to cognitive impairment in elderly individuals (Manderino et al., 2017), and that reducing the level of *Proteobacteria* can improve cognitive function in aging mice (Yang et al., 2020). At the genus level, we found that the abundance of *Alloprevotella* decreased and that of *Parabacteroides* increased in aging mice, and LW reversed these changes. *Alloprevotella* is a beneficial bacterium and is closely related to lipid metabolism in aging mice (Wu et al., 2022), and elevating the abundance of *Alloprevotella* can improve memory function in mice (Liu et al., 2021a). Studies have shown that *Parabacteroides* is an independent risk factor for mild cognitive impairment in elderly individuals (Khine et al., 2020) and that a high abundance of *Parabacteroides* can exacerbate neurodegeneration (Blacher et al., 2019). Further LEfSe analysis revealed that *Lactobacillales* (order), *Clostridiaceae* (class), *Alistipes* (genus), and *Roseburia* (genus) were the dominant microbiota constituents in the LW group. *Lactobacillales* regulates intestinal microbes and enhances immunity and antioxidation (De-Filippis et al., 2020). Previous studies have confirmed that *Lactobacillales* can improve the gut microbiota in aging rats (Hor et al., 2019), inhibit oxidative stress (Wang et al., 2021), and improve cognitive function in aged mice (Ni et al., 2019). Higher *Clostridiaceae* abundance correlates with better "attention continuity" (Komanduri et al., 2021). Previous studies have shown that a high abundance of *Alistipes* can effectively suppress intestinal inflammation and oxidative stress (Wan et al., 2021). *Roseburia* produces short-chain fatty acids, affects intestinal motility, has anti-inflammatory properties and is considered the cornerstone of gut biodiversity (Tamanai-Shacoori et al., 2017). Finally, we found that glycan biosynthesis and metabolism, lipid metabolism, metabolism of other amino acids, exogenous compound biodegradation and metabolism, transport and catabolism, and the nervous system might be the main metabolic pathways in the differential flora through PICRUSt2 analysis.

Increasing evidence suggests that metabolic changes associated with the gut microbiota are important factors associated with various diseases (Liu et al., 2022). Mammalian humoral and tissue metabolomes are greatly influenced by the microbiome, and many health-related metabolites are considered "mammal-microbial cometabolites" (Heinken and Thiele, 2015; Chen et al., 2018). Based on the combined GC–MS and LC–MS/MS whole-spectrum metabolomics platform used in this study, we systematically analyzed endogenous metabolites in the hippocampus of aging mice treated with LW and identified 14 differentially abundant metabolites as potential LW metabolic markers for effects on aging mice. These potential metabolic markers mainly include metabolites closely related to lipid metabolism, such as phosphatidylcholine (PC) and lysoPC. LysoPCs are the most biologically active lysophospholipids; they are key signaling molecules in cell and tissue metabolism and are involved in plasma membrane formation (Shindou et al., 2013), cell growth and death (Makide et al., 2009). In addition,

sphingosine-1-phosphate, a potential metabolic marker, has the ability to modulate the stress resistance, proliferation, differentiation and maturation phenotype of cells in the nervous system (Czubowicz et al., 2019). Studies have confirmed that sphingosine-1-phosphate content in the hippocampus decreases gradually with age (Couttas et al., 2018), and that activation of sphingosine-1-phosphate reduces Aβ deposition and improves cognitive function in Alzheimer's disease (AD) rats (Wang and Yang, 2021). KEGG enrichment analysis revealed that apelin signaling, calcium signaling, phospholipase D signaling, sphingolipid metabolism, neuroactive ligand–receptor interaction and glycerophospholipid metabolism may be the main metabolic pathways involved in the mechanism of action of LW. Apelin, a cytokine produced and secreted by adipocytes, has been shown to be involved in processes such as the regulation of fluid homeostasis, food intake, cell proliferation, and angiogenesis (Zhou et al., 2018). Moreover, apelin has been recently identified as an adipokine involved in energy metabolism, which can act together with leptin and adiponectin on glucose metabolism and lipid metabolism (Bertrand et al., 2015). In an apelin knockout mouse model, the aging rate was accelerated. When apelin content was restored, it was found that not only the vitality of the mice was enhanced but also the behavior and circadian rhythm phenotypes were restored, suggesting that apelin may be an antiaging factor (Rai et al., 2017). Sphingolipids are lipids that are highly enriched in the CNS and are involved in membrane formation and signal transduction, cell proliferation, apoptosis, migration and invasion, inflammation and nervous system development. Disorders of sphingolipid metabolism mediate the occurrence and development of many neurological diseases, such as Parkinson's disease, multiple sclerosis and AD (Alaamery et al., 2021).

Notably, the enrichment analysis based on 16S rRNA sequencing and differential metabolomics in the hippocampus suggested that LW may play a therapeutic role by affecting lipid metabolism in the body. Some studies have suggested that abnormal lipid metabolism is closely related to cognitive dysfunction (Bowers et al., 2020). Therefore, we further explored the effect of LW on the lipid metabolism-related factors ApoE, adiponectin, and FFA in the serum of rapidly aging mice. The results suggested that LW treatment can affect the levels of ApoE, adiponectin and FFA in the serum of aging mice. ApoE is mainly produced in the liver, is able to transport lipids, and plays a central role in lipid metabolism (Yin and Wang, 2018). There is recent evidence for a similar role for ApoE in the brain (Holtzman et al., 2012): as the major CNS apolipoprotein, ApoE is responsible for regulating much of brain lipid metabolism, in particular the transfer of cholesterol and phospholipids from glial cells to neurons (Hudry et al., 2019). Furthermore, loss of ApoE disrupts the blood–brain barrier (BBB) in aging mice (Mulder et al., 2001) and leads to cognitive dysfunction (Zerbi et al., 2014) and cerebrovascular dysfunction (Bell et al., 2012). Adiponectin is a plasma protein capable of crossing the BBB, exerting its modulation and signaling effects through its receptors (Bloemer et al., 2018). Adiponectin has been found to regulate glucose metabolism in hippocampal neurons, increasing rates of glucose uptake, glycolysis and ATP production (Cisternas et al., 2019). St Studies have shown that circulating adiponectin levels are decreased in mild cognitive impairment and AD (Teixeira et al., 2013) and that tail vein injection of adiponectin-overexpressing endothelial progenitor cells can improve cognitive function in aging rats (Huang J. et al., 2020). FFA is closely related to lipid metabolism, and clinical studies have shown that high FFA plasma concentrations are associated with reduced cognitive function (Holloway et al., 2011). Disturbances in lipid metabolism are often accompanied by oxidative stress (Zarrouk et al., 2020), which is often also an important risk factor for aging and cognitive dysfunction (Mecocci et al., 2018). Abnormal oxidative stress can cause protein degeneration, lipid peroxidation, DNA damage and other physiological function changes in cells or tissues, leading to apoptosis and tissue damage, and is a major risk factor for neurodegenerative conditions such as aging (Vatner et al., 2020). Our research shows that the MDA content in the serum and hippocampus of aging mice is significantly increased and that the total SOD (T-SOD) and GSH-Px activities are significantly reduced. LW delays aging and inhibits oxidative damage. Our study showed that the MDA content in the serum and hippocampus of aging mice was significantly increased and that the T-SOD and GSH-Px activities were significantly decreased. Intervention with LW reversed the above changes, suggesting that LW can improve the antioxidant capacity of cells, delay aging and inhibit oxidative damage.

Recently, the microbiota-gut-brain axis has gained extensive attention as a channel for communication and physiological regulation (Li et al., 2020). Experimental evidence suggests that the gut microbiota can alter the levels of multiple cytokines, which in turn can have a significant effect on several brain functions (Giau et al., 2018). *Bacteria* have recently been identified in the brains of AD patients, suggesting that the microbiota may be a contributing factor to related neuroinflammation (Emery et al., 2017). Probiotics can modulate gut microbiota dysbiosis and microbiota–gut–brain axis deficits to improve cognitive dysfunction in aged mice (Yang et al., 2020). Furthermore, gut microbiome activity may promote abnormal lipid deposition and oxidation that damage the brain (Shao et al., 2020). Regulating the composition of the intestinal flora and the abundance of beneficial bacteria (including *Enterorhabdu*s, *Clostridium*, *Bifidobacterium*, and *Parvibacter*) were able to slow down D-gal-induced oxidative stress damage and apoptosis of neurons (Liu et al., 2021c). We found that *Proteobacteria* was positively correlated with FFA and MDA ($p < 0.05$ or $p < 0.01$) and negatively correlated with ApoE, GSH-Px, adiponectin, and SOD ($p < 0.05$), suggesting that the high abundance of *Proteobacteria* may aggravate lipid deposition and promote oxidative stress. Conversely, the high abundance of *Fibrobacterota* may inhibit oxidative stress. Based on the above studies, we speculated that LW might regulate the levels of *Proteobacteria* and *Fibrobacterota* to affect lipid metabolism and oxidative stress to improve age-related cognitive dysfunction, but the mechanism remains to be further investigated.

Notably, there are some limitations of this study. We did not use germ-free mice or fecal bacterial transplantation to determine which flora constituents are related to the therapeutic effect of LW. In addition, the findings still need to be clinically validated,

and the specific mechanisms of differentially abundant bacteria or metabolites and lipid metabolism were not explored in depth and need further investigation.

CONCLUSION

In summary, this study confirmed the ability of LW to improve cognitive function and hippocampal synaptic structure in aging mice, modulate the gut microbial composition and hippocampal metabolic profile in aging mice, and modulate lipid metabolism and oxidative stress. Moreover, this study also showed that the changes in the *Proteobacteria* and *Fibrobacterota* induced by LW may have a potential link with lipid metabolism and oxidative stress, which deserves further investigation.

DATA AVAILABILITY STATEMENT

The datasets presented in this study can be found in online repositories. The names of the repository/repositories and accession number(s) can be found in the article/**Supplementary Material**.

ETHICS STATEMENT

The animal study was reviewed and approved by the Ethics Committee of Laboratory Animal Studies of The First Affiliated Hospital of Hunan University of Chinese Medicine approved all the experimental protocols (No. ZYFY20210710).

AUTHOR CONTRIBUTIONS

BL designed the experiments, analyzed the data, and prepared the manuscript. BC and JY performed the experiments, analyzed the data, and prepared the manuscript. HL, HW, FT, and YL performed the experiments. LX and LL optimized the language of the manuscript. All authors confirmed the final manuscript.

FUNDING

This work was supported by grants from the Hunan Provincial Department of Education Open Platform Fund (20K096), the Hunan Provincial Traditional Chinese Medicine Research Project (2020098), the Changsha Natural Science Foundation (kq2014223), and the Hunan University of Traditional Chinese Medicine Double First-Class Discipline Open Fund (2022ZYX15).

SUPPLEMENTARY MATERIAL

The Supplementary Material for this article can be found online at: https://www.frontiersin.org/articles/10.3389/fnins.2022.949298/full#supplementary-material

Supplementary Table 1 | Chemical composition analysis of LW.

Supplementary Table 2 | Differential metabolites identified by LC-MS.

Supplementary Table 3 | Differential metabolites identified by GC-MS.

Supplementary Material 1 | Chromatographic and MS analytical conditions and data processing methods for LC-MS.

Supplementary Material 2 | Chromatographic and MS analytical conditions and data processing methods for GC-MS.

REFERENCES

Alaamery, M., Albesher, N., Aljawini, N., Alsuwailm, M., Massadeh, S., Wheeler, M., et al. (2021). Role of sphingolipid metabolism in neurodegeneration. *J. Neurochem.* 158, 25–35. doi: 10.1111/jnc.15044

Ali, T., Badshah, H., Kim, T., and Kim, M. (2015). Melatonin attenuates D-galactose-induced memory impairment, neuroinflammation and neurodegeneration via RAGE/NF-K B/JNK signaling pathway in aging mouse model. *J. Pineal Res.* 58, 71–85. doi: 10.1111/jpi.12194

Baker, M. (2011). Metabolomics: from small molecules to big ideas. *Nat. Methods* 8, 117–121.

Bambury, A., Sandhu, K., Cryan, J., and Dinan, T. (2018). Finding the needle in the haystack: systematic identification of psychobiotics. *Br. J. Pharmacol.* 175, 4430–4438. doi: 10.1111/bph.14127

Bell, R., Winkler, E., Singh, I., Sagare, A., Deane, R., Wu, Z., et al. (2012). Apolipoprotein E controls cerebrovascular integrity via cyclophilin a. *Nature* 485, 512–516. doi: 10.1038/nature11087

Bertrand, C., Valet, P., and Castan-Laurell, I. (2015). Apelin and energy metabolism. *Front. Physiol.* 6:115. doi: 10.3389/fphys.2015.00115

Bettio, L., Rajendran, L., and Gil-Mohapel, J. (2017). The effects of aging in the hippocampus and cognitive decline. *Neurosci. Biobehav. Rev.* 79, 66–86. doi: 10.1016/j.neubiorev.2017.04.030

Biagi, E., Nylund, L., Candela, M., Ostan, R., Bucci, L., Pini, E., et al. (2010). Through ageing, and beyond: gut microbiota and inflammatory status in seniors and centenarians. *PLoS One* 5:e10667. doi: 10.1371/journal.pone.0010667

Blacher, E., Bashiardes, S., Shapiro, H., Rothschild, D., Mor, U., Dori-Bachash, M., et al. (2019). Potential roles of gut microbiome and metabolites in modulating ALS in mice. *Nature* 572, 474–480. doi: 10.1038/s41586-019-1443-5

Bloemer, J., Pinky, P., Govindarajulu, M., Hong, H., Judd, R., Amin, R., et al. (2018). Role of adiponectin in central nervous system disorders. *Neural Plast.* 2018:4593530. doi: 10.1155/2018/4593530

Bowers, M., Liang, T., Gonzalez-Bohorquez, D., Zocher, S., Jaeger, B. N., Kovacs, W. J., et al. (2020). FASN-Dependent lipid metabolism links neurogenic Stem/Progenitor cell activity to learning and memory deficits. *Cell Stem Cell* 27, 98–109. doi: 10.1016/j.stem.2020.04.002

Bunker, J., Drees, C., Watson, A., Plunkett, C., Nagler, C., Schneewind, O., et al. (2019). B cell superantigens in the human intestinal microbiota. *Sci. Transl. Med.* 11:u9356. doi: 10.1126/scitranslmed.aau9356

Chen, B., Yi, J., Xu, Y., Zheng, P., Tang, R., and Liu, B. (2022). Construction of a circRNA-miRNA-mRNA network revealed the potential mechanism of Buyang Huanwu Decoction in the treatment of cerebral ischemia. *Biomed. Pharmacother.* 145:112445. doi: 10.1016/j.biopha.2021.112445

Chen, B., Zheng, P., Yi, J., Jia, P., and Liu, B. (2019). Meta-analysis of the efficacy and safety of Liuwei Dihuang Decoction in the treatment of Alzheimer' s disease. *Shizhen Guo Yi Guo Yao* 30, 1274–1277.

Chen, L., Garmaeva, S., Zhernakova, A., Fu, J., and Wijmenga, C. (2018). A system biology perspective on environment-host-microbe interactions. *Hum. Mol. Genet.* 27, R187–R194. doi: 10.1093/hmg/ddy137

Chen, W., Wang, J., Shi, J., Yang, X., Yang, P., Wang, N., et al. (2019). Longevity effect of liuwei dihuang in both *Caenorhabditis elegans* and aged mice. *Aging Dis.* 10, 578–591. doi: 10.14336/AD.2018.0604

Cisternas, P., Martinez, M., Ahima, R., William Wong, G., and Inestrosa, N. (2019). Modulation of glucose metabolism in hippocampal neurons by adiponectin and resistin. *Mol. Neurobiol.* 56, 3024–3037. doi: 10.1007/s12035-018-1271-x

Couttas, T., Kain, N., Tran, C., Chatterton, Z., Kwok, J., and Don, A. (2018). Age-Dependent changes to sphingolipid balance in the human hippocampus are Gender-Specific and may sensitize to neurodegeneration. *J. Alzheimers Dis.* 63, 503–514. doi: 10.3233/JAD-171054

Czubowicz, K., Jęśko, H., Wencel, P., Lukiw, W., and Strosznajder, R. (2019). The role of ceramide and Sphingosine-1-Phosphate in Alzheimer's disease and other neurodegenerative disorders. *Mol. Neurobiol.* 56, 5436–5455. doi: 10.1007/s12035-018-1448-3

de Haas, E. N., and van der Eijk, J. A. J. (2018). Where in the serotonergic system does it go wrong? Unravelling the route by which the serotonergic system affects feather pecking in chickens. *Neurosci. Biobehav. Rev.* 95, 170–188. doi: 10.1016/j.neubiorev.2018.07.007

De-Filippis, F., Pasolli, E., and Ercolini, D. (2020). The food-gut axis: lactic acid bacteria and their link to food, the gut microbiome and human health. *FEMS Microbiol. Rev.* 44, 454–489. doi: 10.1093/femsre/fuaa015

Dinan, T., and Cryan, J. (2017). Brain-Gut-Microbiota axis and mental health. *Psychosom. Med.* 79, 920–926. doi: 10.1097/PSY.0000000000000519

Emery, D. C., Shoemark, D. K., Batstone, T. E., Waterfall, C. M., Coghill, J. A., Cerajewska, T. L., et al. (2017). 16S rRNA next generation sequencing analysis shows bacteria in Alzheimer's Post-Mortem brain. *Front. Aging Neurosci.* 9:195. doi: 10.3389/fnagi.2017.00195

Giau, V., Wu, S., Jamerlan, A., An, S., Kim, S., and Hulme, J. (2018). Gut microbiota and their neuroinflammatory implications in Alzheimer's disease. *Nutrients* 10:1765. doi: 10.3390/nu10111765

Heinken, A., and Thiele, I. (2015). Systems biology of host-microbe metabolomics. *Wiley Interdiscip Rev. Syst. Biol. Med.* 7, 195–219. doi: 10.1002/wsbm.1301

Holloway, C., Cochlin, L., Emmanuel, Y., Murray, A., Codreanu, I., Edwards, L., et al. (2011). A high-fat diet impairs cardiac high-energy phosphate metabolism and cognitive function in healthy human subjects. *Am. J. Clin. Nutr.* 93, 748–755. doi: 10.3945/ajcn.110.002758

Holtzman, D., Herz, J., and Bu, G. (2012). Apolipoprotein E and apolipoprotein E receptors: normal biology and roles in Alzheimer disease. *Cold Spring Harb. Perspect. Med.* 2:a6312. doi: 10.1101/cshperspect.a006312

Hor, Y. Y., Lew, L. C., Jaafar, M. H., Lau, S. Y., and Liong, M. T. (2019). Lactobacillus sp. Improved microbiota and metabolite profiles of aging rats. *Pharmacol. Res.* 146:104312. doi: 10.1016/j.phrs.2019.104312

Huang, J., Hou, B., Zhang, S., Wang, M., Lu, X., Wang, Q., et al. (2020). The protective effect of Adiponectin-Transfected endothelial progenitor cells on cognitive function in D-Galactose-Induced aging rats. *Neural Plast.* 2020:1273198. doi: 10.1155/2020/1273198

Huang, X., Huang, K., Li, Z., Bai, D., Hao, Y., Wu, Q., et al. (2020). Electroacupuncture improves cognitive deficits and insulin resistance in an OLETF rat model of Al/D-gal induced aging model via the PI3K/Akt signaling pathway. *Brain Res.* 1740:146834. doi: 10.1016/j.brainres.2020.146834

Huang, Y., Zhang, H., Yang, S., Qiao, H., Zhou, W., and Zhang, Y. (2012). Liuwei Dihuang decoction facilitates the induction of long-term potentiation (LTP) in senescence accelerated mouse/prone 8 (SAMP8) hippocampal slices by inhibiting voltage-dependent calcium channels (VDCCs) and promoting N-methyl-d-aspartate receptor (n.d.) receptors. *J. Ethnopharmacol.* 140, 384–390. doi: 10.1016/j.jep.2012.01.030

Hudry, E., Klickstein, J., Cannavo, C., Jackson, R., Muzikansky, A., Gandhi, S., et al. (2019). Opposing Roles of apolipoprotein E in aging and neurodegeneration. *Life Sci. Alliance* 2:e201900325. doi: 10.26508/lsa.201900325

Hui, S., Yang, Y., Peng, W., Sheng, C., Gong, W., Chen, S., et al. (2017). Protective effects of *Bushen Tiansui* decoction on hippocampal synapses in a rat model of Alzheimer's disease. *Neural Regen. Res.* 12, 1680–1686. doi: 10.4103/1673-5374.217347

Khine, W., Voong, M., Ng, T., Feng, L., Rane, G., Kumar, A., et al. (2020). Mental awareness improved mild cognitive impairment and modulated gut microbiome. *Aging* 12, 24371–24393. doi: 10.18632/aging.202277

Komanduri, M., Savage, K., Lea, A., McPhee, G., Nolidin, K., Deleuil, S., et al. (2021). The Relationship between Gut Microbiome and Cognition in Older Australians. *Nutrients* 14:64. doi: 10.3390/nu14010064

Lee, K., Lim, B., Chang, H., Yang, H., Bahn, C., Paik, E., et al. (2005). Liuweidihuang-tang improves spatial memory function and increases neurogenesis in the dentate gyrus in rats. *Fitoterapia* 76, 514–519. doi: 10.1016/j.fitote.2005.04.022

Li, B., He, Y., Ma, J., Huang, P., Du, J., Cao, L., et al. (2019). Mild cognitive impairment has similar alterations as Alzheimer's disease in gut microbiota. *Alzheimers Dement.* 15, 1357–1366. doi: 10.1016/j.jalz.2019.07.002

Li, Y., Luo, Z., Hu, Y., Bi, Y., Yang, J., Zou, W., et al. (2020). The gut microbiota regulates autism-like behavior by mediating vitamin B homeostasis in EphB6-deficient mice. *Microbiome* 8:120. doi: 10.1186/s40168-020-00884-z

Liu, X., Tang, S., Zhong, H., Tong, X., Jie, Z., Ding, Q., et al. (2021b). A genome-wide association study for gut metagenome in Chinese adults illuminates complex diseases. *Cell Discov.* 7:9. doi: 10.1038/s41421-020-00239-w

Liu, C., Cheng, Y., Guo, Y., and Qian, H. (2021a). Magnesium-L-threonate alleviate colonic inflammation and memory impairment in chronic-plus-binge alcohol feeding mice. *Brain Res. Bull.* 174, 184–193. doi: 10.1016/j.brainresbull.2021.06.009

Liu, X., Zhao, Y., Zhu, H., Wu, M., Zheng, Y., Yang, M., et al. (2021c). Taxifolin retards the D-galactose-induced aging process through inhibiting Nrf2-mediated oxidative stress and regulating the gut microbiota in mice. *Food Funct.* 12, 12142–12158. doi: 10.1039/d1fo01349a

Liu, W., He, K., Wu, D., Zhou, L., Li, G., Lin, Z., et al. (2022). Natural dietary compound xanthohumol regulates the gut microbiota and its metabolic profile in a mouse model of Alzheimer's disease. *Molecules* 4:1281. doi: 10.3390/molecules27041281

Lu, Y., Wan, H., Wu, Y., Yang, J., Yu, L., He, Y., et al. (2022). Naoxintong capsule alternates gut microbiota and prevents hyperlipidemia in High-Fat-Diet fed rats. *Front Pharmacol.* 13:843409. doi: 10.3389/fphar.2022.843409

Luo, D., Chen, K., Li, J., Fang, Z., Pang, H., Yin, Y., et al. (2020). Gut microbiota combined with metabolomics reveals the metabolic profile of the normal aging process and the anti-aging effect of FuFang Zhenshu TiaoZhi(FTZ) in mice. *Biomed. Pharmacother.* 121:109550. doi: 10.1016/j.biopha.2019.109550

Makide, K., Kitamura, H., Sato, Y., Okutani, M., and Aoki, J. (2009). Emerging lysophospholipid mediators, lysophosphatidylserine, lysophosphatidylthreonine, lysophosphatidylethanolamine and lysophosphatidylglycerol. *Prostaglandins Other Lipid Mediat.* 89, 135–139. doi: 10.1016/j.prostaglandins.2009.04.009

Manderino, L., Carroll, I., Azcarate-Peril, M., Rochette, A., Heinberg, L., Peat, C., et al. (2017). Preliminary evidence for an association between the composition of the gut microbiome and cognitive function in neurologically healthy older adults. *J. Int. Neuropsych. Soc.* 23, 700–705. doi: 10.1017/S1355617717000492

Mecocci, P., Boccardi, V., Cecchetti, R., Bastiani, P., Scamosci, M., Ruggiero, C., et al. (2018). A long journey into aging, brain aging, and Alzheimer's disease following the oxidative stress tracks. *J. Alzheimers Dis.* 62, 1319–1335. doi: 10.3233/JAD-170732

Morgan, A., Mooney, K., Wilkinson, S., Pickles, N., and Mc Auley, M. (2016). Cholesterol metabolism: a review of how ageing disrupts the biological mechanisms responsible for its regulation. *Ageing Res. Rev.* 27, 108–124. doi: 10.1016/j.arr.2016.03.008

Mulder, M., Blokland, A., van den Berg, D. J., Schulten, H., Bakker, A., Terwel, D., et al. (2001). Apolipoprotein E protects against neuropathology induced by a high-fat diet and maintains the integrity of the blood-brain barrier during aging. *Lab. Invest.* 81, 953–960. doi: 10.1038/labinvest.3780307

Ni, Y., Yang, X., Zheng, L., Wang, Z., and Fu, Z. (2019). Lactobacillus and bifidobacterium improves physiological function and cognitive ability in aged mice by the regulation of gut microbiota. *Mol. Nutr. Food Res.* 63:e1900603. doi: 10.1002/mnfr.201900603

Osadchiy, V., Martin, C., and Mayer, E. (2019). The Gut-Brain axis and the microbiome: mechanisms and clinical implications. *Clin. Gastroenterol. Hepatol.* 17, 322–332. doi: 10.1016/j.cgh.2018.10.002

Partridge, L., Fuentealba, M., and Kennedy, B. (2020). The quest to slow ageing through drug discovery. *Nat. Rev. Drug Discov.* 19, 513–532. doi: 10.1038/s41573-020-0067-7

Qin, J., Li, R., Raes, J., Arumugam, M., Burgdorf, K., Manichanh, C., et al. (2010). A human gut microbial gene catalogue established by metagenomic sequencing. *Nature* 464, 59–65. doi: 10.1038/nature08821

Rai, R., Ghosh, A., Eren, M., Mackie, A., Levine, D., Sy, K., et al. (2017). Downregulation of the apelinergic axis accelerates aging, whereas its systemic

restoration improves the mammalian healthspan. *Cell Rep.* 21, 1471–1480. doi: 10.1016/j.celrep.2017.10.057

Shabbir, U., Arshad, M., Sameen, A., and Oh, D. (2021). Crosstalk between gut and brain in Alzheimer's disease: the role of gut microbiota modulation strategies. *Nutrients* 13:690. doi: 10.3390/nu13020690

Shao, A., Lin, S., Wang, L., Tu, S., Lenahan, C., and Zhang, J. (2020). Oxidative stress at the crossroads of aging, stroke and depression. *Aging Dis.* 11, 1537–1566. doi: 10.14336/AD.2020.0225

Sheng, C., Xu, P., Liu, X., Peng, W., Xiang, D., and Luo, S. (2020). *Bushen-Tiansui* formula improves cognitive functions in an $a\beta_{1-42}$ Fibril-Infused rat model of Alzheimer's disease. *Neural Plast.* 2020:8874885. doi: 10.1155/2020/8874885

Shin, N., Whon, T., and Bae, J. (2015). *Proteobacteria*: microbial signature of dysbiosis in gut microbiota. *Trends Biotechnol.* 33, 496–503. doi: 10.1016/j.tibtech.2015.06.011

Shindou, H., Hishikawa, D., Harayama, T., Eto, M., and Shimizu, T. (2013). Generation of membrane diversity by lysophospholipid acyltransferases. *J. Biochem.* 154, 21–28. doi: 10.1093/jb/mvt048

Solé, B., Jiménez, E., Torrent, C., Reinares, M., Bonnin, C., Torres, I., et al. (2017). Cognitive impairment in bipolar disorder: treatment and prevention strategies. *Int. J. Neuropsychopharmacol.* 20, 670–680. doi: 10.1093/ijnp/pyx032

Tamanai-Shacoori, Z., Smida, I., Bousarghin, L., Loreal, O., Meuric, V., Fong, S., et al. (2017). Roseburia spp.: a marker of health?. *Future Microbiol.* 12, 157–170. doi: 10.2217/fmb-2016-0130

Teixeira, A., Diniz, B., Campos, A., Miranda, A., Rocha, N., Talib, L., et al. (2013). Decreased levels of circulating adiponectin in mild cognitive impairment and Alzheimer's disease. *Neuromol. Med.* 15, 115–121. doi: 10.1007/s12017-012-8201-2

Vatner, S., Zhang, J., Oydanich, M., Berkman, T., Naftalovich, R., and Vatner, D. (2020). Healthful aging mediated by inhibition of oxidative stress. *Ageing Res. Rev.* 64:101194. doi: 10.1016/j.arr.2020.101194

Wan, F., Zhong, R., Wang, M., Zhou, Y., Chen, Y., Yi, B., et al. (2021). Caffeic acid supplement alleviates colonic inflammation and oxidative stress potentially through improved gut microbiota community in mice. *Front. Microbiol.* 12:784211. doi: 10.3389/fmicb.2021.784211

Wang, L., Wang, F., Zhang, X., Chen, Q., Xu, J., Li, H., et al. (2022). Transdermal administration of volatile oil from *Citrus aurantium-Rhizoma atractylodis* macrocephalae alleviates constipation in rats by altering host metabolome and intestinal microbiota composition. *Oxid. Med. Cell. Longev.* 2022:9965334. doi: 10.1155/2022/9965334

Wang, W., Liu, F., Xu, C., Liu, Z., and Hou, J. (2021). *Lactobacillus plantarum* 69-2 combined with galacto-oligosaccharides alleviates d-galactose-induced aging by regulating the AMPK/SIRT1 signaling pathway and gut microbiota in mice. *J. Agric. Food Chem.* 69, 2745–2757. doi: 10.1021/acs.jafc.0c06730

Wang, X., and Quinn, P. (2010). Endotoxins: lipopolysaccharides of gram-negative bacteria. *Subcell Biochem.* 53, 3–25. doi: 10.1007/978-90-481-9078-2_1

Wang, X., and Yang, G. (2021). Bone marrow mesenchymal stem cells-derived exosomes reduce Aβ deposition and improve cognitive function recovery in mice with Alzheimer's disease by activating sphingosine kinase/sphingosine-1-phosphate signaling pathway. *Cell Biol. Int.* 45, 775–784. doi: 10.1002/cbin.11522

Wu, L., Liu, X., Hu, R., Chen, Y., Xiao, M., Liu, B., et al. (2022). Agrocybe cylindraceaPrebiotic crude polysaccharides combined with GG postpone aging-related oxidative stress in mice. *Food Funct.* 13, 1218–1231. doi: 10.1039/d1fo02079j

Yang, X., Yu, D., Xue, L., Li, H., and Du, J. (2020). Probiotics modulate the microbiota-gut-brain axis and improve memory deficits in aged SAMP8 mice. *Acta Pharm Sin. B.* 10, 475–487. doi: 10.1016/j.apsb.2019.07.001

Yin, Y., and Wang, Z. (2018). ApoE and neurodegenerative diseases in aging. *Adv. Exp. Med. Biol.* 1086, 77–92. doi: 10.1007/978-981-13-1117-8_5

Zarrouk, A., Hammouda, S., Ghzaiel, I., Hammami, S., Khamlaoui, W., Ahmed, S., et al. (2020). Association between oxidative stress and altered cholesterol metabolism in Alzheimer's disease patients. *Curr. Alzheimer Res.* 17, 823–834. doi: 10.2174/1567205017666201203123046

Zeki, Ö, Eylem, C., Reçber, T., Kır, S., and Nemutlu, E. (2020). Integration of GC-MS and LC-MS for untargeted metabolomics profiling. *J. Pharm. Biomed. Anal.* 190:113509. doi: 10.1016/j.jpba.2020.113509

Zeng, Z., Chen, C., SiTu, Y., Shen, Z., Chen, Y., Zhang, Z., et al. (2022). Anoectochilus roxburghii flavonoids extract ameliorated the memory decline and reduced neuron apoptosis via modulating SIRT1 signaling pathway in senescent mice. *J. Ethnopharmacol.* 296:115361. doi: 10.1016/j.jep.2022.115361

Zerbi, V., Wiesmann, M., Emmerzaal, T., Jansen, D., Van Beek, M., Mutsaers, M., et al. (2014). Resting-state functional connectivity changes in aging apoE4 and apoE-KO mice. *J Neurosci.* 34, 13963–13975. doi: 10.1523/JNEUROSCI.0684-14.2014

Zhou, Q., Chen, L., Tang, M., Guo, Y., and Li, L. (2018). Apelin/APJ system: a novel promising target for anti-aging intervention. *Clin. Chim. Acta* 487, 233–240. doi: 10.1016/j.cca.2018.10.011

Conflict of Interest: The authors declare that the research was conducted in the absence of any commercial or financial relationships that could be construed as a potential conflict of interest.

Publisher's Note: All claims expressed in this article are solely those of the authors and do not necessarily represent those of their affiliated organizations, or those of the publisher, the editors and the reviewers. Any product that may be evaluated in this article, or claim that may be made by its manufacturer, is not guaranteed or endorsed by the publisher.

frontiers | Frontiers in Neuroscience

TYPE Original Research
PUBLISHED 22 August 2022
DOI 10.3389/fnins.2022.943929

OPEN ACCESS

EDITED BY
Xinfeng Guo,
Guangzhou University of Chinese Medicine, China

REVIEWED BY
Mengxing Wang,
Shanghai University of Medicine and Health Sciences, China
Wu Wang,
Shanghai No. Sixth Peoples Hospital, China
Kun zhao,
Beihang University, China

*CORRESPONDENCE
Songjun Lin
lingsozh@163.com
Jianxiang Chen
chenjianxiang1981@126.com
Xiude Qin
qinxiude@foxmail.com

†These authors have contributed equally to this work and share first authorship

SPECIALTY SECTION
This article was submitted to Translational Neuroscience, a section of the journal Frontiers in Neuroscience

RECEIVED 14 May 2022
ACCEPTED 27 July 2022
PUBLISHED 22 August 2022

CITATION
Wang J, Kong F, Zheng H, Cai D, Liu L, Lian J, Lyu H, Lin S, Chen J and Qin X (2022) Lateralized brain activities in subcortical vascular mild cognitive impairment with differential Chinese medicine patterns: A resting-state functional magnetic resonance imaging study.
Front. Neurosci. 16:943929.
doi: 10.3389/fnins.2022.943929

Lateralized brain activities in subcortical vascular mild cognitive impairment with differential Chinese medicine patterns: A resting-state functional magnetic resonance imaging study

Jianjun Wang[1,2,3†], Fanxin Kong[1,2†], Haotao Zheng[1,2], Dongbin Cai[1,2], Lijin Liu[1,2], Jie Lian[1,2], Hanqing Lyu[2,4], Songjun Lin[1,2*], Jianxiang Chen[2,4*] and Xiude Qin[1,2*]

[1]Department of Neurology and Psychology, Shenzhen Traditional Chinese Medicine Hospital, Shenzhen, China, [2]The Fourth Clinical Medical College, Guangzhou University of Chinese Medicine, Shenzhen, China, [3]Harvard Medical School, Global Clinical Scholars Research Training (GCSRT), Boston, MA, United States, [4]Department of Radiology, Shenzhen Traditional Chinese Medicine Hospital, Shenzhen, China

Background: Subcortical vascular mild cognitive impairment (svMCI) is one of the most treatable cognitive impairments, but could be hampered by the high clinical heterogeneities. Further classification by Chinese Medicine (CM) patterns has been proved to stratify its clinical heterogeneities. It remains largely unknown of the spontaneous brain activities regarding deficiency patterns (DPs) and excess patterns (EPs) of svMCI patients based on fMRI data.

Objective: We aim to provide neuroimaging evidence of altered resting-state brain activities associated with DPs and EPs in svMCI patients.

Methods: Thirty-seven svMCI patients (PAs) and 23 healthy controls (CNs) were consecutively enrolled. All patients were categorized into either the EP group (n = 16) and the DP group (n = 21) based on a quantitative CM scale. The fractional amplitude of low-frequency fluctuation (fALFF) value was used to make comparisons between different subgroups.

Results: The DP group showed significant differences of fALFF values in the right middle frontal gyrus and the right cerebellum, while the EP group showed significant differences in the left orbitofrontal gyrus and the left cerebellum, when compared with the CN group. When compared with the EP group, the DP group had markedly increased fALFF values in the left superior temporal gyrus, right middle temporal gyrus and brainstem. The decreased

fALFF values was shown in the right anterior cingulate and paracingulate gyri. Among the extensive areas of frontotemporal lobe, the Montreal Cognitive Assessment (MoCA) scores were significantly correlated with the reduced fALFF value of the right middle frontal gyrus and the left orbitofrontal gyrus.

Conclusion: Our results indicated that the DPs and EPs presented the lateralization pattern in the bilateral frontal gyrus, which will probably benefit the future investigation of the pathogenesis of svMCI patients.

KEYWORDS

subcortical vascular mild cognitive impairment, fALFF, fMRI, Chinese medicine, syndrome differentiation, deficiency pattern, excess pattern, lateralization

Introduction

Subcortical vascular mild cognitive impairment (svMCI) refers to mild cognitive disorder with underlying subcortical lacunar stroke or white matter hyperintensities (WMHs) (T O'Brien et al., 2003). It is one of the most treatable dementia (Rockwood et al., 2000), and has been proposed as a relatively homogeneous subtype of all causes of vascular dementia. However, clinical presentations often differ greatly because of variations in differential subsets of conventional vascular neuroimaging structure (e.g., lacunar and CMBs with differential location, size, and volume, etc.). The resting-state functional magnetic resonance imaging (rs-fMRI) is an emerging and non-invasive technique to detect the brain intrinsic functional architecture and meanwhile overcome the unbalanced distribution of conventional vascular lesions (Vinciguerra et al., 2020; Wang R. et al., 2020). Inspired by the milestone fMRI study to establish subtypes for heterogeneous disease (Drysdale et al., 2017), there is much interest in using rs-fMRI to explore the association of phenotypes and neurobiological subtypes in svMCI.

Interestingly, it is the essence of Chinese medicine (CM) and prerequisite of CM treatment to classify the same biological disease into different etiopathological patterns/subtypes (Tang et al., 2008; Lu et al., 2012). A total of 196 CM patterns have been included in the latest International Classification of Diseases 11th version (ICD-11) coding system (WHO, 2019). Among them, deficiency pattern (DP) and excess pattern (EP), consisting of two contrary and complementary clinical manifestations, have been utilized as two basic patterns/subtypes to ensure reasonable treatment of diseases (Tang et al., 2008). This strategy is especially effective for complicated diseases and has been used in China, Japan, Korea, and elsewhere worldwide (Lam et al., 2019). In a multicenter cohort study of vascular cognitive impairment, DPs exhibited significantly lower naming factor scores relative to EPs (Zheng et al., 2022a), sharpening specific clinical characteristics and treatment targets. The underlying neural mechanisms regarding DPs and EPs in svMCI patients remain to be further elucidated.

It is increasingly accepted that fMRI could help to understand the neural basis behind different CM patterns of disease. Taking major depression for example, the EP subtype is often comorbid with nervousness and irritability, whereas the DP subtype is characterized by excessive pensiveness, suspicion, and timorousness. The functional connectivity of the insular (Liu et al., 2019) and posterior cingulate cortex (Zhang et al., 2015) was found to explain the neural basis of the above clinical alterations, and indicated the sad-face processing variation between DPs and EPs of major depression (Wang et al., 2019). There were also fMRI studies demonstrating the altered resting-state brain activities with different CM patterns in depression with anxiety (Xu et al., 2018; Du et al., 2020) and psychogenic erectile dysfunction (Liu et al., 2015). These studies indicate the methodological possibilities for researching altered cerebral activities based on DPs and EPs in svMCI patients. Further, as an advancing approach to detect spontaneous brain activity with much higher sensitivity and specificity (Zou et al., 2008), the fractional amplitude of low-frequency fluctuations (fALFF) value provides a promising avenue for exploring cerebral alterations that are associated with symptomatic variations between DPs and EPs in svMCI patients.

Taking together, the current study aimed to provide physiological evidence, using functional magnetic resonance imaging (fMRI), to identify altered resting-state brain activity associated with DP and EP patterns in svMCI patients. We

Abbreviations: svMCI, subcortical vascular mild cognitive impairment; fMRI, functional magnetic resonance imaging; DP, deficiency pattern; EP, excess pattern; PA, patient; CN, control; fALFF, fractional amplitude of low-frequency fluctuation; WMHs, white matter hyperintensities; rs-fMRI, resting-state functional magnetic resonance imaging; CM, Chinese medicine; SDSVD, syndrome differentiation score of vascular dementia; MoCA, Montreal Cognitive Assessment; TR, repetition time; TE, echo time; FA, flip angle; FOV, field of view; MNI, Montreal Neurological Institute; FWHM, full-width at half maximum; GS, global signals; WM, white matter; CSF, cerebrospinal fluid; FD, frame-wise displacement.

hypothesize that fALFF values in the DP and EP subgroups of svMCI patients (PAs) were significantly altered compared with healthy controls (CNs). To test this hypothesis, we examined fALFF value differences between (1) PAs and CNs, (2) DPs and CNs, EPs vs. CNs, and DPs vs. EPs.

Material and methods

Participants

We consecutively recruited a total of 60 right-handed participants (Han Chinese) from February 2017 to January 2019. They consisted of 37 svMCI patients and 23 demographically matched healthy controls. All svMCI patients were enrolled from a previous randomized control study (Zheng et al., 2022b), whereas healthy participants were enrolled from community residents by advertisements. Complete recruitment details were described in our prior work (Lyu et al., 2019; Wang J. et al., 2020; Xu J. et al., 2020; Xu Z. et al., 2020). Briefly, the diagnosis criteria of svMCI were performed according to Petersen's criteria (Petersen, 2004). T2 FLAIR images showed WMHs with a Fazekas rating scale score ≥ 2, or multiple (> 3) supratentorial subcortical small infarcts (< 20 mm), or one/more subcortical small infarcts in the caudate nucleus, Globus pallidus, or thalamus (Jia et al., 2016). We excluded patients presenting secondary causes of cognitive deficits according to previously described criteria (Román et al., 2002; Moorhouse and Rockwood, 2008; Jia et al., 2016). Healthy controls had no history of any neurological or psychiatric disorders, no cognitive complaints, and no abnormalities on their conventional brain MRI images. All subjects provided written informed consent to participate in the study. All aspects of this study were approved by the Institutional Review Board of Shenzhen Traditional CM Hospital.

Clinical measures

All subjects underwent a clinical evaluation that assessed their demographic characteristics (age, sex, and level of education), various vascular risk factors (smoking, alcohol, hypertension, diabetes mellitus, and body mass index), as well as brain MRI scanning. All participants underwent a standardized neurological examination and assessment of the Beijing version of the Montreal Cognitive Assessment (MoCA). The scale for the differentiation of syndromes of vascular dementia (SDSVD) = was developed in 2002 (Tian et al., 2002) to power the standardized evaluation of CM syndrome in trials of vascular cognitive impairment (Shi et al., 2014). It was included in the present study to quantitatively assess all patients and divided them into four subtypes, namely kidney essence deficiency (KED), qi and blood deficiency (QBD), phlegm obstruction of orifices (POO), and stasis blocking channels (SBC). KED and QBD are representative of DPs, and POO and SBC are representative of EPs. Each subtype is assigned a score from 0 to 30, with a sum score of at least 7 indicating confirmation of the subtype. If the patients meet more than 2 subtypes, the subtype with the highest score is labeled as the dominant CM pattern, by which the DPs or EPs will be determined (Tian et al., 2002).

Functional magnetic resonance imaging data acquisition

MRI images were acquired using a GE Discovery MR750 3.0T MRI scanner (General Electric Medical Systems, Milwaukee, WI, United States) at the Shenzhen Hospital of Traditional CM. For all subjects, high-resolution structural images were acquired with a three-dimensional MRI sequence using an axial fast spoiled gradient recalled sequence with the following parameters: repetition time (TR) = 8.62 ms, echo time (TE) = 3.224 ms, flip angle (FA) = 12°, data matrix = 512 × 512, field of view (FOV) = 256 × 256 mm^2, and continuous sagittal slices = 152 with 1 mm thickness. Functional images were acquired with an echo-planar imaging (EPI) sequence with the following parameters: TR = 2,000 ms, TE = 35 ms, FA = 90°, data matrix = 64 × 64, resolution = 3.75 × 3.75 mm^2, slices thickness = 4 mm with no inter-slice gap, and volumes = 240 with 38 axial slices. All subjects were required to lie flat, close their eyes, and relax while remaining awake during the scanning process. After the data scanning, all subjects verified that they remained awake during the scan, and the neuroimaging quality was checked.

Functional magnetic resonance imaging data processing

Data preprocessing was performed using statistical parametric mapping (SPM8)[1] (Friston et al., 1994) and DPABI[2] (Yan et al., 2016), following standardized principles and quality control procedures (Polli et al., 2016; Takeuchi et al., 2017; Chen et al., 2018). First, the first 10 volumes in the time series were discarded to avoid non-equilibrium effects in the MR signal. Then the functional images were slice-timing corrected, which was performed by interpolating the voxel time using slice interpolation. Next, all functional images were spatially realigned and co-registered to their corresponding anatomical images. Then, the resulting images were spatially

1 https://www.fil.ion.ucl.ac.uk/spm/

2 http://www.rfmri.org/dpabi

normalized to Montreal Neurological Institute (MNI) space, resampled to 3 mm × 3 mm × 3 mm voxels and further spatially smoothed using a Gaussian kernel with 6 mm full-width at half maximum (FWHM) (Tahmasebi et al., 2009). Finally, potential sources of 24 head motion parameters, global signals (GSs), white matter (WM) signals and cerebrospinal fluid (CSF) signals were regressed out to remove their effects (Murphy et al., 2009). Particularly, given a possible confounding effect of micromovements (Dijk et al., 2012), the framewise displacement (FD) values, which reflected the temporal derivative of the movement parameters (Power et al., 2012; Yang et al., 2014), were calculated for each subject. One subject with svMCI and two healthy subjects who had a mean FD = 0.5 mm or translation > 2 mm or rotation > 2 degrees were excluded. In total, data from the remaining 37 patients with svMCI and 23 healthy controls were used for further analysis.

Fractional amplitude of low-frequency fluctuation analysis

After preprocessing, the linear trend was removed and fALFF analysis was carried out using DPABI software (Yan et al., 2016). The analysis procedure for fALFF was carried out according to the method of previous studies (Zou et al., 2008; Liu et al., 2017). fALFF values were computed in a voxel-wise manner using volumetric fMRI data. The BOLD time series of all brain voxels were converted to the frequency domain *via* the fast Fourier transform (FFT; MATLAB), and normalized power spectrums were subsequently obtained. The fALFF index was computed in a voxel-wise manner as the sum of power in the 0.01–0.1 Hz frequency band divided by the sum of power of the entire frequency range (0.01–0.25 Hz). Finally, the subject-level voxel-wise fALFF maps were standardized into subject-level Z-score maps by subtracting the mean voxel-wise fALFF obtained for the whole brain and dividing by the standard deviation.

Statistics analysis

Participants' baseline characteristics, including demographic information (i.e., age, sex, and body mass index) and clinical scores (i.e., SDSVD and MoCA) were compared between groups. Two-tailed two-sample *t*-tests were performed to examine the significant group-level differences between the PA group and CN group, DP/EP group and CN group, as well as differences between the DP group and EP group. The statistical significance level was set at $p < 0.05$. All statistical tests were performed in IBM SPSS Statistics 21.0 software.

To investigate the effect of differences in fALFF values at the group level, a two-tailed two-sample *t*-test was performed on the individual fALFF maps between different groups (PAs vs. CNs, DPs vs. CNs, EPs vs. CNs and DPs vs. EPs). In particular, age, sex and education level were considered variables of no interest and were regressed out to remove their effects. The threshold of significance was set at a $p = 0.05$ combined with correction for multiple comparisons using the AlphaSim method (a minimum cluster threshold of 178 voxels of 3-mm cubic in MNI space).

Moreover, to identify the relationship of the fALFF values in regions with significant group-level differences and clinical characteristics, the mean fALFF values were calculated first. Then, Pearson's correlation analysis was performed between the mean fALFF values and the cognitive performance of the patients (MoCA).

Results

Demographic and clinical characteristics of subjects

A total of 37 svMCI patients and 23 healthy controls were included for analysis in the present study. Thirty-seven svMCI patients in the PA group were further divided into the EP group ($n = 16$) and DP group ($n = 21$). Demographic and clinical data for all subjects are shown in **Table 1**. MoCA scores were significantly lower in the PA group, DP group and EP group than that in the CN group. The ratio of hypertension in both the DP and EP groups, as well as the education level and age in the DP group, were significantly different from those in the CN group.

Group comparisons

The results obtained from the two-sample *t*-test clearly demonstrated that there were significant differences between different groups when comparing each patient group to the CN group. The PA group exhibited significantly reduced fALFF values in the left superior and medial frontal gyrus, and significantly increased fALFF values in the right cerebellum (**Supplementary Table 1** and **Figure 1A**). However, when the PA group was divided into the DP and EP groups, the DP group exhibited significantly reduced fALFF values in the right middle frontal gyrus, and significantly increased fALFF values in the right cerebellum (**Supplementary Table 1** and **Figure 1B**). In contrast, the EP group exhibited significantly reduced fALFF values in the left orbitofrontal gyrus, and increased fALFF values in the left cerebellum (**Supplementary Table 1** and **Figure 1C**). Further, when the DP group was compared to the EP group, we found significantly increased fALFF values in the left superior temporal gyrus, right middle temporal gyrus, and brainstem, and significantly decreased fALFF values in the right anterior cingulate and paracingulate gyri (**Supplementary Table 1** and **Supplementary Figure 1**).

TABLE 1 Demographic and clinical characteristics in the PA group, DP group, EP group and CN group.

Groups	PA ($N = 37$)	DP ($N = 21$)	EP ($N = 16$)	CN ($N = 23$)	*p*-value			
					PA vs. CN	DP vs. CN	EP vs. CN	DP vs. EP
Gender (male/female)[a]	19/18	9/12	10/6	9/14	0.36	0.80	0.15	0.24
Age (years, mean ± SD)[b]	63.86 ± 6.91	65.67 ± 6.38	61.50 ± 7.05	61.91 ± 4.86	0.24	0.03*	0.83	0.07
Education (years, mean ± *SD*)[b]	8.27 ± 3.73	7.33 ± 3.09	9.50 ± 4.23	9.83 ± 3.55	0.12	0.02*	0.80	0.08
BMI (mean ± *SD*)[b]	23.63 ± 2.73	23.47 ± 2.61	23.84 ± 2.96	23.17 ± 2.36	0.51	0.69	0.44	0.69
Smoking (yes/no)[a]	15/22	9/12	6/10	4/19	0.06	0.06	0.26[Δ]	0.74
Alcohol (yes/no)[a]	9/28	5/16	4/12	4/19	0.75[Δ]	0.72[Δ]	0.69[Δ]	0.93[Δ]
Hypertension (yes/no)[a]	26/11	14/7	12/4	5/18	<0.001*	0.003*	0.001*	0.58[Δ]
Diabetes mellitus (yes/no)[a]	13/24	5/16	8/8	4/19	0.14	0.72[Δ]	0.04[Δ]	0.10
Hyperlipidemia (yes/no)[a]	10/27	5/16	5/11	3/20	0.33[Δ]	0.45[Δ]	0.24[Δ]	0.61
MoCA (mean ± *SD*)[b]	19.49 ± 2.06	18.95 ± 1.91	20.19 ± 2.10	28.83 ± 1.11	<0.001*	<0.001*	< 0.001*	0.07

[a]Binary variables were analyzed using the chi-square test.
[b]Quantitative parameters were analyzed using a two-sample t-test.
*Represents a significant difference between the two groups.
[Δ] Fisher's exact test.
PA, patient; DP, deficiency pattern; EP, excess pattern; CN, control; BMI, body mass index; MoCA, Montreal cognitive assessment.

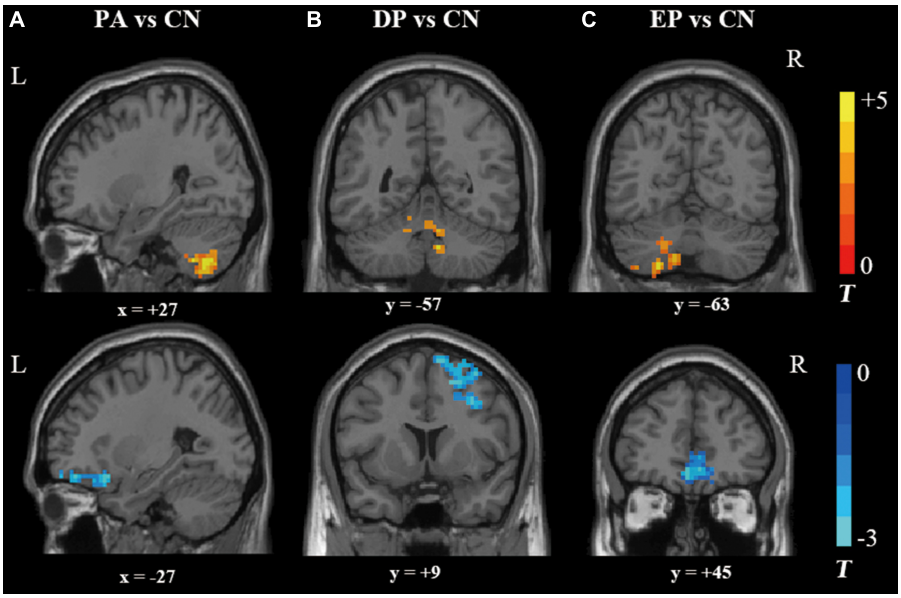

FIGURE 1
Brain regions that showed significant alterations in fALFF values. **(A)** the PA group vs. the CN group, **(B)** the DP group vs. the CN group; and **(C)** the EP group vs. the CN group. fALFF, fractional amplitude of low-frequency fluctuation; PA, patient; DP, deficiency pattern; EP, excess pattern; CN, control; R, right; L, left.

Correlation analysis

The MoCA scores were positively correlated with the fALFF value of the right frontal middle gyrus ($r = 0.544$, $p < 0.001$) (Figure 2A) and the left orbitofrontal gyrus ($r = 0.649$, $p < 0.001$) (Figure 2B). Non-significant correlations were observed between the MoCA scores and the fALFF value of any interested gyrus in the comparison of DP and EP. The whole correlation analysis results can be found in Supplementary Table 2.

Discussion

In the present study, we measured fALFF value alterations before and after svMCI patients were categorized into DP and EP subgroups. We found altered resting-state brain activities in cerebellum, brainstem and widespread frontotemporal area extending to the right middle frontal gyrus, right anterior cingulate gyrus, right middle temporal gyrus, left superior temporal gyrus, and right anterior cingulate and paracingulate. The lateralized activation of the right middle frontal gyrus and

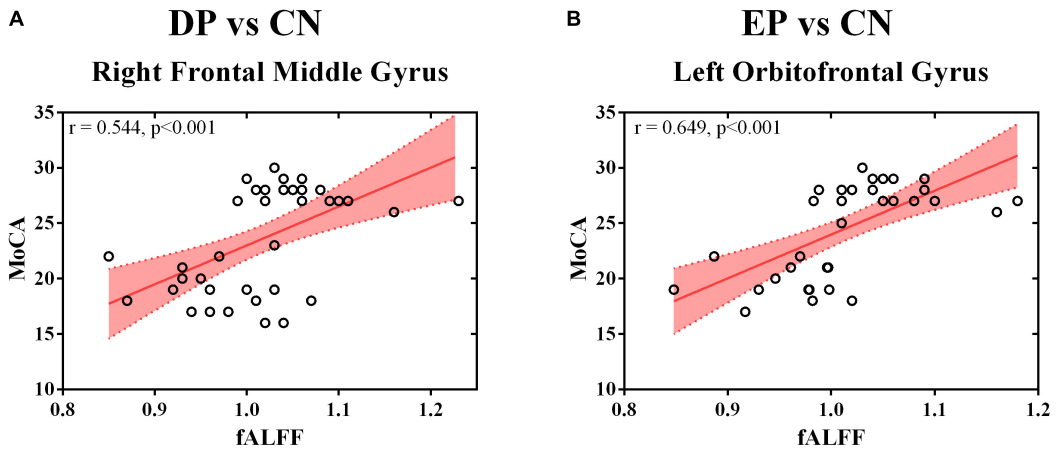

FIGURE 2
Correlation analysis. **(A)** The fALFF value of the right frontal middle gyrus and the MoCA score; **(B)** The fALFF value of the left orbitofrontal gyrus and the MoCA score. fALFF, fractional amplitude of low-frequency fluctuation; DP, deficiency pattern; EP, excess pattern; CN, control; MoCA, the Montreal Cognitive Assessment.

the left orbitofrontal gyrus were found steady and significantly correlated with the MoCA scores. Our findings provide the initial evidence of lateralized brain activation of two contrary CM patterns of DPs and EPs in svMCI patients. These finding might extend our present understanding and allow better stratification of heterogeneous svMCI patients.

We repeatedly found that svMCI patients showed lower prefrontal fALFF values and higher cerebellar fALFF values both before and after the classification of CM patterns. The frontal lobe is one of the most important brain regions subserving cognitive regulation (MacDonald et al., 2000; Arnsten et al., 2021). Dysregulation of the dorsolateral prefrontal cortex leads to clinical cognitive decline and provides the most commonly used targets for non-invasive brain stimulation (Birba et al., 2017). The increased fALFF values were associated with significant improvement of cognitive function after treatment (Qin et al., 2022). According to the "disconnection hypothesis" (Galluzzi et al., 2008), disruption by WMHs or lacunar infarcts of the prefrontal-frontal circuits implicated in the cortical loops and interhemispheric connectivity may primarily result in cognition decline (Puglisi et al., 2018; Vinciguerra et al., 2019; Cantone et al., 2020). Thus, it was not surprising that we found altered frontal fALFF values in svMCI patients due to vascular lesions leading to disrupted plasticity (Yi et al., 2012). Further, we found the increased activities of cerebellar significantly correlated with cognition performance, which could be supported by the recent paradigm shift of cerebellar neuroscience involved in cognition regulation (Schmahmann et al., 2019; Lin et al., 2022). Our study supported the robust biological findings in svMCI patients even in different CM patterns.

It is interesting that we observed opposite sides of brain activation corresponding to DPs and EPs in svMCI patients. Especially, the fALFF value of bilateral clusters of interest was significantly correlated with the disease severity. It is known that EPs and DPs have been clinically utilized for subtype identification and treatment decision making for thousands of years (Jiang et al., 2012; Lee et al., 2015). Functional MRI-derived brain activity has been introduced to explore this mystery based on the development of cognitive neuroscience (Liu et al., 2015; Xu et al., 2018). Consistent with the lateralized pattern in our study, the main differences in posterior cingulate cortex (PCC) functional connectivity between EPs and DPs occurred in the left PCC in depressive patients (Zhang et al., 2015). Meanwhile, we found that the differences in EPs vs. CNs and DPs vs. CNs were totally different from the findings in DPs vs. EPs. This tendency was replicated in functional connectivity analysis in major depression (Zhang et al., 2015), which arises further interests in exploring neural mechanisms behind different CM patterns. Currently, the cell type-specific signature genes were found to significantly correlate with cerebral cortical differences (Li et al., 2021), which provided a novel approach to interpret our findings based on the gene enrichment of the difference map of EPs and DPs. Notably, whenever compared with CNs or EPs, DPs showed decreased resting-state brain activity in the right middle frontal gyrus and anterior cingulate gyrus. These regions are critical for intrinsic connectivity networks that mediated cognitive processing (Zhao et al., 2019). Especially, the reduced activity of the right middle frontal gyrus contributed to the worse cognitive performance. This was of great practical significance because the classical CM theory holds the view that the DP patients always exhibit a long-lasting course of disease with concomitant cognitive impairment (Lin et al., 2020; Wang B. Q. et al., 2020). Interestingly, Ning et al. (2018) demonstrated that the DP individuals had memory and attention impairments by nature even in healthy subjects,

to which the abnormal functional connectivity of the executive control network was attributed. Thus, our study provided neuroimaging response for DPs in svMCI patients and extended our insights into CM patterns with cerebral plasticity.

There are several limitations of this study. First, as participants were recruited from a previous randomized control study (Zheng et al., 2022b) and composed of only partial CM patterns defined by SDSVD, the altered neural activities behind all DPs and EPs should be explained with caution considering the selection bias. Second, the relatively small sample size and potential confounders (e.g., unclear medication consumption) might have compromised the statistical power and the external validity of the analysis. Third, all patients had numerous neuroimaging lesions with small subcortical infarcts and/or randomly distributed WMHs. We cannot exclude the potential effects of these lesions, since it was difficult to assess the randomly distributed location and relatively small volume of all the lesions.

Conclusion

The "DP and EP" theory has long time been utilized for patient treatment in the field of CM. The present study showed a lateralized neural activation paradigm in the bilateral frontal gyrus that may distinguish DPs from EPs in svMCI patients. The right middle frontal gyrus might serve as a brain response to endogenic cognitive impairments of DPs in svMCI patients. Understanding the neural mechanism underlying differential CM patterns will probably benefit the future investigation of the pathogenesis of svMCI, which might improve treatment approaches.

Data availability statement

The datasets generated for this study are available on request to the corresponding authors.

Ethics statement

The studies involving human participants were reviewed and approved by the Ethics Committee of Shenzhen Traditional Chinese Medicine Hospital. The patients/participants provided their written informed consent to participate in this study.

Author contributions

JW, SL, HZ, LL, HL, FK, JC, and XQ: conceptualization and writing—review and editing. JC, JL, and LL: data curation. HZ, DC, and LL: formal analysis. JW, FK, and XQ: funding acquisition. HZ, LL, DC, JL, HL, and FK: investigation. JC, JW, SL, and XQ: methodology. JC, SL, and XQ: supervision. JW and HL: visualization. JW and JC: writing—original draft. All authors contributed to the article and approved the submitted version.

Funding

This work was supported by National Natural Science Foundation of China (Grant no. 82004284), the Guangdong Medical Science Foundation (Grant Nos. A2020370 and A2021199), the Guangdong Administration of Traditional Chinese Medicine Project (Grant Nos. 20211328 and 20221357), the Shenzhen Science and Technology Program (Grant No. RCBS20200714114959156), the Shenzhen Municipal Health and Family Planning System Scientific Research Project (Grant No. SZFZ2018013), and the Sanming Project of Medicine in Shenzhen (SZZYSM202111011).

Acknowledgments

We thank all the volunteers and patients for their participation in our study.

Conflict of interest

The authors declare that the research was conducted in the absence of any commercial or financial relationships that could be construed as a potential conflict of interest.

Publisher's note

Supplementary material

The Supplementary Material for this article can be found online at: https://www.frontiersin.org/articles/10.3389/fnins.2022.943929/full#supplementary-material

References

Arnsten, A. F., Datta, D., and Wang, M. (2021). The genie in the bottle-magnified calcium signaling in dorsolateral prefrontal cortex. *Mol. Psychiatry* 26, 3684–3700. doi: 10.1038/s41380-020-00973-3

Birba, A., Ibáñez, A., Sedeño, L., Ferrari, J., García, A. M., and Zimerman, M. (2017). Non-invasive brain stimulation: A new strategy in mild cognitive impairment? *Front. Aging Neurosci.* 9:16. doi: 10.3389/fnagi.2017.00016

Cantone, M., Lanza, G., Fisicaro, F., Pennisi, M., Bella, R., Di Lazzaro, V., et al. (2020). Evaluation and treatment of vascular cognitive impairment by transcranial magnetic stimulation. *Neural Plast.* 2020:8820881. doi: 10.1155/2020/8820881

Chen, X., Lu, B., and Yan, C. (2018). Reproducibility of R-fMRI metrics on the impact of different strategies for multiple comparison correction and sample sizes. *Hum. Brain Mapp.* 39, 300–318. doi: 10.1002/hbm.23843

Dijk, V., Ra, K., Sabuncu, M. R., and Buckner, R. L. (2012). The influence of head motion on intrinsic functional connectivity MRI. *Neuroimage* 59, 431–438. doi: 10.1016/j.neuroimage.2011.07.044

Drysdale, A. T., Grosenick, L., Downar, J., Dunlop, K., Mansouri, F., Meng, Y., et al. (2017). Resting-state connectivity biomarkers define neurophysiological subtypes of depression. *Nat. Med.* 23, 28–38. doi: 10.1038/nm.4246

Du, Y., Zhao, J., Wang, Y., Han, Y., Deng, L., Jia, H., et al. (2020). Brain functional differences in drug-naive major depression with anxiety patients of different traditional chinese medicine syndrome patterns: A resting-state fMRI study. *Evid. Based Complement. Alternat. Med.* 2020:7504917. doi: 10.1155/2020/7504917

Friston, K., Holmes, A. P., Worsley, K. J., Poline, J.-B., Frith, C., and Frackowiak, R. (1994). Statistical parametric maps in functional imaging: A general linear approach. *Hum. Brain Mapp.* 2, 189–210. doi: 10.1002/hbm.460020402

Galluzzi, S., Beltramello, A., Filippi, M., and Frisoni, G. B. (2008). Aging. *Neurol. Sci.* 29, 296–300. doi: 10.1007/s10072-008-1002-6

Jia, J., Wei, C., Liang, J., Zhou, A., Zuo, X., Song, H., et al. (2016). The effects of DL-3-n-butylphthalide in patients with vascular cognitive impairment without dementia caused by subcortical ischemic small vessel disease: A multicentre, randomized, double-blind, placebo-controlled trial. *Alzheimers Dement.* 12, 89–99. doi: 10.1016/j.jalz.2015.04.010

Jiang, M., Zhang, C., Zheng, G., Guo, H., Li, L., Yang, J., et al. (2012). Traditional Chinese medicine Zheng in the era of evidence-based medicine: A literature analysis. *Evid. Based Complement. Alternat. Med.* 2012:409568. doi: 10.1155/2012/409568

Lam, W. C., Lyu, A., and Bian, Z. (2019). ICD-11: Impact on traditional Chinese medicine and world healthcare systems. *Pharm. Med.* 33, 373–377. doi: 10.1007/s40290-019-00295-y

Lee, J. C., Lee, S., and Jin, H. J. (2015). Development of decision-making rules for pattern identification. *Eur. J. Integr. Med.* 7, 348–353. doi: 10.1016/j.eujim.2015.07.042

Li, J., Seidlitz, J., Suckling, J., Fan, F., Ji, G.-J., Meng, Y., et al. (2021). Cortical structural differences in major depressive disorder correlate with cell type-specific transcriptional signatures. *Nat. Commun.* 12:1647. doi: 10.1038/s41467-021-21943-5

Lin, J., Chen, Y., Xie, J., and Mo, L. (2022). Altered brain connectivity patterns of individual differences in insightful problem solving. *Front. Behav. Neurosci.* 16:905806. doi: 10.3389/fnbeh.2022.905806

Lin, Z. Y., Huang, T. W., Huang, J. S., and Zheng, G. Y. (2020). Tiaobu xinshen recipe (调补心肾方) improved mild cognitive impairment of Alzheimer's disease patients with xin (heart) and shen (kidney) deficiency. *Chin. J. Integr. Med.* 26, 54–58. doi: 10.1007/s11655-019-3073-z

Liu, L. Y., Xu, X. P., Luo, L. Y., Zhu, C. Q., Li, Y. P., Wang, P. R., et al. (2019). Brain connectomic associations with traditional Chinese medicine diagnostic classification of major depressive disorder: A diffusion tensor imaging study. *Chin. Med.* 14:15. doi: 10.1186/s13020-019-0239-8

Liu, Q., Zhang, P., Pan, J., Li, Z., Liu, J., Li, G., et al. (2015). Cerebral activity changes in different traditional Chinese medicine patterns of psychogenic erectile dysfunction patients. *Evid. Based Complement. Alternat. Med.* 2015:503536. doi: 10.1155/2015/503536

Liu, X., Lauer, K. K., Ward, B. D., Roberts, C., Liu, S., Gollapudy, S., et al. (2017). Propofol attenuates low-frequency fluctuations of resting-state fMRI BOLD signal in the anterior frontal cortex upon loss of consciousness. *Neuroimage* 147, 295–301. doi: 10.1016/j.neuroimage.2016.12.043

Lu, A., Jiang, M., Zhang, C., and Chan, K. (2012). An integrative approach of linking traditional Chinese medicine pattern classification and biomedicine diagnosis. *J. Ethnopharmacol.* 141, 549–556. doi: 10.1016/j.jep.2011.08.045

Lyu, H., Wang, J., Xu, J., Zheng, H., Yang, X., Lin, S., et al. (2019). Structural and functional disruptions in subcortical vascular mild cognitive impairment with and without depressive symptoms. *Front. Aging Neurosci.* 11:241. doi: 10.3389/fnagi.2019.00241

MacDonald, A. W., Cohen, J. D., Stenger, V. A., and Carter, C. S. (2000). Dissociating the role of the dorsolateral prefrontal and anterior cingulate cortex in cognitive control. *Science* 288, 1835–1838.

Moorhouse, P., and Rockwood, K. (2008). Vascular cognitive impairment: Current concepts and clinical developments. *Lancet Neurol.* 7, 246–255. doi: 10.1016/S1474-4422(08)70040-1

Murphy, K., Birn, R. M., Handwerker, D. A., Jones, T. B., and Bandettini, P. A. (2009). The impact of global signal regression on resting state correlations: Are anti-correlated networks introduced? *Neuroimage* 44, 893–905. doi: 10.1016/j.neuroimage.2008.09.036

Ning, Y., Yin, D., Jia, W., Zhu, H., Xue, S., Liu, J., et al. (2018). Cognitive impairment in patients with kidney deficiency syndrome: A resting-state fMRI study. *Eur. J. Integr. Med.* 24, 49–53. doi: 10.1016/j.eujim.2018.10.018

Petersen, R. C. (2004). Mild cognitive impairment as a diagnostic entity. *J. Intern. Med.* 256, 183–194. doi: 10.1111/j.1365-2796.2004.01388.x

Polli, A., Weis, L., Biundo, R., Thacker, M., Turolla, A., Koutsikos, K., et al. (2016). Anatomical and functional correlates of persistent pain in Parkinson's disease. *Mov. Disord.* 31, 1854–1864. doi: 10.1002/mds.26826

Power, J. D., Barnes, K. A., Snyder, A. Z., Schlaggar, B. L., and Petersen, S. E. (2012). Spurious but systematic correlations in functional connectivity MRI networks arise from subject motion. *Neuroimage* 59, 2142–2154. doi: 10.1016/j.neuroimage.2011.10.018

Puglisi, V., Bramanti, A., Lanza, G., Cantone, M., Vinciguerra, L., Pennisi, M., et al. (2018). Impaired cerebral haemodynamics in vascular depression: Insights from transcranial doppler ultrasonography. *Front. Psychiatry* 9:316. doi: 10.3389/fpsyt.2018.00316

Qin, Y., Zhang, F., Zhang, M., and Zhu, W. (2022). Effects of repetitive transcranial magnetic stimulation combined with cognitive training on resting-state brain activity in Alzheimer's disease. *Neuroradiol. J.* 12:19714009211067409. doi: 10.1177/19714009211067409

Rockwood, K., Wentzel, C., Hachinski, V., Hogan, D., MacKnight, C., and McDowell, I. (2000). Prevalence and outcomes of vascular cognitive impairment. *Neurology* 54, 447–451. doi: 10.1212/WNL.54.2.447

Román, G. C., Erkinjuntti, T., Wallin, A., Pantoni, L., and Chui, H. C. (2002). Subcortical ischaemic vascular dementia. *Lancet Neurol.* 1, 426–436. doi: 10.1016/s1474-4422(02)00190-4

Schmahmann, J. D., Guell, X., Stoodley, C. J., and Halko, M. A. (2019). The theory and neuroscience of cerebellar cognition. *Annu. Rev. Neurosci.* 42, 337–364. doi: 10.1146/annurev-neuro-070918-050258

Shi, G., Liu, C., Guan, W., Wang, Z., Wang, L., Xiao, C., et al. (2014). Effects of acupuncture on Chinese medicine syndromes of vascular dementia. *Chin. J. Integr. Med.* 20, 661–666. doi: 10.1007/s11655-013-1323-4

T O'Brien, J., Erkinjuntti, T., Reisberg, B., Roman, G., Sawada, T., Pantoni, L., et al. (2003). Vascular cognitive impairment. *Lancet Neurol.* 2, 89–98. doi: 10.1016/S1474-4422(03)00305-3

Tahmasebi, A. M., Abolmaesumi, P., Zheng, Z. Z., Munhall, K. G., and Johnsrude, I. S. (2009). Reducing inter-subject anatomical variation: Effect of normalization method on sensitivity of functional magnetic resonance imaging data analysis in auditory cortex and the superior temporal region. *Neuroimage* 47, 1522–1531. doi: 10.1016/j.neuroimage.2009.05.047

Takeuchi, H., Taki, Y., Nouchi, R., Yokoyama, R., Kotozaki, Y., Nakagawa, S., et al. (2017). Regional homogeneity, resting-state functional connectivity and amplitude of low frequency fluctuation associated with creativity measured by divergent thinking in a sex-specific manner. *Neuroimage* 152, 258–269. doi: 10.1016/j.neuroimage.2017.02.079

Tang, J.-L., Liu, B.-Y., and Ma, K.-W. (2008). Traditional Chinese medicine. *Lancet* 372, 1938–1940. doi: 10.1016/s0140-6736(08)61354-9

Tian, J., Han, M., Tu, J., Zhou, W., Yang, C., Yang, H., et al. (2002). Criteria for diagnosis, syndrome differentiation and treatment effect evaluation of vascular dementia (in Chinese). *Chin. J. Gerontol.* 22, 329–331. doi: 10.3969/j.issn.1005-9202.2002.05.001

Vinciguerra, L., Lanza, G., Puglisi, V., Fisicaro, F., Pennisi, M., Bella, R., et al. (2020). Update on the neurobiology of vascular cognitive impairment: From lab to clinic. *Int. J. Mol. Sci.* 21:2977. doi: 10.3390/ijms21082977

Vinciguerra, L., Lanza, G., Puglisi, V., Pennisi, M., Cantone, M., Bramanti, A., et al. (2019). Transcranial doppler ultrasound in vascular cognitive impairment-no dementia. *PLoS One* 14:e0216162. doi: 10.1371/journal.pone.0216162

Wang, B.-Q., Mei, J., Liu, L., Ju, C.-X., Zhao, J.-N., Zhang, P., et al. (2020). Exploratory study on the safety and effectiveness of Yizhi Qingxin Decoction (capsules) in the treatment of hypertension in the elderly with mild cognitive impairment (deficiency of kidney essence syndrome). *Medicine* 99:e20789. doi: 10.1097/MD.0000000000020789

Wang, J., Lyu, H., Chen, J., Lin, S., Zheng, H., Li, J., et al. (2020). Cortical Alterations are associated with depression in subcortical vascular mild cognitive impairment revealed by surface-based morphometry. *J. Alzheimers Dis.* 78, 673–681. doi: 10.3233/JAD-200156

Wang, R., Liu, N., Tao, Y., Gong, X., Zheng, J., Yang, C., et al. (2020). The application of rs-fMRI in vascular cognitive impairment. *Front. Neurol.* 11:951. doi: 10.3389/fneur.2020.00951

Wang, Y. Z., Han, Y., Zhao, J. J., Du, Y., Zhou, Y., Liu, Y., et al. (2019). Brain activity in patients with deficiency versus excess patterns of major depression: A task fMRI study. *Complement. Ther. Med.* 42, 292–297. doi: 10.1016/j.ctim.2018.12.006

WHO (2019). *International classification of diseases, 11th revision (ICD-11) [Online]*. Available online at: http://www.who.int/classifications/icd/en/ (accessed December 27, 2019).

Xu, J., Wang, J., Lyu, H., Pu, X., Xu, Z., Hu, Y., et al. (2020). Different patterns of functional and structural alterations of hippocampal sub-regions in subcortical vascular mild cognitive impairment with and without depression symptoms. *Brain Imaging Behav.* 15, 1211–1221. doi: 10.1007/s11682-020-00321-7

Xu, Z., Wang, J., Lyu, H., Wang, R., Hu, Y., Guo, Z., et al. (2020). Alterations of whiter matter microstructure in subcortical vascular mild cognitive impairment with and without depressive symptoms. *J. Alzheimers Dis.* 73, 1565–1573. doi: 10.3233/JAD-190890

Xu, Z., Zhang, S., Huang, L., Zhu, X., Zhao, Q., Zeng, Y., et al. (2018). Altered Resting-state brain activities in drug-naïve major depressive disorder assessed by fMRI: Associations with somatic symptoms defined byyin-yangtheory of the traditional Chinese medicine. *Front. Psychiatry* 9:195. doi: 10.3389/fpsyt.2018.00195

Yan, C., Wang, X., Zuo, X., and Zang, Y. (2016). DPABI: Data processing & analysis for (resting-state) brain imaging. *Neuroinformatics* 14, 339–351. doi: 10.1007/s12021-016-9299-4

Yang, Z., Craddock, R. C., Margulies, D. S., Yan, C., and Milham, M. P. (2014). Common intrinsic connectivity states among posteromedial cortex subdivisions: Insights from analysis of temporal dynamics. *Neuroimage* 93, 124–137. doi: 10.1016/j.neuroimage.2014.02.014

Yi, L., Wang, J., Jia, L., Zhao, Z., Lu, J., Li, K., et al. (2012). Structural and functional changes in subcortical vascular mild cognitive impairment: A combined voxel-based morphometry and resting-state fMRI study. *PLoS One* 7:e44758. doi: 10.1371/journal.pone.0044758

Zhang, Y. F., Yu, H., Wang, Y. Z., Zhang, Y. F., Jia, H. X., Jin, E. H., et al. (2015). Characterization of resting-state fMRI-derived functional connectivity in patients with deficiency versus excess patterns of major depression. *Complement. Ther. Med.* 23, 7–13. doi: 10.1016/j.ctim.2014.12.010

Zhao, Q., Sang, X., Metmer, H., Lu, J., and Alzheimer's Disease NeuroImaging Initiative (2019). Functional segregation of executive control network and frontoparietal network in Alzheimer's disease. *Cortex* 120, 36–48. doi: 10.1016/j.cortex.2019.04.026

Zheng, H., Qin, X., Wang, J., Kong, F., Cai, H., Huang, R., et al. (2022a). Correlations between deficiency pattern/excess pattern and cognitive function in patients with vascular cognitive impairment. *Chin. J. Alzheimers Dis. Relat. Disord. (In Chinese)* 5, 27–31. doi: 10.1186/s13054-016-1208-6

Zheng, H., Wang, J., Kong, F., Qin, X., Lin, S., Cai, H., et al. (2022b). A multi-center randomized controlled study of Naosuikang in the treatment of vascular cognitive impairment with deficiency of spleen and kidney and phlegm and blood stasis syndrome. *Chin. J. Integr. Med. (In Chinese)* 42, 160–166.

Zou, Q.-H., Zhu, C.-Z., Yang, Y., Zuo, X.-N., Long, X.-Y., Cao, Q.-J., et al. (2008). An improved approach to detection of amplitude of low-frequency fluctuation (ALFF) for resting-state fMRI: Fractional ALFF. *J. Neurosci. Methods* 172, 137–141. doi: 10.1016/j.jneumeth.2008.04.012

frontiers | Frontiers in Neurology

TYPE Original Research
PUBLISHED 01 September 2022
DOI 10.3389/fneur.2022.963648

OPEN ACCESS

EDITED BY
Jennifer S. Yokoyama,
University of San Francisco,
United States

REVIEWED BY
Evan Fletcher,
University of California, Davis,
United States
Pasquale Mone,
Albert Einstein College of Medicine,
United States

*CORRESPONDENCE
Nan Hee Kim
nhkendo@gmail.com

†These authors have contributed equally to this work

SPECIALTY SECTION
This article was submitted to Dementia and Neurodegenerative Diseases, a section of the journal Frontiers in Neurology

RECEIVED 07 June 2022
ACCEPTED 29 July 2022
PUBLISHED 01 September 2022

CITATION
Yu JH, Kim REY, Park SY, Lee DY, Cho HJ, Kim NH, Yoo HJ, Seo JA, Kim SH, Kim SG, Choi KM, Baik SH, Shin C and Kim NH (2022) Night blood pressure variability, brain atrophy, and cognitive decline.
Front. Neurol. 13:963648.
doi: 10.3389/fneur.2022.963648

Night blood pressure variability, brain atrophy, and cognitive decline

Ji Hee Yu[1], Regina E. Y. Kim[2,3], So Young Park[1], Da Young Lee[1], Hyun Joo Cho[1], Nam Hoon Kim[1], Hye Jin Yoo[1], Ji A Seo[1], Seong Hwan Kim[4], Sin Gon Kim[1], Kyung Mook Choi[1], Sei Hyun Baik[1], Chol Shin[2†] and Nan Hee Kim[1*†]

[1]Division of Endocrinology and Metabolism, Department of Internal Medicine, Korea University College of Medicine, Seoul, South Korea, [2]Institute of Human Genomic Study, Korea University Ansan Hospital, Korea University College of Medicine, Ansan, South Korea, [3]Department of Psychiatry, University of Iowa, Iowa City, IA, United States, [4]Division of Cardiology, Department of Internal Medicine, Korea University College of Medicine, Seoul, South Korea

Background: Although blood pressure variability (BPV) has emerged as a novel risk factor for Alzheimer's disease, few studies have examined the effects of night BPV on brain structure and function. This study investigated the association of night BPV with brain atrophy and cognitive function changes.

Methods: The analysis included 1,398 participants with valid ambulatory blood pressure (BP) monitoring at baseline and both baseline and 4-year follow-up brain magnetic resonance images who were recruited from the Korean Genome and Epidemiology Study. Participants underwent a comprehensive neuropsychological test battery. BPV was derived from ambulatory BP monitoring and calculated as a standard deviation (SD) of 24-h and daytime and nighttime BP.

Results: During the median follow-up of 4.3 years, increased SD of night systolic or diastolic BP was an indicator of total brain volume reduction, while daytime BPV or night average BP was not associated with total brain volume changes. High SD of night systolic BP was associated with reduced gray matter (GM) volume, independent of average night BP, and use of antihypertensive drugs. It also was associated with a reduction of temporal GM volume, mostly driven by atrophy in the left entorhinal cortex and the right fusiform gyrus. In cognitive performance, high variability of night systolic BP was associated with a decrease in visual delayed recall memory and verbal fluency for the category.

Conclusion: Increased night BPV, rather than night mean BP, was associated with reduced brain volume and cognitive decline. High night BPV could be an independent predictor for rapid brain aging in a middle-aged population.

KEYWORDS

night blood pressure, variability, gray matter, brain atrophy, cognition

Introduction

High blood pressure (BP) has been shown to be associated with brain atrophy and cognitive dysfunctions (1–3). Nocturnal hypertension showed significant associations with brain volume and cognitive impairment (1, 4, 5). In addition to the effect of BP level on brain function, the importance of dynamic changes in BP level in cerebrovascular disease has been supported by several observations. Past studies have focused on the effect of circadian BP variation, such as nocturnal BP dipping or non-dipping, and both patterns had adverse effects on brain health. Non-dippers are defined as night BP decrease <10% of the daytime level and showed more frequent silent cerebral infarction than dippers, with a night BP decrease >10% (6). In contrast, the very large nocturnal BP decrease of an extreme dipper could induce cerebral vascular insufficiency (7). Since the advent of 24-h non-invasive ambulatory BP monitoring, most studies have evaluated the association between short-term BP variability (BPV) and cerebral outcomes. High BPV was associated with an increased risk of cerebral small vessel disease, stroke, dementia, and cognitive decline (8–13). Evidence has shown that greater BPV leads to diffuse atherosclerotic progression represented by increased left ventricular mass index or carotid-intima media thickness value (14, 15).

Despite these observations, the relationship between increased nighttime BPV and brain volume atrophy or cognitive function remains poorly understood. Previous studies are limited by small sample sizes (16) or cross-sectional associations with inconsistent results (17–19). Moreover, it is not clear which regional area of the brain is most associated with high night BPV and how it relates to changes in cognitive functions.

In this study, we investigated whether increased night BPV is associated with brain volume atrophy and cognitive decline in a middle-aged population. We analyzed longitudinal associations between night BPV at baseline and changes in brain volume and cognitive function across 4 years.

Materials and methods

Subjects

The study subjects were from the Ansan cohort of the Korean Genome Epidemiology Study (KoGES), an ongoing population-based cohort study that began in 2001. The demographics, medical illness, and medications of KoGES participants have been biennially evaluated. During the 6th and 7th examinations (2011–2014), baseline brain magnetic resonance imaging (MRI) scans and cognitive function tests were acquired. Follow-up brain MRI scans and cognitive function tests were conducted during the 8th and 9th examinations (2015–2018). Further details are described elsewhere (20).

This study included 1,967 subjects who examined 24-h ABPM during the baseline period (2011–2014) (Figure 1). We excluded 224 subjects with the following conditions: (1) valid 24-h ABPM $\leq$ 70% of the readings of total 24-h BP measurements (n = 202); (2) cerebrovascular disease (n = 10); and (3) any cancer (n = 12). Among the remaining 1,743 subjects, 1,438 individuals underwent both baseline and follow-up brain MRI scans. None of them had a history of dementia or any neuropsychiatric disorders. After the exclusion of subjects with missing data (n = 40), 1,398 participants were finally included in this study. This study was performed according to the principles of the Declaration of Helsinki of the World Medical Association and was approved by the Institutional Review Board of Korea University Ansan Hospital.

Assessments

Demographic, anthropometric, and laboratory measurements

All participants responded to an interviewer-administered questionnaire and underwent physical examinations. Lifestyle characteristics, such as smoking status and alcohol consumption, were categorized as never, former, and current. Regular exercise was defined as at least three times a week for 30 min per session during the previous month. Education level was categorized into primary, secondary, and college/university levels. Height was measured to the nearest 0.1 cm using a fixed wall-scale measuring device. Weight was measured to the nearest 0.1 kg using an electronic scale that was calibrated before each measurement. Body mass index (BMI) was calculated as weight in kilograms divided by height in meters squared. Blood was drawn for biochemical analysis after an overnight fast.

24 h ABPM

A Mobil-O-Graph NGversion20, which is a non-invasive oscillometric device, and its hypertension management software (I.E.M. GmbH, Stolberg, Germany) were used for ABPM. A trained researcher informed the participant during a clinic visit how to use the home 24-h ABPM device. A BP cuff was placed on the upper region of the non-dominant arm, and BP was recorded automatically every 30 min (0600–2,300 h) or every hour (2,300–0600 h). The participant was asked to record the time of waking and sleeping over a 24-h period. Daytime and nighttime for each of the participants were ascertained based on the awake and asleep times.

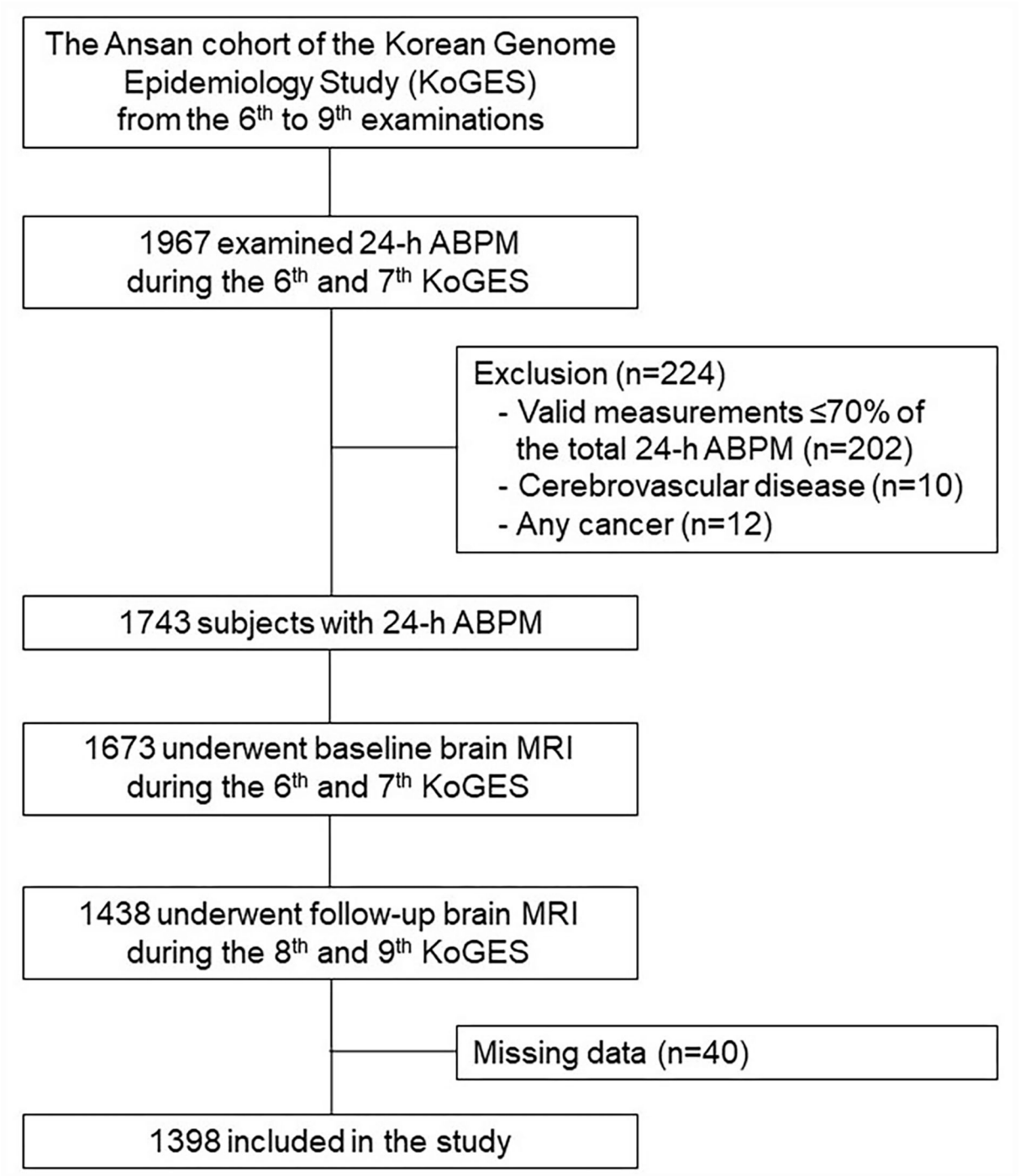

FIGURE 1
A flowchart of the selection process. ABPM, ambulatory blood pressure measurement; MRI, magnetic resonance imaging.

Brain MRI

All 3D T1 MRI scans were acquired using a GE Signa HDxt 1·5 T MRI scanner with an 8-channel head coil. The detailed MRI protocols are described in a previous study (20). Brain MRI images were processed through a well-established fully automated procedure, the BRAINS AutoWorkup in the BRAINSTOOLs package (21, 22). The MRI processing starts with spatial normalization using landmark detection (23), bias-field correction with tissue classification (22), and finally segmentation using ANTs Joint Fusion (24). Two hundred

TABLE 1 Baseline characteristics of the study subjects.

$N = 1,398$	
Age, years	59.7 ± 6.7
Age group	
<60 years	796 (56.9)
60–69 years	454 (32.5)
≥70 years	148 (10.6)
Sex, men	643 (46.0)
Current smoker	132 (9.4)
Current drinker	597 (42.7)
Regular exercise	527 (37.7)
Education, elementary or less	183 (13.1)
Primary	183 (13.1)
Secondary	912 (65.2)
College/university	303 (21.7)
BMI, kg/m^2	24.6 ± 2.9
Day SBP, mmHg	122.6 ± 12.0
Day DBP, mmHg	80.7 ± 10.1
Night SBP, mmHg	112.3 ± 12.8
Night DBP, mmHg	72.1 ± 10.0
SD of day SBP	12.6 ± 4.0
SD of day DBP	9.6 ± 2.5
SD of night SBP	10.1 ± 4.5
SD of night DBP	8.6 ± 3.5
ICV, mL	1396.1 ± 137.1
DM	444 (31.8)
Hypertension	538 (38.5)
Antihypertensive medications	454 (32.5)
Heart disease	107 (7.7)
Obesity	605 (43.3)
Sleep duration, h	6.0 ± 1.2
Snoring	1,072 (77.2)

Data are presented as mean ± SD or number (%).
BMI, body mass index; DBP, diastolic blood pressure; DM, diabetes mellitus; ICV, intracranial volume; SBP, systolic blood pressure; SD, standard deviation.

fifteen independent brain subcompartments were automatically delineated, and the volumes were measured. The high reliability of the longitudinal measurement of two-time point MRI using the BRAINS AutoWorkup has been previously described (20). The sub-compartments were merged into three tissue classes: GM, WM, and cerebrospinal fluid. All the volume measurements were extracted from an individual's original anatomical space. GM and WM volumes were summed to obtain total brain volume.

Neuropsychological tests

KoGES participants were administered the neuropsychological assessment battery described below during the regular examination cycle as part of the baseline measurement of the aging study: (1) story recall test, immediate and delayed recall, and recognition; (2) visual reproduction, immediate and delayed recall, and recognition; (3) verbal fluency; (4) trail making tests; (5) Digit Symbol-coding, incidental learning, and free recall; and (6) Korean-Color Word Stroop Test, word reading, and color reading. Standard administration protocols were used for each testing session, and the tests were conducted by well-trained and experienced psychological examiners. Further details are described elsewhere (25).

Definitions of diabetes mellitus (DM), hypertension, heart disease, and obesity

DM was diagnosed as fasting plasma glucose ≥7.0 mmol/L, 2-h plasma glucose ≥11.1 mmol/L after a 75 g oral glucose tolerance test or use of anti-diabetic medication (26). Hypertension was diagnosed as systolic BP (SBP) or diastolic BP (DBP) equal to or higher than 140 or 90 mmHg, respectively, or use of antihypertensive medications. Participants with a documented history of myocardial infarction, angina, or congestive heart failure were considered to have heart disease. Obesity was defined as BMI ≥25 kg/m^2.

Sleep duration and snoring measurements

All participants were asked to answer sleep-related questions based on the average sleep pattern during the past month. Sleep duration was determined as the answer to, "How many hours did you usually sleep per day during the last month?" Participants were asked if they had ever been reported to snore. Snoring status was confirmed by a bed partner or a family member who lived with the participant for more than 1 year. Further details are described elsewhere (27).

Statistical analysis

As measures of short-term reading-to-reading BPV, we used the SD over daytime and nighttime. Baseline characteristics are presented as number (%) or mean ± SD. The brain volume change was calculated by subtracting the baseline brain volume from the follow-up brain volume. Multivariate linear regression analyses were conducted to evaluate the effects of BPV on brain volume or cognitive function changes. The regression models included brain volume changes as the dependent variable; ICV, age, sex, smoking, alcohol, exercise, education, an average of daytime and nighttime BP, antihypertensive medications, DM, heart disease, baseline brain volume, and time intervals between baseline and follow-up MRI scans were included as the independent variables. For analysis of associations with night systolic BPV, the average SBP during the day and that during

TABLE 2 Associations between 24-h BP indicators and total brain volume changes.

	SBP			DBP		
$N = 1398$	β Estimate	SE	*p*	β Estimate	SE	*p*
Mean day	0.058	0.063	0.357	0.059	0.081	0.470
Mean night	0.0004	0.059	0.995	0.022	0.078	0.773
SD day	−0.055	0.158	0.728	−0.054	0.220	0.807
SD night	−0.278	0.119	**0.020**	−0.375	0.154	**0.015**

All models are adjusted for baseline intracranial volume, age, sex, smoking, alcohol, exercise, education, mean day BP, mean night BP, anti-hypertensive medications, DM, heart disease, time between MRI scans, and baseline brain volume. Brain volume changes were calculated by subtracting baseline brain volumes from follow-up brain volumes.
BP, blood pressure; DBP, diastolic blood pressure; DM, diabetes mellitus; MRI, magnetic resonance imaging; SBP, systolic blood pressure; SD, standard deviation. Bold values indicate *P* value < 0.05.

the night were included in the regression models; for analysis of night diastolic BPV, the average DBP values during both days and night were included. The association of night BPV with brain regional volume changes was further analyzed in sub-compartments of WM and temporal GM. The cognitive function change was calculated by subtracting the baseline cognitive scores from the follow-up scores. The regression models included cognitive function change as the dependent variable, and baseline cognitive scores and time between cognitive tests were entered as variables along with those mentioned above. Sobel's tests were performed to examine whether GM volume atrophy mediated any associations between night systolic BPV and decline in cognition. Statistical significance for non-normally distributed cognitive variables was estimated after logarithmic transformation. A *P*-value <0.05 was considered statistically significant. Statistical analyses were performed using SAS version 9.1 for Windows (SAS Institute Inc., Cary, NC, USA).

Results

Subject characteristics

The descriptive and clinical characteristics of the study population at baseline are presented in Table 1. The mean age of all participants was 59.7 ± 6.7 years (range, 49–79), and 46.0% of the individuals were men. The mean BMI was 24.6 ± 2.9 kg/m^2, and 43.3% of the participants were obese. Approximately, 38.5% of patients had hypertension and 31.8% had diabetes mellitus at baseline. In addition, 13.1% of participants had an education level of elementary school or lower.

Associations between BPV and total brain volume changes

Table 2 presents the associations between the 24-h ambulatory BP indicators and total brain volume changes. The average period between baseline and follow-up brain MRI scans was 4.3 ± 0.5 years. The mean BP during daytime or nighttime was not associated with total brain volume changes. In relation to BPV, only SD of night BP was significantly associated with total brain volume changes. Higher SD of night SBP or DBP was significantly associated with greater total brain volume reduction after full adjustment ($P = 0.020$ for SD of night SBP, $P = 0.015$ for SD of night DBP; Table 2). Further adjustment for sleep duration, snoring, or BMI did not alter the significance of these associations. The SD of night SBP or DBP was positively associated with age, BMI, and an average of day and night BP in the multivariable regression analysis (Supplementary Table 1). Sleep parameters such as sleep duration or snoring were not associated with night BPV.

Effects of night BPV on regional brain volume changes

We evaluated the effects of night BPV on regional brain volume changes, and the results are shown in Table 3. Increased SD of night SBP was associated with greater atrophy in GM volume ($P = 0.033$), particularly with decreased temporal GM ($P = 0.021$). The significance of this finding did not change even after further adjustment for sleep duration, snoring, or BMI. The relationship between night systolic BPV and temporal GM was mostly driven by atrophy of the left entorhinal cortex ($P = 0.010$) and right fusiform gyrus ($P = 0.039$) (Figure 2; Supplementary Table 2). Atrophy of the right fusiform gyrus was also associated with increased SD of night DBP ($P = 0.018$).

SD of night DBP showed a negative association with WM volume changes ($P = 0.049$; Table 3). Higher night diastolic BPV was associated with greater regional WM atrophy in the right precentral ($P = 0.045$), left paracentral ($P = 0.025$), right rostral middle frontal ($P = 0.048$), both superior frontal ($P = 0.024$ for left, 0.049 for right), left precuneus ($P = 0.033$), left transverse temporal ($P = 0.027$), both lingual ($P = 0.016$ for left, 0.034 for right), and right cuneus ($P = 0.029$) gyri (Supplementary Table 3). The volume changes of the

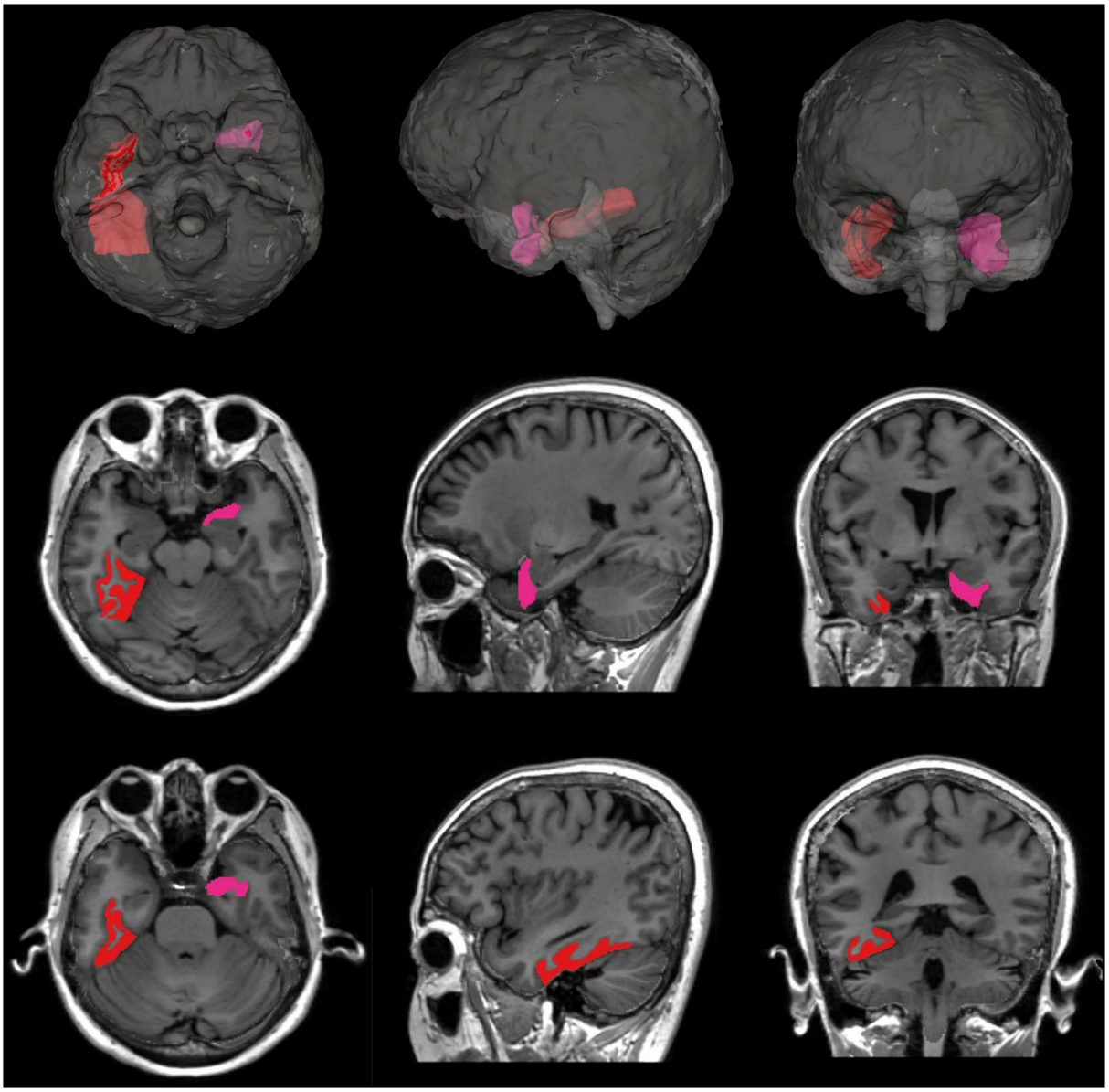

FIGURE 2
Subregions of temporal GM with significant atrophy associated with night systolic BPV. The left entorhinal cortex (marked in pink, $P = 0.010$) and the right fusiform gyrus (marked in red, $P = 0.039$) showed significantly greater atrophy associated with increased night systolic BPV.

hippocampus were not associated with night systolic or diastolic BPV (data not shown).

Effects of night BPV on cognitive performance changes

Table 4 shows the associations between night systolic BPV and cognitive performance changes. High SD of night SBP was significantly associated with a greater decline in visual delayed recall memory ($P = 0.028$) and verbal fluency for category ($P = 0.029$) and with a slower decline in verbal recognition memory ($P = 0.010$) during the follow-up period. Further adjustment for sleep duration and snoring did not alter the significance of these associations. In contrast, night mean SBP or DBP was not associated with any cognitive functional changes (Supplementary Table 4). Night diastolic BPV was also not significantly associated with cognitive decline (data not shown).

We examined whether the relation between night systolic BPV and decline in cognitive function was mediated by GM atrophy (Supplementary Table 5). There was no significant

TABLE 3 Linear regression analyses between night BPV and regional brain volume changes.

	SD of night SBP			SD of night DBP		
Δ ml ($n = 1,398$)	**β Estimate**	**SE**	***p***	**β Estimate**	**SE**	***p***
Δ GM	−0.168	0.079	**0.033**	−0.159	0.102	0.121
Δ Frontal GM	−0.035	0.043	0.422	−0.039	0.056	0.485
Δ Parietal GM	−0.033	0.019	0.090	−0.021	0.025	0.411
Δ Temporal GM	−0.039	0.017	**0.021**	−0.018	0.022	0.407
Δ Occipital GM	−0.014	0.015	0.335	−0.015	0.019	0.442
Δ WM	−0.127	0.092	0.168	−0.234	0.119	**0.049**
Δ Frontal WM	−0.039	0.039	0.318	−0.096	0.050	0.055
Δ Parietal WM	−0.037	0.026	0.160	−0.060	0.034	0.073
Δ Temporal WM	−0.003	0.019	0.885	−0.013	0.025	0.592
Δ Occipital WM	−0.013	0.009	0.171	−0.015	0.012	0.225

All models were adjusted for baseline intracranial volume, age, sex, smoking, alcohol, exercise, education, mean day BP, mean night BP, anti-hypertensive medications, DM, heart disease, time between MRI scans, and baseline brain volume.
Regional brain volume changes were calculated by subtracting baseline regional brain volumes from follow-up volumes.
BP, blood pressure; DBP, diastolic blood pressure; DM, diabetes mellitus; GM, gray matter; MRI, magnetic resonance imaging; SBP, systolic blood pressure; SD, standard deviation; WM, white matter.

evidence of mediation by GM volume atrophy in the relationship between night systolic BPV and cognitive decline in visual delayed recall memory (Sobel's test = 0.437, $P = 0.662$) or verbal fluency for category (Sobel's test = 0.432, $P = 0.666$).

Discussion

We found that higher systolic BPV during the night was associated with the greater decline in brain volume and cognitive function over a mean follow-up of 4.3 years in a Korean population. Increased night BPV was associated with total brain volume atrophy, independent of average BP and the use of antihypertensive drugs. High variability of night SBP was associated with GM volume atrophy, especially temporal GM atrophy. Furthermore, the increase in night systolic BPV was associated with a greater decline in visual delayed recall memory and verbal fluency for category.

In our study, total brain volume atrophy and cognitive decline were associated with increased night BPV, but not with night mean BP. It is well-known that high BP contributes to cognitive impairments and dementia (3, 28). However, despite excellent BP control in a *post-hoc* analysis of the SPRINT MIND trial, higher BPV was associated with an increased risk of dementia (29), suggesting that increased BPV might be an independent factor associated with brain damage. Recent meta-analyses have demonstrated that increased BPV was associated with cerebral small vessel disease progression (10, 30), which is a major cause of cognitive decline (31–33). BPV also increased with age and mean BP level in our study. Therefore, high night BPV might be an epiphenomenon accompanied by the coexistence of various comorbidities or frailty in older adults. Increased BPV was associated with a greater risk of frailty (34), showing a significant correlation with cognitive decline, particularly in elderly hypertensive individuals (35–38).

Temporal GM was the area most affected by high night systolic BPV in our study. The relationship between night systolic BPV and temporal GM was driven most highly by atrophy of the left entorhinal cortex and right fusiform gyrus. To the best of our knowledge, this is the first study to identify the regional area of the brain most affected by night systolic and diastolic BPV. The entorhinal cortex is located in the medial temporal lobe, which functions as a widespread network hub for memory, navigation, and the perception of time (39). The fusiform gyrus is the largest macro-anatomical structure within the ventral temporal cortex and is considered a key structure for functionally specialized computations of high-level vision, such as face perception, object recognition, reading, and visual processing of letters and words (40). However, GM atrophy did not mediate the relationship between increased night systolic BPV and impaired visual delayed recall memory or verbal categorical fluency in our study. It remains to be seen whether brain regional connectivity or microstructural changes are involved in this relationship. More long-term follow-up studies are warranted to clarify the relevant mechanisms. It is unclear why the increased variation in night SBP was associated with slower decline in verbal recognition memory.

High night diastolic BPV was significantly related to WM atrophy, while the increase in night systolic BPV was associated with GM volume reduction in our study. It remains a matter of debate whether the variability of SBP or DBP contributes separately to GM and WM atrophy. Several studies have reported that DBP was strongly associated with WM hyperintensities (41, 42). It has been suggested that large artery stiffness leads to elevated SBP and pulse pressure, whereas

TABLE 4 Linear regression analyses between night systolic BPV and cognitive performance changes.

	n	Estimate	SE	*p*
Story Recall Test-Immediate Recall	1,376	0.015	0.023	0.507
Story recall test-delayed recall	1,367	0.016	0.023	0.490
Story recall test-recognition[a]	1,379	0.003	0.001	**0.010**
Visual reproductions-immediate recall	1,384	−0.019	0.014	0.150
Visual reproductions-delayed recall	1,377	−0.032	0.015	**0.028**
Visual reproductions-recognition	1,380	−0.004	0.006	0.567
Verbal fluency-phonemic	1,347	0.013	0.045	0.768
Verbal fluency-category	1,347	−0.044	0.020	**0.029**
Digit symbol-coding	1,361	−0.022	0.042	0.598
Digit symbol-incidental learning[a]	1,343	0.002	0.004	0.660
Digit symbol-free recall	1,358	−0.003	0.008	0.727
Trails A-Time[a]	1,378	0.003	0.002	0.078
Stroop-color reading	1,333	0.127	0.137	0.352
Stroop-word reading	1,307	0.022	0.046	0.633

All models were adjusted for baseline intracranial volume, age, sex, smoking, alcohol, exercise, education, mean day BP, mean night BP, anti-hypertensive medications, DM, heart disease, the time between cognitive tests, and baseline cognitive scores.
Cognitive performance changes were calculated by subtracting baseline cognitive scores from follow-up scores of cognitive tests.
[a]Statistical significance was estimated after logarithmic transformation.
BP, blood pressure; DM, diabetes mellitus; SBP, systolic blood pressure; SD, standard deviation. Bold values indicate P value < 0.05.

DBP is reflecting peripheral vascular resistance (43). Brain pathology studies have demonstrated venous collagenosis in periventricular WM lesions (44). Therefore, it can be inferred that WM atrophy or lesion loads might be susceptible to changes in peripheral vascular resistance associated with DBP.

The exact mechanism by which increased night BPV, rather than daytime BPV, showed a significant correlation with cognitive decline and brain atrophy remains unknown. Daytime BPV might be directly affected by physical activities or emotional stress that occur during the day, whereas nocturnal BP monitoring could be less influenced by external stimuli. Increased night BPV might better reflect pathophysiological conditions such as baroreflex dysfunction, arterial stiffness neurohormonal activation, or sleep apnea than increased daytime BPV (45). Sleep is another possible key mechanism linked to fluctuations in nighttime BP. Sleep deprivation or fragmentation has been shown to be associated with increased night BPV through sympathetic neuronal activation (46, 47). Poor sleep quality has been linked to reduced brain volume and cognitive deficits (48, 49). However, in our study, there was no association between night BPV and sleep duration or snoring, and the significance of the results was not changed after adjustment for sleep-related indicators. The comprehensive association of several factors might account for the mechanisms associated with negative effects of high night BPV on cerebral vessels, brain structure, and function. Additional longitudinal studies are needed to determine whether dementia occurs more frequently in individuals with increased night BPV and if selective reduction of night BPV in this population could improve outcomes associated with brain health.

Our study has several strengths. First, our study is a 4-year, longitudinal, population-based study with a large sample size and brain MRI imaging data. Second, this study is the first to follow changes in detailed cognitive function tests in conjunction with brain imaging in relation to night BPV. Third, we examined sleep-related indicators as factors that could be associated with an increase in night BPV, although they were based on surveys. However, some limitations of this study should be noted. First, WM hyperintensities or diffusion MRI-based estimates of white matter microstructure were not measured in this study. These indicators of vascular brain injuries might be more sensitive to night BPV than brain volume loss, and further studies will be needed. Second, we did not address any associated neurohormonal changes during nighttime, which made it difficult to elucidate the mechanisms associated with increased night BPV. Third, there is a limit on the determination of the causal relationship between brain structural changes associated with high night BPV and cognitive decline.

To summarize, our study showed that increased nighttime BPV, rather than night mean BP, was associated with total brain volume atrophy and cognitive decline. High night systolic BPV was associated with temporal GM atrophy and impaired visual memory and verbal fluency. Increased nighttime BPV could be an independent predictor for rapid brain aging in a middle-aged population.

Data availability statement

The data analyzed in this study was obtained from The Korea Centers for Disease Control and Prevention (KCDC), the following licenses/restrictions apply: The datasets can be provided after review and evaluation of research plan by the KCDC. Requests to access these datasets should be directed to the KCDC, http://www.cdc.go.kr/CDC/eng/main.jsp.

Ethics statement

The study protocol was reviewed and approved by Institutional Review Board of Korea University Ansan Hospital. The participants provided written informed consent to participate in the cohort study.

Author contributions

JY contributed to the study design and data analysis and wrote the manuscript. RK contributed to the MRI data processing and wrote the manuscript. SP and DL contributed to the literature search and data analysis. HC conducted the statistical analysis. NamK, HY, JS, SeK, SiK, KC, and SB reviewed and critiqued the statistical and MRI analyses and provided feedback on the manuscript text. CS and NanK contributed to data collection, obtained funding, and led the study. All authors read and approved the final manuscript, contributed toward data analysis, drafted and revised the paper, and agreed to be accountable for all aspects of the work.

Funding

This work was supported by funds (2011-E71004-00, 2012-E71005-00, 2013-E71005-00, 2014-E71003-00, 2015-P71001-00, 2016-E71003-00, 2017-E71001-00, and 2018-E71001-00) from the Korean Centers for Disease Control and Prevention, the Bio & Medical Technology Development Program of the National Research Foundation (NRF) funded by the Korean government (MSIT) (2019M3E5D3073102, 2019R1H1A2039682, and 2020R1F1A1074265), a Korea University grant (K1824431 and K1810951), Ansan-Si hidden champion fostering and supporting project funded by Ansan city, and computational resources provided by the University of Iowa, Iowa City, Iowa.

Conflict of interest

The authors declare that the research was conducted in the absence of any commercial or financial relationships that could be construed as a potential conflict of interest.

Publisher's note

All claims expressed in this article are solely those of the authors and do not necessarily represent those of their affiliated organizations, or those of the publisher, the editors and the reviewers. Any product that may be evaluated in this article, or claim that may be made by its manufacturer, is not guaranteed or endorsed by the publisher.

Supplementary material

The Supplementary Material for this article can be found online at: https://www.frontiersin.org/articles/10.3389/fneur.2022.963648/full#supplementary-material

References

1. Nagai M, Hoshide S, Ishikawa J, Shimada K, Kario K. Ambulatory blood pressure as an independent determinant of brain atrophy and cognitive function in elderly hypertension. *J Hypertens.* (2008) 26:1636–41. doi: 10.1097/HJH.0b013e3283018333

2. Papademetriou V. Hypertension and cognitive function. Blood pressure regulation and cognitive function: a review of the literature. *Geriatrics.* (2005) 60:20–4.

3. Levine DA, Springer MV, Brodtmann A. Blood pressure and vascular cognitive impairment. *Stroke.* (2022) 53:1104–13. doi: 10.1161/strokeaha.121.036140

4. Yano Y, Inokuchi T, Hoshide S, Kanemaru Y, Shimada K, Kario K. Association of poor physical function and cognitive dysfunction with high nocturnal blood pressure level in treated elderly hypertensive patients. *Am J Hypertens.* (2011) 24:285–91. doi: 10.1038/ajh.2010.224

5. Yano Y, Butler KR, Hall ME, Schwartz GL, Knopman DS, Lirette ST, et al. Associations of nocturnal blood pressure with cognition by self-identified race in middle-aged and older adults: the GENOA (genetic epidemiology network of arteriopathy) study. *J Am Heart Assoc.* (2017) 6:e007022. doi: 10.1161/jaha.117.007022

6. Ma JF, Sun JL, Zhao J, Wei X, Wang BS, Fu Y. Relationship between nocturnal blood pressure variation and silent cerebral infarction in Chinese hypertensive patients. *J Neurol Sci.* (2010) 294:67–9. doi: 10.1016/j.jns.2010.04.002

7. Kario K, Pickering TG, Matsuo T, Hoshide S, Schwartz JE, Shimada K. Stroke prognosis and abnormal nocturnal blood pressure falls in older hypertensives. *Hypertension.* (2001) 38:852–7. doi: 10.1161/hy1001.092640

8. Ma Y, Wolters FJ, Chibnik LB, Licher S, Ikram MA, Hofman A, et al. Variation in blood pressure and long-term risk of dementia: A population-based cohort study. *PLoS Med.* (2019) 16:e1002933. doi: 10.1371/journal.pmed.1002933

9. Rothwell PM, Howard SC, Dolan E, O'Brien E, Dobson JE, Dahlöf B, et al. Prognostic significance of visit-to-visit variability, maximum

systolic blood pressure, and episodic hypertension. *Lancet.* (2010) 375:895–905. doi: 10.1016/s0140-6736(10)60308-x

10. Ma Y, Song A, Viswanathan A, Blacker D, Vernooij MW, Hofman A, et al. Blood pressure variability and cerebral small vessel disease: a systematic review and meta-analysis of population-based cohorts. *Stroke.* (2020) 51:82–9. doi: 10.1161/strokeaha.119.026739

11. Zhou TL, Kroon AA, van Sloten TT, van Boxtel MPJ, Verhey FRJ, Schram MT, et al. Greater blood pressure variability is associated with lower cognitive performance. *Hypertension.* (2019) 73:803–11. doi: 10.1161/hypertensionaha.118.12305

12. Yoo JE, Shin DW, Han K, Kim D, Lee SP, Jeong SM, et al. Blood pressure variability and the risk of dementia: a nationwide cohort study. *Hypertension.* (2020) 75:982–90. doi: 10.1161/hypertensionaha.119.14033

13. Qin B, Viera AJ, Muntner P, Plassman BL, Edwards LJ, Adair LS, et al. Visit-to-visit variability in blood pressure is related to late-life cognitive decline. *Hypertension.* (2016) 68:106–13. doi: 10.1161/hypertensionaha.116.07494

14. Frattola A, Parati G, Cuspidi C, Albini F, Mancia G. Prognostic value of 24-h blood pressure variability. *J Hypertens.* (1993) 11:1133–7. doi: 10.1097/00004872-199310000-00019

15. Sander D, Kukla C, Klingelhöfer J, Winbeck K, Conrad B. Relationship between circadian blood pressure patterns and progression of early carotid atherosclerosis: A 3-year follow-up study. *Circulation.* (2000) 102:1536–41. doi: 10.1161/01.cir.102.13.1536

16. Goldstein IB, Bartzokis G, Guthrie D, Shapiro D. Ambulatory blood pressure and the brain: a 5-year follow-up. *Neurology.* (2005) 64:1846–52. doi: 10.1212/01.Wnl.0000164712.24389.Bb

17. Yang S, Yuan J, Qin W, Yang L, Fan H, Li Y, et al. Twenty-four-hour ambulatory blood pressure variability is associated with total magnetic resonance imaging burden of cerebral small-vessel disease. *Clin Interv Aging.* (2018) 13:1419–27. doi: 10.2147/cia.S171261

18. Goldstein IB, Bartzokis G, Guthrie D, Shapiro D. Ambulatory blood pressure and brain atrophy in the healthy elderly. *Neurology.* (2002) 59:713–9. doi: 10.1212/wnl.59.5.713

19. Nakanishi K, Jin Z, Homma S, Elkind MSV, Rundek T, Schwartz JE, et al. Night-time systolic blood pressure and subclinical cerebrovascular disease: the cardiovascular abnormalities and brain lesions (CABL) study. *Eur Heart J Cardiovasc Imag.* (2019) 20:765–71. doi: 10.1093/ehjci/jey221

20. Kim RE, Yun CH, Thomas RJ, Oh JH, Johnson HJ, Kim S, et al. Lifestyle-dependent brain change: a longitudinal cohort MRI study. *Neurobiol Aging.* (2018) 69:48–57. doi: 10.1016/j.neurobiolaging.2018.04.017

21. Kim RE, Lourens S, Long JD, Paulsen JS, Johnson HJ. Preliminary analysis using multi-atlas labeling algorithms for tracing longitudinal change. *Front Neurosci.* (2015) 9:242. doi: 10.3389/fnins.2015.00242

22. Young Kim E, Johnson HJ. Robust multi-site MR data processing: iterative optimization of bias correction, tissue classification, and registration. *Front Neuroinform.* (2013) 7:29. doi: 10.3389/fninf.2013.00029

23. Ghayoor A, Vaidya JG, Johnson HJ. Robust automated constellation-based landmark detection in human brain imaging. *Neuroimage.* (2018) 170:471–81. doi: 10.1016/j.neuroimage.2017.04.012

24. Wang H, Yushkevich PA. Multi-atlas segmentation with joint label fusion and corrective learning-an open source implementation. *Front Neuroinform.* (2013) 7:27. doi: 10.3389/fninf.2013.00027

25. Kim H, Au R, Thomas RJ, Yun CH, Lee SK, Han C, et al. Cognitive performance norms from the Korean genome and epidemiology study (KoGES). *Int Psychogeriatr.* (2017) 29:1909–24. doi: 10.1017/s1041610217000990

26. Genuth S, Alberti KG, Bennett P, Buse J, Defronzo R, Kahn R, et al. Follow-up report on the diagnosis of diabetes mellitus. *Diabetes Care.* (2003) 26:3160–7. doi: 10.2337/diacare.26.11.3160

27. Kim J, Pack A, Maislin G, Lee SK, Kim SH, Shin C. Prospective observation on the association of snoring with subclinical changes in carotid atherosclerosis over four years. *Sleep Med.* (2014) 15:769–75. doi: 10.1016/j.sleep.2014.03.009

28. Hughes D, Judge C, Murphy R, Loughlin E, Costello M, Whiteley W, et al. Association of blood pressure lowering with incident dementia or cognitive impairment: a systematic review and meta-analysis. *Jama.* (2020) 323:1934–44. doi: 10.1001/jama.2020.4249

29. de Havenon A, Anadani M, Prabhakaran S, Wong KH, Yaghi S, Rost N. Increased blood pressure variability and the risk of probable dementia or mild cognitive impairment: a *post-hoc* analysis of the sprint mind trial. *J Am Heart Assoc.* (2021) 10:e022206. doi: 10.1161/jaha.121.022206

30. Tully PJ, Yano Y, Launer LJ, Kario K, Nagai M, Mooijaart SP, et al. Association between blood pressure variability and cerebral small-vessel disease: a systematic review and meta-analysis. *J Am Heart Assoc.* (2020) 9:e013841. doi: 10.1161/jaha.119.013841

31. Gyanwali B, Vrooman H, Venketasubramanian N, Wong TY, Cheng CY, Chen C, et al. Cerebral small vessel disease and enlarged perivascular spaces-data from memory clinic and population-based settings. *Front Neurol.* (2019) 10:669. doi: 10.3389/fneur.2019.00669

32. Liu R, Chen H, Qin R, Gu Y, Chen X, Zou J, et al. The altered reconfiguration pattern of brain modular architecture regulates cognitive function in cerebral small vessel disease. *Front Neurol.* (2019) 10:324. doi: 10.3389/fneur.2019.00324

33. Fan Y, Xu Y, Shen M, Guo H, Zhang Z. Total cerebral small vessel disease burden on mri correlates with cognitive impairment in outpatients with amnestic disorders. *Front Neurol.* (2021) 12:747115. doi: 10.3389/fneur.2021.747115

34. Rouch L, De Souto Barreto P, Hanon O, Vidal JS, Amar J, Andrieu S, et al. Visit-to-visit blood pressure variability and incident frailty in older adults. *J Gerontol A Biol Sci Med Sci.* (2021) 76:1369–75. doi: 10.1093/gerona/glab112

35. Mone P, Pansini A, Calabrò F, De Gennaro S, Esposito M, Rinaldi P, et al. Global cognitive function correlates with P-wave dispersion in frail hypertensive older adults. *J Clin Hypertens.* (2022) 24:638–43. doi: 10.1111/jch.14439

36. Mone P, Gambardella J, Lombardi A, Pansini A, De Gennaro S, Leo AL, et al. Correlation of physical and cognitive impairment in diabetic and hypertensive frail older adults. *Cardiovasc Diabetol.* (2022) 21:10. doi: 10.1186/s12933-021-01442-z

37. Mone P, Pansini A, Frullone S, de Donato A, Buonincontri V, De Blasiis P, et al. Physical decline and cognitive impairment in frail hypertensive elders during COVID-19. *Eur J Intern Med.* (2022) 99:89–92. doi: 10.1016/j.ejim.2022.03.012

38. Matsue Y, Kamiya K, Saito H, Saito K, Ogasahara Y, Maekawa E, et al. Prevalence and prognostic impact of the coexistence of multiple frailty domains in elderly patients with heart failure: the FRAGILE-HF cohort study. *Eur J Heart Fail.* (2020) 22:2112–9. doi: 10.1002/ejhf.1926

39. Tsao A, Sugar J, Lu L, Wang C, Knierim JJ, Moser MB, et al. Integrating time from experience in the lateral entorhinal cortex. *Nature.* (2018) 561:57–62. doi: 10.1038/s41586-018-0459-6

40. Weiner KS, Zilles K. The anatomical and functional specialization of the fusiform gyrus. *Neuropsychologia.* (2016) 83:48–62. doi: 10.1016/j.neuropsychologia.2015.06.033

41. Wartolowska KA, Webb AJS. Midlife blood pressure is associated with the severity of white matter hyperintensities: analysis of the UK Biobank cohort study. *Eur Heart J.* (2021) 42:750–7. doi: 10.1093/eurheartj/ehaa756

42. Marcus J, Gardener H, Rundek T, Elkind MS, Sacco RL, Decarli C, et al. Baseline and longitudinal increases in diastolic blood pressure are associated with greater white matter hyperintensity volume: the northern Manhattan study. *Stroke.* (2011) 42:2639–41. doi: 10.1161/strokeaha.111.617571

43. Guo X, Pantoni L, Simoni M, Bengtsson C, Björkelund C, Lissner L, et al. Blood pressure components and changes in relation to white matter lesions: a 32-year prospective population study. *Hypertension.* (2009) 54:57–62. doi: 10.1161/hypertensionaha.109.129700

44. Moody DM, Brown WR, Challa VR, Ghazi-Birry HS, Reboussin DM. Cerebral microvascular alterations in aging, leukoaraiosis, and Alzheimer's disease. *Ann N Y Acad Sci.* (1997) 826:103–16. doi: 10.1111/j.1749-6632.1997.tb48464.x

45. Mancia G, Grassi G. Mechanisms and clinical implications of blood pressure variability. *J Cardiovasc Pharmacol.* (2000) 35:S15–9. doi: 10.1097/00005344-200000004-00003

46. Somers VK, Dyken ME, Mark AL, Abboud FM. Sympathetic-nerve activity during sleep in normal subjects. *N Engl J Med.* (1993) 328:303–7. doi: 10.1056/nejm199302043280502

47. Dettoni JL, Consolim-Colombo FM, Drager LF, Rubira MC, Souza SB, Irigoyen MC, et al. Cardiovascular effects of partial sleep deprivation in healthy volunteers. *J Appl Physiol.* (2012) 113:232–6. doi: 10.1152/japplphysiol.01604.2011

48. Sexton CE, Storsve AB, Walhovd KB, Johansen-Berg H, Fjell AM. Poor sleep quality is associated with increased cortical atrophy in community-dwelling adults. *Neurology.* (2014) 83:967–73. doi: 10.1212/wnl.0000000000000774

49. Benitez A, Gunstad J. Poor sleep quality diminishes cognitive functioning independent of depression and anxiety in healthy young adults. *Clin Neuropsychol.* (2012) 26:214–23. doi: 10.1080/13854046.2012.658439

frontiers | Frontiers in Neurology

TYPE Review
PUBLISHED 07 September 2022
DOI 10.3389/fneur.2022.929781

OPEN ACCESS

EDITED BY
Hansen Chen,
Stanford University, United States

REVIEWED BY
Colwyn Headley,
Stanford University, United States
Salvatore Fusco,
Catholic University of the Sacred Heart, Italy

*CORRESPONDENCE
Lina Sun
sunflm@126.com
Xiaohui Zhang
xhzhang@bnu.edu.cn
Chong Gao
gaoc@zucc.edu.cn

SPECIALTY SECTION
This article was submitted to Dementia and Neurodegenerative Diseases, a section of the journal Frontiers in Neurology

RECEIVED 27 April 2022
ACCEPTED 21 June 2022
PUBLISHED 07 September 2022

CITATION
Sun L, Liu T, Liu J, Gao C and Zhang X (2022) Physical exercise and mitochondrial function: New therapeutic interventions for psychiatric and neurodegenerative disorders. *Front. Neurol.* 13:929781. doi: 10.3389/fneur.2022.929781

Physical exercise and mitochondrial function: New therapeutic interventions for psychiatric and neurodegenerative disorders

Lina Sun[1,2]*, Tianbiao Liu[2], Jingqi Liu[2], Chong Gao[3]* and Xiaohui Zhang[1]*

[1]State Key Laboratory of Cognitive Neuroscience and Learning, Beijing Normal University, Beijing, China, [2]College of P.E and Sport, Beijing Normal University, Beijing, China, [3]Department of Clinical Medicine, Key Laboratory of Novel Targets and Drug Study for Neural Repair of Zhejiang Province, Institute of Brain and Cognitive Science, Zhejiang University City College, Hangzhou, China

Psychiatric and neurodegenerative diseases, including major depression disorder (MDD), bipolar disorder, and Alzheimer's disease, are a burden to society. Deficits of adult hippocampal neurogenesis (AHN) have been widely considered the main hallmark of psychiatric diseases as well as neurodegeneration. Herein, exploring applicable targets for improving hippocampal neural plasticity could provide a breakthrough for the development of new treatments. Emerging evidence indicates the broad functions of mitochondria in regulating cellular behaviors of neural stem cells, neural progenitors, and mature neurons in adulthood could offer multiple neural plasticities for behavioral modulation. Normalizing mitochondrial functions could be a new direction for neural plasticity enhancement. Exercise, a highly encouraged integrative method for preventing disease, has been indicated to be an effective pathway to improving both mitochondrial functions and AHN. Herein, the relative mechanisms of mitochondria in regulating neurogenesis and its effects in linking the effects of exercise to neurological diseases requires a systematic summary. In this review, we have assessed the relationship between mitochondrial functions and AHN to see whether mitochondria can be potential targets for treating neurological diseases. Moreover, as for one of well-established alternative therapeutic approaches, we summarized the evidence to show the underlying mechanisms of exercise to improve mitochondrial functions and AHN.

KEYWORDS

mitochondria, exercise, psychiatric diseases, neurodegenerative diseases, adult neurogenesis

Introduction

In recent decades, psychiatric or neurodegenerative diseases have attracted increased attention due to the growing number of patients. Psychiatric diseases such as depression disorder (MDD) and bipolar disorder usually see patients suffering from anxiety or depressive moods and changes in physical and emotional reactions that would be

exacerbated by even minor environmental changes (1, 2). As for neurodegenerative diseases such as Alzheimer's disease (AD) and Parkinson's disease (PD), the progressive death of neurons commonly induces irreversible neuronal cognitive deficits, motor disability, and complex behavioral dysregulation (3). The unidentified etiology of those diseases strongly limited the development of drugs to prevent the progress of behavioral abnormality. From the angle of symptomatic treatment, it is urgent and necessary to explore supplementary or alternative medicine for improving brain functions.

Neural plasticity provides the ability for the central nervous system (CNS) to adapt to environmental challenges under physiological and pathological conditions (4). In the adult hippocampus, neural plasticity refers to neurogenesis and synaptic plasticity, both of which perform critical roles in regulating emotional and cognitive behaviors. Adult neurogenesis was widely considered as a structural plasticity through its regulation of the neuronal population in certain brain regions. As for the target of alternative or integrative medicine, improving hippocampal neurogenesis could serve as a key therapeutic paradigm against neurological disorders without a clear pathological mechanism (5–7). For this reason, evaluating the mechanism of adult neurogenesis could help explore an applicable pathway to treat neurological diseases.

Emerging evidence indicates mitochondria have a key function in regulating the activity and fate commitment of stem cells (8). In addition, mitochondria have been recognized as key mediators in response to development of neurological disease (9). Physical exercise is an effective way to prevent chronic diseases, including diabetes, neurodegeneration, and psychiatric disorders (10, 11). Through metabolic regulating, exercise is beneficial to mitochondrial functions. It is noteworthy that mitochondria could be the linker between exercise and neurogenesis. Given this, it is necessary to summarize the effects of mitochondria in neural functions and its roles in disease development. In this review, we summarized the functions of mitochondria to regulate adult hippocampal neurogenesis and its potential regulators. Furthermore, we discussed the linkage role of mitochondria to bridge physical exercise and brain functional improvement.

Hippocampal plasticity and neurogenesis in neurological disorders

Adult neurogenesis is a temporal-spatial progress composed by the self-renewal fate commitment of neural stem cells (NSCs) as well as the maturation of neural progenitor cells (NPCs). In the hippocampus, neurogenesis provides the regenerative resources to clear panic memory (12, 13). The enhancement of hippocampal neurogenesis was shown to promote pattern separation behavior, which enables animals to discriminate between environmental cues related to stress experience (14). While declined hippocampal neurogenesis commonly results in an elevated fear response, which subsequently manifests as inappropriate, uncontrollable expression of fear in neutral and safe environments (15). These documents highlight the critical role of AHN in regulating antidepressant behaviors. The critical role of hippocampal neurogenesis in depressive moods could also be seen in an animal model of seizures, which was demonstrated to be triggered by antidepressants (16). The seizures animal model showed abnormal increase of adult neurogenesis with upregulated immature neuronal numbers in the hippocampal DG region (17). Another type of neural plasticity besides neurogenesis is synaptic plasticity, which includes synaptogenesis as well as synaptic functions like long-term potentiation (LTP) and pre-synaptic plasticity. Dysregulation of synaptic plasticity was also shown to be related to the development of neurological disorders. Immobilization-stressed mice presented intensified fear memory and enhanced long-term potentiation (LTP) (18). In terms of synaptic plasticity, adult neurogenesis can provide a regenerative resource to prevent the neurodegenerative progress and simultaneously enhance the ability in emotional regulation (19). Promoting the AHN was documented as an effective approach against psychiatric disorders, particularly depression. *In vivo* calcium imaging to record neuronal activity in the vDG (ventral dentate gyrus) demonstrated increased neurogenesis correlated to decreased activity of stress-responsive cells, which are active during attacks or while mice explore anxiogenic environments (20). Through conditional knockout of the Bcl-gene in NSCs, Sahay et al. established that there is enhanced AHN in mice and found that improving AHN was sufficient to prevent behavioral dysfunctions in a depression model (21). Additionally, blocking AHN with temozolomide (TMZ) could also result in the comprised therapeutic effects of antidepressants such as SSRIs (selective serotonin reuptake inhibitors) and ketamine (22, 23). Thus, exploring factors in regulating ANH would offer the new drug targets for treating neurological diseases.

Mitochondrial function and hippocampal plasticity and neurogenesis

Biological regulation of mitochondria involves multiple aspects, including their metabolism, biogenesis, fission, and fusion dynamics and degradation *via* autophagy. Accumulating evidence has been reported to show that all these biological events participate in the regulation of AHN at different levels or conditions (Table 1). Cell metabolism plays a fundamental role in multiple biological events, including energy supply, cell growth, differentiation, and death. During the self-renewal and differentiation process, stem cells undergo a dramatic metabolic reprogram. At an adult hippocampus, the metabolism

TABLE 1 Mitochondrial biology in regulating AHNs in different aspects.

Research model	Mitochondrial biology	AHNs events	References
Normal adult mice	Mitochondrial mass and dynamics	Enhanced neuron maturation	(24)
Linage tracing mice model	Mitochondrial dynamics	Daughter cells directs between self-renew or differentiation	(25)
Drosophila multipotent hematopoietic progenitors (like human mammalian myeloid progenitors)	ROS scavenge	Prevented the differentiation	(26)
Human embryonic stem cells	SIRT1 downregulation	Neuroretinal morphogenesis	(27)
Optic atrophy	Perturbation of inner mitochondrial membrane	Atrophy of retinal RGCs	(28)
Amyotrophic lateral sclerosis	Mitochondrial fragmentation, disruption of ETC, reduced ATP production and oxidative stress	Increase in proliferation in the SVZ but decrease in proliferation in the SGZ	(29, 30)
Stroke model	ETC disruption and impaired ATP production	Increased proliferation and death of neuroblasts	(31)
Alzheimer's disease model		Increased NSCs and immature neurons in hippocampus	(32, 33)

pattern of NSCs undergoes the switch from glycolysis to oxidative phosphorylation (OXPHOS) following the process of neuronal differentiation (34). In mature neurons, mitochondrial OXPHOS provides high amounts of energy to meet the requirement of neuronal electrophysiological activities (35, 36). Numerous mitochondrial mediators could be applied as therapeutic targets not only for metabolic regulating but also to improve AHN.

Mitochondrial metabolism in regulating neurogenesis

Mitochondria have been primarily identified as cellular organelles that provide energy. In neurons, mitochondrial dysfunction is reported to be involved in multiple neurodegenerative or psychiatric diseases (37, 38). Dysregulated AHN induced by abnormal mitochondrial function is one of the main reasons to these diseases. According to the environmental changes, quiescent NSCs in the hippocampus are undergoing extensive changes along with proliferative activity, cellular growth, and synaptic growth. Adult NSCs display astroglia features, including 100% GFAP expression, as well as glycolytic cellular metabolisms pattern (39). Following neurogenesis, mature neurons require high amounts of ATP for their biological functions, such as presynaptic vesicle recycling. Mature neurons integrated in neural circuits are highly dependent on the mitochondrial electron transport chain (ETC) and OXPHOS (40–42). Single cell transcriptomics shows the dramatic upregulating profile of OXPHOS-related genes during the neural lineage commitment of hippocampal NSCs. Moreover, specific ablation of mitochondrial transcription factor A (Tfam) in adult NSCs reproduces multiple hallmarks of aging in the hippocampus, including declined neurogenesis. Such alteration could be reversed by pharmacological enhancement of mitochondrial function (34). The evidence suggests mitochondrial metabolism has a critical role in regulating hippocampal neurogenesis and relative physiological process. Suppressing mitochondrial OXPHOS could also affect the other types of adult stem cells. In hematopoietic stem cell (HSCs), deleting PTEN-like mitochondrial phosphatase Ptpmt1 could lead to defective hematopoiesis with impaired differentiation of HSCs (43). Additionally, the metabolic pattern of cells could shift from mitochondrial OXPHOS to glycolysis during the reprogramming process of the inducible pluripotent stem cells (iPSCs), indicating that mitochondria also act critically in embryonic stem cells (44). Generally, switching of mitochondrial function is commonly associated with the energetic demands of stem cells to meet the requirement of their self-renewal or differentiation. Most neurological drugs that are widely used in clinic reportedly have an effect on metabolic regulation. Indeed, mitochondria are widely reported as the target for improving brain functions. The brain functional recovery drug piracetam was documented to prevent declined neurogenesis *via* promoting mitochondrial metabolism in an aging model (34, 45). Antioxidants could also reserve the functions of mitochondria (46). However, it is noteworthy that exercise may elevate the level of radial oxidative species (ROS), which has been recently declared as a mechanism in

antidiabetic effects (47). Since antioxidant and exercise can provide effects similar to those of mitochondria, a certain level of ROS might serve as the "second messenger" to promote the fate commitment of the NSCs at the physiological level (48). Hence, exercise could be an effective way to control the level of ROS into physiological reasonable by promoting mitochondrial OXPHOS.

Mitochondria dynamics and NSCs behaviors

Mitochondria are constantly varying between being fragmented or filamentous networks to adapt to the requirements of cellular functions. According to different energetic demands of the stem cells stage between self-renewal and differentiation, dynamics alterations of mitochondrial morphology are critical in regulating stemness (49). Mitochondrial elongation commonly occurs in aging skeletal muscle cells with increased mitochondrial fusion protein MFN1/2 and the accumulated mutation of mitochondrial DNA (50). Following the neural commitment of NSCs, mitochondria shift from the elongated morphology to fragmentation. On the cell metabolic level, increasing mitochondrial fragments are associated with enhanced OXPHOS and production of ROS, previously mentioned as the second messenger to stimulate downstream signaling like NRF2 and downregulate Notch1 for lineage commitment determination (48). Sirtuins were also considered as regulators to link mitochondrial dynamics with adult neurogenesis (25). Physical exercise, the well-known upregulator of SIRT3 and lipid metabolism, could enhance adult neurogenesis in an unpredictable chronic stress depression model (51). Hypoxia inducible factor (HIF) signaling also provides the link between oxygen levels and mitochondrial dynamics (52, 53). The activation of the HIF complex under hypoxia ensures that energy demands meet pathological conditions by increasing levels of glycolytic enzymes and inhibiting oxygen consumption (54). Such mechanisms also mediate self-derived neural repair under stress. In the hypoxia condition, activation of HIF induces NSCs proliferation and switched their migration in subventricular zone, which promotes regenerative progress in infarction region (55). HIF deletion, however, can impair the AHN and induce learning and memory deficit (56). Therefore, mitochondrial dynamics-mediated redox/oxidative status plays a key role in regulating AHN.

Mitophagy in regulating neurogenesis

In starvation conditions, autophagy could be rapidly activated to provides a cell with nutrients to survive (57). The selective autophagy of mitochondria, also known as mitophagy, can be processed such that damaged or unwanted mitochondria require degradation (58). As differentiation of stem cells involves extensive cellular remodeling, autophagy ensures the elimination of unnecessary cellular components to maintain an optimal cellular status. It was demonstrated that pretreatment of antioxidant N-acetylcysteine (NAC) attenuated oxidative stress-induced NSCs' self-renewal disruption by suppressing autophagy signaling mTOR and decreased LC3B-II protein expression (59). In contrast, enhancing autophagy in aged satellite cells prevented the senescence and restored regenerative properties (60). Herein, it could hypothesize that mitochondrial morphology is another effect pathway to regulate mitochondrial dynamics in NSCs. At a physiological level, certain levels of mitophagy might be necessary for controlling the differentiation of adult NSCs. However, there is no systematic evidence that indicates the exact mechanisms of mitophagy to regulate the differentiation and self-renewal of adult NSCs.

Targeting mitochondria in neurological disease treatment

At the cell level, mitochondrial alterations could be regarded as a hallmark for stem cell differentiation. Consistently, impairment of AHN is a well-established biological hallmark of psychiatric diseases and neurodegeneration at the tissue level. Such a relationship indicates that mitochondria could perform be a therapeutic target for neurological diseases. An increasing number of clinical reports have demonstrated substantial mitochondrial damage could contribute to the development of depression and cognitive impairments. Deletion of mtDNA in a child was associated with mitochondrial disease symptoms and mild–moderate unipolar depression (61). Blood sample measurement of mtDNA in bipolar disorder (BD) and MDD patients also showed a lower mtDNA copy number than in controls (62). Another report demonstrated a significant reduction of mtDNA copy numbers in combat PTSD (63), indicating mtDNA or the mitochondrial mass abnormality could be the general phenomena correlated with psychiatric diseases. On the other hand, mitochondria perform as the therapeutic target to psychiatric diseases. SSRIs (selective serotonin reuptake inhibitors) like the antidepressant fluoxetine could promote mitophagy by increasing colocalization of autophagosomes and mitochondria, which thereby eliminates damaged mitochondria in corticosterone-treated astrocytes (64). McCoy et al. compared high novelty responder rats (HRs), which show highly exploratory behavior in a novel environment as well as remarkable resilience to chronic mild stress, and low novelty responder rats (LRs), which are susceptible to chronic stress. They observed that LRs displayed higher cytochrome c oxidase (COX) activity in the dentate gyrus, prefrontal cortex, and dorsal raphe compared to HRs (65). Apart from selected brain regions, a declining skeletal muscle mitochondrial

function in aging adults was also shown to be associated with clinically significant depressive symptoms (66). These lines of evidence support the critical regulatory roles of mitochondria in antidepressant functions.

Environmental factors could also induce psychiatric diseases *via* affecting mitochondrial functions. Glombik et al. reported that maternal stress leads to depression-like behaviors in the offspring of rats; they displayed brain mitochondrial abnormalities, including significant downregulation of Ndufv2 (complex I) (67). Animal studies have suggested that mitochondrial abnormalities were augmented by stress, indicating mitochondria are stress-response modulators and contribute to the stress-induced pathophysiology of psychiatric diseases (68). A possible mechanism might be an enhanced requirement of the neural activity during learning or memory coding, which could induce increased mitochondrial respiration and thereby produce more metabolic products to influence the signaling pathways downstream, e.g., ROS and RNS.

Accumulating evidence suggests that improving mitochondrial functions could help the treatment of neurodegeneration (69, 70). The complex I inhibitor rotenone could be utilized as a PD model for drug development (71). The impairment of complex I was associated with reduced ATP levels, oxidative stress, and calcium-mediated damage in such a pathological model (72). In post-mortem tissue of sporadic AD, scientists found mitochondrial dysfunction is correlated with decreased levels of ATP (73). Growing evidence indicated the medications targeting on mitochondria exert the therapeutic effects to neurodegenerative. Metformin, a type-2 diabetes drug approved by the FDA, was shown to enhance adult neurogenesis and showed promising effects on an animal model of AD and PD (74, 75). Another example is the glycogen-like peptide-(GLP-1) analog. It has been reported that the GLP-1 analog could promote adult neurogenesis and attenuate the behavioral dysfunctions in neurodegenerative disorders including PD and AD (76, 77). Herein, improving mitochondrial functions could also result in protective effects against neurodegeneration.

Physical exercise and mitochondrial function

Alternative and integrative medicine are increasingly proposed as effective strategies to treat psychiatric and neurodegenerative disorders. Due to safety concerns regarding the tolerability and risk of medications (78), an effective alternative therapy is highly requested to attenuate the behavioral disorders. As for neurodegeneration, early prevention of the diseases is currently the most effective strategy due to the limited effects of drugs to halt or prevent the progress of the neuron death. Physical exercise is widely recognized as being part of a healthy lifestyle partly due to its promotion of the maintenance of lifelong mitochondrial quality control (79). Exercise has been increasingly reported for its improvement of adult neurogenesis in both physiological and pathological conditions (80–82). Exercise improves mitochondrial functions *via* its multiple biological effects. It was demonstrated that exercise promoted the production of brain-derived neurotrophic factor (BDNF) levels and could alter mitochondrial function, neuroplasticity, and the rate of apoptosis in the hippocampus and thereby prevented the occurrence of PTSD (83). In a maternal separation depression model, exercise could alter mitochondrial function, serotonin levels, and the rate of apoptosis (84). Herein, mitochondrial functions perform as the linkage between exercise and its neuroprotective effects.

Exercise-mediated mitochondrial functions in neurogenic effects

In aged mice, physical exercise significantly increased DRP1 protein levels and elevated the rates of respiration and ROS production in mitochondria, which is suggestive of its potential in improving brain functions *via* its regulating mitochondrial electron transport chain function and dynamics (85). In an animal model of Alzheimer's disease, 1 h of swimming exercise for 6 days/week consolidated the intact of mitochondrial cristae and edges, raised the brain ATP production as well as the number of synapses by regulating the expression of GLUT1 and GLUT3 expression levels (86). Antidepressant action of running was highly correlated with an increase of hippocampal neurogenesis and plasticity (81). Compared with its promotion of NSCs' proliferation, the accelerating effects of exercise have a longer latency period (about 2 weeks) on the maturation of new neurons (87). Moreover, structural magnetic resonance imaging suggested hippocampus and brain cortex growth in schizophrenia patients and healthy controls after the endurance aerobic physical training. This evidence indicates exercise can also serve as a promising candidate for pathophysiology-based add-on interventions for schizophrenia (88). A recent study indicates that free wheel running could promote the activation of the quiescent NSCs in the hippocampus by regulating cellular ROS level (89). Therefore, exercise could engage broad effects of neural functions *via* multiple molecular mechanisms.

Multiple effects of exercise in brain tissue

Exercise could exert multiple biological effects in additional to its roles in mitochondrial functions. Brain inflammation is another key target of exercise for neural tissue. A recent study showed the systematic regulatory mechanism of exercise influenced adult neurogenesis. Injecting plasma derived from voluntary running mice resulted in elevated density of hippocampal DCX^{+} neurons correlating with

improved working memory, which were shown to rely on the inflammatory regulation *via* clusterin (90). This report further suggested the effects of exercise mediated AHN may depend on its effects on the peripheral circulation system. It was indicated that LPS could reduce the number of new neurons in aged but not adult mice, while such dysfunctions could be prevented by free wheel running (91). Exercise could also attenuate the inflammatory response in subjects with depression. A study on 61 university students assigned to 6 weeks of different models of exercise including high-intensity interval training (HIT), moderate continuous training (MCT), or no exercise (CON) suggested that MCT exercise could have a positive effect on the promotion of mental health by decreasing TNF-α level (92). Neuroinflammation has been suggested to negatively affect adult

TABLE 2 Functional impacts of exercise on neuronal mitochondrial fitness/health.

Exercise model	Impacts to mitochondria	Impacts to neural tissue	References
Wheel running	Promoted autophagy/lysosome system	No direct evidence	(95)
High-intensity exercise	Activated partial mitochondrial biogenesis	Promoted AHN, attenuated the inflammation	(96)
Regular running exercise	Activated POMC neuronal mitohormesis	Induced the hypothalamic mediated thermogenesis	(97)
Treadmill exercise	Increase mitochondrial biogenesis and OXPHOS level	Possible protective effects to PD animal model	(98)
Treadmill exercise	Prevented mitochondria-mediated caspase-dependent apoptotic pathways	Suppressed neural apoptosis in aging model	(99)
Voluntary exercise	Increased oxygen consumption and ATP production *via* oxidative phosphorylation	Improved dopaminergic functions in PD model	(100)
Low-intensity treadmill	Attenuated apoptosis, H_2O_2 emission and permeability transition pore	Elevated cognitive function and neurogenesis	(101)
Treadmill exercise	Increased TFAM	Decreased the expression of BAD and BAX, increased the expression of BCL-2	(102)
Treadmill exercise	Inhibited mitochondrial outer membrane permeabilization	Reduced neurobehavioral scores and cerebral infarction volumes in stroke model	(103)

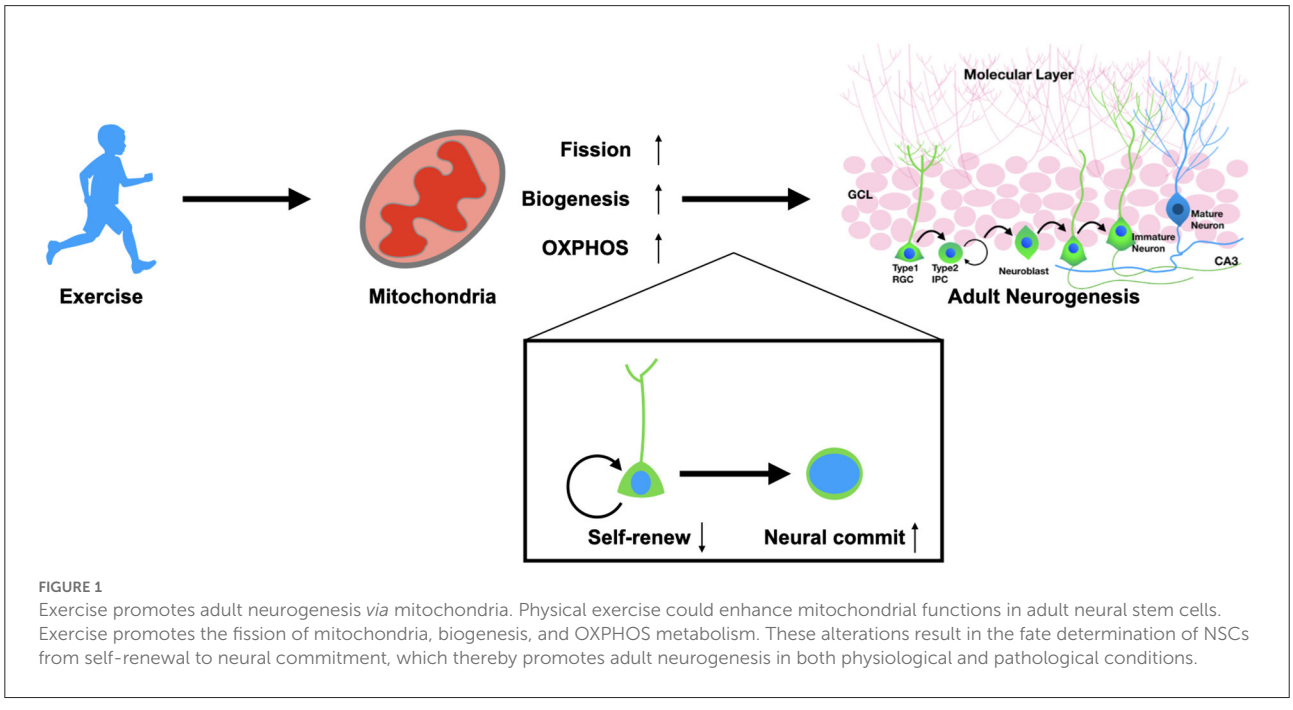

FIGURE 1
Exercise promotes adult neurogenesis *via* mitochondria. Physical exercise could enhance mitochondrial functions in adult neural stem cells. Exercise promotes the fission of mitochondria, biogenesis, and OXPHOS metabolism. These alterations result in the fate determination of NSCs from self-renewal to neural commitment, which thereby promotes adult neurogenesis in both physiological and pathological conditions.

neurogenesis, and physical exercise could promote AHN by buffering the inflammation response in neural tissue (93). The activation of microglia mediated the proinflammatory factors, including interleukin-6, TNF-α, ROS, and nitric oxide, which all have anti-neurogenic properties (94). Table 2 summarizes the recent evidence in support of the effects of exercise, showing different patterns of mitochondrial biology as well as neuronal functions (Table 2). However, limited evidence has shown the possible role of mitochondria during exercise and their ability to mediate the functions of neural tissue, particularly adult NSCs.

Conclusion

Mitochondria are key organelles in the mediation of energy functions. Based on this mechanism, recent studies have demonstrated that mitochondria mediate multiple cellular behaviors that are far beyond energy supply, e.g., the fate commitment and proliferation of somatic stem cells as well as the reprogramming and differentiation process of pluripotent stem cells (104, 105). Improving mitochondrial function has also been considered a therapeutic strategy against neurological diseases. Therapeutic approaches targeting mitochondria should focus on future pre-clinical exploration for treating neurodegenerative and psychiatric disorders. Mitochondria play the critical roles in regulating stem cell behaviors including self-renew and fate commitment of the adult NSCs (Figure 1). Therefore, a systematic strategy to improve mitochondrial functions throughout the body is preferable; we should not only promote neuronal regeneration but also focus on regulating the NSCs environment, including the peripheral factors and the neurogenic niche. With such requirements, exercise is the ideal option, accompanied as it is by considerable healing effects and relatively few safety issues.

Author contributions

All authors listed have made a substantial, direct, and intellectual contribution to the work and approved it for publication.

Funding

This work was supported by National Natural Science Foundation of China (32000835), and Open Research Fund of the State Key Laboratory of Cognitive Neuroscience and Learning (CNLZD2104).

Conflict of interest

The authors declare that the research was conducted in the absence of any commercial or financial relationships that could be construed as a potential conflict of interest.

Publisher's note

All claims expressed in this article are solely those of the authors and do not necessarily represent those of their affiliated organizations, or those of the publisher, the editors and the reviewers. Any product that may be evaluated in this article, or claim that may be made by its manufacturer, is not guaranteed or endorsed by the publisher.

References

1. Cohen JA, Deblinger E, Mannarino AP, Steer RA. A multisite, randomized controlled trial for children with sexual abuse-related PTSD symptoms. *J Am Acad Child Adolesc Psychiatry.* (2004) 43:393–402. doi: 10.1097/00004583-200404000-00005

2. Raskind MA, Peskind ER, Kanter ED, Petrie EC, Radant A, Thompson CE, et al. Reduction of nightmares and other PTSD symptoms in combat veterans by prazosin: a placebo-controlled study. *Am J Psychiatry.* (2003) 160:371–3. doi: 10.1176/appi.ajp.160.2.371

3. Breijyeh Z, Karaman R. Comprehensive review on Alzheimer's disease: causes and treatment. *Molecules.* (2020) 25:25245789. doi: 10.3390/molecules25245789

4. Sharma N, Classen J, Cohen LG. Neural plasticity and its contribution to functional recovery. *Handb Clin Neurol.* (2013) 110:3–12. doi: 10.1016/B978-0-444-52901-5.00001-0

5. Adamec RE, Blundell J, Burton P. Relationship of the predatory attack experience to neural plasticity, pCREB expression and neuroendocrine response. *Neurosci Biobehav Rev.* (2006) 30:356–75. doi: 10.1016/j.neubiorev.2005.04.004

6. Nissen C, Holz J, Blechert J, Feige B, Riemann D, Voderholzer U, et al. Learning as a model for neural plasticity in major depression. *Biol Psychiatry.* (2010) 68:544–52. doi: 10.1016/j.biopsych.2010.05.026

7. Phillips ML, Ladouceur CD, Drevets WC. A neural model of voluntary and automatic emotion regulation: implications for understanding the pathophysiology and neurodevelopment of bipolar disorder. *Mol Psychiatry 13 829.* (2008) 833–57. doi: 10.1038/mp.2008.65

8. Khacho M, Harris R, Slack RS. Mitochondria as central regulators of neural stem cell fate and cognitive function. *Nat Rev Neurosci.* (2019) 20:34–48. doi: 10.1038/s41583-018-0091-3

9. Kim Y, Vadodaria KC, Lenkei Z, Kato T, Gage FH, Marchetto MC, et al. Mitochondria, metabolism, and redox mechanisms in psychiatric disorders. *Antioxid Redox Signal.* (2019) 31:275–317. doi: 10.1089/ars.2018.7606

10. Barnes JN. Exercise, cognitive function, and aging. *Adv Physiol Educ.* (2015) 39:55–62. doi: 10.1152/advan.00101.2014

11. Jenkins DW, Jenks A. Exercise and diabetes: a narrative review. *J Foot Ankle Surg.* (2017) 56:968–74. doi: 10.1053/j.jfas.2017.06.019

12. Clelland CD, Choi M, Romberg C, Clemenson GDJr, Fragniere A, Tyers P, et al. A functional role for adult hippocampal neurogenesis in spatial pattern separation. *Science.* (2009) 325:210–3. doi: 10.1126/science.1173215

13. Kheirbek MA, Klemenhagen KC, Sahay A, Hen R. Neurogenesis and generalization: a new approach to stratify and treat anxiety disorders. *Nat Neurosci.* (2012) 15:1613–20. doi: 10.1038/nn.3262

14. Sahay A, Scobie KN, Hill AS, O'Carroll CM, Kheirbek MA, Burghardt NS, et al. Increasing adult hippocampal neurogenesis is sufficient to improve pattern separation. *Nature.* (2011) 472:466–70. doi: 10.1038/nature09817

15. Besnard A, Sahay A. Adult hippocampal neurogenesis, fear generalization, and stress. *Neuropsychopharmacology.* (2016) 41:24–44. doi: 10.1038/npp.2015.167

16. Gorska N, Slupski J, Cubala WJ, Wiglusz MS, Galuszko-Wegielnik M. Antidepressants in epilepsy. *Neurol Neurochir Pol.* (2018) 52:657–61. doi: 10.1016/j.pjnns.2018.07.005

17. Lybrand ZR, Goswami S, Zhu J, Jarzabek V, Merlock N, Aktar M, et al. A critical period of neuronal activity results in aberrant neurogenesis rewiring hippocampal circuitry in a mouse model of epilepsy. *Nat Commun.* (2021) 12:1423. doi: 10.1038/s41467-021-21649-8

18. Nijholt I, Farchi N, Kye M, Sklan EH, Shoham S, Verbeure B, et al. Stress-induced alternative splicing of acetylcholinesterase results in enhanced fear memory and long-term potentiation. *Mol Psychiatry.* (2004) 9:174–83. doi: 10.1038/sj.mp.4001446

19. Mahar I, Bambico FR, Mechawar N, Nobrega JN. Stress, serotonin, and hippocampal neurogenesis in relation to depression and antidepressant effects. *Neurosci Biobehav Rev.* (2014) 38:173–92. doi: 10.1016/j.neubiorev.2013.11.009

20. Anacker C, Luna VM, Stevens GS, Millette A, Shores R, Jimenez JC, et al. Hippocampal neurogenesis confers stress resilience by inhibiting the ventral dentate gyrus. *Nature.* (2018) 559:98–102. doi: 10.1038/s41586-018-0262-4

21. Hill AS, Sahay A, Hen R. Increasing adult hippocampal neurogenesis is sufficient to reduce anxiety and depression-like behaviors. *Neuropsychopharmacology.* (2015) 40:2368–78. doi: 10.1038/npp.2015.85

22. Ma Z, Zang T, Birnbaum SG, Wang Z, Johnson JE, Zhang CL, et al. TrkB dependent adult hippocampal progenitor differentiation mediates sustained ketamine antidepressant response. *Nat Commun.* (2017) 8:1668. doi: 10.1038/s41467-017-01709-8

23. Santarelli L, Saxe M, Gross C, Surget A, Battaglia F, Dulawa S, et al. Requirement of hippocampal neurogenesis for the behavioral effects of antidepressants. *Science.* (2003) 301:805–9. doi: 10.1126/science.1083328

24. Steib K, Schaffner I, Jagasia R, Ebert B, Lie DC. Mitochondria modify exercise-induced development of stem cell-derived neurons in the adult brain. *J Neurosci.* (2014) 34:6624–33. doi: 10.1523/JNEUROSCI.4972-13.2014

25. Iwata R, Casimir P, Vanderhaeghen P. Mitochondrial dynamics in postmitotic cells regulate neurogenesis. *Science.* (2020) 369:858–62. doi: 10.1126/science.aba9760

26. Owusu-Ansah E, Banerjee U. Reactive oxygen species prime Drosophila haematopoietic progenitors for differentiation. *Nature.* (2009) 461:537–41. doi: 10.1038/nature08313

27. Calvanese V, Lara E, Suarez-Alvarez B, Abu Dawud R, Vazquez-Chantada M, Martinez-Chantar ML, et al. Sirtuin 1 regulation of developmental genes during differentiation of stem cells. *Proc Natl Acad Sci USA.* (2010) 107:13736–41. doi: 10.1073/pnas.1001399107

28. Alavi MV, Fuhrmann N. Dominant optic atrophy, OPA1, and mitochondrial quality control: understanding mitochondrial network dynamics. *Mol Neurodegener.* (2013) 8:32. doi: 10.1186/1750-1326-8-32

29. Galan L, Gomez-Pinedo U, Guerrero A, Garcia-Verdugo JM, Matias-Guiu J. Amyotrophic lateral sclerosis modifies progenitor neural proliferation in adult classic neurogenic brain niches. *BMC Neurol.* (2017) 17:173. doi: 10.1186/s12883-017-0956-5

30. Muyderman H, Chen T. Mitochondrial dysfunction in amyotrophic lateral sclerosis - a valid pharmacological target? *Br J Pharmacol.* (2014) 171:2191–205. doi: 10.1111/bph.12476

31. Marti-Fabregas J, Romaguera-Ros M, Gomez-Pinedo U, Martinez-Ramirez S, Jimenez-Xarrie E, Marin R, et al. Proliferation in the human ipsilateral subventricular zone after ischemic stroke. *Neurology.* (2010) 74:357–65. doi: 10.1212/WNL.0b013e3181cbccec

32. Boekhoorn K, Joels M, Lucassen PJ. Increased proliferation reflects glial and vascular-associated changes, but not neurogenesis in the presenile Alzheimer hippocampus. *Neurobiol Dis.* (2006) 24:1–14. doi: 10.1016/j.nbd.2006.04.017

33. Jin K, Peel AL, Mao XO, Xie L, Cottrell BA, Henshall DC, et al. Increased hippocampal neurogenesis in Alzheimer's disease. *Proc Natl Acad Sci USA.* (2004) 101:343–7. doi: 10.1073/pnas.2634794100

34. Beckervordersandforth R, Ebert B, Schaffner I, Moss J, Fiebig C, Shin J, et al. Role of mitochondrial metabolism in the control of early lineage progression and aging phenotypes in adult hippocampal neurogenesis. *Neuron.* (2017) 93:60–573 e566. doi: 10.1016/j.neuron.2016.12.017

35. Kann O. The interneuron energy hypothesis: implications for brain disease. *Neurobiol Dis.* (2016) 90:75–85. doi: 10.1016/j.nbd.2015.08.005

36. Kwon SK, Sando R. 3rd, Lewis TL, Hirabayashi Y, Maximov A, Polleux F. LKB1 regulates mitochondria-dependent presynaptic calcium clearance and neurotransmitter release properties at excitatory synapses along cortical axons. *PLoS Biol.* (2016) 14:e1002516. doi: 10.1371/journal.pbio.1002516

37. Chen J, Vitetta L. Mitochondria could be a potential key mediator linking the intestinal microbiota to depression. *J Cell Biochem.* (2020) 121:17–24. doi: 10.1002/jcb.29311

38. Joshi AU, Minhas PS, Liddelow SA, Haileselassie B, Andreasson KI, Dorn GW, et al. Fragmented mitochondria released from microglia trigger A1 astrocytic response and propagate inflammatory neurodegeneration. *Nat Neurosci.* (2019) 22:1635–48. doi: 10.1038/s41593-019-0486-0

39. Alberini CM, Cruz E, Descalzi G, Bessieres B, Gao V. Astrocyte glycogen and lactate: New insights into learning and memory mechanisms. *Glia.* (2018) 66:1244–62. doi: 10.1002/glia.23250

40. Alle H, Roth A, Geiger JR. Energy-efficient action potentials in hippocampal mossy fibers. *Science.* (2009) 325:1405–8. doi: 10.1126/science.1174331

41. Attwell D, Laughlin SB. An energy budget for signaling in the grey matter of the brain. *J Cereb Blood Flow Metab.* (2001) 21:1133–45. doi: 10.1097/00004647-200110000-00001

42. Hall CN, Klein-Flugge MC, Howarth C, Attwell D. Oxidative phosphorylation, not glycolysis, powers presynaptic and postsynaptic mechanisms underlying brain information processing. *J Neurosci.* (2012) 32:8940–51. doi: 10.1523/JNEUROSCI.0026-12.2012

43. Yu WM, Liu X, Shen J, Jovanovic O, Pohl EE, Gerson SL, et al. Metabolic regulation by the mitochondrial phosphatase PTPMT1 is required for hematopoietic stem cell differentiation. *Cell Stem Cell.* (2013) 12:62–74. doi: 10.1016/j.stem.2012.11.022

44. Folmes CD, Nelson TJ, Martinez-Fernandez A, Arrell DK, Lindor JZ, Dzeja PP, et al. Somatic oxidative bioenergetics transitions into pluripotency-dependent glycolysis to facilitate nuclear reprogramming. *Cell Metab.* (2011) 14:264–71. doi: 10.1016/j.cmet.2011.06.011

45. Stockburger C, Miano D, Pallas T, Friedland K, Muller WE. Enhanced neuroplasticity by the metabolic enhancer piracetam associated with improved mitochondrial dynamics and altered permeability transition pore function. *Neural Plast.* (2016) 2016:8075903. doi: 10.1155/2016/8075903

46. Oyewole AO, Birch-Machin MA. Mitochondria-targeted antioxidants. *FASEB J.* (2015) 29:4766–71. doi: 10.1096/fj.15-275404

47. Watson JD. Type 2 diabetes as a redox disease. *Lancet.* (2014) 383:841–3. doi: 10.1016/S0140-6736(13)62365-X

48. Khacho M, Clark A, Svoboda DS, Azzi J, MacLaurin JG, Meghaizel C, et al. Mitochondrial dynamics impacts stem cell identity and fate decisions by regulating a nuclear transcriptional program. *Cell Stem Cell.* (2016) 19:232–47. doi: 10.1016/j.stem.2016.04.015

49. Chen H, Chan DC. Mitochondrial dynamics in regulating the unique phenotypes of cancer and stem cells. *Cell Metab.* (2017) 26:39–48. doi: 10.1016/j.cmet.2017.05.016

50. Berliocchi L, Maiaru M, Varano GP, Russo R, Corasaniti MT, Bagetta G, et al. Spinal autophagy is differently modulated in distinct mouse models of neuropathic pain. *Mol Pain.* (2015) 11:3. doi: 10.1186/1744-8069-11-3

51. Santos SS, Moreira JB, Costa M, Rodrigues RS, Sebastiao AM, Xapelli S, et al. The mitochondrial antioxidant sirtuin3 cooperates with lipid metabolism to safeguard neurogenesis in aging and depression. *Cells.* (2021) 11:11010090. doi: 10.3390/cells11010090

52. Chen X, Yao JM, Fang X, Zhang C, Yang YS, Hu CP, et al. Hypoxia promotes pulmonary vascular remodeling via HIF-1alpha to regulate mitochondrial dynamics. *J Geriatr Cardiol.* (2019) 16:855–71. doi: 10.11909/j.issn.1671-5411.2019.12.003

53. Jiang N, Zhao H, Han Y, Li L, Xiong S, Zeng L, et al. HIF-1alpha ameliorates tubular injury in diabetic nephropathy via HO-1-mediated control of mitochondrial dynamics. *Cell Prolif.* (2020) 53:e12909. doi: 10.1111/cpr.12909

54. Kim JW, Tchernyshyov I, Semenza GL, Dang CV. HIF-1-mediated expression of pyruvate dehydrogenase kinase: a metabolic switch required for cellular adaptation to hypoxia. *Cell Metab.* (2006) 3:177–85. doi: 10.1016/j.cmet.2006.02.002

55. Chen X, Zhou B, Yan T, Wu H, Feng J, Chen H, et al. Peroxynitrite enhances self-renewal, proliferation and neuronal differentiation of neural stem/progenitor cells through activating HIF-1alpha and Wnt/beta-catenin signaling pathway. *Free Radic Biol Med.* (2018) 117:158–67. doi: 10.1016/j.freeradbiomed.2018.02.011

56. Carrica L, Li L, Newville J, Kenton J, Gustus K, Brigman J, et al. Genetic inactivation of hypoxia inducible factor 1-alpha (HIF-1alpha) in adult hippocampal progenitors impairs neurogenesis and pattern discrimination learning. *Neurobiol Learn Mem.* (2019) 157:79–85. doi: 10.1016/j.nlm.2018.12.002

57. Leidal AM, Levine B, Debnath J. Autophagy and the cell biology of age-related disease. *Nat Cell Biol.* (2018) 20:1338–48. doi: 10.1038/s41556-018-0235-8

58. Gustafsson AB, Dorn GW 2nd. Evolving and expanding the roles of mitophagy as a homeostatic and pathogenic process. *Physiol Rev.* (2019) 99:853–92. doi: 10.1152/physrev.00005.2018

59. Xiong G, Zhao L, Yan M, Wang X, Zhou Z, Chang X. N-acetylcysteine alleviated paraquat-induced mitochondrial fragmentation and autophagy in primary murine neural progenitor cells. *J Appl Toxicol.* (2019) 39:1557–67. doi: 10.1002/jat.3839

60. Garcia-Prat L, Martinez-Vicente M, Perdiguero E, Ortet L, Rodriguez-Ubreva J, Rebollo E, et al. Autophagy maintains stemness by preventing senescence. *Nature.* (2016) 529:37–42. doi: 10.1038/nature16187

61. Koene S, Kozicz TL, Rodenburg RJ, Verhaak CM, de Vries MC, Wortmann S, et al. Major depression in adolescent children consecutively diagnosed with mitochondrial disorder. *J Affect Disord.* (2009) 114:327–32. doi: 10.1016/j.jad.2008.06.023

62. Tsujii N, Otsuka I, Okazaki S, Yanagi M, Numata S, Yamaki N, et al. Mitochondrial DNA copy number raises the potential of left frontopolar hemodynamic response as a diagnostic marker for distinguishing bipolar disorder from major depressive disorder. *Front Psychiatry.* (2019) 10:312. doi: 10.3389/fpsyt.2019.00312

63. Bersani FS, Morley C, Lindqvist D, Epel ES, Picard M, Yehuda R, et al. Mitochondrial DNA copy number is reduced in male combat veterans with PTSD. *Prog Neuropsychopharmacol Biol Psychiatry.* (2016) 64:10–7. doi: 10.1016/j.pnpbp.2015.06.012

64. Shu X, Sun Y, Sun X, Zhou Y, Bian Y, Shu Z, et al. The effect of fluoxetine on astrocyte autophagy flux and injured mitochondria clearance in a mouse model of depression. *Cell Death Dis.* (2019) 10:577. doi: 10.1038/s41419-019-1813-9

65. McCoy CR, Sabbagh MN, Huaman JP, Pickrell AM, Clinton SM. Oxidative metabolism alterations in the emotional brain of anxiety-prone rats. *Prog Neuropsychopharmacol Biol Psychiatry.* (2019) 95:109706. doi: 10.1016/j.pnpbp.2019.109706

66. Brown PJ, Brennan N, Ciarleglio A, Chen C, Garcia CM, Gomez S, et al. Declining skeletal muscle mitochondrial function associated with increased risk of depression in later life. *Am J Geriatr Psychiatry.* (2019) 27:963–71. doi: 10.1016/j.jagp.2019.03.022

67. Glombik K, Stachowicz A, Slusarczyk J, Trojan E, Budziszewska B, Suski M, et al. Maternal stress predicts altered biogenesis and the profile of mitochondrial proteins in the frontal cortex and hippocampus of adult offspring rats. *Psychoneuroendocrinology.* (2015) 60:151–62. doi: 10.1016/j.psyneuen.2015.06.015

68. Picard M, McManus MJ, Gray JD, Nasca C, Moffat C, Kopinski PK, et al. Mitochondrial functions modulate neuroendocrine, metabolic, inflammatory, and transcriptional responses to acute psychological stress. *Proc Natl Acad Sci USA.* (2015) 112:E6614–23. doi: 10.1073/pnas.1515733112

69. Beirne K, Rozanowska M, Votruba M. Photostimulation of mitochondria as a treatment for retinal neurodegeneration. *Mitochondrion.* (2017) 36:85–95. doi: 10.1016/j.mito.2017.05.002

70. Li PA, Hou X, Hao S. Mitochondrial biogenesis in neurodegeneration. *J Neurosci Res.* (2017) 95:2025–9. doi: 10.1002/jnr.24042

71. Radad K, Al-Shraim M, Al-Emam A, Wang F, Kranner B, Rausch WD, et al. Rotenone: from modelling to implication in Parkinson's disease. *Folia Neuropathol.* (2019) 57:317–26. doi: 10.5114/fn.2019.89857

72. Greenamyre JT, Sherer TB, Betarbet R, Panov AV. Complex I and Parkinson's disease. *IUBMB Life.* (2001) 52:135–41. doi: 10.1080/15216540152845939

73. Hoyer S. Oxidative energy metabolism in Alzheimer brain. Studies in early-onset and late-onset cases. *Mol Chem Neuropathol.* (1992) 16:207–24. doi: 10.1007/BF03159971

74. Barini E, Antico O, Zhao Y, Asta F, Tucci V, Catelani T, et al. Metformin promotes tau aggregation and exacerbates abnormal behavior in a mouse model of tauopathy. *Mol Neurodegener.* (2016) 11:16. doi: 10.1186/s13024-016-0082-7

75. Kang H, Khang R, Ham S, Jeong GR, Kim H, Jo M, et al. Activation of the ATF2/CREB-PGC-1alpha pathway by metformin leads to dopaminergic neuroprotection. *Oncotarget.* (2017) 8:48603–18. doi: 10.18632/oncotarget.18122

76. Bae CS, Song J. The role of glucagon-like peptide 1 (GLP1) in type 3 diabetes: GLP-1 controls insulin resistance, neuroinflammation and neurogenesis in the brain. *Int J Mol Sci.* (2017) 18:18112493. doi: 10.3390/ijms18112493

77. Grieco M, Giorgi A, Gentile MC, d'Erme M, Morano S, Maras B, et al. Glucagon-like peptide-1: a focus on neurodegenerative diseases. *Front Neurosci.* (2019) 13:1112. doi: 10.3389/fnins.2019.01112

78. Carvalho AF, Sharma MS, Brunoni AR, Vieta E, Fava GA. The safety, tolerability and risks associated with the use of newer generation antidepressant drugs: a critical review of the literature. *Psychother Psychosom.* (2016) 85:270–88. doi: 10.1159/000447034

79. Balan E, Schwalm C, Naslain D, Nielens H, Francaux M, Deldicque L. Regular endurance exercise promotes fission, mitophagy, and oxidative phosphorylation in human skeletal muscle independently of age. *Front Physiol.* (2019) 10:1088. doi: 10.3389/fphys.2019.01088

80. Choi SH, Bylykbashi E, Chatila ZK, Lee SW, Pulli B, Clemenson GD, et al. Combined adult neurogenesis and BDNF mimic exercise effects on cognition in an Alzheimer's mouse model. *Science.* (2018) 361:aan8821. doi: 10.1126/science.aan8821

81. Micheli L, Ceccarelli M, D'Andrea G, Tirone F. Depression and adult neurogenesis: Positive effects of the antidepressant fluoxetine and of physical exercise. *Brain Res Bull.* (2018) 143:181–93. doi: 10.1016/j.brainresbull.2018.09.002

82. Poulose SM, Miller MG, Scott T, Shukitt-Hale B. Nutritional factors affecting adult neurogenesis and cognitive function. *Adv Nutr.* (2017) 8:804–11. doi: 10.3945/an.117.016261

83. Seo JH, Park HS, Park SS, Kim CJ, Kim DH, Kim TW. Physical exercise ameliorates psychiatric disorders and cognitive dysfunctions by hippocampal mitochondrial function and neuroplasticity in post-traumatic stress disorder. *Exp Neurol.* (2019) 322:113043. doi: 10.1016/j.expneurol.2019.113043

84. Park SS, Park HS, Kim CJ, Baek SS, Kim TW. Exercise attenuates maternal separation-induced mood disorder-like behaviors by enhancing mitochondrial functions and neuroplasticity in the dorsal raphe. *Behav Brain Res.* (2019) 372:112049. doi: 10.1016/j.bbr.2019.112049

85. Gusdon AM, Callio J, Distefano G, O'Doherty RM, Goodpaster BH, Coen PM, et al. Exercise increases mitochondrial complex I activity and DRP1 expression in the brains of aged mice. *Exp Gerontol.* (2017) 90:1–13. doi: 10.1016/j.exger.2017.01.013

86. Pang R, Wang X, Pei F, Zhang W, Shen J, Gao X, et al. Regular exercise enhances cognitive function and intracephalic GLUT expression in Alzheimer's disease model mice. *J Alzheimers Dis.* (2019) 72:83–96. doi: 10.3233/JAD-190328

87. Patten AR, Sickmann H, Hryciw BN, Kucharsky T, Parton R, Kernick A, et al. Long-term exercise is needed to enhance synaptic plasticity in the hippocampus. *Learn Mem.* (2013) 20:642–7. doi: 10.1101/lm.030635.113

88. Maurus I, Hasan A, Roh A, Takahashi S, Rauchmann B, Keeser D, et al. Neurobiological effects of aerobic exercise, with a focus on patients with schizophrenia. *Eur Arch Psychiatry Clin Neurosci.* (2019) 269:499–515. doi: 10.1007/s00406-019-01025-w

89. Adusumilli VS, Walker TL, Overall RW, Klatt GM, Zeidan SA, Zocher S, et al. ROS dynamics delineate functional states of hippocampal neural stem cells and link to their activity-dependent exit from quiescence. *Cell Stem Cell.* (2021) 28:300–14 e306. doi: 10.1016/j.stem.2020.10.019

90. De Miguel Z, Khoury N, Betley MJ, Lehallier B, Willoughby D, Olsson N, et al. Exercise plasma boosts memory and dampens brain inflammation via clusterin. *Nature.* (2021) 600:494–9. doi: 10.1038/s41586-021-04183-x

91. Littlefield AM, Setti SE, Priester C, Kohman RA. Voluntary exercise attenuates LPS-induced reductions in neurogenesis and increases microglia expression of a proneurogenic phenotype in aged mice. *J Neuroinflammation.* (2015) 12:138. doi: 10.1186/s12974-015-0362-0

92. Paolucci EM, Loukov D, Bowdish DME, Heisz JJ. Exercise reduces depression and inflammation but intensity matters. *Biol Psychol.* (2018) 133:79–84. doi: 10.1016/j.biopsycho.2018.01.015

93. Ryan SM, Nolan YM. Neuroinflammation negatively affects adult hippocampal neurogenesis and cognition: can exercise compensate? *Neurosci Biobehav Rev.* (2016) 61:121–31. doi: 10.1016/j.neubiorev.2015.12.004

94. Voloboueva LA, Giffard RG. Inflammation, mitochondria, and the inhibition of adult neurogenesis. *J Neurosci Res.* (2011) 89:1989–96. doi: 10.1002/jnr.22768

95. Huang J, Wang X, Zhu Y, Li Z, Zhu YT, Wu JC, et al. Exercise activates lysosomal function in the brain through AMPK-SIRT1-TFEB pathway. *CNS Neurosci Ther.* (2019) 25:796–807. doi: 10.1111/cns.13114

96. Lezi E, Burns JM, Swerdlow RH. Effect of high-intensity exercise on aged mouse brain mitochondria, neurogenesis, and inflammation. *Neurobiol Aging.* (2014) 35:2574–83. doi: 10.1016/j.neurobiolaging.2014.05.033

97. Kang GM, Min SH, Lee CH, Kim JY, Lim HS, Choi MJ, et al. Mitohormesis in hypothalamic POMC neurons mediates regular exercise-induced high-turnover metabolism. *Cell Metab.* (2021) 33:334–49 e336. doi: 10.1016/j.cmet.2021.01.003

98. Ferreira AFF, Binda KH, Singulani MP, Pereira CPM, Ferrari GD, Alberici LC, et al. Physical exercise protects against mitochondria alterations in the 6-hidroxydopamine rat model of Parkinson's disease. *Behav Brain Res.* (2020) 387:112607. doi: 10.1016/j.bbr.2020.112607

99. Liu YJ, Cui ZY, Yang AL, Jallow AW, Huang HL, Shan CL, et al. Anti-apoptotic and pro-survival effect of exercise training on early aged hypertensive rat cerebral cortex. *Aging.* (2021) 13:20495–510. doi: 10.18632/aging.203431

100. Lai JH, Chen KY, Wu JC, Olson L, Brene S, Huang CZ, et al. Voluntary exercise delays progressive deterioration of markers of metabolism and behavior in a mouse model of Parkinson's disease. *Brain Res.* (2019) 1720:146301. doi: 10.1016/j.brainres.2019.146301

101. Park HS, Kim CJ, Kwak HB, No MH, Heo JW, Kim TW. Physical exercise prevents cognitive impairment by enhancing hippocampal neuroplasticity and mitochondrial function in doxorubicin-induced chemobrain. *Neuropharmacology.* (2018) 133:451–61. doi: 10.1016/j.neuropharm.2018.02.013

102. Navazani P, Vaseghi S, Hashemi M, Shafaati MR, Nasehi M. Effects of treadmill exercise on the expression level of BAX, BAD, BCL-2, BCL-XL, TFAM, and PGC-1alpha in the hippocampus of thimerosal-treated rats. *Neurotox Res.* (2021) 39:1274–84. doi: 10.1007/s12640-021-00370-w

103. Pan G, Zhang H, Zhu A, Lin Y, Zhang L, Ye B, et al. Treadmill exercise attenuates cerebral ischaemic injury in rats by protecting mitochondrial function via enhancement of caveolin-1. *Life Sci.* (2021) 264:118634. doi: 10.1016/j.lfs.2020.118634

104. Arrazola MS, Andraini T, Szelechowski M, Mouledous L, Arnaune-Pelloquin L, Davezac N, et al. Mitochondria in developmental and adult neurogenesis. *Neurotox Res.* (2019) 36:257–67. doi: 10.1007/s12640-018-9942-y

105. Jia ZW. Mitochondria and pluripotent stem cells function. *Yi Chuan.* (2016) 38:603–11. doi: 10.16288/j.yczz.16-001

frontiers | Frontiers in Neurology

TYPE Systematic Review
PUBLISHED 06 October 2022
DOI 10.3389/fneur.2022.988034

OPEN ACCESS

EDITED BY
Guowei Li,
Guangdong Second Provincial General Hospital, China

REVIEWED BY
Kah Hui Wong,
University of Malaya, Malaysia
Wei Shao,
Mayo Clinic Florida, United States

*CORRESPONDENCE
Lihua Gu
kmglh169@163.com
Qigang Chen
179981715@qq.com

†These authors have contributed equally to this work and share first authorship

SPECIALTY SECTION
This article was submitted to Dementia and Neurodegenerative Diseases, a section of the journal Frontiers in Neurology

RECEIVED 06 July 2022
ACCEPTED 14 September 2022
PUBLISHED 06 October 2022

CITATION
Liao Y, He S, Liu D, Gu L, Chen Q, Yang S and Li D (2022) The efficacy and safety of Chinese herbal medicine as an add-on therapy for amyotrophic lateral sclerosis: An updated systematic review and meta-analysis of randomized controlled trials. *Front. Neurol.* 13:988034. doi: 10.3389/fneur.2022.988034

The efficacy and safety of Chinese herbal medicine as an add-on therapy for amyotrophic lateral sclerosis: An updated systematic review and meta-analysis of randomized controlled trials

Yingdi Liao†, Sijin He†, Duo Liu, Lihua Gu*, Qigang Chen*, Shuang Yang and Daiying Li

Department of Rehabilitation, Kunming Municipal Hospital of Traditional Chinese Medicine, Kunming, China

Background: Amyotrophic lateral sclerosis (ALS) has attracted widespread attention because of its unknown pathogenesis, rapid progression, and life-threatening and incurable characteristics. A series of complementary therapies, including Chinese herbal medicine (CHM), is available for use in the clinic and has been the focus of much research. However, it is unclear as to whether supplementary CHM relieves disease symptoms or extends life span; thus, we conducted this updated meta-analysis to validate the efficacy and safety of this practice.

Methods: We searched six electronic databases for randomized controlled trials involving CHM and patients with ALS that were published up to April 2022. Two researchers independently screened the literature, assessed the risk of bias for each trial, and then extracted data. The methodological quality of the included trials was assessed using the Cochrane risk of bias tool, and a pooled data analysis was performed using RevMan 5.3.

Results: A total of 14 trials led to the publication of 15 articles featuring 1,141 participants during the study period; the articles were included in the systematic review. In terms of increasing ALS functional rating scale (ALSFRS) scores, CHM was superior to the placebo after 3 months of treatment [mean difference (MD):0.7; 95% CI:0.43 to 0.98; $P < 0.01$] and to riluzole after 4 weeks of treatment (MD: 2.87; 95% CI: 0.81 to 4.93; $P < 0.05$), and it was superior to conventional medicine (CM) alone when used as an add-on therapy after 8 weeks of treatment (MD: 3.5; 95% CI: 0.51 to 6.49; $P < 0.05$). The change in the modified Norris score (m-Norris) from baseline to the end of more than 3 months of treatment was significantly different when compared between the CHM plus CM group and the CM alone group (MD: 2.09; 95% CI: 0.62 to 3.55; $P < 0.01$). In addition, CHM had a significantly better effect on increase in clinical effective rate (RR: 1.54; 95% CI: 1.23 to 1.92; $P < 0.01$) and improvement in forced vital capacity (MD: 7.26; 95% CI: 2.92 to 11.6; $P < 0.01$). However, there was no significant difference between the CHM therapy and CM in terms

of improving life quality (MD: 5.13; 95% CI: −7.04 to 17.31; $P = 0.41$) and decreasing mortality (RR: 0.41; 95% CI: 0.04 to 4.21; $P = 0.46$).

Conclusion: The analysis suggested that the short-term adjunct use of CHM could improve the ALSFRS score and clinical effect with a good safety profile when compared with the placebo or riluzole alone. However, future research should be centered on the long-term efficacy of patient-oriented outcomes.

Systematic review registration: https://www.crd.york.ac.uk/PROSPERO/display_record.php?RecordID=323047, identifier: CRD42022323047.

KEYWORDS

Chinese herbal medicine, amyotrophic lateral sclerosis, meta-analysis, systematic review, randomized controlled (clinical) trial

Introduction

Amyotrophic lateral sclerosis (ALS) is a progressive neurodegenerative condition involving upper motor neurons (UMNs) and lower motor neurons (LMNs) in the cerebral cortex, brain stem, and spinal cortex. The clinical neurological manifestations of ALS include muscle stiffness, spasm, hyperreflexia, and pathological reflexes as a sign of UMN injury and muscle weakness and atrophy as a sign of LMN damage with difficulty walking, speaking, and swallowing (1, 2). The prognosis of ALS is fatal, resulting in death due to respiratory failure or other associated conditions. Furthermore, there is no cure for ALS (1). This condition progresses rapidly, and the median survival duration is around 3–5 years from primary symptoms to death (3). This disease has an incidence of 2.5 per 100,000 persons-years and is more prevalent in men than in women (4). The cause of ALS has yet to be elucidated; however, ∼5–10% of patients with ALS are thought to suffer from a familial form of ALS that exerts familial genetic characteristics and feature mutations in several genes including *C9orf72*, *SOD1*, *FUS*, and *TARDBP*. The remaining 90% of patients are considered as sporadic cases of ALS associated with abnormalities of the immune system, toxic exposure, mitochondrial dysfunction, oxidative stress, neuroinflammation, or glutamate poisoning (2–5).

Riluzole, an anti-glutamate drug, is currently the only drug approved by the Food and Drug Administration (FDA) to prolong the life span of patients with ALS. However, this drug is expensive and is associated with several detrimental side effects including fatigue and diarrhea (4). Furthermore, an increasing body of evidence supports the fact that antioxidants may represent a potential treatment without serious clinical adverse effects although the efficacy of this treatment remains uncertain (6). Consequently, there is an urgent need to identify new and effective integrated therapies to slow the progression of ALS and increase the survival rate of patients. According to a previous survey on the use of integrated therapies conducted in Shanghai, China, Traditional Chinese Medicine (TCM) is the most commonly used form of complementary and supplementary therapy for treating ALS (7).

The clinical symptoms of ALS suggest that it could be defined as a "wilt disease" in the TCM system. Chinese Herbal Medicine (CHM), a form of TCM therapy, has been used to treat a wilt disease for thousands of years (8). A recent scoping review analyzed the research trends for the use of traditional herbal medicine in the treatment of ALS and identified many case reports, clinical observation studies, and randomized controlled trials (RCTs) involving the use of traditional herbal medicine for the treatment of ALS in East Asia, thus indicating that CHM may represent a potentially unique and effective therapy for ALS (4). However, the mechanisms and targets of CHM in the treatment of ALS were not described in this previous scoping review. A preclinical study showed that TCM compounds could inhibit the deleterious aggregation of abnormally phosphorylated nerve filaments around the nucleus, thus maintaining the integrity of the cytoskeleton, reducing axonal atrophy, and improving axoplasmic transport to delay neuronal degeneration (9). Over recent years, single TCM drugs, Chinese medicine compounds, Chinese patent medicines, and injections of Chinese medicines have all been proven to be effective in the treatment of ALS in clinical trials. However, there is insufficient evidence to support the efficacy and safety of CHM for ALS. Thus, it is necessary to evaluate the documented efficacy of this form of treatment by performing a systematic review and meta-analysis of RCTs. We aimed to answer the following questions: (1) whether CHM can improve clinical symptoms in patients with ALS, (2) whether CHM reduces mortality in patients with ALS, (3) whether CHM improves the quality of life of patients with ALS, (4) whether CHM improves the clinical effective rate of patients with ALS, and (5) whether CHM is safe when used alone or as an adjunct therapy.

Methods

The review protocol was registered on PROSPERO (Reference: CRD42022323047) and was performed according to the checklist of Preferred Reporting Items for Systematic Reviews and Meta-Analyses (10).

Eligibility criteria

Types of study

Randomized controlled trials (RCTs) on Chinese herbal medicine for ALS; the publication language was restricted to English and Chinese.

Participants

Participants with ALS of any age and race were eligible. The included trials needed to provide definite and universal diagnostic criteria for ALS formulated by the World Federation of Neurology Sub-Committee on Neuromuscular Diseases at El Escorial (11) or the Neurology Branch of the Chinese Medical Association (12).

Interventions

The Chinese herbal medicine was used on the treatment group alone or in combination with a conventional medicine (CM) such as riluzole, mecobalamin, vitamin, and other antioxidants. The Chinese herbal medicine included Chinese patent medicine, traditional herbal decoction, and other single Chinese medicines or compounds. The route of administration for the Chinese herbal medicine was not restricted. The controls included placebo or routine pharmacotherapies such as riluzole, mecobalamin, vitamin, and other antioxidants. When the treatment group was CHM plus another treatment, the adjunct therapy needed to be the same as the control.

Outcomes

The primary outcome was the assessment of functional changes in patients with ALS, as appraised with the ALS functional rating scales (ALSFRS) or the revised ALS functional rating scales (ALSFRS-r) and modified Norris scale (m-Norris) at the end of the treatment duration or after the follow-up. The ALSFR is a 10-item instrument, while the ALSFRS-r is a 12-item instrument that integrates all aspects of myelination symptoms, motor symptoms, and respiratory symptoms. The ALSFRS scores range from 0 to 40 (ALSFRS-r from 0 to 48); higher scores indicate less severe neurological impairment (13). m-Norris is a comprehensive scale that is used mainly to evaluate myelination and limb function; the score ranges from 0 to 99, with lower values implying more severe functional impairment (14).

The secondary outcomes were as follows: (1) the overall clinical effective rate was defined according to universally approved criteria, which are divided into markedly effective, effective, and ineffective; (2) changes in the number of points allocated for TCM syndrome as assessed by main and minor symptoms. The main symptoms include four items: fleshy atrophy, wilting limb, swallowing difficulty, and sluggish speech; these are graded as 0, 2, 4, and 6 points, respectively. The minor symptoms include shortness of breath, fatigue, spontaneous sweating, thirst, dry throat, being upset, waist knee soreness, and tinnitus; each item is graded as 0, 1, 2, and 3 points; (3) the assessment of life quality in patients with ALS; (4) pulmonary function, as assessed by forced vital capacity (FVC); (5) composite endpoint events including mortality, and noninvasive or invasive ventilation; (6) adverse events (AEs).

Exclusion criteria

Articles were excluded for the following reasons: (1) repeated publications and not related to ALS, (2) involved animal research or were not RCTs, (3) devoid of relevant outcomes or provided an incomplete dataset for analysis, and (4) the treatment group included acupuncture, moxibustion, massage, or treatments other than traditional Chinese medicine.

Study selection and data extraction

A systematic and comprehensive literature search was performed from inception to March 2022 using a range of online databases including PubMed, Embase, the Cochrane Library, China National Knowledge Infrastructure, Wangfang, and the China Biomedical Database. The search terms were as follows: amyotrophic lateral sclerosis, Chinese herbal, preparation, and randomized controlled trials. The retrieval strategy is shown in Appendix. Additional manual searches were based on previous related studies (4). Two authors (YL and SH) identified and selected the studies. Based on the above inclusion and exclusion criteria, titles and abstracts were identified and checked by the two authors. The full text of all relevant articles was obtained and screed by the reviewers. Disagreements were resolved by discussion.

Data extraction was performed independently and involved a cross-check by the two authors (YL and SH). Then, we extracted the following information from eligible studies into Microsoft Excel 2007: (1) basic information including authors, publication year, study design, and diagnostic criteria of ALS; (2) patient characteristics including total number, age, gender, and disease history; (3) types of interventions including intervention

name, dose, treatment duration, frequency, usage, and follow-up; (4) outcomes and AEs. Disagreements were resolved by discussion.

Risk of bias assessment

The two authors (YL and SH) assessed the risk of bias in the included studies by applying tools developed by the Cochrane Collaboration. These tools covered the following seven domains: random sequence generation, allocation concealment, blinding of participants and personnel, blinding of outcome assessment, incomplete outcome data, selective reporting, and other forms of bias. The risk of bias judgments was categorized as low, high or, unclear. Disagreements were resolved by discussion.

Statistical analysis

Data analysis was performed with the Review Manager software (RevMan version 5.3; The Cochrane Collaboration, Oxford, United Kingdom). Continuous data are presented as the mean difference (MD) with 95% CI, while dichotomous data are presented as relative risk (RR) with 95% CI. The heterogeneity of the included RCTs was evaluated by chi-squared tests. Fixed-effects models were used to estimate the effect for studies with low heterogeneity ($I^2 < 50\%$, $P > 0.1$). If the I^2 value was more than 50%, we performed a subgroup analysis to identify the source of the heterogeneity. In addition, a subgroup analysis was carried out for different durations, and random-effects models were used for estimation. A sensitivity analysis was performed to assess the robustness of results by only including trials with a low risk of bias for blinding of participants and allocation concealment. Funnel plots were used to assess publication bias if more than 10 RCTs reported the same outcome.

Results

Literature search

The initial search identified 3,586 articles from the selected databases. According to the eligibility criteria, a total of 26 full texts were further screened after checking the titles and abstracts. Twelve articles were excluded for the following reasons: not RCTs, contained invalid data, featured duplicate data, reported unrelated outcomes, and inappropriate controls. In some cases, the full text was not available. Finally, 15 articles were included in our analysis (15–29). However, two articles (17, 18) published different outcomes for the same trial. Therefore, a total of 14 original studies were included in our meta-analysis. Supplementary Figure 1 shows a flowchart that describes the strategy used for screening articles.

Characteristics of the included studies

All of the included studies, featuring 1,141 participants, were RCTs and were published between 2006 and 2020 (15–29). One study was published in English (28), while the remaining articles were published in Chinese. The treatment duration ranged from 4 weeks to 6 months. Ten studies reported follow-up data at the end of treatment (16, 20–28). Nine articles mentioned the course of ALS within 5 years (15–19, 22, 24, 27, 29). In three trials, the treatment group was treated with CHM combined with riluzole (16, 21, 22). One trial combined CHM with a coenzyme, vitamin E, and mecobalamine (20). Eight trials used only CHM in the experimental group (15, 17–19, 24–26, 28, 29). Two trials were double-blinded, double-dummy RCTs (23, 27). The control group was treated with conventional medicine alone or with a CHM placebo. The most frequent herb was *huangqi*, followed by *baizhu, shengdi, rensheng, yingyanghuo, dansghe*, and *fuling*. The most frequent Chinese preparations were Jia Wei Si Jun Zi decoctions, Ji Wei Ling preparations, and Fu Yuan Sheng Ji granules. The characteristics of the included studies are shown in Tables 1, 2.

Risk of bias assessment for the included studies

Eleven studies (15–18, 20, 21, 23–25, 27–29) reported appropriate methods of random sequence generation, including random number tables and computer software. Three other studies (19, 22, 26) mentioned randomized trials but did not report the randomization methods in detail. Allocation concealment was unclear in all the studies because of limited information, although one study (23) reported the use of sequentially numbered containers to conceal allocation. Three trials (15, 19, 24) reported a high risk of blinding because blindness could have been disrupted by applying different methods of administration in the control and treatment groups. Three trials (20, 23, 27) were reported in a double blinded manner to participants and personnel; we considered this as a low risk. However, the remaining studies (15–19, 21, 22, 24–26, 28, 29) did not report blinding to the participants and personnel. One trial (27) reported the blinding of outcome assessment, while the other 10 trials (16–18, 20–23, 25, 26, 28, 29) lacked detailed information related to the blinding of outcome assessment; we considered this as an unclear risk. One trial (20) reported a dropout but did not provide a clear reason for the dropout. The reporting bias for all trials (15–29) was assessed as a low risk because they all reported predefined outcomes in their Methods sections. For all the studies, other forms of bias were considered to be an unclear risk because of lack of information. Detailed results related to risk of bias are shown in Supplementary Figures 2, 3.

TABLE 1 Basic features of the included studies.

Included studies	Sample size (T/C)	Ages: mean (SD)/range, T/C	Gender (M/F)		Course of disease (month)	Followup (day)	Outcome	
			T	C			Primary outcome	Secondary outcome
Zhang (15)	42/42	45.36(6.52)/45.51(6.38)	34/8	36/6	6–60	NA	ALSFRS-r, clinical effect	
Li et al. (16)	30/28	56.43(11.08)/55.79(10.06)	19/11	19/9	2–36	540	m-Norris,	FVC, Endpoint events
Wang et al. (17)	100/25	55.11(13.52)/56.64(11.18)	60/40	16/9	<60	NA	Clinical effect	TCM syndrome score, AEs
Ren et al. (18)	100/25	55.11(13.52)/56.64(11.18)	60/40	16/9	<60	NA	m-Norris, Clinical effect	AEs
Chen et al. (19)	240/80	54.67(10.23)/53.56(10.31)	147/93	46/34	6–36	NA	Clinical effect	
Zhu et al. (20)	24/21	NA	15/9	14/7	NA	365	ALSFRS-r	AEs
Wang et al. (21)	30/30	53.07(11.19)/53.07(11.19)	32/28		NA	56	ALSFRS-r	Endpoint events, AEs,FVC
Su et al. (22)	25/10	60.2(14.1)/59.4(9.0)	13/12	6/4	<60	90	m-Norris	TCM syndrome score
Pan (23)	38/38	49.38(8.96)/50.05(8.10)	26/12	25/13	NA	90	ALSFRS, m-Norris, Clinical effect	Life quality, AEs
Wang (24)	30/30	44.57(9.55)/48.13(8.54)	20/10	22/8	3–60	28	ALSFRS, Clinical effect	Life quality, FVC, AEs
Sui et al. (25)	33/31	54.00(11.96)/54.00(11.92)	18/15	20/11	NA	84	m-Norris, Clinical effect	TCM syndrome score, AEs
Wu et al. (26)	16/16	41.1/42.9	13/3	12/4	NA	90	Clinical effect	
Ma (27)	30/30	48.33(10.24)/48.68(11.06)	9/21	10/20	5–28	28	ALSFRS, m-Norris, Clinical effect	Life quality, FVC, AEs
Pan et al. (28)	23/19	51.6(7.2)/50.1(4.2)	14/9	11/8	NA	180	ALSFRS-r	Life quality, Endpoint events, AEs
Wenjie et al. (29)	40/40	24∼76/20∼79	25/15	27/13	<60	NA	m-Norris, Clinical effect	TCM syndrome score,

T, treatment group; C, control group; NA, data are not available; M, male; F, female; ALSFRS-r, revised ALS functional rating scales; ALSFRS, ALS functional rating scales; m-Norris, modified Norris scales; FVC, forced vital capacity; AEs, adverse events; TCM, Traditional Chinese Medicine.

10.3389/fneur.2022.988034

TABLE 2 Details of interventions in the included studies.

Included studies	Interventions		Principle of syndrome differentiation and treatment	Ingredients of the treatment group	Treatment duration
	T	C			
Zhang (15)	Shen Mai injection 20 ml ivd qd + neurotrophin 2000 u ivd qd+ Cobamamide 0.5mg po qd + adenosine triphosphate disodium tablets 40 mg po qd	Neurotrophin 2000 u ivd qd+ Cobamamide 0.5mg po qd + adenosine triphosphate disodium tablets 40 mg po qd	NA	*hongsheng, maidong*	45 d
Li et al. (16)	Fu Yuan Sheng Ji granules 1 pack po bid + Riluzole tablets 50 mg po bid	Riluzole tablets 50 mg po bid	Fortify spleen and tonify kidney	*huangqi, yingyanghuo, baizhu, shanyurou, shengdi, xianlingpi, gancao*	180 d
Wang et al. (17)	Fu Yuan Sheng Ji granules 15 g po bid	Riluzole tablets 50 mg po bid	Fortify spleen and tonify kidney	*huangqi, yingyanghuo, baizhu, shanyurou, shengdi, xianlingpi, gancao*	84 d
Ren et al. (18)	Fu Yuan Sheng Ji granules 15 g po bid	Riluzole tablets 50 mg po bid	Fortify spleen and tonify kidney	*huangqi, yingyanghuo, baizhu, shanyurou, shengdi, xianlingpi, gancao*	84 d
Chen et al. (19)	Ji Wei Ling injection 48 ml qd ivd+ Ji Wei Ling capsule	Riluzole tablets 50 mg po bid + neurotrophin 2000 u ivd qd	Reinforce source qi, tonify nutrient aspect and promote muscle vitality	*rensheng, lurong, heshouwu*	75 d
Zhu et al. (20)	Jia Wei Si Jun Zi decoction 1 pack + coenzyme Q10 + vitamin E + mecobalamine	Placebo + coenzyme Q10 + vitamin E + mecobalamine	Fortify spleen and tonify qi	*huangqi, dangshen, baizhu, fuling, zhigancao, danggui*	9 m
Wang et al. (21)	Jian Pi Yi Fei granules 1 pack po bid + Riluzole tablets 50 mg po bid	Riluzole tablets 50 mg po bid	Fortify spleen and tonify lung	*huangqi, dangshen, baizhu, wuweizi, duzhong, tusizi, maidong, chenpi, fabanxia, baijiangcan, xinren, jiegeng, chaihu, zhimaqianzi, zhigancao*	8 w
Su et al. (22)	Yi Qi Qiang Ji decoction 1 pack po bid + Riluzole tablets50 mg po bid	Riluzole tablets 50 mg po bid	Tonify qi and nourish ying and yang	*huangqi, dangshen, fuling, gancao, shengdi, yingyanghuo, zhidahuang, shengma,*	90 d
Pan (23)	Shen Zhe Jiang Qi powder 5 g po tid +Riluzole placebo 50mg po tid	Shen Zhe Jiang Qi placebo 5 g po tid + Riluzole tablets 50mg po tid	Regulate qi	*dangshen, zheshi, guiban, roucongrong, shanzhuyu, roucongrong, jiegeng, zhike, wugong*	90 d
Wang (24)	Ji Wei Ling injection 24 ml ivd qd	Riluzole Tablets 50 mg po bid	Reinforce source qi, tonify nutrient aspect and promote muscle vitality	*rensheng, lurong, heshouwu*	28 d
Sui et al. (25)	Huo Ling Sheng Ji decoction 1 pack po bid	Riluzole tablets 50 mg po bid	Replenish qi and tonify spleen, warm kidney	*huangqi, yingyanghuo, fuchaobaizhu, shanzhuyu, fuling, shengdihuang*	12 w
Wu et al. (26)	Huangqi powder 60 g po tid	Riluzole Tablets 50 mg po bid	Tonify spleen, lung and kidney, replenish qi and blood	*huangqi*	90 d
Ma et al. (27)	Ji Wei Ling injection 32 ml ivd qd + Riluzole placebo 50 mg po bid	Ji Wei Ling injection placebo 32 ml ivd qd+Riluzole tablets 50 mg po bid	Reinforce source qi, tonify nutrient aspect and promote muscle vitality	*rensheng, lurong,heshouwu*	28 d
Pan et al. (28)	Jia Wei Si Jun Zi decoction 1 pack po bid	Riluzole tablets 50 mg po bid	Nourish spleen and enrich vitality	*huangqi,renshen, baizhu, fuling, zhigancao, roucongrong*	6 m
Wenjie et al. (29)	Zi Ni Fang 1 pack po bid	Riluzole tablets 50 mg po bid	Tonify kidney, fortify the spleen and soothe the liver	*huangqi, shengdihuang, xianlingpi, bajitian, shanzhuyu, fuling, shihu, huainiuxi, chaihu, yujin*	6m

T, treatment group; C: control group; NA, data are not available; d, days; m, months; w, weeks.

10.3389/fneur.2022.988034

Effects of interventions

Primary outcome measures

CHM alone vs. controls

In terms of assessment of ALS function, one double-blind, double-dummy RCT with 60 participants measured outcome with the ALSRF scale and reported that CHM plus a placebo for riluzole was more effective than riluzole plus a placebo for CHM after 3 months of treatment (MD: 2.78; 95% CI: 0.15 to 5.41; $P < 0.05$) (27). Another RCT, with the same methodological design, measured the outcome with the swallowing item in ALSFRS; the results showed that the experimental group had a better effect on improving swallow function than the control group after 3 months of treatment (MD:0.68; 95% CI: 0.41 to 0.95; $P < 0.01$) (23). The results are shown in Figure 1. Another RCT with 60 participants showed that CHM was superior to riluzole in improving ALSRF scores after 4 weeks of treatment (MD: 2.87; 95% CI: 0.81 to 4.93; $P < 0.05$) (24). In terms of ALSRF-r scores, one trial with 48 participants showed that there was no significant difference between the CHM group and the riluzole group after 6 months of treatment (MD: 1.8; 95% CI: −2.62 to 6.22; $P > 0.05$) (28).

With regard to ALS function, as measured with the m-Norris scale, CHM plus a placebo for riluzole was not superior to riluzole plus a placebo for CHM after 3 months of treatment (MD: 2.57; 95% CI: −3.36 to 8.5; $P = 0.4$; $I^2 = 60\%$; $n = 2$ RCTs; 136 participants) (23, 27). CHM alone was not better than riluzole in improving the m-Norris scale score after 12 weeks of treatment (MD: −1.53; 95% CI: −7.22 to 4.17; $P = 0.6$; $I^2 = 0\%$; $n = 2$ RCTs; 189 participants) (18, 25). The results are shown in Figure 2. The other trial was not analyzed because the data were reported as medians rather than means; however, there was no significant difference between the CHM group and the riluzole group after 6 months of treatment ($P > 0.05$) (29).

CHM plus conventional medicine vs. controls

With regard to ALS function, as assessed with the ALSFRS-r scale, one RCT featuring 45 participants showed that CHM was no more effective than a placebo based on CM after 9 months of treatment (MD: 5; 95% CI: −0.08 to 10.08; $P = 0.05$) and after 3 months of follow-up (MD: 1.24; 95% CI: −4.44 to 6.92; $P = 0.67$) (20). At the end of 7 to 8 weeks of treatment, CHM plus CM had a better effect than CM alone (MD: 3.9; 95% CI: 2.49 to 5.31; $P < 0.001$; $I^2 = 0\%$; $n = 2$ RCTs; 138 participants) (15, 21). The results are shown in Figure 3.

With regard to ALS function, as assessed with the m-Norris scale, two trials reported changes from baseline to the end of treatment; adding CHM significantly increased this trend for change when compared to riluzole alone after 3 months of treatment (MD: 2.09; 95% CI: 0.62 to 3.55; $P < 0.01$; $I^2 = 0\%$; $n = 2$ RCTs; 93 participants) (16, 22). The results are shown in Figure 4.

Secondary outcomes

Overall clinical effective rate

CHM alone vs. controls

Two RCTs reported clinical effective rate as assessed by ALS symptoms and life quality; the clinical effect of CHM plus a placebo for riluzole was better than that of riluzole plus a placebo for CHM after 4 weeks of treatment (RR: 1.54; 95% CI: 1.23 to 1.92; $P < 0.001$; $I^2 = 0\%$; $n = 2$ RCTs; 136 participants) (23, 27). The results are shown in Supplementary Figure 4.

Six trials compared CHM with conventional therapy and assessed the overall effective rate with different criteria (17–19, 24–26, 29); four trials measured the effective rate with the m-Norris scale and showed that there was no significant difference between the two groups (RR:0.94; 95% CI: 0.6 to 1.47; $P = 0.78$; $I^2 = 16\%$; $n = 4$ RCTs; 301 participants) (18, 25, 26, 29). The remaining RCTs measured the effective rate with other criteria and showed that the CHM group had a better effect than the TCM group (as assessed by TCM syndrome points: RR: 2.75; 95% CI: 1.65 to 4.57; $P < 0.001$; $I^2 = 41\%$; $n = 2$ RCTs; 269 participants; as assessed by ALS clinical symptoms: RR: 22.78; 95% CI: 7.5 to 69.21; $P < 0.01$; $n = 1$ RCT; 320 participants; as assessed by ALS bulbar paralysis clinical symptoms scores: RR: 2.38; 95% CI: 1.24 to 4.56; $P < 0.01$; $n = 1$ RCT; 60 participants) (17, 19, 24, 25). The results are shown in Supplementary Figure 5.

CHM plus conventional medicine vs. controls

Only one trial reported the effective rate as assessed by ALS clinical symptoms and showed that the CHM plus CM group had a better effect than the CM group (RR: 1.26; 95% CI: 1.03 to 1.53; $P < 0.05$; 84 participants) (15).

Traditional Chinese medicine syndrome

One trial featuring 35 participants reported a change in TCM syndrome score from baseline to the end of treatment and showed that CHM plus riluzole had a better effect on reducing the change in TCM syndrome score than riluzole alone after 3 months of treatment (MD: 3.9; 95% CI: 1.77 to 6.03; $P < 0.001$) (22). Another trial showed that CHM had a better effect on reducing changes in TCM syndrome scores than riluzole after 6 months of treatment ($P < 0.05$) (29). However, we did not perform an analysis for this study because data were reported as medians rather than means (29). Two trials reported TCM syndrome score after 12 weeks of treatment; the pooled data showed that the effect of CHM on reducing the TCM syndrome score was better than that of riluzole (MD: −3.27; 95% CI: −5.4 to −1.14; $P < 0.01$; $I^2 = 0\%$; $n = 2$ RCTs; 189 participants) (17, 28). However, there was no significant difference between the two groups with regard to reducing fleshy atrophy symptom score and limb wilt score (fleshy atrophy symptom score: MD: −0.25; 95% CI: −0.73 to 0.24; $P = 0.89$; $I^2 = 0\%$; $n = 2$ RCTs; 189 participants; limb wilt symptom score: MD:0.19; 95% CI: −0.24

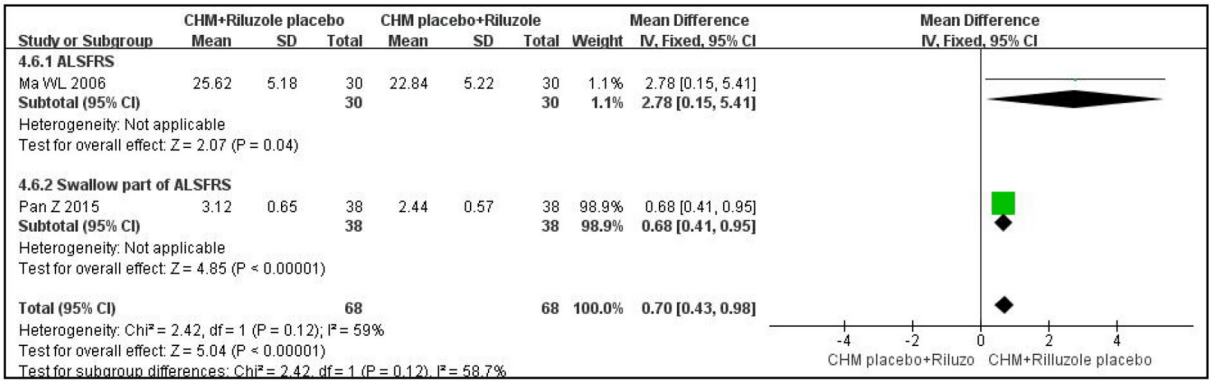

FIGURE 1
Forest plot of ALSRF for ALS compared CHM with controls. ALSFRS, ALS functional rating scales; CHM, Chinese herbal medicine; ALS, amyotrophic lateral sclerosis.

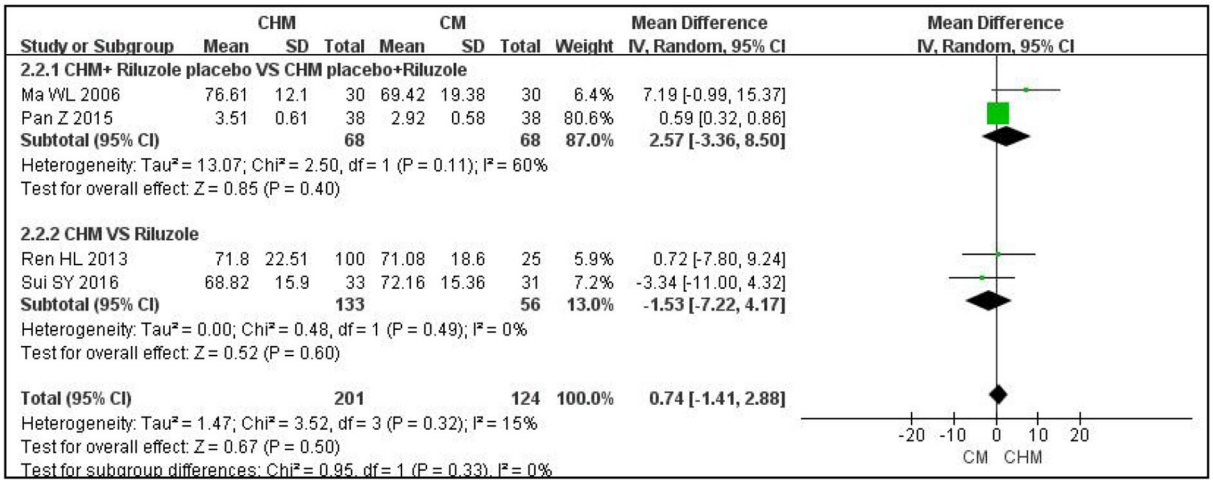

FIGURE 2
Forest plot of m-Norris for ALS compared CHM with controls. m-Norris, modified Norris scales; CHM, Chinese herbal medicine; ALS, amyotrophic lateral sclerosis.

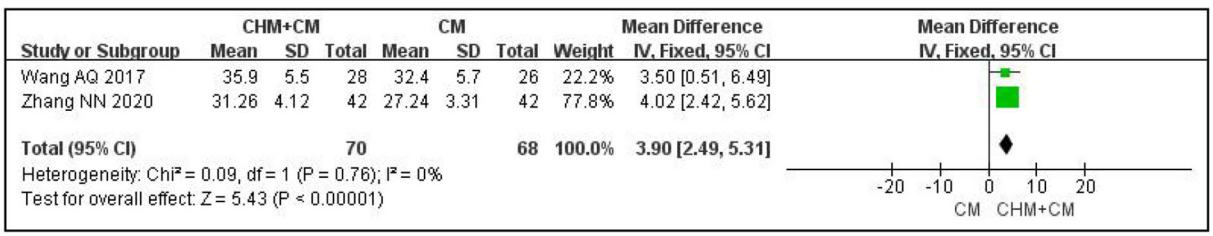

FIGURE 3
Forest plot of ALSFRS-r for ALS compared CHM plus CM with CM. r-ALSFRS, revised ALS functional rating scales; CHM, Chinese herbal medicine; ALS, amyotrophic lateral sclerosis; CM, conventional medicine.

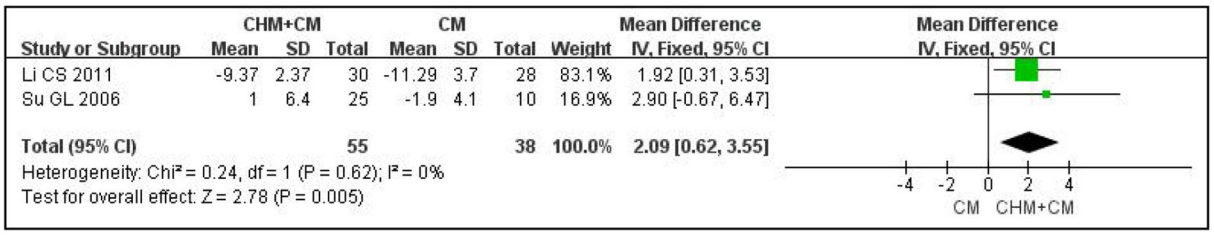

FIGURE 4
Forest plot of m-Norris for ALS compared CHM plus CM with CM. m-Norris, modified Norris scales; CHM, Chinese herbal medicine; ALS, amyotrophic lateral sclerosis; CM, conventional medicine.

to.62; $P = 0.38$; $I^2 = 0\%$; $n = 2$ RCTs; 189 participants) (17, 28). The results are shown in Supplementary Figure 6.

Assessment of life quality of ALS patients

Two double-blinded, double-dummy trials reported the quality of life as measured with the ALS assessment questionnaire (ALSAQ-40) and showed that there was no significant difference between the experimental group and the control group (MD: 5.13; 95% CI: −7.04 to 17.31; P =0.41; $I^2 = 73\%$; $n = 2$ RCTs; 136 participants) (23, 27). The results are shown in Supplementary Figure 7. The other two trials compared CHM with riluzole but used different scales to measure life quality (24, 28); therefore, we did not perform a pooled analysis. However, the published results showed that there was a significant difference between the two groups [ALSAQ-40: MD: 3.33; 95% CI: −4.02 to 10.68; P = 0.37; n = 1 RCT; 60 participants; SF-36 physical functioning (PF) subscale: MD: 1.30; 95% CI: −2.7 to 5.3; $P = 0.52$; $n = 1$ RCT; 42 participants].

Pulmonary function as assessed by forced vital capacity

One trial featuring 60 participants reported FVC data and showed that CHM plus a placebo for riluzole improved the FVC in a manner more superior to that of riluzole plus a placebo for CHM after 4 weeks of treatment (MD: 7.26; 95% CI: 2.92 to 11.6; $P < 0.01$) (27). Wang et al. compared CHM plus conventional therapy with conventional therapy alone and showed that there was no significant differences between the CHM plus CM group and the CM alone group after 8 weeks of treatment (MD: 2.14; 95% CI: −7.93 to 12.21; $P = 0.68$) (21). Two trials reported FVC changes from baseline to the end of treatment (16, 24). Wang et al. reported that CHM had a better effect than riluzole on improving FVC values after 4 weeks of treatment (MD: 2.31; 95% CI:0.62 to 4; P <0.01) (24). However, Li et al. showed that there were no significant differences between a CHM plus CM group and a CM alone group after 6 months of treatment (MD:0.84; 95% CI: −0.4 to 2.08; $P = 0.18$) (16).

Composite endpoint events

Three trials (16, 21, 28) reported the outcome after long-term treatment or follow-up including death, tracheotomy, gastrostomy, and coma. The incidence of non-favorable clinical events was 13.6%. One trial featuring 42 participants compared CHM alone with riluzole with regard to mortality and revealed that there was no significant difference between the two groups after 6 months of treatment (RR:0.41; 95% CI: 0.04 to 4.21; P = 0.46) (28). Another trial featuring 58 participants reported mortality due to respiratory failure at the end of 18 months follow-up and showed that there was no significant difference between the CHM plus riluzole group and the riluzole alone group (MD:0.35; 95% CI: 0.1 to 1.19; P = 0.09) (16). This trial also reported that three patients underwent tracheotomy in the experimental group (16). Wang et al. reported that two patients underwent tracheotomy with mechanical breathing, one underwent gastrostomy, and one patient who fell into a coma after injury, at the end of 2 months of follow-up but did not mention whether the event occurred in the control group or the treatment group (21).

Adverse events

Adverse events were monitored in eight studies (17, 18, 20, 21, 23–25, 27, 28). Two of these studies found no adverse events in the two groups (17, 18, 20). Five studies reported that the incidence of adverse events in the CHM group was around 2%, and that the incidence of adverse events in the riluzole group was about 32%. We performed a meta-analysis for the frequency of adverse events. The results showed that the group that received CHM plus a placebo for riluzole had fewer adverse events than the group that received riluzole plus a placebo for CHM (RR: 0.02; 95% CI: 0 to 0.14; $P < 0.001$; $I^2 = 0\%$; $n = 2$ RCTs; 136 participants) (23, 27). The CHM group had fewer adverse events than the riluzole group (RR:0.15; 95% CI: 0.07 to 0.3; $P < 0.001$; $I^2 = 0\%$; $n = 3$ RCTs; 166 participants) (24, 25, 28). Furthermore, there was no significant difference between CHM plus riluzole and riluzole (RR: 1; 95% CI: 0.36 to 2.75; P = 0.64; $n = 1$ RCT; 60 participants) (21). The results are shown in Supplementary Figure 8. The adverse events in the CHM group

were mainly nausea ($n = 3$), abdominal distention ($n = 2$), and constipation ($n = 2$). The adverse events in the riluzole group were mainly nausea ($n = 22$), dizziness ($n = 6$), loss of appetite ($n = 11$), constipation ($n = 3$), diarrhea ($n = 5$), abdominal distention ($n = 10$), increased levels of transaminase ($n = 49$), fatigue ($n = 11$), and itchy skin ($n = 4$).

Other analysis

Subgroup analysis

The subgroup-analysis for ALSFRS or ALSFRS-r based on treatment duration and CHM preparation is shown in Table 3. The results of subgroup analyses suggested that there was a greater effect of CHM on improving functional ability in terms of ALSFRS or ALSFRS-r when the optimal therapeutic duration of DZSM seems to be 3 months or administered intravenously. Table 3 details the full statistical results of the subgroup analyses. For m-Norris, a subgroup analysis was not performed because of lack of sufficient number of studies.

Sensitivity analysis and publication bias

Because of the lack of a sufficient number of trials, we could not perform an additional analysis.

Discussion

Summary of findings and applicability

We comprehensively and systematically searched electronic databases to perform the updated meta-analysis to evaluate the efficacy and safety of CHM for ALS. Conventional pharmacotherapies may sometimes fail to cure ALS, such as riluzole or other antixodants with disadvantages of being expensive and having side effects and uncertain efficacy, whereas ALS is reported to be improved with alternative and complementary medicine based on traditional Chinese theory (4). Although there have been some systematic reviews or scoping reviews on CHM, no study evaluated the overall efficacy and safety of Chinese patent medicines, traditional herbal decoctions, or Chinese medicine compounds for ALS based on a meta-analysis.

In our study, we used the ALSFRS and m-Norris scales as the primary outcome to assess the efficacy of CHM for ALS function because these scales are the most representative tools to evaluate the physical function of daily life in ALS clinical trials, with tested reliability, sensitivity, and stability (30, 31). Our findings showed that CHM was superior to both the placebo and riluzole in terms of ALSFR and was superior to riluzole alone when used as an add-on therapy in terms of ALSFR after 3 months of treatment. Our subgroup analysis results suggest that 3 months of treatment can significantly improve the ALSFRS or ALSFRS-r scores, and that the different administrations of CHM may lead to different effects. These data imply that the course of treatment may affect the efficacy of functional change in patients with ALS as measured by ALSFRS or ALSFRS-r. Furthermore, we found that the effect was similar between the CHM group and the placebo or riluzole group with regard to improvements in m-Norris score after treatment regardless of the length of treatment. However, the change in m-Norris score from baseline to the end of more than 3 months of treatment was significantly different when compared between the CHM plus CM group and the CM alone group. This means that the determination of outcome measures may lead to different results.

The other findings in this review, which estimated the effect on secondary outcome, revealed that CHM had a better effect than the placebo and CM with regard to increasing the clinical effective rate and was superior to CM alone when used as an add-on therapy. In terms of TCM syndrome scores, CHM also had a better effect than CM although there was no obvious advantage of CHM with regard to improving fleshy atrophy symptoms and limb wilt symptoms in the TCM system. Extensive research is still needed to demonstrate the effectiveness of CHM in improving TCM syndrome scores. Only one RCT featuring a double blind and double dummy design reported improvement in FVC values (27). However, the data do not mean that CHM could improve pulmonary function in the clinic because we only used FVC as an evaluation measure. The existing evidence is insufficient to prove the efficacy of CHM in terms of improving pulmonary function. In addition, patients appear to be concerned about whether CHM can prolong survival, reduce mortality, or improve life quality. Our results showed that CHM did not significantly improve life quality and did not reduce endpoint events such as mortality and the need for tracheotomy. Therefore, we did not find any evidence to support the fact that CHM did provide a greater benefit with regard to prolonging survival or improving life quality. A more rigorous and multi-center study on a larger number of subjects is required to prove the efficacy in the future.

A previous investigation from China showed that the mean price of TCM decoctions and compounds range from 10.23 to 72.87 RMB/per day, and that riluzole costs 160 RMB/per day (7). The trial in our included studies also reported that CHM was cheaper than riluzole (28). Therefore, CHM could be a promising therapy for ALS because of its considerable efficacy and appreciable price. Moreover, this treatment option is safe as severe adverse events have not been reported. Moreover, there were fewer adverse events in the CHM group.

Interpretation of different CHM potential mechanisms

The mechanisms underlying the effects of CHM prescriptions when dealing with ALS remain incompletely clear; some studies, however, provide evidence for the

TABLE 3 Subgroup analysis of ALSFRS or ALSFRS-r based on treatment duration and preparation of CHM.

Subgroup		No. study	No. participants	Estimated effect (MD, 95% CI)	I^2	*P* value	Analysis model
CHM vs. placebo							
Treatment duration	3 m	2	105	2.98 [0.77,5.19]	0%	<0.01	Fixed model
	6 m	1	45	2.88 [-1.38,7.14]	-	0.18	Fixed model
	9 m	1	45	5.00 [-0.08,10.08]	-	0.05	Fixed model
Preparation of CHM	Decoction or granules	2	121	0.69 [0.42,0.97]	43%	<0.01	Fixed model
	Injection	1	60	2.78 [0.15,5.41]	-	0.04	Fixed model
CHM vs. riluzole							
Treatment duration	3 m	2	108	2.68 [0.81,4.55]	0%	<0.01	Fixed model
	6 m	1	42	3.80 [-1.41,9.01]	-	0.15	Fixed model
Preparation of CHM	Decoction	1	48	1.80 [-2.62,6.22]	-	0.42	Fixed model
	Injection	1	60	2.87 [0.81,4.93]	-	<0.01	Fixed model

T, treatment group; CHM, Chinese herbal medicine; ALSFRS, ALS functional rating scales; ALSFRS-r, revised ALS functional rating scales; m, months; MD, mean difference.

relationship between CHM intake and ALS prognosis, as well as the mechanisms underlying the effects.

Our studies demonstrated that the most frequent formulae were Jia Wei Si Jun Zi decoction. Zhu observed the effect of supplementary Sijunzi decoction on SOD1 transgenic ALS mice and explored the mechanisms involved; the results showed that the Sijunzi decoction may reduce the abnormal aggregation of abnormally phosphorylated neurofilaments around the nuclei probably by inhibiting the abnormal phosphorylation of neurofilament, thus maintaining the integrity of the cytoskeleton, alleviating axonal atrophy, improving axonal transport, delaying neuronal degeneration, and exerting neuroprotective effects (9).

ALS is a form of a wilt disease in traditional medicine (32). TCM physicians believe that the pathogenesis of a wilt disease is mostly related to deficiencies in the spleen, kidneys, lungs, and liver, and consider that the therapeutic principles of invigorating the spleen, soothing the liver, and tonifying the kidneys and lungs are beneficial for ALS from a syndrome differentiation point of view; thus, therapeutic prescriptions such as Jianpi Bushen, Jianpi Yifei, and Bushen Jianpi Shugan prescriptions are used extensively. Zhu et al. showed that Jianpi Bushen prescription could improve the activity ability as well as balance in a ADAR2-knockout ALS mouse; this may be associated with the delayed degeneration and loss of anterior horn neurons as well as the inhibition of ADAR2 immunoreaction generated by CHM (33). Pan et al. found that Jianpi Yifei prescription may play a neuroprotective role by inhibiting the activation of microglia and by downregulating the expression of the p38 MAPK protein and inflammatory factors by mediating the p38 MAPK pathway in a mouse model of ALS (34). These results demonstrate the potential of a CHM prescription as a supplementary treatment for ALS.

A previous study analyzed a CHM prescription for a wilt disease and ALS by data mining and found that the commonly used herbs were *dangshen, huangqi, fuling, baizhu, dihuang*, and *danggui* (35); the results were consistent with our present findings. The TCM theory suggests that *dihuang* can tonify the kidney, nourish *yin*, and fill lean pulps, that *dangshen* can replenish the spleen and lung *qi*, that *huangqi, fuling*, and *baizhu* can tonify *qi* and strengthen the spleen, and that *danggui* can tonify blood circulation and relieve pain. Evidence from modern medicine shows that the pathogenesis of ALS mainly involves excitotoxicity, oxidative stress, mitochondrial abnormality, and immune inflammatory response (36). Patients with ALS have elevated levels of glutamate (Glu) in the cerebrospinal fluid and elevated levels of Glu release were found in the spinal cord of ALS transgenic mice (37), thus aggravating excitotoxicity. It has been shown that *dihuang* extract exerts cytoprotective effects on Glu-induced PC12 cytotoxic injury *via* pathways related to energy metabolism (38). *Dangshen, fuling*, and *baizhu* may benefit ALS by antioxidation (39–42). On the other hand, the combination of *huangqi* and *danggui* may be beneficial for ALS by regulating the gene expression of T cells and cytokines, thus playing a role in immune regulation (43, 44).

Strengths of this study compared to those published previously

A previous systematic review and meta-analysis on tonic class prescriptions for ALS was published in 2016 and showed that CHM was superior to conventional therapy in terms of improving clinical effects and m-Norris scale score (45). However, our present study is very different. First, the previous studies did not register the associated protocol in advance on PROSPERO or other platforms and used the Jadad scale to assess the quality of studies. In our study, we registered our review protocol on PROSPERO (Reference: CRD42022323047) to avoid selection bias and used the Cochrane risk and bias

tool to evaluate the quality of the included studies. Second, we performed our systematic and comprehensive literature search from inception to March 2022 to gather more up-to-date trials from six databases. We only included Chinese herbal compounds or decoctions and excluded other forms of Chinese medicines such as acupuncture and massage. Third, we assessed different outcomes from different perspectives especially patient-centered outcomes such as mortality and quality of life.

Limitations and implications for research

There are some limitations associated with our meta-analysis that need to be considered, i.e., the included trials were conducted in China. In the future, we must incorporate more RCT results from other countries or different races. We also restricted the retrieval language to both Chinese and English; this may have led to a potential publication bias. ALS is also a progressive disease; we did not collect detailed characteristics of the disease or grade the severity of ALS. Therefore, we were unable to evaluate the efficacy of CHM for different grades of ALS. Furthermore, the outcomes were mainly subjective, and the blinding of outcome assessors was mostly unclear; this may have affected the credibility of the efficacy data. Further studies need to evaluate hard endpoints such as survival and mortality or consider objective indices such as electromyogram results. Future research should exhibit more conformity in terms of outcome measures. Furthermore, the designs of the included studies were relatively poor; future studies should involve randomization and triple blinding and recruit a larger number of participants to conduct a more rigorous and methodological study. Personnel should perform follow-up studies to demonstrate the long-term efficacy of CHM. We were unable to identify a specific important ingredient. However, Jia Wei Si Jun Zi decoctions, Ji Wei Ling preparations, and Fu Yuan Sheng Ji granules had relatively more studies in our review, and subjects numbers should be priorities for further research. It is also hoped that future research will continue to explore the mechanisms and efficacy of specific drugs or active ingredients.

Conclusion

Our study suggests that short-term adjunct use of CHM could improve ALSFRS score and exert beneficial clinical effects with a good safety profile when compared with a placebo or riluzole alone. However, future research or clinical studies should focus on the long-term efficacy of patient-oriented outcomes.

Data availability statement

The original contributions presented in the study are included in the article/Supplementary material, further inquiries can be directed to the corresponding author/s.

Author contributions

LG and QC conceived and designed the study. YL and SH drafted the manuscript, screened the studies, and extracted the data. YL performed the meta-analysis. DLiu, SY, and DLi interpreted the results and revised the manuscript. All authors have read and agreed to the published version of the manuscript.

Funding

This study was funded and supported by the Yunnan Provincial Science and Technology Department-Applied Basic Research Joint Special Funds of Chinese Medicine (Youth Project: 202101AZ070001-127) and by Kunming Health Science and Technology Talents Training Project (Number: 2019-SW-province-20).

Acknowledgments

The authors would like to express their gratitude to EditSprings (https://www.editsprings.cn) for the expert linguistic services provided.

Conflict of interest

The authors declare that the research was conducted in the absence of any commercial or financial relationships that could be construed as a potential conflict of interest.

Publisher's note

Supplementary material

The Supplementary Material for this article can be found online at: https://www.frontiersin.org/articles/10.3389/fneur.2022.988034/full#supplementary-material

References

1. Ustyantseva EI, Medvedev SP. Zakian, SM. Studying ALS: current approaches, effect on potential treatment strategy. *Adv Exp Med Biol.* (2020) 1241:195–217. doi: 10.1007/978-3-030-41283-8_11

2. Hulisz D. Amyotrophic lateral sclerosis: disease state overview. *Am J Manag Care.* (2018) 24:S320—6.

3. Zhu J, Shen L, Lin X, Hong Y, Feng Y. Clinical research on traditional chinese medicine compounds and their preparations for amyotrophic lateral sclerosis. *Biomed Pharmacother.* (2017) 96:854–64. doi: 10.1016/j.biopha.2017.09.135

4. Suh WJ, Seo Y, Jin C, Cho SY, Park SU, Jung WS, et al. Traditional east asian herbal medicine for amyotrophic lateral sclerosis: a scoping review. *Evid Based Complement Alternat Med.* (2021) 5674142. doi: 10.1155/2021/5674142

5. Meyer T. Amyotrophic lateral sclerosis (ALS) - diagnosis, course of disease and treatment options. *Dtsch Med Wochenschr.* (2021) 146:1613–8. doi: 10.1055/a-1562-7882

6. Orrell RW, Lane RJ, Ross M. Antioxidant treatment for amyotrophic lateral sclerosis / motor neuron disease. *Cochrane Database Syst Rev.* (2007) 1:CD002829. doi: 10.1002/14651858.CD002829.pub4

7. Pan W, Chen X, Bao J, Bai Y, Lu H, Wang Q, et al. The use of integrative therapies in patients with amyotrophic lateral sclerosis in Shanghai, China. *Evid-based Complement Altern Med.* (2013) 2013:613596. doi: 10.1155/2013/613596

8. Li J, Deng T. *Great Dictionary of Chinese Medicine. 1st ed.* Beijing: People's Medical Pulishing House. (1995).

9. Zhu X, Chen J, Weng W, Sun Y, Li H, Sheng X, et al. Neuroprotective effects of Modified Sijunzi Decoction on transgenic mouse model of amyotrophic lateral sclerosis. *J Tradit Chin Med.* (2017) 51:10. doi: 10.16305/j.1007-1334.2017.S1.051

10. Moher D, Liberati A, Tetzlaff J, Altman DG. PRISMA Group Preferred reporting items for systematic reviews and meta-analyses: the PRISMA statement. *BMJ.* (2009) 339:b2535. doi: 10.1136/bmj.b2535

11. Brooks BR. El Escorial World Federation of Neurology criteria for the diagnosis of amyotrophic lateral sclerosis. Subcommittee on motor neuron diseases/amyotrophic lateral sclerosis of the world federation of neurology research group on neuromuscular diseases and the El Escorial "Clinical limits of amyotrophic lateral sclerosis" workshop contributors. *J Neurol Sci.* (1994) 124:96–107. doi: 10.1016/0022-510X(94)90191-0

12. Chinese Society of Neurology. Diagnostic criteria for amyotrophic lateral sclerosis (draft). *Chin J Neurol.* (2001) 34:190. doi: 10.3760/j.issn:1006-7876.2001.03.032

13. Cedarbaum JM, Stambler N, Malta E, Fuller C, Hilt D, Thurmond B, et al. The ALSFRS-R: a revised ALS functional rating scale that incorporates assessments of respiratory function. BDNF ALS study group (Phase III). *J Neurol Sci.* (1999) 169:13–21. doi: 10.1016/S0022-510X(99)00210-5

14. Appel V, Stewart SS, Smith G, Appel SH, A. rating scale for amyotrophic lateral sclerosis: description and preliminary experience. *Ann Neurol.* (1987) 22:328–33. doi: 10.1002/ana.410220308

15. Zhang N.Effect of Shenmai injection in adjuvant treatment of motor neuron disease patients with amyotrophic lateral sclerosis. *Chin Med J.* (2020) 32:49–50.doi: 10.3969/j.issn.1672-0369.2020.08.019

16. Li C, Hu L, Kong L, Gao J, Zhu X, Zhi H.Efficacy of Fuyuanshengji Granule on the short period prognosis of the patients with amyotrophic lateral sclerosis. *J Neuro Rehabilitation.* (2011) 8:61–64. doi: 10.3969/j.issn.1672-7061.2011.02.002

17. Wang J, Gao J, Guo Y, Qing B, Ren H, Xu W, et al. Clinical study of the effect of fuyuanshegnji granule on symptoms of the patients with amyotrophic lateral sclerosis. *J Neuro Rehabilitation.* (2009) 6:173–5. doi: 10.3969/j.issn.1672-7061.2009.03.003

18. Ren H, Zhi H, Gao J. Ma D. Randomized controlled clinical trial on Fuyuan Shengji granule and riluzole for treatment of amyotrophic lateral sclerosis. *J Liaoning University of Trad Chin Med.* (2013) 5:154–6. doi: 10.13194/j.jlunivtcm.2013.07.156.renhl.110

19. Chen J, Ping Y, Wang D.Clinical observation on 240 cases of amyotrophic lateral sclerosis treated with Jiweiling series preparation. *N Chin Med.* (2005) 09:38–9. doi: 10.3969/j.issn.0256-7415.2005.09.018

20. Zhu X, Zhang H, Li H, Zhang S, Chen J, Wang J, et al. Clinical efficacy and safety evaluation of supplementary Sijunzi decoction in treatment of ALS patients with Splenasthenic syndrome. *Clini Misdiagnosis Misther.* (2017) 30:81–7. doi: 10.3969/j.issn.1002-3429.2017.01.028

21. Wang A, Li X, Ren Z, Hou X, Lu M, Du B, et al. Clinical efficacy of spleen-invigorating and lung-replenishing therapy for patients with amyotrophic lateral sclerosis. *World Chin Med.* (2017) 12:1364–7. doi: 10.3969/j.issn.1673-7202.2017.06.038

22. Su G, Zhang J, Hong Y. Treatment of 25 cases of amyotrophic lateral sclerosis with Yiqi Qiangji Decoction. *Chin J Integr Med.* (2006) 4:452–3. doi: 10.3969/j.issn.1672-1349.2006.05.046

23. Pan Z. *Clinical Study on Treatment of Chong Meridian qi Adversely Ascending Type Amyotrophic Lateral Sclerosis by Shenzhe Jiangqi Powder.* Hebei Medical University. (2015). doi: 10.7666/d.Y2784845

24. Wang X. *The Clinical Study of JIWEILING Injection in Dealing With Amyotrophic Lateral Sclerosis Buibar Paralysis.* Hebei Medical University. (2007). doi: 10.7666/d.y1156662

25. Sui S, Wang Y, Zhi H, Hong Y, Feng Y. Effect of "Huoling Shengji Formula"in treatment of amyotrophic lateral sclerosis. *J Tradit Chin Med.* (2016) 30:23–6. doi: 10.16306/j.1008-861x.2016.02.006

26. Wu Y, Zheng Z, Bai X, Yang S, Wang R. F wave analysis of the dry prognosis of astragalus root in amyotrophic lateral sclerosis. *China J Chin Materia Medica.* (2016):1454—5.

27. Ma W. *The clinical study of JIWEILING injection in dealing with amyotrophic lateral sclerosis buibar paralysis.* Hebei Medical University. (2006). doi: 10.7666/d.y969929

28. Pan W, Su X, Bao J, Wang J, Zhu J, Cai D, et al. Open randomized clinical trial on JWSJZ decoction for the treatment of ALS patients. *Evid Based Complement Alternat Med.* (2013) 2013:347525. doi: 10.1155/2013/347525

29. Wenjie X, Hongli R, Huiping Z. Effects of kidney-tonifying,spleen-strengthening and liver-soothing method on amyotrophic lateral sclerosis. *J Tradit Chin Med.* (2011) 25:4. doi: 10.16306/j.1008-861x.2011.05.014

30. Listed N. The Amyotrophic Lateral Sclerosis Functional Rating Scale. Assessment of activities of daily living in patients with amyotrophic lateral sclerosis. The ALS CNTF treatment study (ACTS) phase I-II Study Group. *Arch Neurol.* (1996) 53:141–7. doi: 10.1001/archneur.1996.00550020045014

31. Wang J, Zhou S, Chen J, Ma Consistency W, andsynergistic effects of the four clinical scale methods for evaluating amyotrophic lateral sclerosis. *Chinese J. Rehabilitation Med.* (2005) 9:24–6. doi: 10.3321/j.issn:1673-8225.2005.29.011

32. Yao S. Wilting disease (Amyotrophic lateral sclerosis). *N Chin Med.* (1985) 05:36.

33. Zhu W, Wang M, Li T, LIU Y, Pan W, Study on the mechanism of Jian-Pi-Bu-Shen decoction in the treatment of amyotrophic lateral sclerosis. *J Neurol.* (2021) 17:57–62.

34. Pan X, Yang B, Du B, Zheng Y, Li H. Effect of Jianpi Yifei prescription on p38 MAPK protein and inflammatory factors expression in spinal cord of ALS hSOD1-G93A transgenic mice. *Chin Med J (Engl).*(2018) 24:155–60. doi: 10.1155/2018/5897817

35. He P. *Study on the Law and Mechanism of Drug Use in Literature of Ancient Dysfunction Syndrome and Modern Amyotrophic Lateral Sclerosis.* Bejing University of Chinese Medicine. (2021).

36. Oskarsson B, Gendron TF, Staff NP. Amyotrophic lateral sclerosis: an update for 2018. *Mayo Clin Proc.* (2018) 93:1617–28. doi: 10.1016/j.mayocp.2018.04.007

37. Guo Y, Li S, Zhang H, Wu Y. Advance in pathogenesis of amyotrophic lateral sclerosis (review). *Chin J Rehabil.* (2017) 23:685–9. doi: 10.3969/j.issn.1006-9771.2017.06.014

38. Liu Y, Liu L, Ying XX, et al. Dried Rehmannia root protects against glutamate-induced cytotoxity to PC12 cells through energy metabolism-related pathways. *Neural Regen Res.* (2017) 12:1338–46. doi: 10.4103/1673-5374.213556

39. Puentes F, Malaspina A, van Noort JM, Amor S. Non-neuronal Cells in ALS: Role of Glial, Immune cells and Blood-CNS Barriers. *Brain Pathol.* (2016) 26:248–57. doi: 10.1111/bpa.12352

40. Xie Q, Cheng X, Hu F, Wang C. Research advance on chemical constituents, pharmacological action and quality control of Radix Codonopsis. *J Tradit Chin Med.* (2020) 54:94–104. doi: 10.16305/j.1007-1334.2020.08.013

41. Den T, Peng D, Yu N, Wang L, Zhang Y, Ding Z, et al. Research progress on chemical composition and pharmacological effects of Poria COCOS and predictive analysis on quality markers. *Chin Tradit Herb*. (2020) 51:2703–17 doi: 10.7501/j.issn.0253-2670.2020.10.013

42. Du H, He S, Hu H, Li H. Review of pharmacological effects of active ingredient of Atractylodes macrocephala. *J Tradit Chin Med Sci*. (2022)54:76–80. doi: 10.19844/j.cnki.1672-397X.2022.05.023

43. Lyon MS, Wosiski-Kuhn M, Gillespie R, Caress J, Milligan C. Inflammation immunity and amyotrophic lateral sclerosis: *Etiology* I. and pathology. *Muscle Nerve*. (2019) 59:10–22. doi: 10.1002/mus.26289

44. Xiang L, Zhang Q, Zhao Q, Qin L, Gong W. Research progress on chemical constituents, pharmacological effects and clinical applications of Astragali Radix- Angelicae Sinensis Radix. *Chin Tradit Herb*. (2022) 53:2196–213. doi: 10.7501/j.issn.0253-2670.2022.07.030

45. Li X, Liu M, Ying A, Han C, Liu Y, Liu J. Meta analysis on traditional chinese medicine tonic class prescriptions intreatment of amyotrophic lateral sclerosis. *Chin J Exp Tradit Medical Formulae*. (2016) 22:7. doi: 10.13422/j.cnki.syfjx.2016040201

Appendix

Search strategy

#1 "amyotrophic lateral sclerosis"[MeSH Terms]
#2 "randomized controlled trial"[tw] OR "controlled clinical trial"[tw] OR "randomized"[tw] OR "placebo"[tw] OR "randomly"[tw]
#3 (((((("Medicine, Chinese Traditional"[Mesh]) OR "Drugs, Chinese Herbal"[Mesh]) OR "Medicine, Traditional" [Mesh]) OR "Plants, Medicinal" [Mesh]) OR "Phytotherapy" [Mesh]) OR "Pharmacognosy" [Mesh]) OR "Plant Extracts" [Mesh]) OR "Ethnopharmacology" [Mesh]
#4 (traditional [tw] or Chinese [tw] or "traditional Chinese" [tw] or folk [tw] or therapy [tw] or preparation [tw]) and (drug? [tw] or herbal [tw] or plant? [tw] or extract? [tw]) or indigenous [tw] or Kampo [tw] or Kanpo [tw]) and (medici*[tw] or remedies[tw] or herb? [tw] or pharmaceutical [tw] or healing [tw])
#5 #3 OR #4
#6 #1 AND #2 AND #5

frontiers | Frontiers in Neurology

TYPE Review
PUBLISHED 15 November 2022
DOI 10.3389/fneur.2022.1034243

OPEN ACCESS

EDITED BY
Guowei Li,
Guangdong Second Provincial General Hospital, China

REVIEWED BY
David James Brooks,
Newcastle University, United Kingdom
Teodorico Castro Ramalho,
Universidade Federal de Lavras, Brazil

*CORRESPONDENCE
Xianfu Lu
ahluxianfu@163.com
Yi Lyu
19111360001@fudan.edu.cn

SPECIALTY SECTION
This article was submitted to Dementia and Neurodegenerative Diseases, a section of the journal Frontiers in Neurology

RECEIVED 01 September 2022
ACCEPTED 31 October 2022
PUBLISHED 15 November 2022

CITATION
Cao Y, Yu F, Lyu Y and Lu X (2022) Promising candidates from drug clinical trials: Implications for clinical treatment of Alzheimer's disease in China. *Front. Neurol.* 13:1034243. doi: 10.3389/fneur.2022.1034243

Promising candidates from drug clinical trials: Implications for clinical treatment of Alzheimer's disease in China

Yuxia Cao[1], Feng Yu[1], Yi Lyu[2]* and Xianfu Lu[3,4]*

[1]School of Basic Medicine and Clinical Pharmacy, China Pharmaceutical University, Nanjing, China, [2]Department of Anesthesiology, Minhang Hospital, Fudan University, Shanghai, China, [3]Department of Anesthesiology (High-Tech Branch), The First Affiliated Hospital of Anhui Medical University, Hefei, China, [4]Department of Anesthesiology, Anqing First People's Hospital of Anhui Medical University, Anqing, China

Alzheimer's disease is the most common neurodegenerative disease. Prior to 2017, National Medical Products Administration approved only four drugs to treat Alzheimer's disease, including three cholinesterase inhibitors and one N-methyl-D-aspartate receptor antagonist. We queried ClinicalTrials.gov to better understand Alzheimer's drug development over the past 5 years and found 16 promising candidates that have entered late-stage trials and analyzed their impact on clinical treatment of Alzheimer's disease in China. The 16 compounds selected include disease-modifying therapies and symptomatic therapies. The research and development pipeline now focuses on disease-modifying therapies such as gantenerumab, aducanumab, ALZ-801, ALZT-OP1, donanemab, lecanemab, simufilam, NE3107, semaglutide, and GV-971, which could put an end to the situation where Alzheimer's patients in China have no effective treatment alternatives. The reuse of drugs or combinations currently under investigation for the psychiatric treatment of Alzheimer's disease, including AXS-05, AVP-786, nabilone, brexpiprazole, methylphenidate, and pimavanserin, could provide physicians with additional treatment options. Although most of these drugs have not been explored in China yet, due to the current development trend in this field in China, it is expected that China will be involved in research on these drugs in the future.

KEYWORDS

Alzheimer's disease, clinical trials, drug development, clinical treatment, China

Introduction

Alzheimer's disease (AD) is a form of dementia that affects memory, thinking, and behavior. It is the most common disease among neurodegenerative disorders. Symptoms include cognitive dysfunction, mental problems, behavioral disturbances, and difficulty performing activities of daily living, all of which have a significant impact on patients' daily lives (1). As the world's population continues to age, the incidence of AD is increasing. According to the 2019 Global Burden of Disease Study, AD is the leading cause of death in people over 75 years of age (2). Incidence rates in people over 65

and 85 are 5% and more than 30%, respectively (3). There are an estimated 50 million worldwide, including 10 million in China. It is estimated that there will be about 130 million Alzheimer's patients worldwide by 2050 (3).

In the Chinese Guidelines for the Diagnosis and Treatment of Alzheimer's Disease published in 2020 (4), there are mainly two types of drugs approved to alleviate cognitive impairment in AD patients, including cholinesterase inhibitors (donepezil, rivastigmine, and galantamine) and glutamate receptor antagonists (memantine), as well as drugs to treat psychiatric symptoms in AD patients. All of the above medications treat symptoms only and have limited effects on AD patients. These medications are far from meeting the needs of the current medical system in light of the increasing prevalence of AD. As research found, amyloid-beta (Aβ) accumulation, the growth of neurofibrillary tangles (NFT), and tau protein hyperphosphorylation are the major causes of AD (5). Increased accumulation of reactive oxygen species (ROS) induces oxidative stress and neuronal cell abnormalities which is one of the pathogenesis of AD (5). Anti-Aβ drugs, anti-tau drugs, and antioxidants, among others, may become promising preventive and therapeutic species for AD. However, these drugs are still under active development, and future research results are unknown.

The development of novel drugs has increased dramatically due to the enormous and largely unmet clinical need. However, failures in this area of drug development are common. According to reliable sources, the failure rate for cancer drug development is 92%, while the failure rate for AD clinical trial development can be as high as 99.6% (6). It can be argued that pharmacological research and development (R&D) in the field of AD treatment is slow compared to other disease areas and is in a state of constant wandering and investigation. Research progress on potentially effective neuroprotectors and therapeutic strategies that prevent the development of AD is stalled because of a lack of adequate understanding of the intricate mechanisms of neurodegeneration (7). Apart from the above reasons, imperfect preclinical models and lack of validated diagnosis contribute to the high failure rate in the development of AD (8). The huge demand for AD drugs and the high failure rate in R&D require us to capture the latest AD candidates in late-stage development and then explore their potential impact on the treatment of AD patients in China in the future. In this paper, we conduct an annual review of the AD drug development pipeline and present the results of our 2017–2021 pipeline analysis as presented on ClinicalTrials.gov.

A total of 473 studies were included in our database. These studies are mainly conducted in the United States (US), Europe, China, and other increasingly aging regions. Phase I and Phase II studies accounted for a substantial proportion of the total, 36.36 and 41.86%, respectively. From these studies, we selected 16 compounds that are in late-stage development. Figure 1 illustrates various therapeutic targets in AD.

Disease-modifying therapy

Anti-amyloid strategies

Aducanumab

Aducanumab, marketed as aduhelm, is an Aβ-direct antibody manufactured by Biogen. Treatment with aducanumab should be initiated in patients with mild cognitive impairment (MCI) or mild dementia (9). It is suitable for all genotypes of early AD (10). The chemical structure of aducanumab is not available online, but studies have found that it binds to the N-terminus of Aβ in an extended conformation (11). Its mechanism of action (MOA) involves binding of aggregated forms of Aβ rather than monomers. Aβ may contribute to cell death and tissue loss in parts of the brain critical for memory, thinking, learning, and behavior. In a first-in-human study (NCT01397539), a dose of 30 mg/kg demonstrated an acceptable safety and tolerability profile, although patients receiving 60 mg/kg of aducanumab experienced serious adverse events (SAEs) and symptomatic amyloid-related imaging abnormalities (ARIA) that resolved at weeks 8–15 (12). Biogen announced in December 2014 that the drug had entered Phase III. However, ARIA-edema (ARIA-E) and ARIA-hemorrhage (ARIA-H), two of the most common adverse events (AEs), occurred in 362 of the 1,029 patients (35.2%) in the 10 mg/kg group in the phase 3 randomized clinical trials (RCTs) of aducanumab EMERGE (NCT02484547) and ENGAGE (NCT02477800) (13). In March 2019, Biogen and Eisai announced that all ongoing aducanumab trials would be discontinued due to the likelihood that EMERGE and ENGAGE would miss their primary endpoints in the interim analysis. Fortunately, Biogen later announced that EMERGE had met its primary endpoint. Key endpoints were significantly reduced in participants who received a high dose, and secondary endpoints declined less. Although patient progress was delayed in the low-dose group, the differences were not statistically significant compared with the placebo group. Although the primary objective of the ENGAGE study was not met, an exploratory analysis showed that patients taking 10 or more mg/kg deteriorated more slowly (14). Based on the results of the above studies, aducanumab may produce a dose-dependent reduction in amyloid and some reduction in phospho-tau (p-tau) in the cerebrospinal fluid (CSF). The Food and Drug Administration (FDA) granted fast-track approval for aducanumab on the condition that Biogen complete a post-approval clinical trial in August 2021 to confirm the drug's efficacy (15).

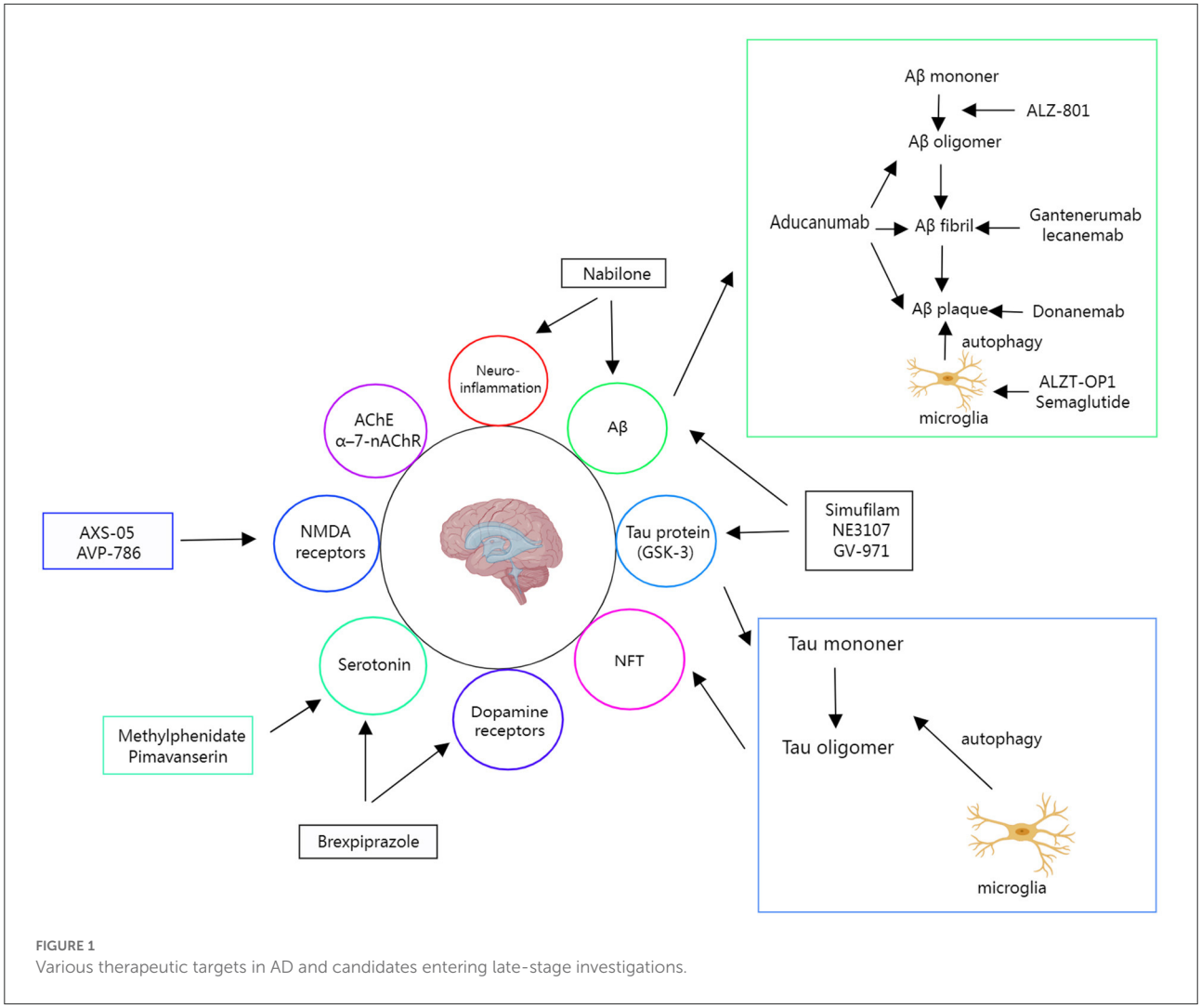

FIGURE 1
Various therapeutic targets in AD and candidates entering late-stage investigations.

ALZ-801

Alzheon developed ALZ-801 (Figure 2A). Several ALZ-801 molecules surround and engage with Aβ monomers using an enveloping MOA, maintaining their structure and preventing the synthesis of neurotoxic oligomers (16). This prevents the hippocampus' shrinkage, which is linked to the onset and progression of the disease (16). ALZ-801 is an orally accessible valine-conjugated tramiprosate prodrug (17). It and tramiprosate are both converted to 3-sulfo-propanic acid (3-SPA), which is present in the brain and inhibits Aβ42 aggregation (17). Compared to tramiprosate, ALZ-801 has better gastrointestinal tolerability and more stable plasma levels, resulting in higher brain penetration (18). Patients with moderate AD and APOE4/4 homozygotes are the target population (19). Alzheon began a phase II open-label biomarker study in September 2020 (NCT04693520) with results expected in July 2023. Patients with early AD and one or two copies of APOE4 are enrolled in the study. Alzheon presented interim results in February 2022 on 80 patients treated for 6 months, reporting a 29% decrease in plasma P-tau18 from baseline, a similar decrease in the p-tau181/Aβ42 ratio, and improvement in the Rey Auditory Verbal Learning Test (RAVLT) (20). From May 2021 to April 2024, the phase 3 trial (NCT04770220) is ongoing. It intends to enroll 300 APOE4 homozygotes with early to mild AD who receive 265 mg of ALZ-801 or placebo twice daily for 18 months. To date, data from these two studies has not been published. Depending on the progress of the studies, Alzheon decides to submit its marketing application to the FDA in 2025.

Gantenerumab

Gantenerumab is a purely human IgG1 antibody developed by Roche that targets Aβ fibrils. Its primary study population consists of patients with early AD of all genotypes. Its chemical structure remains a mystery. The therapeutic rationale for this antibody is that it eliminates amyloid plaques *via* Fcγ

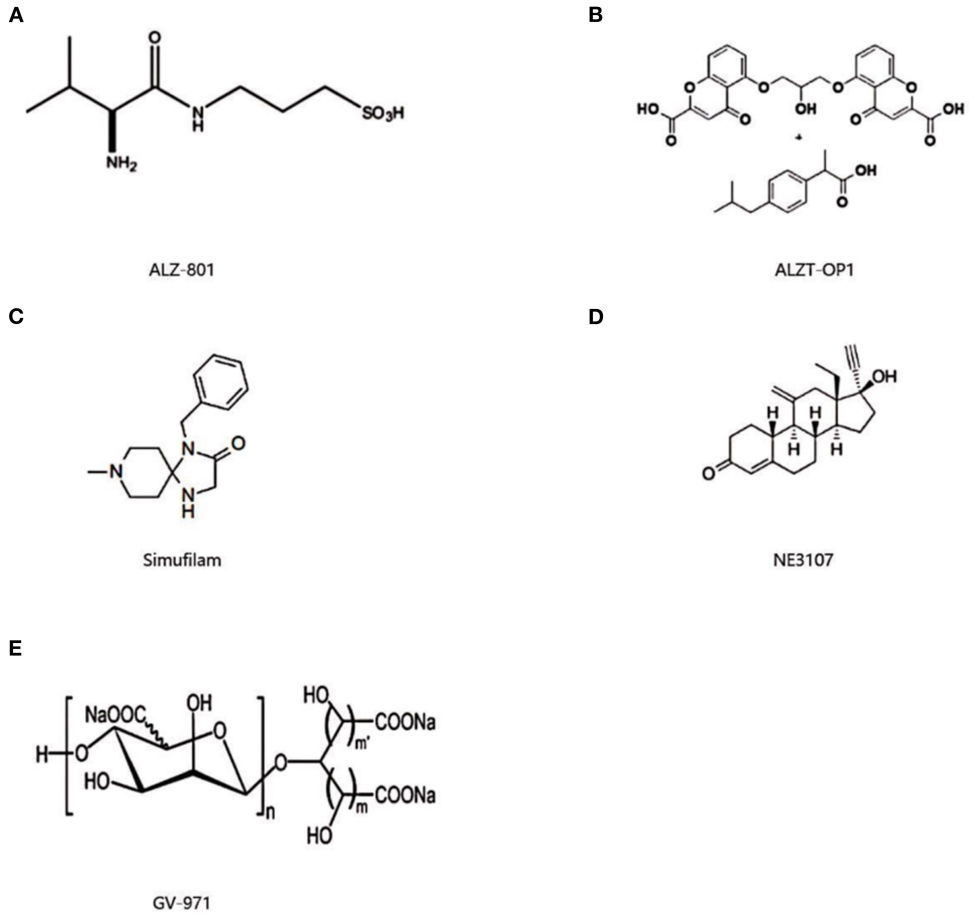

FIGURE 2
Chemical structure of ALZ-801 **(A)**, ALZT-OP1 **(B)**, simufilam **(C)**, NE3107 **(D)**, and GV-971 **(E)**.

receptor-mediated microglial phagocytosis and binds with high affinity to aggregated Aβ-species (21–23). *In vivo*, gantenerumab suppresses oligomeric Aβ42's neurotoxic effects (23). The PK profile of gantenerumab after subcutaneous administration was shown to attain a peak plasma concentration at a median time of 119h (about 5 days) and then fell in a mono-exponential way in a Phase I study (NCT02882009) (24). It showed that subcutaneous gantenerumab injections at rates of 5 and 15 s were well-tolerated in healthy volunteers, potentially allowing patients with AD or their caretakers to administer the drug at home (24). Aβ plaque levels were below the Aβ positive criterion in 37 and 51% of patients at years 1 and 2, respectively, in a positron emission tomography (PET) sub-study interim analysis of Roche's Scarlet RoAD (NCT01224106) and Marguerite RoAD (NCT02051608) (25). At 2 years, 51% patients receiving up to 1,200 mg of gantenerumab had PET amyloid levels consistent with sparse to non-neuritic Aβ (25). In 2021, the FDA designated gantenerumab as a breakthrough therapy. According to the favorable procedure of gantenerumab, Roche intends to submit a new drug application (NDA) in 2022.

Lecanemab

Biogen and Eisal collaborated on the development of lecanemab, formerly known as BAN2401. The target population of lecanemab is early AD patients of all genotypes and APOE4 carriers (10). There is no information available online about the chemical structure of lecanemab. Lecanemab is an antibody that binds to a soluble, poisonous form of Aβ (26). The binding is intended to neutralize Aβ and "tag" them so that the immune system can clear them from the brain before they aggregate and become plaques (26). The humanized IgG1 variant of the mouse monoclonal antibody mAb158 binds preferentially to soluble monomeric forms of Aβ. MAb158 has been shown to reduce Aβ protofibrils in the

brain (42% less) and CSF in tg-ArcSwe mice (53% less) (27). In addition, mAb158 was found to protect neurons and reduce the toxicity of Aβ-protofibrils in neuron-glia co-cultures of mice by counteracting the abnormal accumulation of these protofibrils in astrocytes (28). Compared with the anti-amyloid antibodies aducanumab and gantenerumab, lecanemab was found to bind most strongly to Aβ-protofibrils, preferring the other highly aggregated forms (29). The sponsor conducted a combined single- and multiple-ascending dose study (NCT01767311) in August 2010 to evaluate the safety, tolerability, immunogenicity, pharmacodynamic response, and pharmacology of intravenous lecanemab in participants with mild to moderate AD. The incidence of ARIA-E/H on magnetic resonance imaging (MRI) was comparable to that of the placebo group. In all cases, lecanemab was extremely safe (30). However, the 12-month primary endpoint was not met (31). According to Bayesian and frequentist analyses, lecanemab at a dose of 10 mg/kg every 2 weeks reduced brain amyloid (0.306 SUVr units) and showed a difference between drug and placebo in favor of active treatment by 27 and 30% on the Alzheimer's Disease Composite Score (ADCOMS), 56 and 50% on the 14-item Alzheimer's Disease Assessment Scale, Cognitive Subscale (ADAS-Cog14), and 33 and 26% on the Clinical Dementia Rating Scale-Sum of Boxes (CDR-SB) compared with placebo at 18 months (31). Biomarkers in the CSF confirmed the treatment effect (31). Eisal initiated a phase III study called Clarity AD (NCT03887455) in March 2019 to evaluate the safety and efficacy of lecanemab in people with early AD. The Alzheimer's Clinical Trial Consortium (ACTC) launched a large trial (NCT04468659) next year that is expected to last until 2027 and was co-funded by the National Institutes of Health (NIH) and Eisal. The FDA designated lecanemab as a breakthrough therapy in June 2021 and granted it fast-track designation in late 2021 to expedite its review. The sponsors submitted the NDA to the FDA for approval in September 2021.

Donanemab

Lilly is exploring donanemab, a biologic that binds to deposited amyloid plaques in the brain, for the treatment of early AD in all genotypes (10). The chemical structure of donanemab has not yet been published. Donanemab targets an N-terminal pyroglutamate Aβ epitope found only in existing plaques (32–34). It is epitope specific, with no off-target binding to other Aβ species, neurotransmitters, or their receptors, and no known symptomatic effect (35). The MOA of donanemab is not just about preventing plaque deposition or growth, but rather about targeting deposited plaques to eliminate the existing amyloid burden in the brain. Some previous plaque-binding antibodies have been withdrawn because they caused microbleeds in the brain (36). Donanemab was well-tolerated in a dose-escalation study up to 10 mg/kg. And even 10 mg/kg caused significant changes in amyloid deposition (40–50%). It was observed that increasing the dose prolonged the mean terminal elimination half-life (34). Lilly undertook TRAILBLAZER-ALZ, a Phase II trial (NCT03367403) in early symptomatic AD to evaluate the safety, tolerability, and efficacy of donanemab. Reductions in amyloid plaques and global tau burden with donanemab were 85.06 centiloids and 0.01 greater than with placebo, respectively, at 76 weeks (35). Despite mixed secondary outcomes, donanemab has a better composite score for cognition and ability to perform activities of daily living than placebo (35). In two phase II studies, both infusion reactions occurred. Lilly began recruiting in TRAILBLAZER-ALZ 2 (NCT04437511), a phase II safety and efficacy study, in October 2020. It was then expanded to a Phase III registration study with 1,500 participants, with results expected in the first half of 2023 (36). Lilly is currently conducting three Phase III studies: TRAILBLAZER-EXT (NCT04640077), TRAILBLAZER-ALZ 3 (NCT05026866) and TRAILBLAZER-ALZ 4 (NCT05108922). In June 2021, the FDA granted donanemab breakthrough therapy designation to accelerate its development. Lilly submitted a regulatory filing in October 2021, with study data being submitted on a rolling basis.

ALZT-OP1

ALZT-OP1 is a combination product developed by AZ Therapies that includes a dry powder inhaler with cromolyn (ALZT-OP1a) and an oral tablet containing ibuprofen (ALZT-OP1b) (Figure 2B) (37). The target population is mild AD APOE4/4 homozygotes (10). Ibuprofen, a non-steroidal anti-inflammatory drug (NSAID) that is a cyclooxygenase (COX)-1 and COX-2 inhibitor and an agonist of peroxisome proliferator-activated receptors (PPARs), reduces nitric oxide (NO) synthesis, protects neurons from glutamate toxicity, and decreases production of pro-inflammatory cytokines. Ibuprofen penetrates the blood-brain barrier (BBB) and decreases neuritic plaque pathology and inflammation in the brains of people with AD. Ibuprofen is also a potent free radical scavenger that may help minimize lipid peroxidation and free radical formation. Because of its neuroprotective potential, relative safety, and long-standing use, ibuprofen has the potential to treat AD (38). Cromolyn sodium has been shown to effectively disrupt Aβ aggregation *in vitro* and dramatically reduce the amount of soluble Aβ *in vivo* after 1 week. Cromolyn sodium, alone or in combination with ibuprofen, significantly reduced aggregated Aβ levels and induced a neuroprotective microbial activation state favoring Aβ phagocytosis vs. a pro-neuroinflammatory state in $APP^{Swedish}$-expressing Tg2576 mice (39). In a Phase I plasma/CSF PK crossover trial (NCT02482324) conducted in June and July 2015 with 26 healthy volunteers at Panax Clinical Research in Florida, AZ Therapies evaluated two ALZT-OP1 dosing regimens, each lasting 2 days. The combination was found to be safe; three patients reported mild to moderate AEs

(37). Cromolyn and ibuprofen levels in CSF are thought to be sufficient to titrate the estimated daily amyloid production of 17.7 ng and the associated inflammatory response (40). In September 2015, ALZT-OP1 entered phase III. The study (NCT02547818) which evaluated the safety and efficacy of ALZT-OP1 in subjects with early AD, was completed in November 2020. Further information remains to be seen.

Semaglutide

Semaglutide is being explored to improve insulin resistance in the treatment of AD. Semaglutide, an approved anti-diabetic drug, is a synthetic, long-acting version of glucagon-like peptide-1 (GLP-1) (Figure 3). GLP-1 is a hormone produced in the gut that stimulates the release of insulin and improves insulin sensitivity by activating receptors in the pancreas, liver, and gut (41). GLP-1 has the ability to cross the BBB and may improve insulin signaling in the brain (42, 43). It also enhances synaptic plasticity, cognition, and cell survival in the hippocampus nucleus (44). GLP-1 can be engineered to penetrate the BBB and exhibit neuroprotective properties *via* lowering inflammation, oxidative stress, and other factors (42). Semaglutide has been shown in preclinical studies to increase LC3II, Beclin-1, and P62, all of which block Aβ25-35 and hence accelerate autophagy. It also prevents apoptosis by reducing Bax expression caused by Aβ25 and enhancing Bcl2 expression decreased by Aβ25-35 (45). The Alzheimer's Association's Part the Cloud program supported a Phase II trial, yet it has not been registered. Novo Nordisk ran a Phase IIIa trial in December 2020 for people with early AD. When compared to the placebo group, the semaglutide group had a 53% lower risk of acquiring dementia. In March 2021, the sponsor registered two Phase 3 trials, EVOKE (NCT04777396) and EVOKE Plus (NCT04777409), to evaluate the efficacy and safety of semaglutide in the treatment of early AD. Both will last till April 20, 2026.

Anti-tau strategies

Tau proteins currently represent one of most promising targets to treat AD. Compared to anti-Aβ therapeutic strategies with a long history of equivocal results and minimal therapeutic benefit, anti-tau therapeutic strategies emerged relatively late and showed the potential for better therapeutic effect. However, candidates that target only tau are still at an early stage of development, so they have not been included in this review.

Anti-amyloid and tau strategies

Simufilam

Simufilam, formerly PTI-125, is a unique small-molecule (oral) agent that represents a completely novel method for treating AD (Figure 2C). It returns altered filamin A (FLNA), a brain scaffolding protein, back to its original structure and function. FLNA is a scaffolding protein that modulates the actin cytoskeleton (46). It is required for the normal folding and function of Aβ and tau. FLNA in its altered form hinders the Aβ and tau proteins from folding properly. This leads them to cluster together in the brain, forming plaques and tangles. Simufilam binds to FLNA and attempts to restore its activity, which may alleviate disease symptom (47). In 2017, Cassava Sciences launched a Phase I safety study (NCT03784300) in which 24 healthy adults were given 50, 100, or 200 mg of simufilam (46). In early 2019, the company conducted a NIH-funded Phase IIa trial (NCT03748706) in people with mild to severe AD. The results showed total tau, neurogranin, and the light chain of the neurofilament all dropped by 20, 32, and 22%, respectively (48). P-tau (pT181) was diminished by 34% (48). Biomarkers of neuroinflammation in the CSF (YKL-40 and inflammatory cytokines) dropped by 5–14%, and the outcomes were similar in plasma (48). Aβ42 increased somewhat, which is a nice sign because a low Aβ42 level implies AD (48). According to the findings, simufilam prevents disease and slows neurodegeneration. The organization executed an NIH-funded Phase IIb study (NCT04079803) at 10 sites across the US from September 2019 to March 2020. The firm registered two Phase III trials (NCT04994483 and NCT05026177) in the fall of 2021. However, Cassava's trial data has been extensively attacked, the clinical trials' scientific integrity has been called into question, and some have even urged them to be halted immediately. Cassava has currently reached an agreement with the FDA to conduct the Phase III trial. Cassava stated as recently as the beginning of October that it had begun the analysis of the late-stage project plan.

NE3107

NE3107 (previously HE 3286) is an anti-inflammatory, blood-brain permeable small molecule insulin sensitizer that binds to extracellular regulated protein kinases (ERK) (Figure 2D) (49). It has been demonstrated to reduce inflammation-driven ERK- and nuclear factor kappa-B (NF-κB)-stimulated inflammatory mediators, including tumor necrosis factor (TNF-α), without interfering with their homeostatic functions (50). NE3107 inhibits inflammation and improves insulin sensitivity, all of which have been proven to diminish AD pathogenesis in preclinical and clinical trials. It reduces inflammation by blocking EPIC, which is located upstream of Aβ and p-tau. It has no known interactions with nuclear hormone receptors, passes the BBB, has a high safety profile, and no indication of immunosuppression (50). The goal of an ongoing pivotal phase 3 trial in mild and moderate AD (NCT04669028) that began in May 2021 is to see if NE3107's impact on inflammation and insulin resistance will help slow the rate of cognitive loss. The trial is now enrolling patients

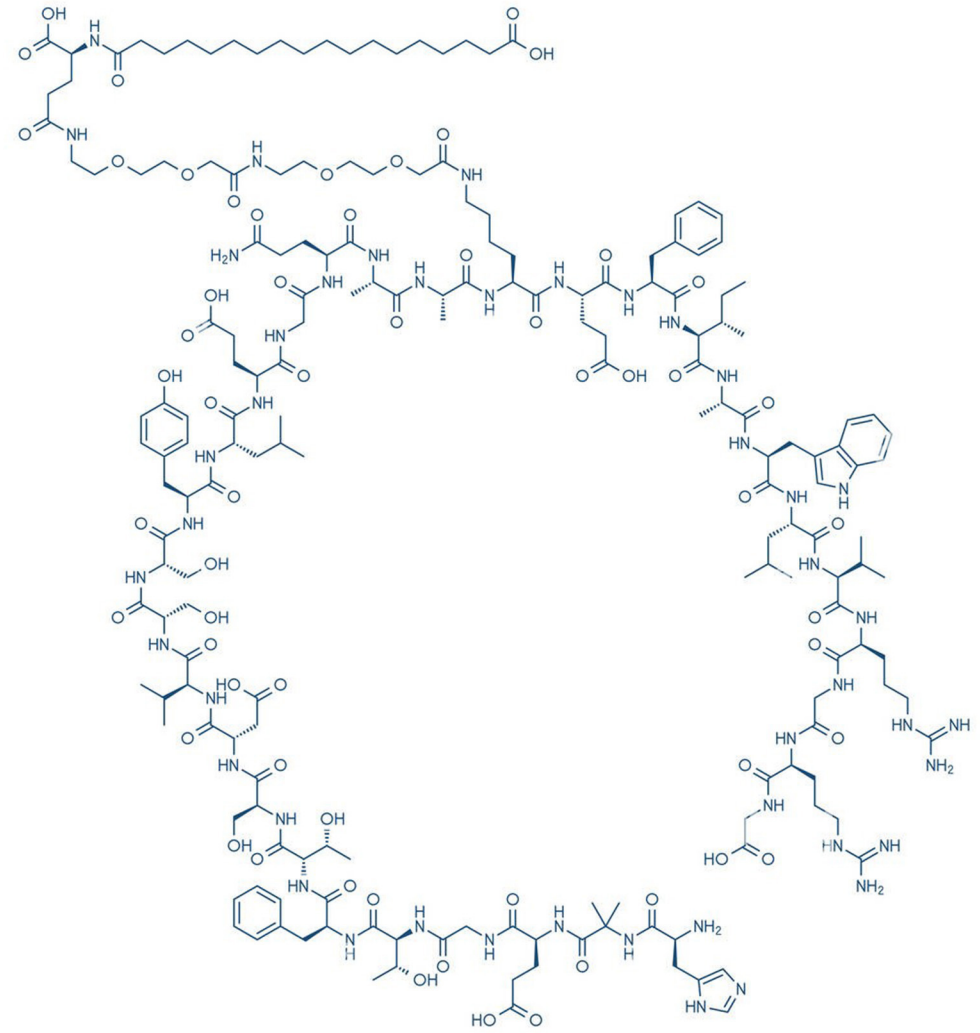

FIGURE 3
Chemical structure of semaglutide.

and expanding to 45 sites. The data readout is scheduled for mid-2023.

GV-971

GV-971, also known as sodium oligomannate, is an oligosaccharide combination derived from the marine algae Ecklonia kurome that is used in China to treat AD (Figure 2E) (51). The agent suppressed neuroinflammation by significantly modifying gut microbiota composition and modulating amino acid metabolism (including a significant reduction in phenylalanine and isoleucine levels) (51). As a result, sodium oligomannate impaired the relationship between brain Th1 cells and gut microbiota changes (51). In sodium oligomannate-treated mice, there was a reduction in brain Th1 cells, microglial activation, and various brain cytokines, as well as a reduction in Aβ plaque aggregation and tau phosphorylation, as well as an improvement in discrimination learning (52). The MOA by which GV-971 may act is yet to be defined. GV-971 has a limited oral bioavailability, and food has little influence on absorption of this compound (53). There are no human studies on GV-971 metabolites, and the excretion pathways are unknown (51). GV-971 PK has not been examined in certain groups, such as individuals with hepatic or renal impairment (53). Green Valley began a Phase III trial (NCT02293915) at 34 sites in China in April 2014. At 4, 12, 24, and 36 weeks, the treatment group outperformed the placebo group in terms of Alzheimer's disease Assessment Scale–Cognitive Subscale (ADAS-Cog) scores, as reported at Clinical Trials on Alzheimer's disease (CTAD) 2018. The Canadian International Business Immigration Consultant (CIBIC) showed a trend toward improvement, but no other secondary outcomes changed (54). A subgroup analysis revealed

that drug effects were larger in those with lower Mini–Mental State Examination (MMSE) scores at the start of the study. GV-971 was well-tolerated. The experiment was completed by 80% of participants, and the rates of AEs were comparable in the treatment and placebo groups. The results of a 36-week experiment revealed that GV-971 displayed high efficacy in improving cognition, with persistent improvement throughout all observation periods (55). In November 2019, GV-971 gained its first approval in China for the treatment of mild to severe AD to improve cognitive function (51).

All the Disease-modifying therapy medications cited in this article have been listed in Table 1.

Symptomatic therapy

Symptomatic for agitation

AXS-05

AXS-05 is an innovative, fixed-dose oral combination of two authorized medications being developed to treat agitation in AD (Figure 4A). Dextromethorphan (DM), one of the ingredients, is a weak antagonist of N-methyl-D-aspartate (NMDA) receptors, an agonist of sigma 1 receptors (endoplasmic reticulum membrane molecular chaperones), and an inhibitor of serotonin and norepinephrine transporters, nicotinic acetylcholine receptors, and microglial activation. Bupropion is another component whose major role is to increase the bioavailability of dextromethorphan by decreasing its metabolism and boosting its plasma levels while also reducing norepinephrine (NE) and dopamine reuptake (56). There is no information on Phase I trials in the trial register or the peer-reviewed literature. Axsome commenced a Phase II /III trial called ADVANCE-1 (NCT03226522) in July 2017 to evaluate the efficacy and safety of AXS-05 for the treatment of agitation in AD patients. The sponsor announced topline data in April 2020, citing a statistically significant 15.4 points reduction in Cohen-Mansfield Agitation Inventory (CMAI) with therapy, compared to 11.5 points with placebo and 10.0 points with bupropion alone. AXS-05 fulfilled the primary endpoint and resulted in a clinical response on the CMAI in over 70% of patients in this trial, defined as a 30% or higher improvement. It was also statistically significantly better than bupropion in terms of component contribution. AXS-05 was generally safe and well-tolerated, and was not associated with sedation-induced cognitive impairment (57). The FDA approved AXS-05 breakthrough therapy designation for treating agitation in AD in June 2020. Alongside that, Axsome announced that two trials to support the NDA for agitation in AD would begin before the end of 2020. The first will be a Phase III efficacy study (NCT04797715) while the second will be an open-label long-term safety study.

AVP-786

Avanir and Concert Pharmaceuticals created AVP-786, a deuterated second-generation version of AVP-923 (Figure 4B). It comprises DM and quinidine, two approved medicines. DM is the agent's neuroactive ingredient (58). Quinidine improves DM bioavailability by blocking the BBB protein pump P-glycoprotein and decreasing its oxidative metabolism by the liver enzyme cytochrome P450-2D6. AVP-923 is linked to less agitation in people with neurocognitive impairments, including AD (59). AVP-786 is distinct from AVP-923 in that it incorporates deuterium into the DM, which has been shown to reduce first-pass metabolism in the liver. Because of the lower metabolic rate, AVP-786 requires ultra-low quinidine doses, which improves overall safety and tolerability by reducing drug-drug interactions and adverse cardiac effects (60, 61). The safety, tolerability, and PK of DM dextromethorphan were evaluated in a phase I trial. At lower quinidine dosages, AVP-786 had the same steady-state plasma levels of DM as AVP-923. In November 2015, the FDA fast-tracked AVP-786 for agitation. The sponsor also ran two Phase III trials in the same year, TRIAD-1 and TRIAD-2 (NCT02442765 and NCT02442778), to analyze the drug in moderate AD patients with clinically significant agitation. Avanir revealed in March 2019 that the TRIAD-1 sequential design study had accomplished its primary endpoint, whereas TRIAD-2 had failed. There were no treatment-related deaths, although falls, urinary tract infections, headaches, and diarrhea were common AEs. The sponsors are currently undertaking the investigation on AVP-786 in AD agitation globally, with four trials registered on ClinicalTrials.gov (NCT04464564, NCT04408755, NCT03393520, and NCT02446132). In the future, positive outcomes are expected.

Nabilone

Cannabinoids (CB) have previously been shown to have a neuroprotective impact by activating the G-protein coupled receptors: CB1 and 2 (CB1/2) receptors (Figure 4C). CB1 receptors, which are found in the cerebral cortex and hippocampus, can impair learning and memory function in Alzheimer's patients and are also linked to anxiety-like and aggressive behavior in animals. CB2 receptors were engaged at the same time, reducing the generation of pro-inflammatory chemicals and removing Aβ plaques (62). Nabilone, a synthetic CB that acts as an agonist at CB1/2 receptors, has been studied to see if it improves agitation in AD. Sunnybrook Health Sciences Centre sponsored a Phase II/III trial (NCT02351882) in January 2015 to test the impact of 6 weeks of nabilone treatment on agitation symptoms compared to placebo (63). CMAI, Neuropsychiatric Inventory-Nursing Home version (NPI-NH) total, NPI-NH caregiver distress, and standardized MMSE were all favored by nabilone using a linear mixed model (64). Treatment differences favored placebo in those who completed the

TABLE 1 Disease-modifying therapy in active development from 2017 to 2021.

Candidate	Target	MOA	Sponsor	Phase globally	Phase in China	Last completed trial (Phase)	Patient enrolled	Disease stage	Reduce Aβ or/and tau burden
Aducanumab	Aβ	Remove aggregated forms of Aβ	Biogen; Eisai	Approved	N	NCT02484547 (III)	1,643	Early AD	+
						NCT02477800 (III)	1,653		–
ALZ-801	Aβ	Prevent Aβ42 from forming oligomers	Alzheon	III	N	NCT04157712 (I)	127	HV	N/A
						NCT04585347 (I)			
Gantenerumab	Aβ	Disassemble and degrade Aβ fibrils	Roche	III	III	NCT01224106 (III)	194	Prodromal AD	+
						NCT04623242 (III)	799	Mild AD	+
lecanemab	Aβ	Disassemble and degrade Aβ fibrils	Eli Lilly	III	III	NCT01767311 (II)	856	Early AD	+
Donanemab	Aβ	Remove Aβ plaques	Eli Lilly	III	N	NCT03367403 (II)	272	Early AD	±
ALZT-OP1	COX-1; PPARs	Promote microglia recruitment to plaques, and phagocytosis of Aβ deposits	AZ Therapies	III	N	NCT02547818 (III)	620	Early AD	Unknow
Semaglutide	GLP1 receptor	Accelerate autophagy of Aβ25-35	Novo Nordisk	III	III	/	/	/	/
Simufilam	FLNA	Restore of normally folded Aβ and tau proteins	Cassava Sciences	III	N	NCT03748706 (II)	13	Mild-to-moderate AD	+
						NCT04079803 (II)	64		+
NE3107	NF-κB	Reduces inflammation by blocking EPIC, which is located upstream of Aβ and p-tau	BioVie	III	N	/	/	/	/
GV-971	N/A	De-aggregate Aβ and reduce tau hyperphosphorylation	Shanghai Green Valley Pharmaceutical	Approved	Approved	NCT02293915 (III)	818	Mild-to-moderate AD	N/A

N/A, Not applicable.

10.3389/fneur.2022.1034243

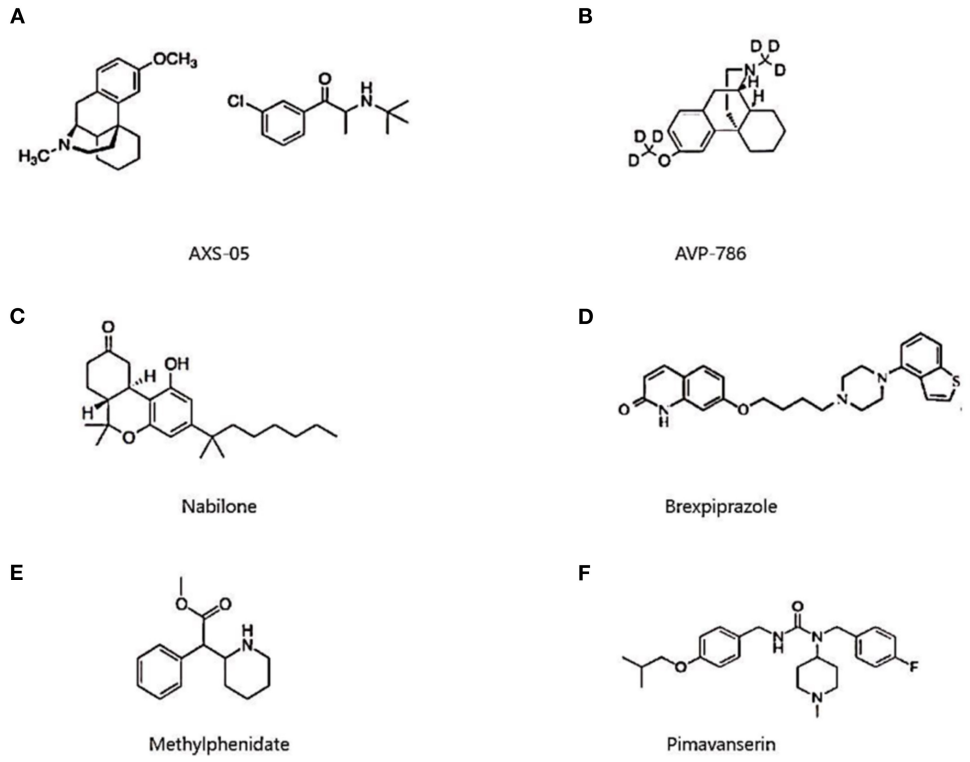

FIGURE 4
Chemical structure of AXS-05 **(A)**, AVP-786 **(B)**, nabilone **(C)**, brexpiprazole **(D)**, methylphenidate **(E)**, and pimavanserin **(F)**.

simultaneous integrated boost (SIB) ($n = 25$) (64). The difference in Certified Gastroenterology Coder (CGIC) improvement between nabilone (47%) and placebo (23%) was not statistically significant (McNemar's test, exact $p = 0.09$) (64). Sedation was higher during the nabilone (45%) vs. placebo (16%) phases (McNemar's test, exact $p = 0.02$), although treatment-limiting sedation was not substantially different (McNemar's test, exact $p = 0.22$), hence sedation and cognitive function must be continuously monitored (64). Following the completion of the study, the sponsor commenced a Phase 3 trial (NCT04516057) in February 2021. It will last until October 2025.

Brexpiprazole

Brexpiprazole is a unique third-generation antipsychotic that functions as a partial agonist for dopamine D2 receptors, a partial agonist for serotonin 5-HT1A receptors, an antagonist for serotonin 5-HT2A/5-HT2B receptors, and a partial antagonist for noradrenaline α1B/α2C receptors (Figure 4D) (65). Brexpiprazole may be beneficial in the treatment of dementia sufferers since serotonin, dopamine, and noradrenaline neurotransmitter systems are linked to behavioral symptoms of dementia, such as agitation (66). Otuska and Lundbeck collaborated in 2013 to conduct two 12-week Phase III studies (NCT01862640 and NCT01922258) to assess the efficacy, safety, and tolerability of brexpiprazole in patients with agitation associated with AD dementia. In the study (NCT01862640), brexpiprazole 2 mg and 1 mg significantly reduced total CMAI scores by 21.6 and 17.6 points, respectively, at 12 weeks, compared to 17.8 points in the placebo group, and greatly decreased NPI-NH agitation/aggression scores by 58.34 and 51.71%, respectively, at 12 weeks, compared to 47.12% for placebo (66). Brexpiprazole 0.5–2 mg/day did not establish statistical advantage over placebo in study (NCT01922258). In *post-hoc* studies, however, patients titrated to the maximal brexpiprazole dose of 2 mg/day indicated a benefit when compared to similarly titrated placebo patients (66). Brexpiprazole provoked treatment-emergent adverse events (TEAEs) in both studies, including headache, insomnia, urinary tract infection, and others. The bulk of the TEAEs were mild to moderate in severity (66). In 2018, the sponsors commenced three Phase III trials l (NCT03594123, NCT03548584, and NCT03724942) and one Phase II/III trial (NCT03620981), all of which are scheduled to run through 2022.

Symptomatic for apathy

Methylphenidate

Methylphenidate has been approved for narcolepsy and attention deficit hyperactivity disorder (ADHD) (Figure 4E). Methylphenidate hinders presynaptic neurons from reabsorbing two neurotransmitters, adrenaline and dopamine. It inhibits the transporters of these neurotransmitters, resulting in an increase in dopamine and adrenaline levels in the synaptic cleft (67). It is also a mild agonist at the 5-HT1A receptor, which is another mechanism that contributes to higher dopamine levels (68). Methylphenidate can promote neuroprotection *via* increasing dopamine levels (69). Apathy in people with AD is thought to be caused by reduced dopaminergic neurotransmission (70). It is being investigated as a treatment for apathy in patients with AD as a mild CNS stimulant. Methylphenidate may benefit non-cognitive, apathy-like behavior (as demonstrated by decreased exploration) in the 5xFAD mouse model, but it has little ability to enhance chronic Alzheimer's typical learning and memory deficiencies (71). It was shown that methylphenidate was well-tolerated and alleviated apathy in patients with AD in two open-label studies (72, 73). Another placebo-controlled crossover trial found that, in comparison to placebo, methylphenidate patients' apathy was considerably improved (74). A Phase II study called ADMET (NCT01117181) was established in June 2010 to further verify methylphenidate's involvement in AD. Methylphenidate improved NPI apathy scores by 1.8 points more than placebo, and further findings showed that methylphenidate reduced apathy in Alzheimer's patients and enhanced global cognition with few AEs (75). Methylphenidate was then evaluated in Phase III (NCT02346201) in 2016 for its ability to minimize the severity of apathy in AD. The NPI apathy score in those receiving methylphenidate decreased more from baseline to 6 months than in those taking placebo, and its safety was clearly proven in this experiment (76).

Symptomatic for other psychosis

Pimavanserin

Pimavanserin has been approved for the treatment of Parkinson's disease psychosis (PDP) (Figure 4F). It is a selective inverse agonist/antagonist of the 5-HT2A receptor with little affinity for the 5-HT2C receptor and no affinity for dopaminergic, muscarinic, histaminergic, or adrenergic receptors (77). Previous research revealed that activation at the 5-HT2A receptor could possibly help with AD psychosis (78). It is now being developed for the treatment of psychosis in Alzheimer's patients. A prior study found that serotonin signaling attenuated Aβ *in vitro* and in animal models of AD (79). Pimavanserin administration interfered with Aβ deposition by altering the balance between two 5-HT2A signaling pathways that were antagonists of Gq/11 signaling and agonists of Gαi1 signaling, according to the findings (80). From November 2013 through September 2019, Acadia launched a Phase II trial (NCT02035553). At the primary endpoint (week 6), pimavanserin had an effect on psychosis and was well-tolerated. Further follow-up through week 12 revealed no meaningful benefits for pimavanserin as compared to placebo (81). A subsequent subgroup analysis revealed that ≥30% improvement was 88.9 vs. 43.3% ($p < 0.001$) and ≥50% improvement was 77.8 vs. 43.3% ($p = 0.008$) for pimavanserin and placebo, respectively, in this severe subgroup with a baseline Neuropsychiatric Inventory-Nursing Home Version psychosis score (NPI-NH-PS) ≥12 ($n = 27$ pimavanserin; $n = 30$ placebo) (82). The next Phase II study, SERENE (NCT03118947), was terminated in February 2017. The findings of this experiment do not support pimavanserin's function. Pimavanserin entered Phase III from 2017 to 2019. The trial (NCT03325556) sought to examine the efficacy of pimavanserin vs. placebo in preventing the return of psychotic symptoms in dementia-related psychosis patients who responded to 12 weeks of open-label pimavanserin treatment. According to the findings, 13% of the pimavanserin group relapsed, compared to 28% of the placebo group. The trial was also halted due to ineffectiveness. Longer and larger trials are needed to confirm the efficacy of pimavanserin on psychosis in AD (83). The sponsors submitted an NDA to the FDA in December 2021 for permission to treat AD.

All the symptomatic therapy medications cited in this article have been cited in Table 2.

Conclusion and future expectations

Available drugs for AD are only symptomatic in China, and even in the world. Prior to 2017, the four approved drugs for AD were acetylcholinesterase (AChE) inhibitors and NMDA antagonists. By lowering AChE activity, these medications temporarily halt the loss of cognitive function, resulting in increased ACh levels and enhanced brain function (84). However, they only provide minor benefits in terms of symptom management and do not prevent neuronal death, brain shrinkage, and cognitive decline (85).

Due to a lack of powerful drugs to slow the progression of AD, huge efforts have been undertaken to find novel molecules with the potential to change the illness's course: disease-modifying therapy (DMT) (86). Since AD evolves concurrently with the accumulation of Aβ, causing the expansion of tau pathology (87), these prospective DMT are essentially addressing the two pathogenic hallmarks of AD: Aβ and tau-protein (86). The amyloid hypothesis has been the subject of contemporary study (86). Aβ is the most popular target in Phase III drug development programs (87). Gantenerumab,

TABLE 2 Symptomatic therapy in active development from 2017 to 2021.

Candidate	Target	MOA	Sponsor	Phase globally	Phase in China	Last completed trial (Phase)	Patient enrolled	Disease stage	Relieve symptoms
AXS-05	NMDA receptor; Sigma 1 receptor	Inhibit serotonin and NA transporters, N acetylcholine receptors, and microglial activation	Axsome Therapeutics	III	N	NCT03226522 (II/III)	366	AD agitation	+
AVP-786	NMDA receptor; Sigma 1 receptor	Inhibit serotonin and NA transporters, N acetylcholine receptors, and microglial activation	Avanir Pharmaceuticals; Concert Pharmaceuticals; Otsuka Pharmaceutical	III	N	NCT02442765 (III) NCT02442778 (III)	410 522	AD agitation	+ –
Nabilone	CB1/2 receptor	Reduce the generation of pro-inflammatory chemicals; Remove Aβ plaques	Other Hospital/Academic/ Medical Center	III	N	NCT02351882 (II/III)	38	AD agitation	+
Brexpiprazole	D2 receptor; 5-HT1A receptor; 5-HT2A/B receptor; NAα1B/α2C	D2 and 5-HT1A receptor partial agonist; 5-HT2A/5-HT2B receptor antagonist; NAα1B/α2C partial antagonist	Lundbeck	III	N	NCT01862640 (III) NCT01922258 (III) NCT03724942 (III) NCT03548584 (III)	433 270 164 345	AD agitation	+ + Unknown Unknown
Methylphenidate	5-HT1A receptor; SLC6A2	Block NE and DA reuptake; 5-HT1A receptor agonist	Other Hospital/ Academic/Medical Center	IV	N	NCT02346201 (III)	200	AD apathy	+
Pimavanserin	5-HT2A receptor	5-HT2A receptor agonist	ACADIA Pharmaceuticals	III	N	NCT03325556 (III)	392	AD psychosis	+

10.3389/fneur.2022.1034243

aducanumab, ALZ-801, ALZT-OP1, donanemab, lecanemab, and semaglutide are among the selected agents aimed at eliminating Aβ. They are engaged in secondary prevention trials in people with preclinical, prodromal, mild, or moderate-to-severe AD (87). The risk of AD is 60–80% heritable, with more than 40 AD-associated genetic risk loci already identified, the APOE alleles having the strongest association with the disease (87). AD patients with APOE4/4 homozygotes are the target population for ALZ-801 and ALZT-OP1. Gantenerumab, aducanumab, and donanemab are beneficial in all genotypes of AD patients. Lecanemab is distinct in that it is intended for patients of all genotypes, including APOE4/4 homozygotes (19). According to prior studies, insulin resistance has been linked to neurodegeneration (88). Semaglutide is an anti-diabetic medication that has been approved in China. A trial in China is now underway to treat MCI and mild dementia caused by AD. Other agents, such as aducanumab, which has been approved in the US and is advised for clinical therapy, have not been studied in China aside from gantenerumab, lecanemab, and semaglutide. China has been paying attention to drug R&D in this field in recent years, and these promising candidates are expected to be expanded to China for future research. Tau biology adds to the list of potentially relevant targets for DMT (89). The anti-tau strategies, on the other hand, are still in the early stages of clinical studies (86). However, there are candidates that target both Aβ and tau, such as simufilam, NE3107, and GV-971. FLNA is a unique target in that recovered FLNA can restore normal Aβ and tau function. According to the existing data, simufilam is rather effective in AD. Neuro-inflammation is recognized as a major component of the pathology of AD, contributing to disease progression and neurodegeneration (87), in addition to aberrant Aβ protein deposition and hyperphosphorylation of tau protein. Therefore, medications targeting this pathway are also being developed to alleviate the condition of AD patients. NE3107 is a candidate that significantly targets inflammation, and some other candidates have anti-inflammatory properties as well. In addition to its anti-inflammatory properties, NE3107 has the potential to reduce insulin resistance. However, NE3107 is presently only being tested in clinical studies in the US. GV-971 belongs to DMT as well, although its MOA is undetermined and may be related to gut flora. It was approved in China in 2019, following a phase III trial that indicated cognitive enhancement in the same country (52). However, due to the difficulties to get more clinical reports for GV-971 in order to assess the quality of the evidence, the current Chinese guidelines have been unable to make adequate recommendations, and we only hope to augment it when the guidelines are revised in the future (4). All the agents described above were devised to combat the pathogenic mechanism of AD and, therefore, can interfere with the disease process. And, in disorders like Alzheimer's, pathogenic alterations occur before symptoms manifest. If patients can be diagnosed early, these compounds could become the top choice for the prevention and treatment of AD, changing the existing status of no cure.

Cognitive impairment and psycho-behavioral dysfunction are the two primary categories of AD symptoms. The four approved Alzheimer's medications are generally used to modify cognitive impairment, and more are being developed to improve patients' cognition by delaying the disease process in the past 5 years. Antipsychotic behavioral disorder drug investigation accounts for a significant portion of AD symptomatic treatment. Pimavanserin is an inverse agonist for the 5-HT2A receptor that has been investigated for dementia-related psychosis (87). Only the treatment of hallucinations and delusions associated with psychosis in Parkinson's disease (PD) has been studied with pimavanserin in China. However, because pimavanserin relieves hallucinations and delusions while having no harmful effects on cognition, the Chinese guideline makes the following recommendation: Pimavanserin has a short-term effect on AD dementia mental symptoms (4). Apathy is one of the symptoms of depression, which is common in Alzheimer's patients. The guidelines show that tandospirone, but not sertraline or mirtazapine, is beneficial for depression in Alzheimer's patients (4). In recent research, methylphenidate has been considered to be an effective symptom-modifying drug (90). In China, methylphenidate is recommended for respiratory depression, narcolepsy, ADHD, and other conditions. Agitation is a prevalent symptom of dementia, affecting up to 70% of patients with AD during their illness (91). Some atypical antipsychotics (such as olanzapine, risperidone, and quetiapine, among others) and serotonin medications (such as pimavanserin, buspirone, and citalopram, among others) have been recorded in the guidelines for the effect of alleviating psychological symptoms, mainly agitation, in AD patients (4). Recent studies have demonstrated that AXS-05, AVP-786, nabilone, and brexpiprazole are significantly effective in treating agitation. Clinical studies for AXS-05 and AVP-786 are not being conducted in China. As nabilone is illegal in China, it cannot be used clinically. Brexpiprazole was initially developed for depression and schizophrenia and has not been linked to the agitation of AD in China. It's challenging to compare the efficacy of the above-mentioned drugs since the primary endpoints of clinical trials are inconsistent, but they've all shown curative effects, giving doctors more options to treat AD patients with psychiatric symptoms in the future.

In the last 5 years, the R&D pipeline for AD has been primarily focused on DMT, with the goal of improving the embarrassing status of no viable pharmacological treatment in clinic. Agents targeting Aβ have a distinct advantage over late-stage agents, despite the fact that many agents' development processes are tortuous. Tau protein, a new intriguing target, may be more effective than Aβ in treating AD, and the future pipeline may focus on this target. If the tau protein

study continues to make significant progress, it will be a tremendous step forward in the treatment of AD. New targets for different pathogenic pathways, like FLNA and improving blood glucose, provide new opportunities for future R&D pipelines. In the R&D pipeline of AD, drugs that relieve symptoms still have a place. Although the number of potential pharmaceuticals developed in China is still limited, China is actively introducing and looking forward to participating in the development of these drugs. Once approved by the National Medical Products Administration (NMPA), these drugs will be able to remedy the shortages of radically curative drugs and provide more therapeutic alternatives for symptomatic therapy.

Author contributions

YC searched the database and conducted analysis. YC and YL wrote original draft. YL and XL did review and editing and were responsible for supervision.

Funding

This work was supported by Department Resource.

Conflict of interest

The authors declare that the research was conducted in the absence of any commercial or financial relationships that could be construed as a potential conflict of interest.

Publisher's note

References

1. Burns A, Iliffe S. Alzheimer's disease. *BMJ.* (2009) 338:b158. doi: 10.1136/bmj.b158

2. Natalia V. Global burden of 369 diseases and injuries in 204 countries and territories, 1990–2019: a systematic analysis for the global burden of disease study 2019. *Lancet.* (2020) 396:1204–22.

3. World Alzheimer's Day. *Caring for the Elderly, Please Pay Attention to Alzheimer's Disease.* Chinese Center for Disease Control and Prevention (2019).

4. Jinzhou T, Hengge X, Luning W. Chinese guidelines for the diagnosis and treatment of Alzheimer's Disease (Version 2020). *Chin J Gerontol.* (2021) 40:269–83. doi: 10.3760/cma.j.issn.0254-9026.2021.03.001

5. Teixeira JP, de Castro AA, Soares FV, da Cunha EFF, Ramalho TC. Future therapeutic perspectives into the Alzheimer's disease targeting the oxidative stress hypothesis. *Molecules.* (2019) 24:4410. doi: 10.3390/molecules24234410

6. *"Wandering" and "Exploring" in the Field of Alzheimer's Disease (Ad) Treatment* (2022).

7. Abramov AY, Bachurin SO. Neurodegenerative disorders—Searching for targets and new ways of diseases treatment. *Med Res Rev.* (2021) 41:2603–5. doi: 10.1002/med.21794

8. America PRaMo. *Researching Alzheimer's Medicines: Setbacks and Stepping Stones, 2012.* PhRMA (2016).

9. Biogen. *Aduhelm^{TM} Instruction*. FDA (2021).

10. Tolar M, Hey J, Power A, Abushakra S. Neurotoxic soluble amyloid oligomers drive Alzheimer's pathogenesis and represent a clinically validated target for slowing disease progression. *Int J Mol Sci.* (2021) 22:6355. doi: 10.3390/ijms22126355

11. Arndt JW, Qian F, Smith BA, Quan C, Kilambi KP, Bush MW, et al. Structural and kinetic basis for the selectivity of aducanumab for aggregated forms of amyloid-B. *Sci Rep.* (2018) 8:6412. doi: 10.1038/s41598-018-24501-0

12. Ferrero J, Williams L, Stella H, Leitermann K, Mikulskis A, O'Gorman J, et al. First-in-human, double-blind, placebo-controlled, single-dose escalation study of aducanumab (Biib037) in mild-to-moderate Alzheimer's disease. *Alzheimers Dement.* (2016) 2:169–76. doi: 10.1016/j.trci.2016.06.002

13. Salloway S, Chalkias S, Barkhof F, Burkett P, Barakos J, Purcell D, et al. Amyloid-related imaging abnormalities in 2 phase 3 studies evaluating aducanumab in patients with early Alzheimer disease. *JAMA Neurol.* (2022) 79:13–21. doi: 10.1001/jamaneurol.2021.4161

14. Neurimmune, Biogen. *Aduhelm*. (2021). Available online at: https://www.alzforum.org/therapeutics/aduhelm (accessed May 16, 2022).

15. Cavazzoni P. *Fda's Decision to Approve New Treatment for Alzheimer's Disease.* FDA (2021).

16. Dutton G. *New Drug Approval Could Be on Horizon for Alzheimer's after 17-Year Drought*. BioSpace (2021).

17. Hey JA, Kocis P, Hort J, Abushakra S, Power A, Vyhnálek M, et al. Discovery and identification of an endogenous metabolite of tramiprosate and its Prodrug Alz-801 that inhibits beta amyloid oligomer formation in the human brain. *CNS Drugs.* (2018) 32:849–61. doi: 10.1007/s40263-018-0554-0

18. Abushakra S, Porsteinsson A, Scheltens P, Sadowsky C, Vellas B, Cummings J, et al. Clinical effects of tramiprosate in Apoe4/4 homozygous patients with mild Alzheimer's disease suggest disease modification potential. *J Prev Alzheimers Dis.* (2017) 4:149–56. doi: 10.14283/jpad.2017.26

19. Tolar M, Abushakra S, Hey JA, Porsteinsson A, Sabbagh M. Aducanumab, Gantenerumab, Ban2401, and Alz-801—The first wave of amyloid-targeting drugs for Alzheimer's disease with potential for near term approval. *Alzheimers Res Ther.* (2020) 12:95. doi: 10.1186/s13195-020-00663-w

20. Alzheon. *Alz-801*. (2022). Available online at: https://www.alzforum.org/therapeutics/alz-801 (accessed February 16, 2022).

21. Novakovic D, Feligioni M, Scaccianoce S, Caruso A, Piccinin S, Schepisi C, et al. Profile of gantenerumab and its potential in the treatment of Alzheimer's disease. *Drug Des Devel Ther.* (2013) 7:1359. doi: 10.2147/DDDT.S53401

22. Ostrowitzkis S, Deptula D, Thurfjell L, Barkhof F, Bohrmann B, Brooks DJ, et al. Mechanism of amyloid removal in patients with Alzheimer disease treated with gantenerumab. *Arch Neurol.* (2012) 69:198–207. doi: 10.1001/archneurol.2011.1538

23. Bohrmann B, Baumann K, Benz J, Gerber F, Huber W, Knoflach F, et al. Gantenerumab: a novel human anti-Aβ antibody demonstrates sustained cerebral amyloid-B binding and elicits cell-mediated removal of human amyloid-B. *J Alzheimers Dis.* (2012) 28:49–69. doi: 10.3233/JAD-2011-110977

24. Portron A, Jordan P, Draper K, Muenzer C, Dickerson D, van Iersel T, et al. A Phase I study to assess the effect of speed of injection on pain, tolerability, and pharmacokinetics after high-volume subcutaneous administration of gantenerumab in healthy volunteers. *Clin Ther.* (2020) 42:108–20. e1. doi: 10.1016/j.clinthera.2019.11.015

25. Klein G, Delmar P, Voyle N, Rehal S, Hofmann C, Abi-Saab D, et al. Gantenerumab reduces amyloid-B plaques in patients with prodromal to moderate Alzheimer's disease: a pet substudy interim analysis. *Alzheimers Res Therapy.* (2019) 11:101. doi: 10.1186/s13195-019-0559-z

26. *Lecanemab (Also Called Ban2401)*. ALS News Today (2021).

27. Tucker S, Moller C, Tegerstedt K, Lord A, Laudon H, Sjodahl J, et al. The murine version of Ban2401 (Mab158) selectively reduces amyloid-beta protofibrils in brain and cerebrospinal fluid of Tg-Arcswe Mice. *J Alzheimers Dis.* (2015) 43:575–88. doi: 10.3233/JAD-140741

28. Sollvander S, Nikitidou E, Gallasch L, Zysk M, Soderberg L, Sehlin D, et al. The abeta protofibril selective antibody Mab158 prevents accumulation of abeta in astrocytes and rescues neurons from abeta-induced cell death. *J Neuroinflammation.* (2018) 15:98. doi: 10.1186/s12974-018-1134-4

29. ALZFORUM. *Lecanemab Sweeps up Toxic Aβ Protofibrils, Catches Eyes of Trialists* (2021).

30. Logovinsky V, Satlin A, Lai R, Swanson C, Kaplow J, Osswald G, et al. Safety and tolerability of Ban2401–a Clinical study in Alzheimer's Disease with a protofibril selective abeta antibody. *Alzheimers Res Ther.* (2016) 8:14. doi: 10.1186/s13195-016-0181-2

31. Swanson CJ, Zhang Y, Dhadda S, Wang J, Kaplow J, Lai RYK, et al. A randomized, double-blind, phase 2b proof-of-concept clinical trial in early Alzheimer's disease with lecanemab, an anti-abeta protofibril antibody. *Alzheimers Res Ther.* (2021) 13:80. doi: 10.1186/s13195-021-00813-8

32. DeMattos RB, Lu J, Tang Y, Racke MM, DeLong CA, Tzaferis JA, et al. A plaque-specific antibody clears existing B-amyloid plaques in Alzheimer's disease mice. *Neuron.* (2012) 76:908–20. doi: 10.1016/j.neuron.2012.10.029

33. Irizarry MC, Sims JR, Lowe SL, Nakano M, Hawdon A, Willis BA, et al. O4-08-06: safety, pharmacokinetics (Pk), and Florbetapir F-18 positron emission tomography (Pet) after multiple dose administration of Ly3002813, a B-amyloid plaque-specific antibody, in Alzheimer's Disease (Ad). *Alzheimers Dement.* (2016) 12:P352–P3. doi: 10.1016/j.jalz.2016.06.665

34. Lowe SL, Willis BA, Hawdon A, Natanegara F, Chua L, Foster J, et al. Donanemab (Ly3002813) dose-escalation study in Alzheimer's Disease. *Alzheimers Dement.* (2021) 7:e12112. doi: 10.1002/trc2.12112

35. Mintun MA, Lo AC, Duggan Evans C, Wessels AM, Ardayfio PA, Andersen SW, et al. Donanemab in early Alzheimer's Disease. *New Engl J Med.* (2021) 384:1691–704. doi: 10.1056/NEJMoa2100708

36. Co EL. *Donanemab*. (2021). Available online at: https://www.alzforum.org/therapeutics/donanemab (accessed November 2, 2022).

37. AZTherapies. *Alzt-Op1*. (2019). Available online at: https://www.alzforum.org/therapeutics/alzt-op1 (accessed November 29, 2019).

38. Dokmeci D. Ibuprofen and Alzheimer's disease. *Folia Med.* (2004) 46:5–10.

39. Zhang C, Griciuc A, Hudry E, Wan Y, Quinti L, Ward J, et al. Cromolyn reduces levels of the Alzheimer's disease-associated amyloid beta-protein by promoting microglial phagocytosis. *Sci Rep.* (2018) 8:1144. doi: 10.1038/s41598-018-19641-2

40. Brazier D, Perry R, Keane J, Barrett K, Elmaleh DR. Pharmacokinetics of cromolyn and ibuprofen in healthy elderly volunteers. *Clin Drug Investig.* (2017) 37:1025–34. doi: 10.1007/s40261-017-0549-5

41. Knudsen LB, Lau J. The discovery and development of liraglutide and semaglutide. *Front Endocrinol.* (2019) 10:155. doi: 10.3389/fendo.2019.00155

42. Hölscher C. Novel dual Glp-1/Gip receptor agonists show neuroprotective effects in Alzheimer's and Parkinson's disease models. *Neuropharmacology.* (2018) 136(Pt B):251–9. doi: 10.1016/j.neuropharm.2018.01.040

43. Salameh TS, Rhea EM, Talbot K, Banks WA. Brain uptake pharmacokinetics of incretin receptor agonists showing promise as Alzheimer's and Parkinson's disease therapeutics. *Biochem Pharmacol.* (2020) 180:114187. doi: 10.1016/j.bcp.2020.114187

44. During MJ, Cao L, Zuzga DS, Francis JS, Fitzsimons HL, Jiao X, et al. Glucagon-like peptide-1 receptor is involved in learning and neuroprotection. *Nat Med.* (2003) 9:1173–9. doi: 10.1038/nm919

45. Chang YF, Zhang D, Hu WM, Liu DX Li L. Semaglutide-mediated protection against abeta correlated with enhancement of autophagy and inhibition of apotosis. *J Clin Neurosci.* (2020) 81:234–9. doi: 10.1016/j.jocn.2020.09.054

46. Cassava. *Simufilam*. (2021). Available online at: https://www.alzforum.org/therapeutics/simufilam (accessed September 26, 2022).

47. MS MW. *Simufilam (Pti-125)*. Alzheimer's News Today (2022).

48. Wang HY, Pei Z, Lee KC, Lopez-Brignoni E, Nikolov B, Crowley CA, et al. Pti-125 reduces biomarkers of Alzheimer's disease in patients. *J Prev Alzheimers Dis.* (2020) 7:256–64. doi: 10.14283/jpad.2020.6

49. Reading CL, Frincke JM, White SK. Molecular targets for 17α-ethynyl-5-androstene-3β, 7β, 17β-triol, an anti-inflammatory agent derived from the human metabolome. *PLoS ONE.* (2012) 7:e32147. doi: 10.1371/journal.pone.0032147

50. Reading CL, Ahlem CN, Murphy MF. Nm101 Phase Iii study of Ne3107 in Alzheimer's disease: rationale, design and therapeutic modulation of neuroinflammation and insulin resistance. *Neurodegener Dis Manag.* (2021) 11:289–98. doi: 10.2217/nmt-2021-0022

51. Syed YY. Sodium oligomannate: first approval. *Drugs.* (2020) 80:441–4. doi: 10.1007/s40265-020-01268-1

52. Wang X, Sun G, Feng T, Zhang J, Huang X, Wang T, et al. Sodium oligomannate therapeutically remodels gut microbiota and suppresses gut bacterial amino acids-shaped neuroinflammation to inhibit Alzheimer's disease progression. *Cell Res.* (2019) 29:787–803. doi: 10.1038/s41422-019-0216-x

53. Shanghai Green Valley Pharmaceuticals Co. L. *Sodium Oligomannate Capsules: Chinese Prescribing Information.* ALZFORUM (2020).

54. ALZFORUM. *Fits and Starts: Trial Results from the Ctad Conference* (2018).

55. Xiao S, Chan P, Wang T, Hong Z, Wang S, Kuang W, et al. A 36-week multicenter, randomized, double-blind, placebo-controlled, parallel-group, phase 3 clinical trial of sodium oligomannate for mild-to-moderate Alzheimer's dementia. *Alzheimers Res Ther.* (2021) 13:62. doi: 10.1186/s13195-021-00795-7

56. Axsome. *Axs-05*. ALZFORUM (2020). Available online at: https://www.alzforum.org/therapeutics/axs-05 (accessed April 5, 2022).

57. Jacobson M. *Advance-1 Phase 2/3 Trial of Axs-05 in Alzheimer's Disease Agitation Topline Results.* Axsome (2020).

58. Khoury R, Marx C, Mirgati S, Velury D, Chakkamparambil B, Grossberg GT. Avp-786 as a promising treatment option for Alzheimer's disease including agitation. *Expert Opin Pharmacother.* (2021) 22:783–95. doi: 10.1080/14656566.2021.1882995

59. US. *FDA Drug Approval Package: Nuedexta (Dextromethorphan Hydrobromide and Quinidine Sulfate) Capsules.* CISION (2011).

60. Inc AP. *Avanir Pharmaceuticals Announces Initiation of Phase Iii Trial of Avp-786 for Agitation in Patients with Alzheimer's Disease* (2015).

61. Avanir. *Avanir Pharmaceuticals Announces Initiation of Phase Iii Trial of Avp-786 for Agitation in Patients With Alzheimer's Disease*. (2015).

62. Liu CS, Chau SA, Ruthirakuhan M, Lanctot KL, Herrmann N. Cannabinoids for the treatment of agitation and aggression in Alzheimer's disease. *CNS Drugs.* (2015) 29:615–23. doi: 10.1007/s40263-015-0270-y

63. Ruthirakuhan MT, Herrmann N, Gallagher D, Andreazza AC, Kiss A, Verhoeff N, et al. Investigating the safety and efficacy of nabilone for the treatment of agitation in patients with moderate-to-severe Alzheimer's disease: study protocol for a cross-over randomized controlled trial. *Contemp Clin Trials Commun.* (2019) 15:100385. doi: 10.1016/j.conctc.2019.100385

64. Herrmann N, Ruthirakuhan M, Gallagher D, Verhoeff N, Kiss A, Black SE, et al. Randomized placebo-controlled trial of nabilone for agitation in Alzheimer's disease. *Am J Geriatr Psychiatry.* (2019) 27:1161–73. doi: 10.1016/j.jagp.2019.05.002

65. Maeda K, Sugino H, Akazawa H, Amada N, Shimada J, Futamura T, et al. Brexpiprazole I: *in vitro* and *in vivo* characterization of a novel serotonin-dopamine activity modulator. *J Pharmacol Exp Ther.* (2014) 350:589–604. doi: 10.1124/jpet.114.213793

66. Grossberg GT, Kohegyi E, Mergel V, Josiassen MK, Meulien D, Hobart M, et al. Efficacy and safety of brexpiprazole for the treatment of agitation in Alzheimer's dementia: two 12-week, randomized, double-blind, placebo-controlled trials. *Am J Geriatr Psychiatry.* (2020) 28:383–400. doi: 10.1016/j.jagp.2019.09.009

67. Capp PK, Pearl PL, Conlon C. Methylphenidate Hcl: therapy for attention deficit hyperactivity disorder. *Expert Rev Neurother.* (2005) 5:325–31. doi: 10.1586/14737175.5.3.325

68. Markowitz J, DeVane C, Ramamoorthy S, Zhu H-J. The Psychostimulant D-Threo-(R, R)-methylphenidate binds as an agonist to the 5ht1a Receptor. *Die Pharmazie.* (2009) 64:123–5.

69. Verghese C, Abdijadid S. *Methylphenidate.* StatPearls (2021).

70. van Dyck CH, Arnsten AFT, Padala PR, Brawman-Mintzer O, Lerner AJ, Porsteinsson AP, et al. Neurobiologic rationale for treatment of apathy in Alzheimer's disease with methylphenidate. *Am J Geriatr Psychiatry.* (2021) 29:51–62. doi: 10.1016/j.jagp.2020.04.026

71. Schneider F, Baldauf K, Wetzel W, Reymann KG. Effects of methylphenidate on the behavior of male 5xfad mice. *Pharmacol Biochem Behav.* (2015) 128:68–77. doi: 10.1016/j.pbb.2014.11.006

72. Galynker I, Ieronimo C, Miner C, Rosenblum J, Vilkas N, Rosenthal R. Methylphenidate treatment of negative symptoms in patients with dementia. *J Neuropsychiatry Clin Neurosci.* (1997) 9:231–9. doi: 10.1176/jnp.9.2.231

73. Padala PR, Burke WJ, Shostrom VK, Bhatia SC, Wengel SP, Potter JF, et al. Methylphenidate for apathy and functional status in dementia of the alzheimer type. *Am J Geriatr Psychiatry.* (2010) 18:371–4. doi: 10.1097/JGP.0b013e3181cabcf6

74. Herrmann N, Rothenburg LS, Black SE, Ryan M, Liu BA, Busto UE, et al. Methylphenidate for the treatment of apathy in Alzheimer disease: prediction of response using dextroamphetamine challenge. *J Clin Psychopharmacol.* (2008) 28:296–301. doi: 10.1097/JCP.0b013e318172b479

75. Rosenberg PB, Lanctot KL, Drye LT, Herrmann N, Scherer RW, Bachman DL, et al. Safety and efficacy of methylphenidate for apathy in Alzheimer's disease: a randomized, placebo-controlled trial. *J Clin Psychiatry.* (2013) 74:810–6. doi: 10.4088/JCP.12m08099

76. Mintzer J, Lanctot KL, Scherer RW, Rosenberg PB, Herrmann N, van Dyck CH, et al. Effect of methylphenidate on apathy in patients with Alzheimer disease: the admet 2 randomized clinical trial. *JAMA Neurol.* (2021) 78:1324–32. doi: 10.1001/jamaneurol.2021.3356

77. Hacksell U, Burstein ES, McFarland K, Mills RG, Williams H. On the discovery and development of pimavanserin: a novel drug candidate for Parkinson's psychosis. *Neurochem Res.* (2014) 39:2008–17. doi: 10.1007/s11064-014-1293-3

78. Assal F, Alarcón M, Solomon EC, Masterman D, Geschwind DH, Cummings JL. Association of the serotonin transporter and receptor gene polymorphisms in neuropsychiatric symptoms in Alzheimer disease. *Arch Neurol.* (2004) 61:1249–53. doi: 10.1001/archneur.61.8.1249

79. Sheline YI, West T, Yarasheski K, Swarm R, Jasielec MS, Fisher JR, et al. An antidepressant decreases csf abeta production in healthy individuals and in transgenic ad mice. *Sci Transl Med.* (2014) 6:236re4. doi: 10.1126/scitranslmed.3008169

80. Gründer G, Cumming P. *Serotonin and Amyloid Deposition: A Link between Depression and Alzheimer's Disease? An Editorial Highlight on "Pimavanserin, a 5ht2a Receptor Inverse Agonist, Rapidly Suppresses Aβ Production and Related Pathology in a Mouse Model of Alzheimer's Disease" on Page 658*. Wiley Online Library (2021). p. 560–2.

81. Ballard C, Banister C, Khan Z, Cummings J, Demos G, Coate B, et al. Evaluation of the safety, tolerability, and efficacy of pimavanserin versus placebo in patients with Alzheimer's disease psychosis: a phase 2, randomised, placebo-controlled, double-blind study. *Lancet Neurol.* (2018) 17:213–22. doi: 10.1016/S1474-4422(18)30039-5

82. Ballard C, Youakim JM, Coate B, Stankovic S. Pimavanserin in Alzheimer's disease psychosis: efficacy in patients with more pronounced psychotic symptoms. *J Prev Alzheimers Dis.* (2019) 6:27–33. doi: 10.14283/jpad.2018.30

83. Tariot PN, Cummings JL, Soto-Martin ME, Ballard C, Erten-Lyons D, Sultzer DL, et al. Trial of pimavanserin in dementia-related psychosis. *N Engl J Med.* (2021) 385:309–19. doi: 10.1056/NEJMoa2034634

84. Hung SY, Fu WM. Drug candidates in clinical trials for Alzheimer's disease. *J Biomed Sci.* (2017) 24:47. doi: 10.1186/s12929-017-0355-7

85. Alzheimer's disease facts and figures. *Alzheimers Dement.* (2020) 16:391–460. doi: 10.1002/alz.12068

86. Vaz M, Silvestre S. Alzheimer's disease: recent treatment strategies. *Eur J Pharmacol.* (2020) 887:173554. doi: 10.1016/j.ejphar.2020.173554

87. Scheltens P, De Strooper B, Kivipelto M, Holstege H, Chetelat G, Teunissen CE, et al. Alzheimer's disease. *Lancet.* (2021) 397:1577–90. doi: 10.1016/S0140-6736(20)32205-4

88. Kellar D, Craft S. Brain insulin resistance in Alzheimer's disease and related disorders: mechanisms and therapeutic approaches. *Lancet Neurol.* (2020) 19:758–66. doi: 10.1016/S1474-4422(20)30231-3

89. Cummings J, Blennow K, Johnson K, Keeley M, Bateman RJ, Molinuevo JL, et al. Anti-tau trials for Alzheimer's disease: a report from the Eu/Us/Ctad Task Force. *J Prev Alzheimers Dis.* (2019) 6:157–63. doi: 10.14283/jpad.2019.14

90. Ruthirakuhan MT, Herrmann N, Abraham EH, Chan S, Lanctot KL. Pharmacological interventions for apathy in Alzheimer's Disease. *Cochrane Database Syst Rev.* (2018) 5:CD012197. doi: 10.1002/14651858.CD012197.pub2

91. Halpern R, Seare J, Tong J, Hartry A, Olaoye A, Aigbogun MS. Using electronic health records to estimate the prevalence of agitation in Alzheimer disease/dementia. *Int J Geriatr Psychiatry.* (2019) 34:420–31. doi: 10.1002/gps.5030

frontiers | Frontiers in Neurology

TYPE Original Research
PUBLISHED 26 January 2023
DOI 10.3389/fneur.2022.1064639

OPEN ACCESS

EDITED BY
Alfredo Costa,
University of Pavia, Italy

REVIEWED BY
Yanlin Bi,
Qingdao Municipal Hospital, China
Qisheng Su,
Guangxi Medical University, China

*CORRESPONDENCE
Erdong Zhang
✉ zhanged15@lzu.educn
Xiangchun Shen
✉ sxc@gmc.edu.cn

†These authors have contributed equally to this work

SPECIALTY SECTION
This article was submitted to Dementia and Neurodegenerative Diseases, a section of the journal Frontiers in Neurology

RECEIVED 08 October 2022
ACCEPTED 29 December 2022
PUBLISHED 26 January 2023

CITATION
Zhang E, Dai F, Chen T, Liu S, Xiao C and Shen X (2023) Diagnostic models and predictive drugs associated with cuproptosis hub genes in Alzheimer's disease. *Front. Neurol.* 13:1064639. doi: 10.3389/fneur.2022.1064639

Diagnostic models and predictive drugs associated with cuproptosis hub genes in Alzheimer's disease

Erdong Zhang[1,2*†], Fengqiu Dai[3†], Tingting Chen[4], Shanhui Liu[5], Chaolun Xiao[3] and Xiangchun Shen[1,2*]

[1]State Key Laboratory of Functions and Applications of Medicinal Plants, Guizhou Medical University, Guiyang, Guizhou, China, [2]Key Laboratory of Optimal Utilization of Natural Medicinal Resources, Guizhou Medical University, Guiyang, Guizhou, China, [3]Department of Anatomy, School of Basic Medical Sciences, Guizhou Medical University, Guiyang, China, [4]Guiyang Maternal and Child Health-Care Hospital, Guiyang, Guizhou, China, [5]Key Laboratory of Urological Diseases in Gansu Province, Gansu Nephro-Urological Clinical Center, Institute of Urology, Lanzhou University Second Hospital, Lanzhou, Gansu, China

Alzheimer's disease (AD) is a chronic neurodegenerative disease, and its underlying genes and treatments are unclear. Abnormalities in copper metabolism can prevent the clearance of β-amyloid peptides and promote the progression of AD pathogenesis. Therefore, the present study used a bioinformatics approach to perform an integrated analysis of the hub gene based on cuproptosis that can influence the diagnosis and treatment of AD. The gene expression profiles were obtained from the Gene Expression Omnibus database, including non-demented (ND) and AD samples. A total of 2,977 cuproptosis genes were retrieved from published articles. The seven hub genes associated with cuproptosis and AD were obtained from the differentially expressed genes and WGCNA in brain tissue from GSE33000. The GO analysis demonstrated that these genes were involved in phosphoribosyl pyrophosphate, lipid, and glucose metabolism. By stepwise regression and logistic regression analysis, we screened four of the seven cuproptosis genes to construct a diagnostic model for AD, which was validated by GES15222, GS48350, and GSE5281. In addition, immune cell infiltration of samples was investigated for correlation with these hub genes. We identified six drugs targeting these seven cuproptosis genes in DrugBank. Hence, these cuproptosis gene signatures may be an important prognostic indicator for AD and may offer new insights into treatment options.

KEYWORDS

cuproptosis, Alzheimer's disease, diagnostic, drug, immune

Introduction

Alzheimer's disease is a neurodegenerative disease characterized by aging and irreversibility. It is predicted that dementia prevalence will double in Europe and triple globally by 2050 (1). The number of Americans with Alzheimer's dementia is estimated at 6.5 million over the age of 65 (2). The number of people with AD is forecast to grow to 13.8 million by 2060 without medical breakthroughs to prevent, slow, or treat it (2). According to the Alzheimer's Disease Foundation, Alzheimer's disease is the fifth leading cause of death among Americans aged 65 and older (3). It should be noted that about 5% of patients with AD inherit the disease in a chromosomal-dominant manner, and carriers can develop the disease as late as 40–60 years of age (3). Heritable familial AD (FAD) is most commonly caused by presenilin and the amyloid precursor protein (4). A major pathological feature of AD is the deposit of extracellular amyloid plaques and neurofibrillary tangles (NTFs) in the brain (5). According to the consensus, tau and amyloid β-protein (Aβ) are both essential to the neurodegenerative process in AD, and Aβ is located upstream of tau in the pathway (5). There is evidence indicating that amyloid

plaque is not as detrimental as the soluble oligomeric form of Aβ, which causes synaptic dysfunction (6). However, the exact pathogenic form of Aβ and the molecular mechanism by which pathogenic Aβ causes subsequent synaptic and neurotoxic processes are yet unclear (7). Currently, the U.S. Food and Drug Administration (FDA) has licensed six medications (including donepezil, rivastigmine, galantamine, minocycline, and donepezil) to temporarily treat Alzheimer's symptoms without affecting the underlying brain changes or changing the course of the illness (3). Consequently, finding novel, potent targeted agents is urgently needed to further AD diagnosis and care.

In addition to Aβ and NTFs, neuroinflammation plays a significant role in the development of AD (1). It has been shown that Aβ causes microglia to release cytokines that pass through the blood-brain barrier with increasing age, leading to an accumulation of Aβ (8–10). Aβ-activated microglia secrete neurotoxic cytokines and chemokines (TNF, IL-6, IL-1, and CCL2), which cause neurological dysfunction and death (11). Clinical studies suggest anti-inflammatory cytokines (IL-2, IL-4, and IL-33) can modulate microglia activation and mitigate AD pathology (12, 13). The permeability of immune cells and molecules that pass through the blood-brain barrier increases with age, contributing to neurodegeneration in AD (14). Although a relationship between AD and neuroinflammation has been identified, it is unclear whether it is a cause or a consequence of the disease. Therefore, further research into the relationship between AD and inflammation could enhance our understanding of AD and contribute to developing more effective AD treatments.

A metal with redox activity, copper is involved in several metabolic processes in the brain (15). It serves as the active site for several copper enzymes, including cytochrome oxidase, ceruloplasmin, SOD1, and lysinase (16). The uptake and secretion of intracellular and extracellular copper ions are mediated by CTR1 and ATP7A/B (17). There is evidence that ATP7B (K832R) mutations may increase the risk of AD (18). A large number of copper ions accumulate in neurons in the brains of patients with Alzheimer's disease, primarily in amyloid plaques and tangles (19). It has been shown that copper ions can reduce copper ions in neurons and tissues of the brain when APP expression is increased (20, 21). The deficiency of intracellular copper ions can promote the production of Aβ, while the accumulation of extracellular copper ions can promote the aggregation of Aβ (22, 23). Copper ions can affect the division and proliferation of neutrophils in the peripheral circulation and have a positive correlation with the severity of AD (24). The neutrophil can cross the blood-brain barrier and aggregate near Aβ plaques in the AD mouse model (25). Depletion of neutrophils enhanced cognitive performance, reduced microglia, and reduced Aβ 1–42 levels in 3xTg-AD mouse brain homogenates (26). Thus, regulation of intracellular and extracellular copper iron transport is still under research for the treatment of AD. As one of the causes of neuronal ROS, copper ions combined with Tau protein can lead to the production of H_2O_2 *in vitro*. It was shown that intracellular delivery of copper ions reduced intracellular Tau phosphorylation in a mouse animal model of AD (APP/PS1) (27). Therefore, the relationship between copper ion-related metabolism, immune cells, and molecules and AD is not negligible.

Through the analysis of differentially expressed genes (DEGs) and Weighted gene co-expression network analysis (WGCNA) between ND and AD on the GSE33000 dataset, we identified seven hub genes related to cuproptosis and AD. The biological processes and pathways of seven hub genes have been analyzed using GO and gene set enrichment analysis (GSEA) in patients with AD. We developed a diagnostic model for AD based on stepwise regression and logistic regression analyses and validated it in the GSE15222, GSE48350, and GSE5281 datasets, respectively. It is evident from the AUC value of ROC that the model has good diagnostic performance and may be useful in the diagnosis of AD. Symptoms of neuroinflammation can be accompanied by tangles of tau, which can result from interactions with amyloid plaques. Thus, the significance of immune infiltrating cells for these hub genes was explored in AD samples. Finally, we retrieved drugs targeting seven hub genes from the DrugBank database, which have implications for the treatment of AD. The flowchart of the research is shown in Figure 1.

Materials and methods

Data acquisition

In total, 2,977 genes associated with cuproptosis were found in the published literature (28). In this study, all expression profiles were obtained from public databases. Gene expression data were obtained from the GEO database (https://www.ncbi.nlm.nih.gov/geo/). GSE33000 expression data were obtained using the GPL10558 platform, containing 155 ND samples and 310 AD samples. GSE15222 expression data was used with the GPL2700 platform, containing 40 ND samples and 31 AD samples. GSE48350 expression data was used with the GPL570 platform, containing 27 ND samples and 21 AD samples. GSE5281 expression data was used with the GPL570 platform, containing 11 ND samples and 22 AD samples.

Differential expression analysis

Here, we used the "limma" package (version 3.40.6) for differential analysis to obtain differential genes between the AD and ND groups (29). Specifically, we obtained the expression profile dataset, performed multiple linear regression using the lmFit function, and further used the eBays function to compute moderated *t*-statistics, moderated *F*-statistics, and log-odds of differential expression by empirical Bayes moderation of the standard errors toward a common value, finally obtaining the differential significance of each gene. The differentially expressed genes (DEGs) between AD and AD were filtered with the threshold $|\log FC| > 1$ and adj.*p*.val < 0.05.

Weighted gene co-expression network analysis

Weighted gene co-expression network analysis is a method for analyzing gene expression patterns of multiple samples (30). It can cluster genes by similar gene expression patterns, form modules, and analyze the relationships between modules and the clinical information of patients (30). First, we calculated the MAD (median absolute deviation) of each gene separately using the gene expression profile, and then we eliminated the top 50% of genes with the smallest MAD, removed the outlier genes and samples using the

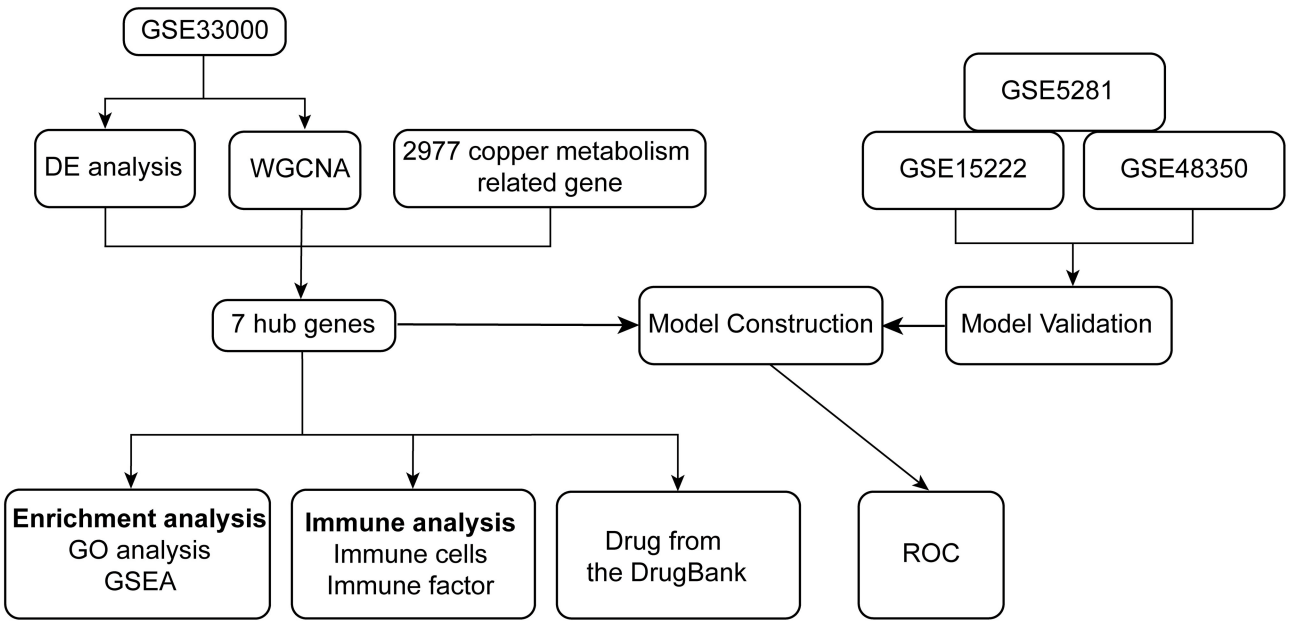

FIGURE 1
The flowchart of the analyses.

goodSamplesGenes method of the R package WGCNA, and further constructed a scale-free co-expression network using WGCNA. First, Pearson's correlation matrices and the average linkage method were both performed for all pair-wise genes. Then, a weighted adjacency matrix was constructed using a power function $A_{mn} = |C_{mn}|^{\beta}$ (C_{mn} = Pearson's correlation between $Gene_m$ and $Gene_n$; A_{mn} = adjacency between $Gene_m$ and $Gene_n$). β was a soft-thresholding parameter that could emphasize strong correlations between genes and penalize weak correlations. After choosing the power of 7, the adjacency was transformed into a topological overlap matrix (TOM), which could measure the network connectivity of a gene defined as the sum of its adjacency with all other genes for network generation, and the corresponding dissimilarity (1-TOM) was calculated. To classify genes with similar expression profiles into gene modules, average linkage hierarchical clustering was conducted according to the TOM-based dissimilarity measure with a minimum size (gene group) of 30 for the gene dendrogram. The sensitivity is 3. To further analyze the module, we calculated the dissimilarity of module eigengenes, chose a cut line for the module dendrogram, and merged some modules. In addition, we merged modules with distances <0.25 and finally obtained 13 co-expression modules. Notably, the gray module was considered a set of genes that could not be assigned to any module. Finally, we calculated the correlation between module vectors and gene expression to obtain MM (MM >0.8), and 206 genes with high connectivity in the clinically significant module were identified as hub genes.

Identification of hub genes

To obtain genes related to cuproptosis genes and AD, DEGs, intersections of genes obtained by WGCNA and cuproptosis genes were taken using the "VeenDiagram" package in R software. The differential expression of the hub gene in ND and AD was represented using violin plots. The hypothesis tests used were the *t*-test and the Mann–Whitney *U*-test. The former was used if the data conformed to a normal distribution, and the latter if not. Significance was defined as $p < 0.05$.

Enrichment analysis

To investigate the biological mechanisms affecting the hub gene for AD, we performed a functional enrichment analysis. We first analyzed the biological process (BP) of gene ontology (GO) in which these genes are involved and presented the final results as a chord plot using the "GOplot" package in the R software. We obtained the GSEA software (version 4.3) from the GSEA (http://software.broadinstitute.org/gsea/index.jsp) website, divided the samples into high (≥50%) and low (<50%) expression groups based on the expression levels of hub genes, and downloaded the c2.cp.kegg.v7.5.1.symbols.gmt subset from the Molecular Signatures Database (http://www.gsea-msigdb.org/gsea/downloads.jsp); the c2.cp.kegg.v7.5.1.symbols.gmt subset was downloaded to evaluate the relevant pathways and molecular mechanisms based on gene expression profiles and phenotypic groupings, setting a minimum gene set of 5 and a maximum gene set of 5,000, with 1,000 resamples. Screening conditions of $p < 0.05$ and FDR < 0.25 were considered to be statistically significant.

We used a query of multiple protein names ("IFI30," "CLIC1," "LYZ," "PYGL," "PLA1A," "ALOX5AP," and "A4GALT") and organisms ("*Homo sapiens*") to search the STRING website (https://string-db.org/). Following that, we set the following main parameters, namely, network type ("full STRING network"), network edge meaning ("evidence"), active interaction sources ("experiments"), the minimum required interaction score ["low confidence (0.150)"], and the maximum number of interactors to show ("no more than 50

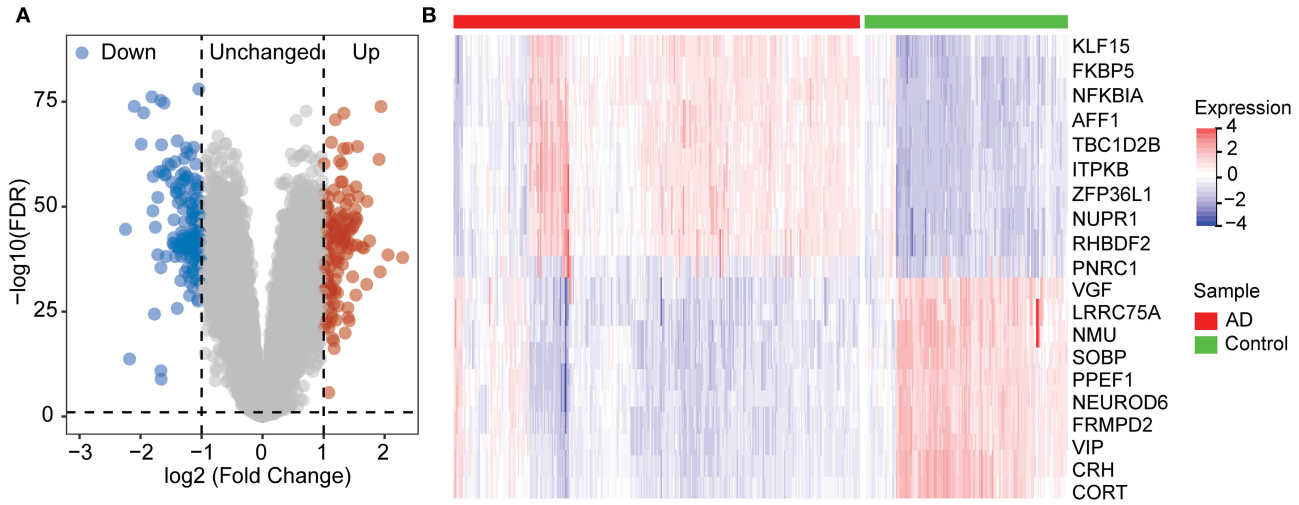

FIGURE 2
Differentially expression gene between ND and AD samples. **(A)** Volcano plot showing the significant genes found by limma analysis. Red genes represent significantly high expression in AD, blue genes indicate significantly high expression in ND, and gray genes mean no changes. **(B)** The top 20 genes significantly expressed in AD or ND samples, showing by the heatmap.

interactors" in the first shell). Finally, the available experimentally determined binding proteins were obtained and visualized by Cytoscape software (version 3.9.1).

Signature for patients with AD

A logistic model is a statistical model that simulates the probability of an event by making the logarithm of the event a linear combination of one or more independent variables and is often used in disease diagnosis (31). In this study, logistic regression with two response variables was used, with 1 representing the AD sample and 0 representing the ND sample. Stepwise regression analysis was used to eliminate factors that were not significant for the response variable and only those that were significant were retained to simplify the model. Stepwise regression iteratively adds or removes variables from the model until the statistical value of the Akaike information criterion (AIC) is minimized. After that, logistic regression was used to fit the relationship between these significant factors and the response variables.

Finally, we performed ROC analysis using the R package pROC (version 1.18.0) to obtain the AUC. Specifically, we obtained the patient's risk score, performed ROC analysis using the roc function of pROC, and evaluated the AUC and confidence interval using the ci function of pROC to obtain the final AUC result of 0.91.

Immune infiltration

CIBERSORT, a deconvolution algorithm, was used to estimate 22 types of infiltration immune cells in patients with ND and AD by using the normalized gene expression (32). In this study, we analyzed the abundance of infiltrating immune cells in ND and AD tissues using CIBERSORT of the LM22 gene file, including plasma cells, naïve B cells, memory B cells, memory $CD4^+$ T cells (activated and resting), naïve $CD4^+$ T cells, $CD8^+$ T cells, follicular helper T cells, γδ T cells, Tregs, macrophages (M0, M1, and M2), mast cells (activated and resting), dendritic cells (activated and resting), NK cells (activated and resting), neutrophils, monocytes, and eosinophils.

Drugs from the DrugBank

DrugBank (www.drugbank.ca) is a comprehensive, freely available web resource containing detailed drug, drug target, drug action, and drug interaction information on FDA-approved drugs and experimental drugs undergoing the FDA approval process (33). In this research, the "Targets" module of the DrugBank database was used to analyze the seven hub genes of drug targeting.

Statistical analysis

All statistical analyses in this study were performed using the R language. The *t*-test and the Mann–Whitney *U*-test were selected according to whether the data conformed to a normal distribution. Statistical significance was defined as $p < 0.05$.

Results

Identification of hub genes for AD and cuproptosis

To identify genes associated with AD, we analyzed a total of 299 differential genes between ND and AD in the GSE33000 dataset using the limma package with the screening criteria of adj.*p*.val < 0.05 and $|\log FC| > 1$, including 139 upregulated genes and 160 downregulated genes (Supplementary Table S1). Expression differential genes were

10.3389/fneur.2022.1064639

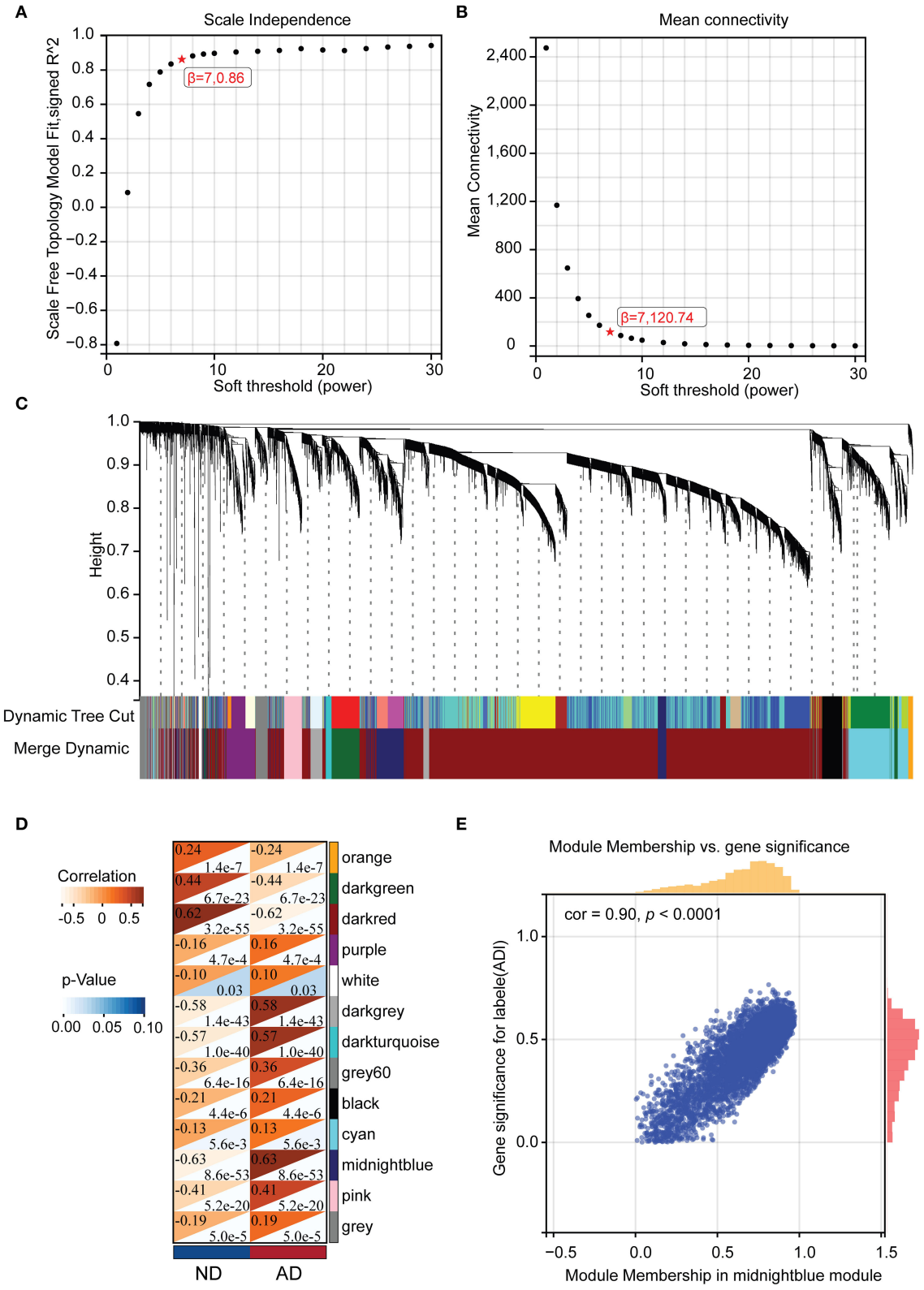

FIGURE 3
The WGCNA results. **(A)** Analysis of the scale-free fit index for various soft-thresholding powers (β). **(B)** The mean connectivity for the soft-thresholding powers. **(C)** Clustering dendrograms of genes, with dissimilarity based on the topological overlap, together with assigned module colors. **(D)** Correlations between different modules and clinical traits. **(E)** Correlation of module membership and gene significance in the midnight blue module.

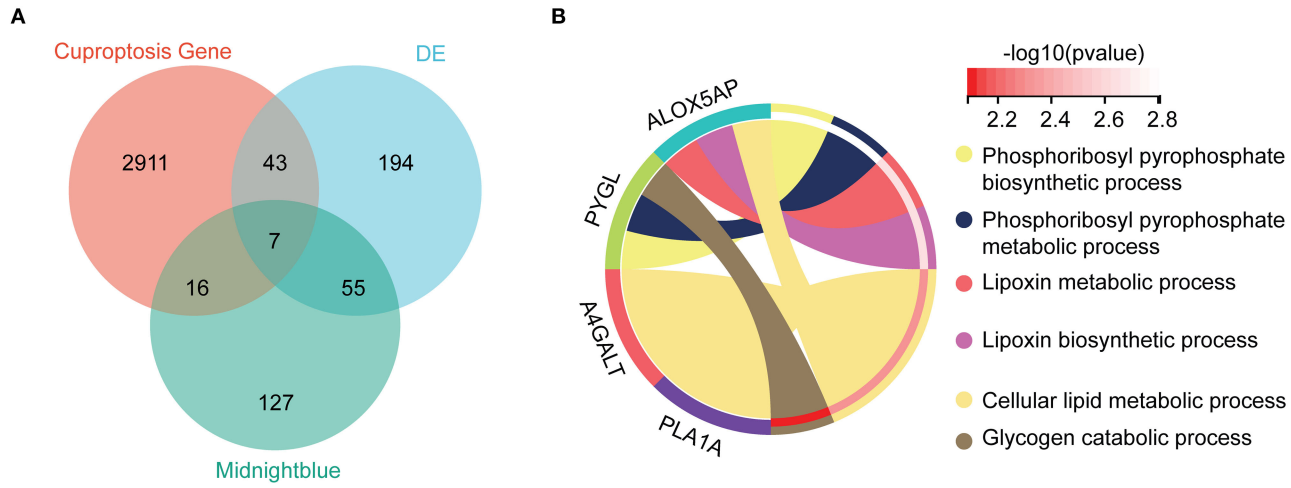

FIGURE 4
Hub genes and GO analysis. **(A)** The intersections of the DE, cuproptosis genes, and midnight blue genes. **(B)** Biological processes in which the seven hub genes were involved.

presented in a volcano plot (Figure 2A), and heat maps of the top 10 differentially expressed genes that were upregulated and downregulated, respectively, were plotted (Figure 2B).

After removing outlier genes and samples using the goodSamplesGenes method in the WGCNA package, the expression profiles of 7,595 genes and 465 samples were taken from GSE33000 for constructing a weighted gene co-expression network (soft threshold force: 7, scale independence: 0.86, average linkage: 120.74, Figures 3A, B). The 13 different co-expression modules were obtained through dynamic tree cutting (module merging threshold: 0.25, minimum module: 30, Figure 3C). The correlation analysis was then performed for each module with clinical traits. It was shown that the midnight blue ($r = 0.64$, $p = 8.6e\text{-}53$) and dark red module ($r = -0.62$, $p = 3.2e\text{-}55$) had the highest positive and negative correlation with AD, respectively (Figure 3D). Thus, we selected the midnight blue module (containing 453 genes) with the highest correlation coefficients for further analysis. GS- and MM-related scatterplots showed that these genes were highly correlated with both modules and phenotypes (cor = 0.90, $p < 0.001$; Figure 3E).

By taking the intersection of 299 differential genes in GSE33000, 453 genes in the midnight blue module of WGCNA, and 2,977 genes related to cuproptosis genes, we finally obtained the seven hub genes of cuproptosis associated with AD (Figure 4A). The results of the violin plot showed that the seven hub genes were highly expressed in patients with AD ($p < 0.05$, Figure 5). In addition, the expression of these genes in GSE15222, GSE48350, and GSE5281 is shown in Supplementary Figure S1.

Enrichment for the hub gene

To further investigate the molecular mechanism of the seven hub genes in AD, we attempted to screen out the targeting of the hub gene binding protein. Based on the STRING tool, we found a total of binding proteins, which were validated by experimental data (Supplementary Figure S2). We performed an enrichment analysis to investigate the potential biological role of these hub genes. The GO analysis showed that four of the seven hub genes were involved in biological processes (BP), including phosphoribosyl pyrophosphate biosynthetic process, phosphoribosyl pyrophosphate metabolic process, lipoxin metabolic process, lipoxin biosynthetic process, cellular lipid metabolic process, and glycogen catabolic process (Figure 4B).

The results of the GSEA analysis showed that these hub genes were associated with neurodegenerative diseases (AD and Parkinson's disease), oxidative phosphorylation, leukocyte transendothelial migration, leishmania infection, hematopoietic cell lineage, complement and coagulation cascades, citrate cycle (TCA cycle), B cell receptor signaling pathway, systemic lupus erythematosus, cytokine receptor interaction, ECM receptor interaction, and Jak stat signaling pathway (Figure 6).

Construction and validation of diagnostic models

Logistic regression was used to perform a multi-gene prediction model based on GSE33000. Logistic regression was used to perform a multi-gene prediction model based on GSE33000. The prediction model was constructed for four of the seven cuproptosis genes, including *IFI30*, *PLA1A*, *ALOX5AP*, and *A4GALT*. The results showed that the constructed model had good diagnostic performance, and the area under the ROC curve was 0.91 (Figure 7A). We used the GSE48350, GSE15222, and GSE5281 datasets for validation, and the results showed that the area under the ROC curve was 0.75, 0.76, and 0.91, respectively (Figures 7B–D). The formula was as follows: [expression level of *IFI30* × (−0.7449)] + [expression level of *PLA1A* × 0.6557] + [Expression level of *ALOX5AP* × 1.1483)] + [expression level of *A4GALT* × 1.4343] + 0.8891.

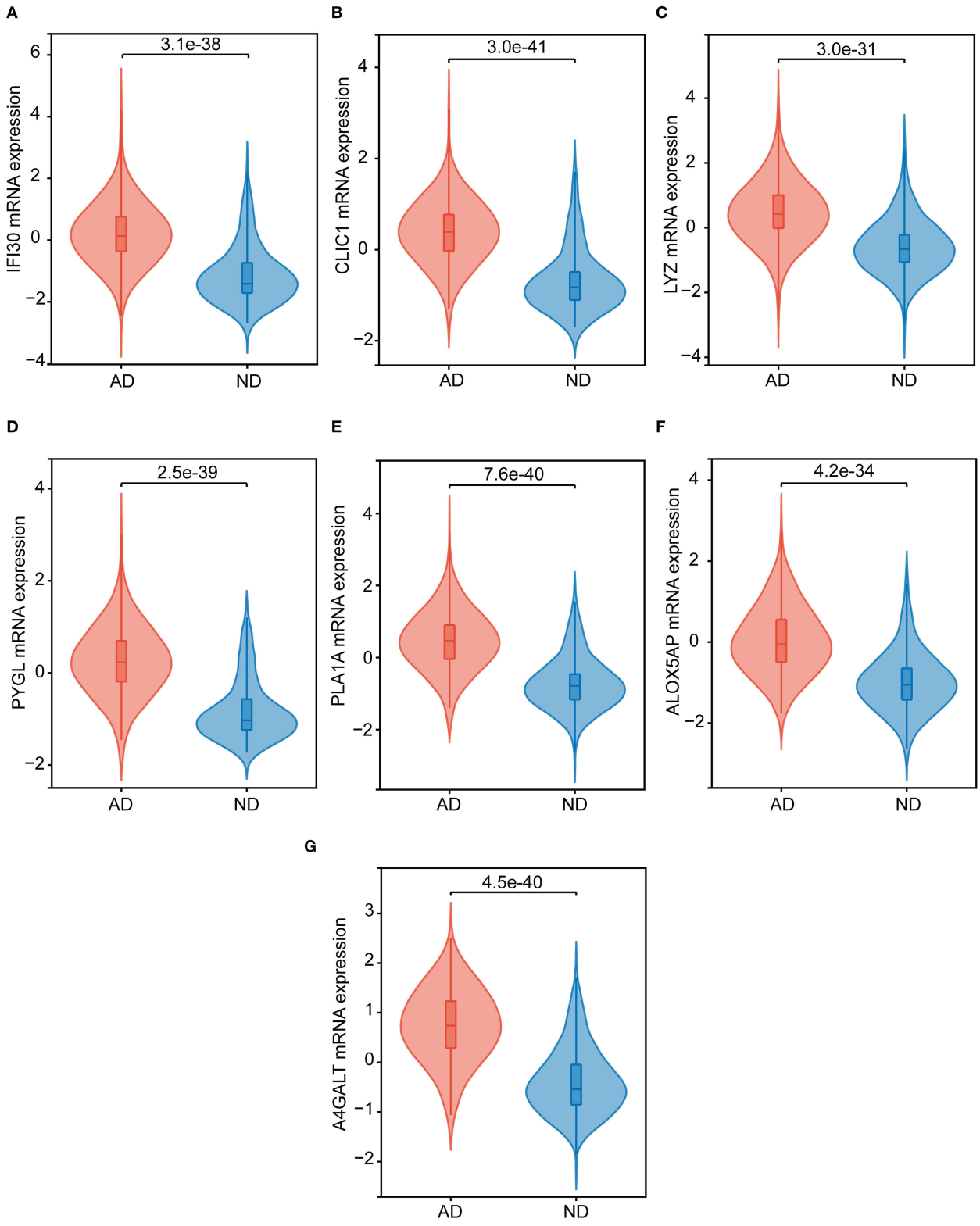

FIGURE 5
The hub genes expression in the ND and AD samples of GSE33000. **(A)** IFI30, **(B)** CLIC1, **(C)** LYZ, **(D)** PYGL, **(E)** PLA1A, **(F)** ALOX5AP, and **(G)** A4GALT.

Immune infiltration in patients with AD

Immune cells, extracellular matrix, and other factors in the body are important for clinical therapeutic sensitivity and disease diagnosis. In this study, we used CIBERSORT to compare the proportion of 22 immune infiltrating cells in ND and AD samples (Figure 8A). The immune cell infiltration was compared between AD and ND samples in the boxplot (Figure 8B). The results showed that

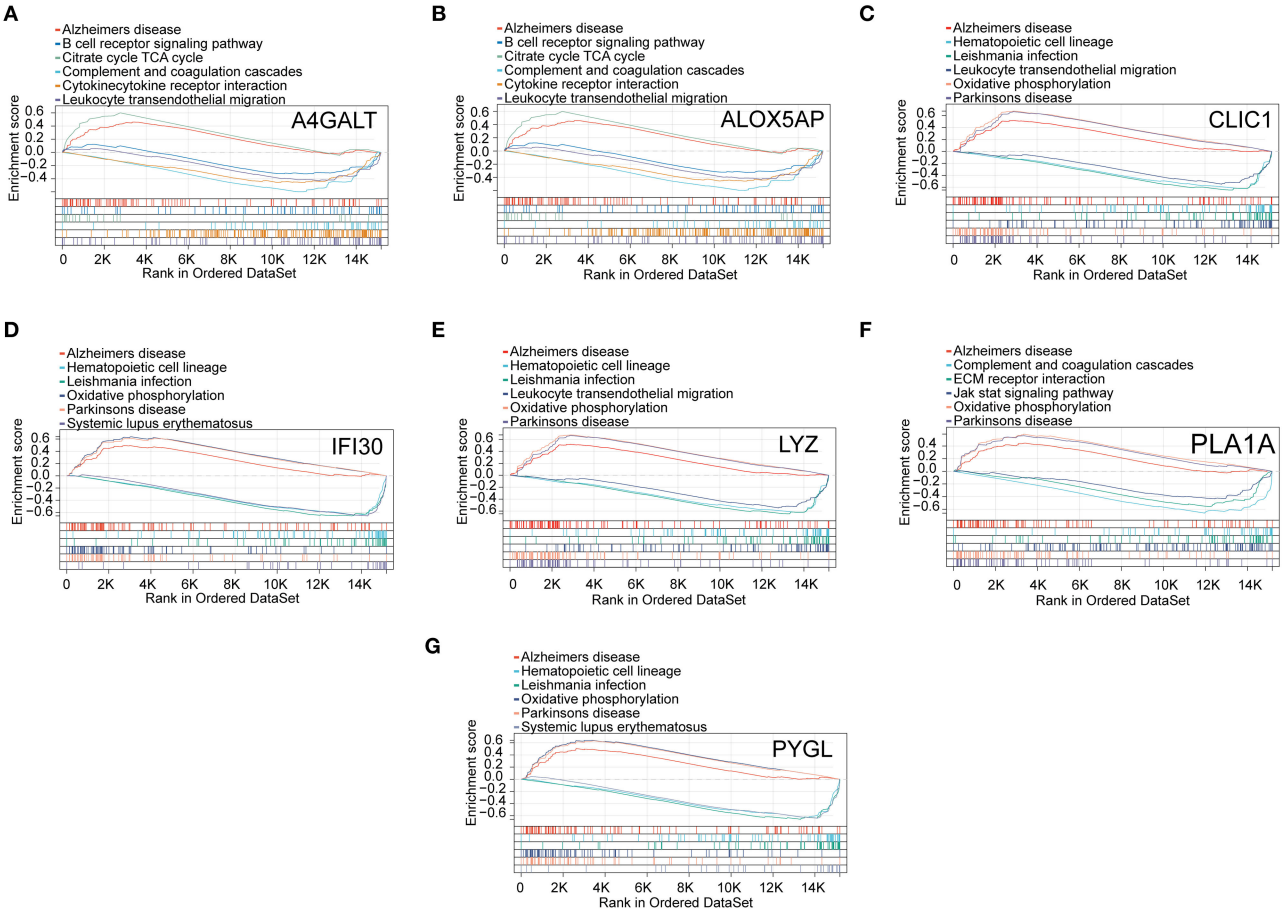

FIGURE 6
GSEA revealed the enriched pathways of the hub genes. **(A)** A4GALT, **(B)** ALOX5AP, **(C)** CLIC1, **(D)** IFI30, **(E)** LYZ, **(F)** PLA1A, and **(G)** PYGL.

memory B cells, naïve $CD4^+$ T cells, resting memory $CD4^+$ T cells, NK cells resting, macrophages M2, activated mast cells, eosinophils, and neutrophils were significantly higher in patients with AD. In contrast, plasma cells, $CD8^+$ T cells, activated memory $CD4^+$ T cells, follicular helper T cells, regulatory T cells (Tregs), activated NK cells and resting mast cells were significantly lower in patients with AD.

Subsequently, the relationship between hub genes and immune infiltration was analyzed. The hub genes were significantly negatively associated with plasma cells, $CD8^+$ T cells, activated memory $CD4^+$ T cells, follicular helper T cells, Tregs, activated NK cells, and resting mast cells, while the opposite was true with resting memory $CD4^+$ T cells, resting NK cells, monocytes, macrophages M1, macrophages M2, and neutrophils (Figure 9). The results suggest that the hub genes may play an important role in the immune microenvironment.

Drug from DrugBank

In this study, we searched the DrugBank database for drugs targeting seven cuproptosis genes (Table 1). The FDA has approved six of these drugs; several others are being investigated intermittently; and one drug has been discontinued. There are no studies available for the *A4GALT*, *PLA1A*, and *PYGL* genes. It is believed that copper (DB09130) does have an effect on the *CLIC1* gene and is mostly used in emergency contraception, non-traceable elements, and dietary supplements, although the exact mechanism is unknown due to the wide spectrum of enzymes that use copper ions as co-factors. Acting as a ligand for *CLIC1* target genes, Artenimol (DB11638) also acts as a regulator of the cell cycle and inserts into membranes to form chloride channels at appropriate pH levels (34). In tissues and body fluids, sucrose (DB02772) acts as a nutritional supplement to Lysozyme C (encoded by the LYZ gene), which has an important role in enhancing immune responses (35, 36). As a feed additive, arsanilic acid (DB03006) is a toxic compound containing arsenic that induces blindness in animals. It has received approval for use in veterinary medicine for treating intestinal diseases in pigs and poultry (36). It is known that propyl alcohol (DB03175) is one of the best targets for lysozyme C and is primarily used for skin disinfection as well as a preservative that can be used in both clinical and domestic settings (35). Known as part of the non-essential amino acid family, aspartic acid (DB00128) can act on lysozyme C, but it needs to be studied further. Rose bengal (DB11182) is used as a diagnostic agent and is recommended for eye examinations, cornea, or conjunctiva (37) (Supplementary Table S2).

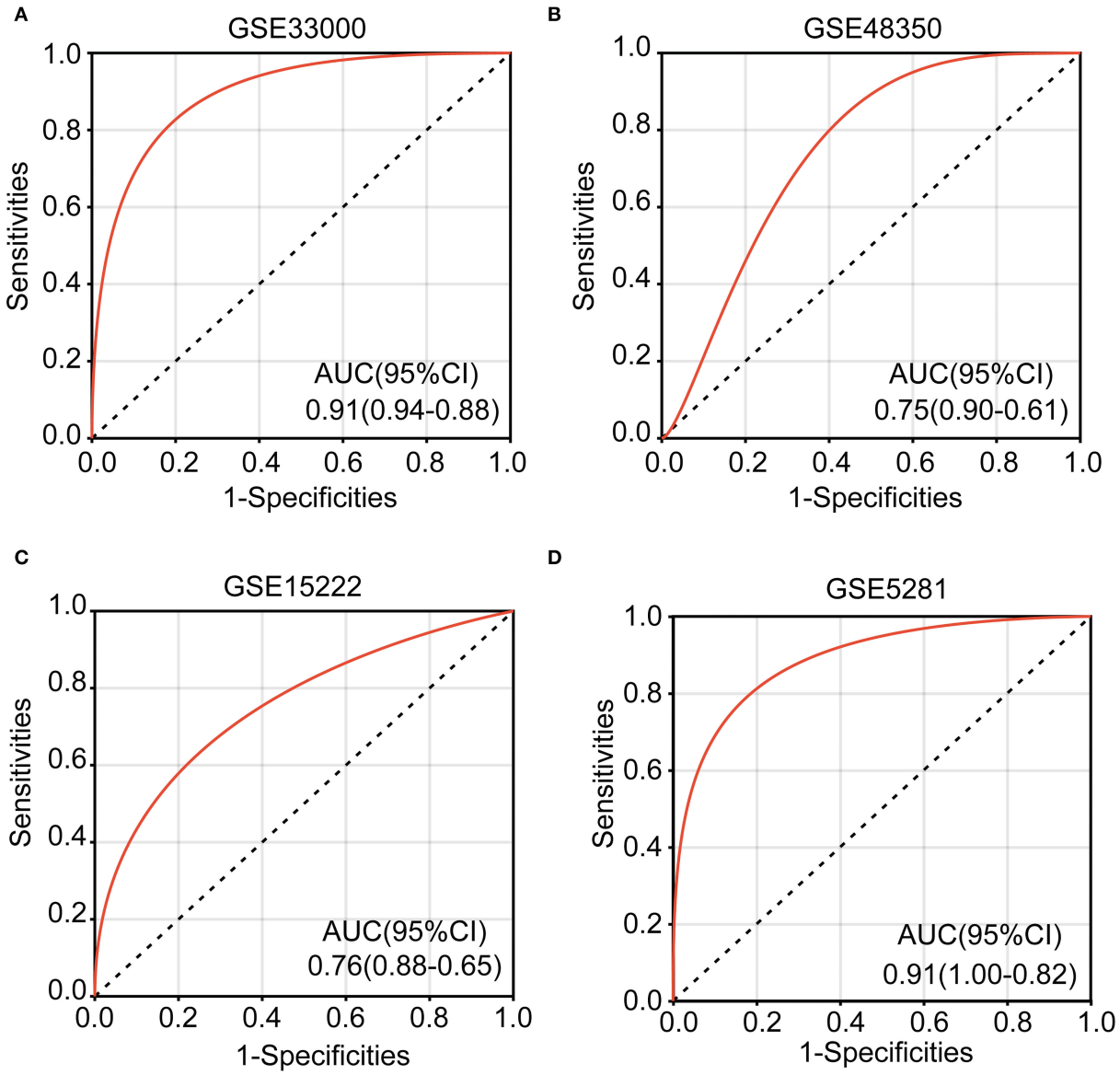

FIGURE 7
Receiver operating characteristic (ROC) curves and corresponding AUC values for the four expression cohorts. **(A)** GSE33000, **(B)** GSE48350, **(C)** GSE15222, and **(D)** GSE5281.

Discussion

In this study, seven cuproptosis genes were screened for association with AD using the public dataset GSE33000. GO analysis showed that they were involved in the phosphoribosyl pyrophosphate and lipoxin biological processes, as well as the cellular lipid metabolic process and glycogen catabolic process. There is no doubt that elevated levels of PRPP in humans are associated with an excess of uric acid production and accumulation, which is negatively correlated with Alzheimer's disease prevalence (38). Neuroinflammation may be beneficial for patients with early-onset Alzheimer's disease, and it may help reverse or at least slow tau protein accumulation in the brain, preventing dementia (25). By helping macrophage differentiation and activation, lipoxin, derived from arachidonic acid, could reduce the immune response in early patients with AD by releasing cytokines that decrease inflammation (39, 40). Based on these cuproptosis genes, prediction models were developed and validated using the GSE48350, GSE5281, and GSE15222 datasets, respectively. Furthermore, GSEA demonstrated that all of these pivotal genes were associated with neurodegenerative diseases, particularly AD, which validated these gene selections to some extent (Figure 6).

The diagnostic models developed from four of the seven cuproptosis genes (including IFI30, PLA1A, ALOX5AP, and A4GALT) can serve as a guide to the clinical diagnosis of AD. An antigen-presenting cell (APC)-expressing gamma-interferon-induced lysosomal thiol reductase (GILT, encoded by IFI30) reduces disulfide bonds through endocytic proteins, presenting

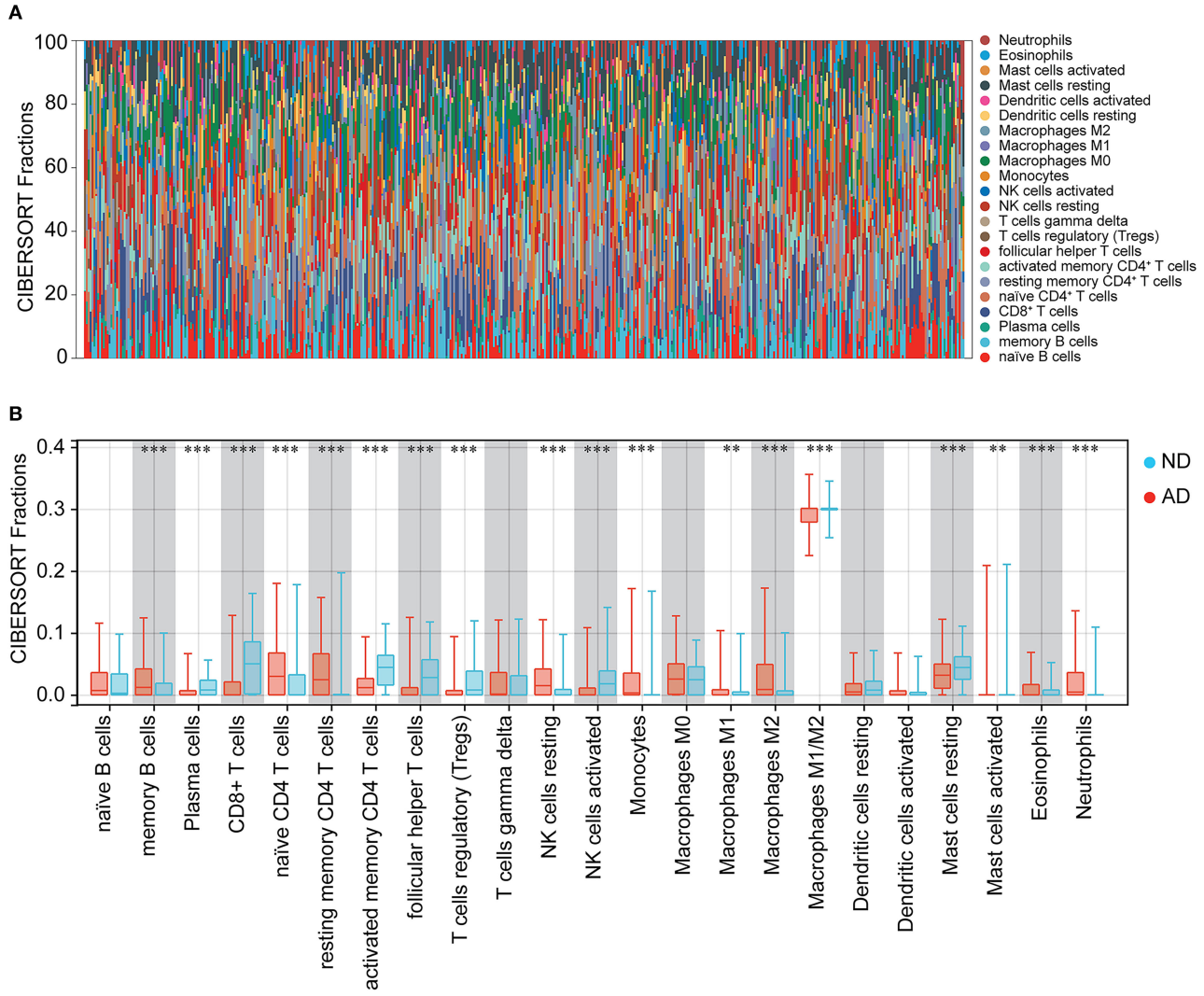

FIGURE 8
Immune cell infiltration between ND and AD samples. **(A)** The percentage of 22 immune cells in each sample. **(B)** Different levels of immune infiltrating cells between ND and AD samples.

immunogenic peptides bound to the major histocompatibility complex (MHC) class II (41). Consistent with our findings that the IFI30 gene is highly expressed in patients with AD, GILT is highly expressed in microglia surrounding Aβ and is involved in Aβ clearance (42, 43). Abnormalities of lipid metabolism in the brain are characteristic of AD (44, 45). It is possible to reduce the risk of AD by converting phosphatidylcholine to lysophosphatidylcholine-DHA in liver tissues and transporting it into the brain across the blood-brain barrier (46, 47). The 5-lipoxygenase-activating protein (FLAP, encoded by ALOX5AP) is widely distributed in the central nervous system and functions to regulate the activation of the 5-lipoxygenase enzyme (48). It has been shown that selective pharmacological inhibition of FLAP significantly reduces Aβ levels and deposition in amyloid precursor protein (APP) transgenic mice (49) and regulates endogenous tau metabolism *in vivo* (50). A4GALT is involved in regulating the synthesis of glycosphingolipids, which is associated with several neurodegenerative diseases, including AD and Parkinson's disease (36, 37). Neuroinflammation is more prevalent in patients with mild cognitive impairment and AD. There is research showing that a combination therapy that reduces amyloid plaque formation and limits neuroinflammation may be more effective than treating either alone (51).

Here, we further explored the level of infiltration of immune infiltrating cells in patients with AD. The results showed that the M0 macrophages were not significantly different in both AD and ND, while the M1/M2 macrophages were significantly lower in AD. According to the results, increased activation and differentiation of M0 macrophages into M2 macrophages reduces inflammation and contributes to delaying the onset of AD. Tregs, the subset of $CD4^+$ T cells, are essential for maintaining immune homeostasis and downregulating patients with AD. The results have shown that early depletion of Tregs is associated with accelerated cognitive impairment and that restoring Tregs reduces Aβ deposition

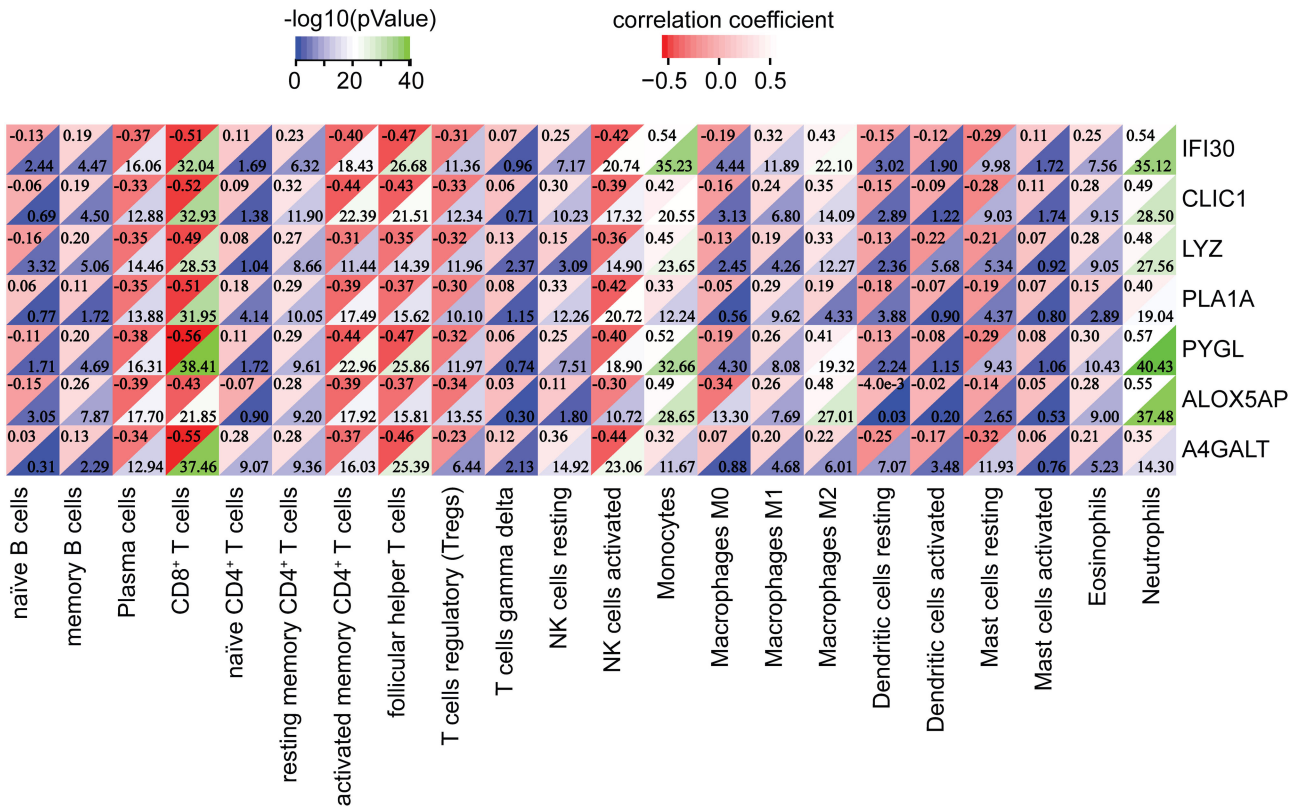

FIGURE 9
Correlation between the hub genes and immune infiltrating cells. $^{**}p < 0.01$, $^{***}p < 0.001$.

and improves cognition, but the results of this study remain controversial (52). Neutrophils are also upregulated in AD. A significant increase in neutrophils was found in AD brains and AD model mice, and hyperactivity of neutrophils is associated with AD (53). It was found that neutrophils may play a role in AD as they produce large quantities of reactive oxygen species, thereby causing AD and cognitive decline through the LFA-1 integrin (25).

The gamma interferon-inducible lysosomal thiol reductase (GILT, encoded by IFI30) is expressed in antigen-presenting cells (APCs), such as dendritic cells, monocytes/macrophages, and B cells, and it is highly expressed in microglia in the AD brain (42). The chloride intracellular channel 1 (CLIC1) protein, a potential marker of neurodegenerative processes, is significantly increased in peripheral blood mononuclear cells of patients with AD (54). The LYZ gene, a significant member of non-specific immunity, is upregulated in the cerebrospinal fluid (CSF) of patients with AD and inhibits the appearance of toxic Aβ oligomers (55). Abnormal brain glucose catabolic processes are associated with the formation of amyloid plaques in the brain and the onset of memory loss (56). In contrast, the relationship between PYGL (glucose metabolizing enzyme) and AD remains unclear.

Finally, the drugs targeting the above genes were retrieved from the DrugBank database. An excess of copper (DB09130) acts as a catalyst for a variety of biological processes (57), accumulating in neurofibrillary tangles and regulating APP gene expression (45, 46). Aβ peptide interaction with copper and other metals is thought to promote gain-of-function activity and lead to neurotoxicity (15). As an immunomodulator and neuroinflammatory drug, Artenimol (DB11638) inhibits neuronal apoptosis, modulates Tau autophagy, and protects AD mice from neuronal damage (58–60). There is no doubt that sucrose (DB02772) is a valuable nutritional supplement, but excessive consumption can lead to type 2 diabetes, and type 2 diabetes is associated with a high incidence of Alzheimer's disease (61). There is an increase in LYZ in the brains of transgenic mice and humans with AD, pointing to new therapeutic strategies to slow its progression (55). Propyl alcohol (DB03175) acts on the LYZ target, but its function still needs further study. In addition to its functionality in protein synthesis, aspartic acid (DB00128) is also involved in the urea cycle and gluconeogenesis and affects AD indirectly (62, 63). There is a xanthene dye, rose bengal (DB11182), which has been used to treat colon cancer (64). Furthermore, rose bengal inhibits the toxic effects caused by Aβ aggregation (65) and has a therapeutic effect on Tau aggregation (66).

Conclusion

In summary, we investigated seven cuproptosis genes and AD-related hub genes by using bioinformatics techniques. The

TABLE 1 Drugs targeting these seven hub genes obtained from the DrugBank database.

Gene symbol	Protein	UniProt ID	DrugBank ID	Name	Drug group	Actions
IFI30	Tryptophan-tRNA ligase, cytoplasmic	P23381	DB00150	Tryptophan	Approved, nutraceutical, withdrawn	Inhibitor
			DB01831	Tryptophanyl-5'amp	Experimental	
			DB04537	Tryptophanamide	Experimental	
A4GALT						
ALOX5AP	Arachidonate 5-lipoxygenase-activating protein	P20292	DB05225	AM103	Investigational	Inhibitor
			DB04929	DG031	Investigational	
			DB06346	Fiboflapon	Investigational	
			DB16739	MK-886	Experimental	Inhibitor
			DB16346	Veliflapon	Investigational	Inhibitor
CLIC1	Chloride intracellular channel protein 1	O00299	DB09130	Copper	Approved, investigational	
			DB11638	Artenimol	Approved, experimental, investigational	Ligand
LYZ	Lysozyme C	P61626	DB02772	Sucrose	Approved, experimental, investigational	
			DB03006	Arsanilic acid	Experimental, vet_approved	
			DB03120	p-Toluenesulfonic acid	Experimental	
			DB03189	Cu-Cyclam	Experimental	
			DB03487	(S)-Aspartimide	Experimental	
			DB02759	4-methyl-umbelliferyl-N-acetyl-chitobiose	Experimental	
			DB03013	N-acetyl-beta-D-glucosaminyl-(1->4)-N-acetyl-beta-D-glucosamine	Experimental	
			DB03175	Propyl alcohol	Approved	
			DB02159	(R)-Propylene glycol	Experimental	
			DB04194	Triacetylchitotriose	Experimental	
			DB04268	Methylumbelliferyl chitotriose	Experimental	
			DB00128	Aspartic acid	Approved, nutraceutical	
			DB06912	UNDECA-3,7-DIENE-1,3,7,11-TETRACARBALDEHYDE	Experimental	
			DB03967	Dodecyl sulfate	Experimental	
			DB11182	Rose bengal	Approved, investigational	ligand
PLA1A	Phospholipase A1 member A	Q53H76				
PYGL	Glycogen phosphorylase, liver form	P06737				

biological role of these genes in AD development was explored. Further experiments are needed to confirm the function. Based on logistic regression analysis, we constructed a diagnostic model that can diagnose patients with AD by detecting the expression of several genes in the brain tissues. Additionally, immune cells expressed themselves more strongly in AD, indicating that they may be crucial to the immunological microenvironment. However, further research is needed to explore their specific effects. Currently, only a few drugs targeting these pivotal genes are predicted to alleviate AD, suggesting that additional drugs need to be developed.

Data availability statement

The original contributions presented in the study are included in the article/Supplementary material, further inquiries can be directed to the corresponding authors.

Author contributions

EZ and FD contributed to the conception, design of the study, and wrote the first draft of the manuscript. TC and SL organized the

database. EZ, FD, and CX performed the statistical analysis. XS wrote sections of the manuscript. All authors contributed to the manuscript revision and read and approved the submitted version.

Funding

This study was supported by the Doctoral Scientific Research Foundation of Guizhou Medical University (No. YJ20066), the National Natural Science Foundation of China Cultivation Project of Guizhou Medical University (No. 20NSP051), the Scientific and Technological Project of Guizhou Province [No. ZK (2022) 398], and the Fund of Science and Technology Project of Guizhou provincial health commission (No. Gzwkj2023-564).

Acknowledgments

We thank all the patients who participated in the study. We also thank Dr. Jianming Zeng and his bioinformatics team for their reference codes.

Conflict of interest

The authors declare that the research was conducted in the absence of any commercial or financial relationships that could be construed as a potential conflict of interest.

Publisher's note

Supplementary material

The Supplementary Material for this article can be found online at: https://www.frontiersin.org/articles/10.3389/fneur.2022.1064639/full#supplementary-material

SUPPLEMENTARY FIGURE 1
Expression of hub genes in the AD and ND samples GSE15222, GSE48350, and GSE5281.

SUPPLEMENTARY FIGURE 2
Protein-protein interaction of seven hub genes.

SUPPLEMENTARY TABLE 1
Differentially expressed genes between AD and ND samples in GSE33000.

SUPPLEMENTARY TABLE 2
Information on drugs targeting these seven hub genes.

References

1. Scheltens P, Strooper BD, Kivipelto M, Holstege H, Chételat G, Teunissen CE, et al. Alzheimer's disease. *Lancet.* (2021) 397:1577–90. doi: 10.1016/S0140-6736(20)32205-4

2. Rajan KB, Weuve J, Barnes LL, McAninch EA, Wilson RS, Evans DA. Population estimate of people with clinical Alzheimer's disease and mild cognitive impairment in the United States (2020-2060). *Alzheimers Dement.* (2021) 17:1966–75. doi: 10.1002/alz.12362

3. Alzheimer's disease facts and figures. *Alzheimers Dement.* (2022) 18:700–89. doi: 10.1002/alz.12638

4. Tanzi RE, Bertram L. Twenty years of the Alzheimer's disease amyloid hypothesis: a genetic perspective. *Cell.* (2005) 120:545–55. doi: 10.1016/j.cell.2005.02.008

5. Lewis J, Dickson DW, Lin WL, Chisholm L, Corral A, Jones G, et al. Enhanced neurofibrillary degeneration in transgenic mice expressing mutant tau and APP. *Science.* (2001) 293:1487–91. doi: 10.1126/science.1058189

6. Masters CL, Selkoe DJ. Biochemistry of amyloid β-protein and amyloid deposits in Alzheimer disease. *Cold Spring Harb Perspect Med.* (2012) 2:a006262. doi: 10.1101/cshperspect.a006262

7. Benilova I, Karran E, De Strooper B. The toxic Aβ oligomer and Alzheimer's disease: an emperor in need of clothes. *Nat Neurosci.* (2012) 15:349–57. doi: 10.1038/nn.3028

8. Zhu M, Wang X, Sun L, Schultzberg M, Hjorth E. Can inflammation be resolved in Alzheimer's disease? *Ther Adv Neurol Disord.* (2018) 11:1756286418791107. doi: 10.1177/1756286418791107

9. Blasko I, Veerhuis R, Stampfer-Kountchev M, Saurwein-Teissl M, Eikelenboom P, Grubeck-Loebenstein B. Costimulatory effects of interferon-gamma and interleukin-1beta or tumor necrosis factor alpha on the synthesis of Abeta1-40 and Abeta1-42 by human astrocytes. *Neurobiol Dis.* (2000) 7:682–9. doi: 10.1006/nbdi.2000.0321

10. Hu J, Akama KT, Krafft GA, Chromy BA, Van Eldik LJ. Amyloid-beta peptide activates cultured astrocytes: morphological alterations, cytokine induction and nitric oxide release. *Brain Res.* (1998) 785:195–206. doi: 10.1016/S0006-8993(97)01318-8

11. DiSabato DJ, Quan N, Godbout JP. Neuroinflammation: the devil is in the details. *J Neurochem.* (2016) 139 Suppl 2:136–53. doi: 10.1111/jnc.13607

12. Alves S, Churlaud G, Audrain M, Michaelsen-Preusse K, Fol R, Souchet B, et al. Interleukin-2 improves amyloid pathology, synaptic failure and memory in Alzheimer's disease mice. *Brain.* (2017) 140:826–42. doi: 10.1093/brain/aww330

13. Kiyota T, Okuyama S, Swan RJ, Jacobsen MT, Gendelman HE, Ikezu T, et al. CNS expression of anti-inflammatory cytokine interleukin-4 attenuates Alzheimer's disease-like pathogenesis in APP+PS1 bigenic mice. *FASEB J.* (2010) 24:3093–102. doi: 10.1096/fj.10-155317

14. Newcombe EA, Camats-Perna J, Silva ML, Valmas N, Huat TJ, Medeiros R. Inflammation: the link between comorbidities, genetics, and Alzheimer's disease. *J Neuroinflammation.* (2018) 15:276. doi: 10.1186/s12974-018-1313-3

15. Roberts BR, Ryan TM, Bush AI, Masters CL, Duce JA. The role of metallobiology and amyloid-β peptides in Alzheimer's disease. *J Neurochem.* (2012) 120(Suppl 1):149–66. doi: 10.1111/j.1471-4159.2011.07500.x

16. Barnham KJ, Masters CL, Bush AI. Neurodegenerative diseases and oxidative stress. *Nat Rev Drug Discov.* (2004) 3:205–14. doi: 10.1038/nrd1330

17. Scheiber IF, Mercer JFB, Dringen R. Metabolism and functions of copper in brain. *Prog Neurobiol.* (2014) 116:33–57. doi: 10.1016/j.pneurobio.2014.01.002

18. Mercer SW, Wang J, Burke R. *In vivo* modeling of the pathogenic effect of copper transporter mutations that cause Menkes and Wilson Diseases, motor neuropathy, and susceptibility to Alzheimer's disease. *J Biol Chem.* (2017) 292:4113–22. doi: 10.1074/jbc.M116.756163

19. Ayton S, Lei P, Bush AI. Metallostasis in Alzheimer's disease. *Free Radic Biol Med.* (2013) 62:76–89. doi: 10.1016/j.freeradbiomed.2012.10.558

20. White AR, Reyes R, Mercer JF, Camakaris J, Zheng H, Bush AI, et al. Copper levels are increased in the cerebral cortex and liver of APP and APLP2 knockout mice. *Brain Res.* (1999) 842:439–44. doi: 10.1016/S0006-8993(99)01861-2

21. Maynard CJ, Cappai R, Volitakis I, Cherny RA, White AR, Beyreuther K, et al. Overexpression of Alzheimer's disease amyloid-beta opposes the age-dependent elevations of brain copper and iron. *J Biol Chem.* (2002) 277:44670–6. doi: 10.1074/jbc.M204379200

22. Ma QF, Li YM, Du JT, Kanazawa K, Nemoto T, Nakanishi H, et al. Binding of copper (II) ion to an Alzheimer's tau peptide as revealed by MALDI-TOF MS, CD, and NMR. *Biopolymers.* (2005) 79:74–85. doi: 10.1002/bip.20335

23. Zhou L-X, Du J-T, Zeng Z-Y, Wu W-H, Zhao Y-F, Kanazawa K, et al. Copper (II) modulates *in vitro* aggregation of a tau peptide. *Peptides.* (2007) 28:2229–34. doi: 10.1016/j.peptides.2007.08.022

24. Scali C, Prosperi C, Bracco L, Piccini C, Baronti R, Ginestroni A, et al. Neutrophils CD11b and fibroblasts PGE(2) are elevated in Alzheimer's disease. *Neurobiol Aging.* (2002) 23:523–30. doi: 10.1016/S0197-4580(01)00346-3

25. Zenaro E, Pietronigro E, Della Bianca V, Piacentino G, Marongiu L, Budui S, et al. Neutrophils promote Alzheimer's disease-like pathology and cognitive decline *via* LFA-1 integrin. *Nat Med.* (2015) 21:880–6. doi: 10.1038/nm.3913

26. Stock AJ, Kasus-Jacobi A, Pereira HA. The role of neutrophil granule proteins in neuroinflammation and Alzheimer's disease. *J Neuroinflammation.* (2018) 15:240. doi: 10.1186/s12974-018-1284-4

27. Crouch PJ, Hung LW, Adlard PA, Cortes M, Lal V, Filiz G, et al. Increasing Cu bioavailability inhibits Abeta oligomers and tau phosphorylation. *Proc Natl Acad Sci U S A.* (2009) 106:381–6. doi: 10.1073/pnas.0809057106

28. Tsvetkov P, Coy S, Petrova B, Dreishpoon M, Verma A, Abdusamad M, et al. Copper induces cell death by targeting lipoylated TCA cycle proteins. *Science.* (2022) 375:1254–61. doi: 10.1126/science.abf0529

29. Ritchie ME, Phipson B, Wu D, Hu Y, Law CW, Shi W, et al. limma powers differential expression analyses for RNA-sequencing and microarray studies. *Nucleic Acids Res.* (2015) 43:e47. doi: 10.1093/nar/gkv007

30. Langfelder P, Horvath S. WGCNA: an R package for weighted correlation network analysis. *BMC Bioinformatics.* (2008) 9:559. doi: 10.1186/1471-2105-9-559

31. Tolles J, Meurer WJ. Logistic regression: relating patient characteristics to outcomes. *JAMA.* (2016) 316:533–4. doi: 10.1001/jama.2016.7653

32. Newman AM, Liu CL, Green MR, Gentles AJ, Feng W, Xu Y, et al. Robust enumeration of cell subsets from tissue expression profiles. *Nat Methods.* (2015) 12:453–7. doi: 10.1038/nmeth.3337

33. Wishart DS, Feunang YD, Guo AC, Lo EJ, Marcu A, Grant JR, et al. DrugBank 5.0: a major update to the DrugBank database for 2018. *Nucleic Acids Res.* (2018) 46:D1074–82. doi: 10.1093/nar/gkx1037

34. Finaurini S, Basilico N, Corbett Y, D'Alessandro S, Parapini S, Olliaro P, et al. Dihydroartemisinin inhibits the human erythroid cell differentiation by altering the cell cycle. *Toxicology.* (2012) 300:57–66. doi: 10.1016/j.tox.2012.05.024

35. Overington JP, Al-Lazikani B, Hopkins AL. How many drug targets are there? *Nat Rev Drug Discov.* (2006) 5:993–6. doi: 10.1038/nrd2199

36. Imming P, Sinning C, Meyer A. Drugs, their targets and the nature and number of drug targets. *Nat Rev Drug Discov.* (2006) 5:821–34. doi: 10.1038/nrd2132

37. Lee YC, Park CK, Kim MS, Kim JH. *In vitro* study for staining and toxicity of rose bengal on cultured bovine corneal endothelial cells. *Cornea.* (1996) 15:376–85. doi: 10.1097/00003226-199607000-00008

38. Tana C, Ticinesi A, Prati B, Nouvenne A, Meschi T. Uric acid and cognitive function in older individuals. *Nutrients.* (2018) 10:975. doi: 10.3390/nu10080975

39. Strosznajder AK, Wójtowicz S, Jezyna MJ, Sun GY, Strosznajder JB. Recent insights on the role of PPAR-β/δ in neuroinflammation and neurodegeneration, and its potential target for therapy. *Neuromolecular Med.* (2021) 23:86–98. doi: 10.1007/s12017-020-08629-9

40. Gerrits E, Brouwer N, Kooistra SM, Woodbury ME, Vermeiren Y, Lambourne M, et al. Distinct amyloid-β and tau-associated microglia profiles in Alzheimer's disease. *Acta Neuropathol.* (2021) 141:681–96. doi: 10.1007/s00401-021-02263-w

41. West LC, Cresswell P. Expanding roles for GILT in immunity. *Curr Opin Immunol.* (2013) 25:103–8. doi: 10.1016/j.coi.2012.11.006

42. Satoh J-I, Kino Y, Yanaizu M, Ishida T, Saito Y. Microglia express gamma-interferon-inducible lysosomal thiol reductase in the brains of Alzheimer's disease and Nasu-Hakola disease. *Intractable Rare Dis Res.* (2018) 7:251–7. doi: 10.5582/irdr.2018.01119

43. Chai K, Zhang X, Chen S, Gu H, Tang H, Cao P, et al. Application of weighted co-expression network analysis and machine learning to identify the pathological mechanism of Alzheimer's disease. *Front Aging Neurosci.* (2022) 14:837770. doi: 10.3389/fnagi.2022.837770

44. Di Paolo G, Kim T-W. Linking lipids to Alzheimer's disease: cholesterol and beyond. *Nat Rev Neurosci.* (2011) 12:284–96. doi: 10.1038/nrn3012

45. Penke B, Paragi G, Gera J, Berkecz R, Kovács Z, Crul T, et al. The role of lipids and membranes in the pathogenesis of Alzheimer's disease: a comprehensive view. *Curr Alzheimer Res.* (2018) 15:1191–212. doi: 10.2174/1567205015666180911151716

46. Ylilauri MPT, Voutilainen S, Lönnroos E, Virtanen HEK, Tuomainen T-P, Salonen JT, et al. Associations of dietary choline intake with risk of incident dementia and with cognitive performance: the Kuopio Ischaemic Heart Disease Risk Factor Study. *Am J Clin Nutr.* (2019) 110:1416–23. doi: 10.1093/ajcn/nqz148

47. Semba RD. Perspective: the potential role of circulating lysophosphatidylcholine in neuroprotection against Alzheimer disease. *Adv Nutr.* (2020) 11:760–72. doi: 10.1093/advances/nmaa024

48. Peters-Golden M, Brock TG. 5-lipoxygenase and FLAP. *Prostaglandins Leukot Essent Fatty Acids.* (2003) 69:99–109. doi: 10.1016/S0952-3278(03)00070-X

49. Chu J, Praticò D. Involvement of 5-lipoxygenase activating protein in the amyloidotic phenotype of an Alzheimer's disease mouse model. *J Neuroinflammation.* (2012) 9:127. doi: 10.1186/1742-2094-9-127

50. Chu J, Lauretti E, Di Meco A, Praticò D. FLAP pharmacological blockade modulates metabolism of endogenous tau *in vivo*. *Transl Psychiatry.* (2013) 3:e333. doi: 10.1038/tp.2013.106

51. Pascoal TA, Benedet AL, Ashton NJ, Kang MS, Therriault J, Chamoun M, et al. Microglial activation and tau propagate jointly across Braak stages. *Nat Med.* (2021) 27:1592–9. doi: 10.1038/s41591-021-01456-w

52. Dansokho C, Ait Ahmed D, Aid S, Toly-Ndour C, Chaigneau T, Calle V, et al. Regulatory T cells delay disease progression in Alzheimer-like pathology. *Brain.* (2016) 139:1237–51. doi: 10.1093/brain/awv408

53. Katayama H. Anti-interleukin-17A and anti-interleukin-23 antibodies may be effective against Alzheimer's disease: role of neutrophils in the pathogenesis. *Brain Behav.* (2020) 10:e01504. doi: 10.1002/brb3.1504

54. Carlini V, Verduci I, Cianci F, Cannavale G, Fenoglio C, Galimberti D, et al. CLIC1 protein accumulates in circulating monocyte membrane during neurodegeneration. *Int J Mol Sci.* (2020) 21:E1484. doi: 10.3390/ijms21041484

55. Sandin L, Bergkvist L, Nath S, Kielkopf C, Janefjord C, Helmfors L, et al. Beneficial effects of increased lysozyme levels in Alzheimer's disease modelled in *Drosophila melanogaster*. *FEBS J.* (2016) 283:3508–22. doi: 10.1111/febs.13830

56. Yang Y, Tapias V, Acosta D, Xu H, Chen H, Bhawal R, et al. Altered succinylation of mitochondrial proteins, APP and tau in Alzheimer's disease. *Nat Commun.* (2022) 13:159. doi: 10.1038/s41467-021-27572-2

57. Gaggelli E, Kozlowski H, Valensin D, Valensin G. Copper homeostasis and neurodegenerative disorders (Alzheimer's, prion, and Parkinson's diseases and amyotrophic lateral sclerosis). *Chem Rev.* (2006) 106:1995–2044. doi: 10.1021/cr040410w

58. Zhao Y, Long Z, Liu Y, Luo M, Qiu Y, Idris NFB, et al. Dihydroartemisinin ameliorates decreased neuroplasticity-associated proteins and excessive neuronal apoptosis in APP/PS1 mice. *Curr Alzheimer Res.* (*2020*) 17:916–925. doi: 10.2174/1567205017666201215124746

59. Xia L, Pang Y, Li J, Wu B, Du Y, Chen Y, et al. Dihydroartemisinin induces O-GlcNAcylation and improves cognitive function in a mouse model of tauopathy. *J Alzheimers Dis.* (2021) 84:239–48. doi: 10.3233/JAD-210643

60. Gao Y, Cui M, Zhong S, Feng C, Nwobodo AK, Chen B, et al. Dihydroartemisinin ameliorates LPS-induced neuroinflammation by inhibiting the PI3K/AKT pathway. *Metab Brain Dis.* (2020) 35:661–72. doi: 10.1007/s11011-020-00533-2

61. Cao D, Lu H, Lewis TL Li L. Intake of sucrose-sweetened water induces insulin resistance and exacerbates memory deficits and amyloidosis in a transgenic mouse model of Alzheimer disease *. *J Biol Chem.* (2007) 282:36275–82. doi: 10.1074/jbc.M703561200

62. Chen PE, Geballe MT, Stansfeld PJ, Johnston AR, Yuan H, Jacob AL, et al. Structural features of the glutamate binding site in recombinant NR1/NR2A N-methyl-D-aspartate receptors determined by site-directed mutagenesis and molecular modeling. *Mol Pharmacol.* (2005) 67:1470–84. doi: 10.1124/mol.104.008185

63. Kreamer BL, Siegel FL, Gourley GR. A novel inhibitor of beta-glucuronidase: L-aspartic acid. *Pediatr Res.* (2001) 50:460–6. doi: 10.1203/00006450-200110000-00007

64. Qin J, Kunda N, Qiao G, Calata JF, Pardiwala K, Prabhakar BS, et al. Colon cancer cell treatment with rose bengal generates a protective immune response *via* immunogenic cell death. *Cell Death Dis.* (2017) 8:e2584. doi: 10.1038/cddis.2016.473

65. Lee JS, Lee BI, Park CB. Photo-induced inhibition of Alzheimer's β-amyloid aggregation *in vitro* by rose bengal. *Biomaterials.* (2015) 38:43–9. doi: 10.1016/j.biomaterials.2014.10.058

66. Dubey T, Gorantla NV, Chandrashekara KT, Chinnathambi S. Photodynamic exposure of Rose-Bengal inhibits Tau aggregation and modulates cytoskeletal network in neuronal cells. *Sci Rep.* (2020) 10:12380. doi: 10.1038/s41598-020-69403-2

frontiers | Frontiers in Neurology

TYPE Original Research
PUBLISHED 09 March 2023
DOI 10.3389/fneur.2023.1029370

OPEN ACCESS

EDITED BY
Giovanni Rizzo,
IRCCS Institute of Neurological Sciences of Bologna (ISNB), Italy

REVIEWED BY
David James Brooks,
Newcastle University, United Kingdom
Yuriy L. Orlov,
I. M. Sechenov First Moscow State Medical University, Russia
Saivageethi Nuthikattu,
University of California, Davis, United States

*CORRESPONDENCE
Jia-jun Chen
✉ cjj@jlu.edu.cn

SPECIALTY SECTION
This article was submitted to Dementia and Neurodegenerative Diseases, a section of the journal Frontiers in Neurology

RECEIVED 27 August 2022
ACCEPTED 09 February 2023
PUBLISHED 09 March 2023

CITATION
Xu J, Li J, Sun Y-j, Quan W, Liu L, Zhang Q-h, Qin Y-d, Pei X-c, Su H and Chen J-j (2023) Identification of key genes and signaling pathways associated with dementia with Lewy bodies and Parkinson's disease dementia using bioinformatics. *Front. Neurol.* 14:1029370. doi: 10.3389/fneur.2023.1029370

Identification of key genes and signaling pathways associated with dementia with Lewy bodies and Parkinson's disease dementia using bioinformatics

Jing Xu, Jia Li, Ya-juan Sun, Wei Quan, Li Liu, Qing-hui Zhang, Yi-dan Qin, Xiao-chen Pei, Hang Su and Jia-jun Chen*

Department of Neurology, China–Japan Union Hospital of Jilin University, Changchun, Jilin, China

Objective: Dementia with Lewy bodies (DLB) and Parkinson's disease dementia (PDD) are collectively known as Lewy body dementia (LBD). Considering the heterogeneous nature of LBD and the different constellations of symptoms with which patients can present, the exact molecular mechanism underlying the differences between these two isoforms is still unknown. Therefore, this study aimed to explore the biomarkers and potential mechanisms that distinguish between PDD and DLB.

Methods: The mRNA expression profile dataset of GSE150696 was acquired from the Gene Expression Omnibus (GEO) database. Differentially expressed genes (DEGs) between 12 DLB and 12 PDD were identified from Brodmann area 9 of human postmortem brains using GEO2R. A series of bioinformatics methods were applied to identify the potential signaling pathways involved, and a protein–protein interaction (PPI) network was constructed. Weighted gene co-expression network analysis (WGCNA) was used to further investigate the relationship between gene co-expression and different LBD subtypes. Hub genes that are strongly associated with PDD and DLB were obtained from the intersection of DEGs and selected modules by WGCNA.

Results: A total of 1,864 DEGs between PDD and DLB were filtered by the online analysis tool GEO2R. We found that the most significant GO- and KEGG-enriched terms are involved in the establishment of the vesicle localization and pathways of neurodegeneration-multiple diseases. Glycerolipid metabolism and viral myocarditis were enriched in the PDD group. A B-cell receptor signaling pathway and one carbon pool by folate correlated with DLB in the results obtained from the GSEA. We found several clusters of co-expressed genes which we designated by colors in our WGCNA analysis. Furthermore, we identified seven upregulated genes, namely, SNAP25, GRIN2A, GABRG2, GABRA1, GRIA1, SLC17A6, and SYN1, which are significantly correlated with PDD.

Conclusion: The seven hub genes and the signaling pathways we identified may be involved in the heterogeneous pathogenesis of PDD and DLB.

KEYWORDS

Lewy body dementias, dementia with Lewy bodies, Parkinson's disease dementia, weighted gene co-expression network analysis, hub gene, biomarker

1. Introduction

Lewy body dementia (LBD) is the second most prevalent form of neurodegenerative dementia after Alzheimer's disease (AD) in patients older than 65 years (1). Parkinson's disease dementia (PDD) and dementia with Lewy bodies (DLB), collectively known as LBD, are synucleinopathies morphologically characterized by neuronal loss, inclusions containing Lewy body/α-synuclein and β-amyloid, and tau pathologies, often reported as part of the same spectrum (2, 3). Cognitive decline in the LBD may, in part, be due to a general loss of synapses and related functional failure (4, 5). There is an average of 30–40% loss of synapses in the frontal and the temporal cortex in DLB (6), and in PDD, a reduction of the synaptophysin immunoreactivity of the cortical neuropil was 8.2% (7). Synaptic functional failure happens in the early stages of synucleinopathies due to altered transport of vesicles, synaptic proteins, and mitochondria, which lead to presynaptic terminal loss, dendritic damage, axonal dystrophy, and eventually degeneration of selective neuronal populations within the striatonigral and cortico-limbic systems, among others (6). Clinical distinctions between the two refer to the "so-called 1-year rule" (1, 8, 9), that is, the term DLB is used if dementia occurs before or concurrently with parkinsonism or within 1 year of onset of the motor symptoms; PDD describes dementia starting 1 year or more after Parkinson's disease (PD) becomes well-established (1). This mode of distinction is clearly arbitrary and based on the distinction between the time of onset of cognitive and motor symptoms (3). The mechanisms underlying these differences in clinical manifestations are unclear, and it is necessary to explore the mechanisms by which differences occur to differentiate from the early stages of the disease or even from differences at the genetic or molecular level, and hopefully to provide targeted treatments for these differences. Therefore, it is important to further study the differences in the pathogenesis between the two dementias (10). To this end, we used bioinformatics methods to delve deep into the mechanisms of their heterogeneity.

2. Materials and methods

2.1. Data source

Gene expression datasets were obtained from the GEO database. After a careful review of the datasets, we chose the series of mRNA expression profile datasets of GSE150696 (https://www.ncbi.nlm.nih.gov/geo/query/acc.cgi?acc=GSE150696) (11). Consensus criteria used for clinical diagnoses of PDD and DLB with neuropathologic confirmation have been previously described in detail (12). The samples processed in each group were matched for age, sex, and postmortem interval. The Brodmann area 9 from human postmortem brains was chosen for analysis. A total of 12 (6 women/6 men) PDD samples and 12 (6 women/6 men) DLB samples were retrieved from GSE150696 and published on 24 May 2021. All brain samples were provided by the Brains for Dementia Research, UK. Data were freely available online, and our study did not involve any experiments in the lab performed by any of the authors.

2.2. Data processing of differentially expressed genes

The GEO2R online analysis tool (https://www.ncbi.nlm.nih.gov/geo/geo2r/) was used to detect differentially expressed genes (DEGs) between PDD and DLB samples, and the *P*-value and |log (FC)| (FC-fold change) were calculated. Genes that met the cutoff criteria, $P < 0.05$ and $|\log FC| \geq 1.0$, were considered DEGs (11). Genes with $P < 0.05$ and $\log FC \geq 1.0$ were considered upregulated genes, and genes with $P < 0.05$ and $\log FC \leq -1.0$ were considered downregulated genes (11). GraphPad Prism 9 (GraphPad Software, San Diego, CA, USA; www.graphpad.com), graphing software that can perform data analysis and data visualization, was used to visualize volcano maps of all identified DEGs and a heat map of the top 50 genes (11).

2.3. GO and KEGG pathway analysis

The R software (version 4.2.1) was used for the GO annotation, the KEGG pathway enrichment analysis, and the visualization of DEGs (13). An online analysis tool Metascape website (http://metascape.org) was used for GO and KEGG analyses of gene modules selected by weighted gene co-expression network analysis (WGCNA) (14).

2.4. Gene set enrichment analysis

Gene Set Enrichment Analysis (GSEA) is a promising and widely used software package (15) that derives gene sets to find the different biological functions of the whole genes between PDD and DLB. The potential contribution of the whole altered genes to LBD was explored using the GSEA software (version 4.2.3). A normalized enrichment score (NES) was calculated, and NES is the enrichment score for the gene set after it has been normalized across analyzed gene sets. The gene set was deemed to be significantly enriched when the *P*-value was <5% and |NES| was >1 for each analysis (16).

2.5. Weighted gene co-expression network analysis

Weighted gene co-expression network analysis (WGCNA) can cluster genes with higher co-expression levels, assemble them into modules, and establish connections between their modules and phenotypes to find the hub genes of the phenotype. We selected a WGCNA package of the R software to filter the top 6,000 median absolute deviation genes to construct a representation matrix and the scale-free network (17). The β-value was selected as long as R^2 was >0.8. The β-value was a soft threshold. The algorithm introduces an approximate scale-free topology to accurately calculate the soft threshold and then replaces the hard threshold of the previous traditional algorithm; Scale-free topologies are more realistic when compared with random networks (18). Based on the selected soft threshold, network

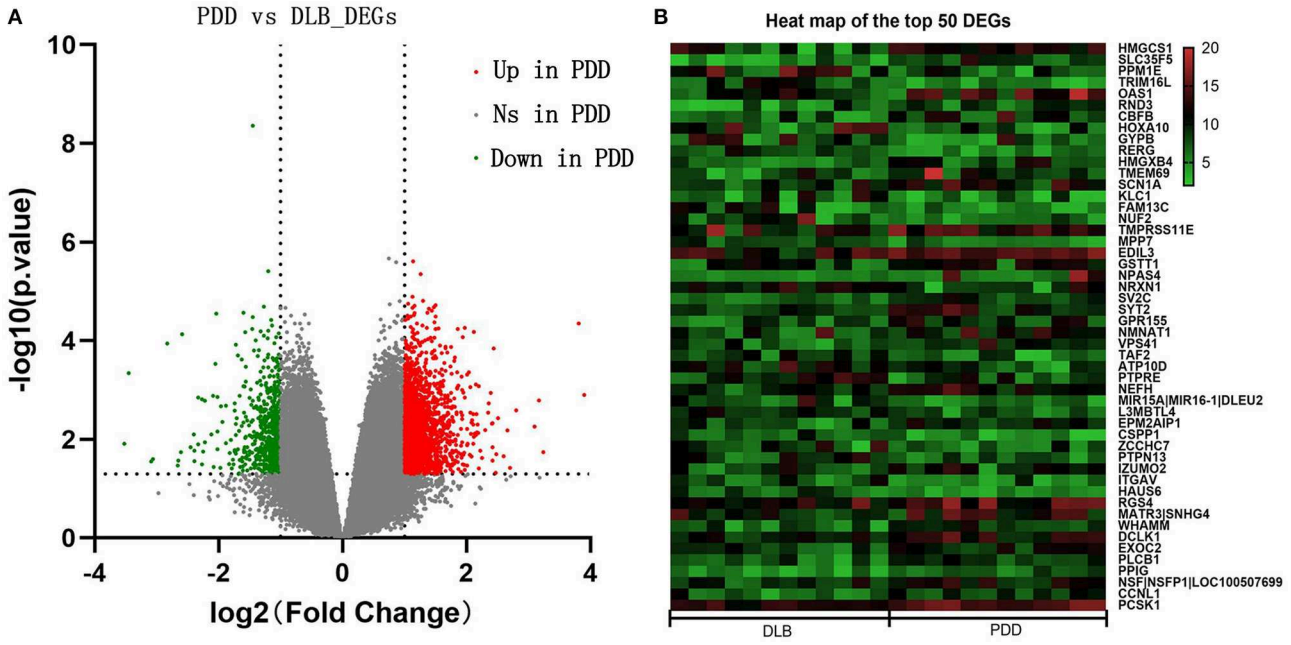

FIGURE 1
(A) Volcano maps of all differentially expressed genes (DEGs) between Parkinson's disease dementia (PDD) and Dementia with Lewy bodies (DLB). The red color represents upregulated genes, and the green color represents downregulated genes in PDD; gray represents genes that are not differentially expressed. The dashed horizontal and vertical axes indicate the log fold change absolute threshold of 1 and the *P*-value threshold of 0.05, respectively. **(B)** Heat map of the top 50 DEGs. The color gradient from green to red indicates gene regulation from downregulation to upregulation in PDD or DLB. Numbers 5–20 indicate gene expression levels.

modules were constructed by clustering the gene topology matrix using the dynamic shear tree algorithm. The minimum number of genes included in the network module was set to 20. The module color was established by using the degree of dissimilarity automatically by WGCNA software (18). The relationships between modules and LBD haplotypes are shown with a heatmap. We measured the module membership (mM) and gene significance (GS) of individual genes, and the hub genes in the selected modules with |mM| >0.8 and |GS| >0.2 were screened for further analysis (19, 20).

2.6. Protein–protein interaction network construction and hub gene identification

We used the online Search Tool for the Retrieval of Interacting Genes database tool (STRING-DB) (http://string-db.org/) to analyze protein–protein interaction (PPI) information (21). PPI pairs were extracted with a combined score of >0.4, and the results were calculated with their automatically cited parameters. Subsequently, the PPI network was visualized using the CytoHubba plug-in in Cytoscape software (version 3.9.1; https://www.cytoscape.org/) was used to calculate the degree of each protein node (11). We considered the top 30 identified genes as the hub genes in our study. Finally, we screened the hub genes by intersecting them in the selected modules, mentioned earlier, and in the DEG-PPI network.

3. Results

3.1. Identification of DEGs

The samples of PDD and DLB obtained from Brodmann area 9 of postmortem brains were selected for the present study from the GSE150696 series. On the basis of the criteria of $P < 0.05$ and $|\log FC| \geq 1.0$, 1,864 DEGs between PDD and DLB were filtered by the online analysis tool GEO2R. It included 1240 upregulated and 624 downregulated DEGs in patients with PDD (Supplementary Table S1). A volcano map of all identified DEGs is shown in Figure 1A. In addition, a heat map of the top 50 DEGs is shown in Figure 1B.

3.2. Functional and pathway enrichment

3.2.1. Analyses for DEGs

The GO and KEGG enrichment analyses were performed on 1,864 DEGs between PDD and DLB, and the findings were visualized with the cluster profiler package of R software (22). The mainly enriched biological process of GO analysis included the establishment of vesicle localization, vesicle-mediated transport in the synapse, and learning and memory. The cellular component of GO analysis included the presynapse axon part and the glutamatergic synapse. The molecular function of GO analysis included ATPase activity and motor activity (Figure 2A). The results of GO analysis of up and down DEGs between PDD and DLB are shown in Supplementary Figures S1A, S2. In addition,

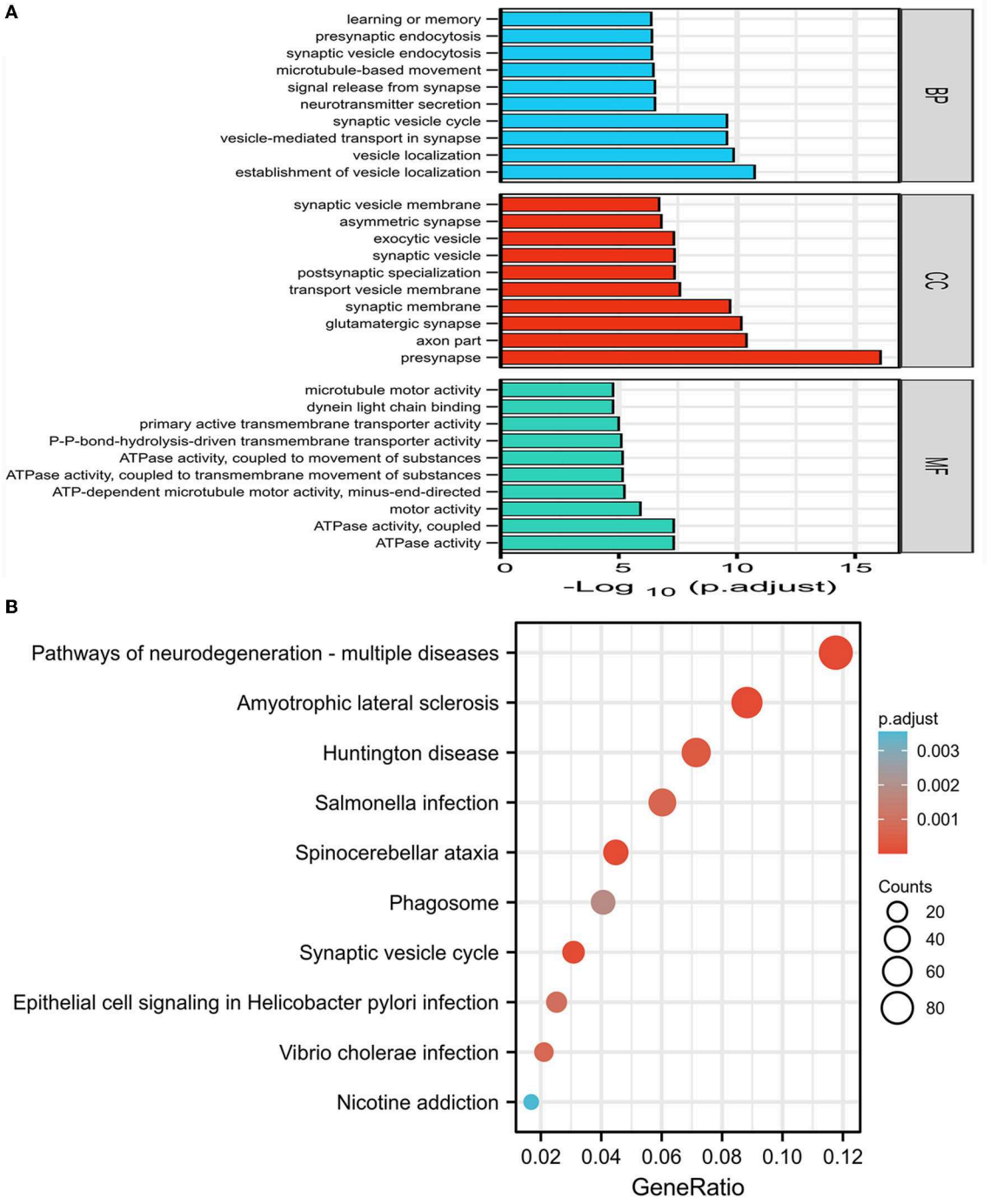

FIGURE 2
(A) The results of gene ontology (GO) enrichment categories of the DEGs for both Parkinson's disease dementia (PDD) and Dementia with Lewy bodies (DLB) groups including biological process (BP), cellular component (CC), and molecular function (MF). **(B)** The results of the Kyoto encyclopedia of genes and genomes (KEGG) pathway enrichment analyses of the DEGs for both PDD and DLB, the abscissa represents GeneRatio (the number of genes enriched in this KEGG entry/the total number of genes), and the ordinate represents KEGG terms. P-adjust refers to the *P*-value after correction, the darker the red color, the greater the correlation. Counts refer to the number of genes enriched in this KEGG entry, the larger the circle, the more the number of genes.

the results of the KEGG pathway analysis showed that DEGs were mainly enriched in pathways in neurodegeneration-multiple diseases, Amyotrophic lateral sclerosis, and Huntington's disease (Figure 2B). The results of the KEGG pathway enrichment analysis in up DEGs are shown in Supplementary Figure S1B (down DEGs were not enriched by the corresponding KEGG pathway).

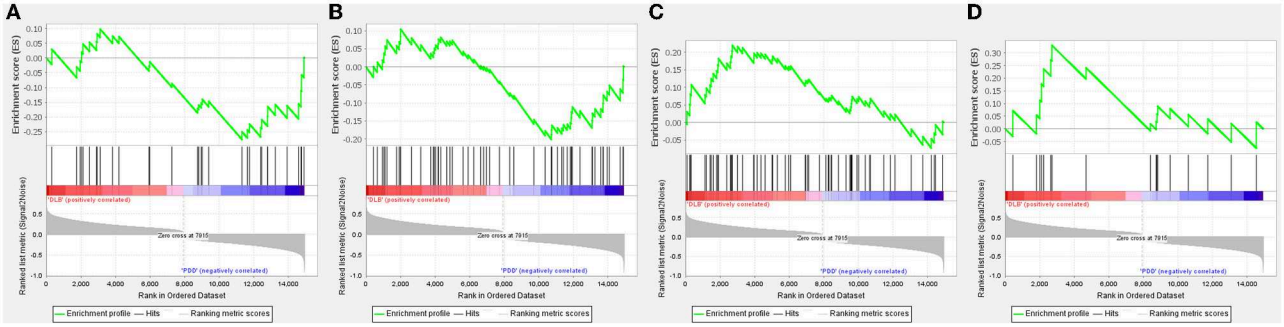

FIGURE 3
Gene set enrichment analysis (GSEA) plots of the most enriched gene sets in the Parkinson's disease dementia (PDD) and Dementia with Lewy bodies (DLB) groups. The enriched pathways positively correlated with PDD: **(A)** glycerolipid metabolism; **(B)** viral myocarditis. The enriched pathways positively correlated with DLB: **(C)** One carbon pool by folate; **(D)** B-cell receptor signaling pathway.

3.2.2. Gene set enrichment analysis

The GSEA analysis was used to filter unique pathways involved in the pathogenesis of PDD or DLB. When the green line plot was in the negative direction, the gene on the right side of the maximum enrichment score value was the core gene, the pathway was positively correlated with the PDD group, contrarily, the pathway was positively correlated with the DLB group. As shown in Figures 3A–D, the pathways of glycerolipid metabolism and viral myocarditis were positively correlated with the PDD group. The pathways of the B-cell receptor signaling pathway and one carbon pool by folate signaling pathways were positively correlated with the DLB group.

3.3. Weighted gene co-expression network analysis

We used WGCNA software to identify the associations between the key gene modules related to PDD and DLB. As shown in Figures 4A, B, the power was set as 6 for further analysis and satisfied the scale-free co-expression network relationships, with the mean value of the adjacency function gradually approaching 0. According to the module-trait relationships, eight modules were identified by the average linkage hierarchical clustering method from the co-expression network, and the colors were defined by the software automatically (Figure 4C). Based on the correlation between different modules and subtypes of LBD shown in the heatmap, we found the green module was significantly positively associated with the PDD group (cor = 0.75, P-value < 0.01); the yellow module was significantly positively associated with the DLB group (cor = 0.75, P-value < 0.01) (Figure 4D); and the gray module represented genes that were not assigned to each network. Other modules such as black, turquoise, red, brown, and blue also suggest a clear correlation.

3.4. Enrichment analyses of module genes identified by WGCNA

We used the Metascape tool to perform GO annotation and KEGG pathway enrichment analyses to analyze the features of the module genes. The number of genes within the blue and yellow modules was 2,530 and 182, respectively. As shown in Figures 5A, C, genes in the blue module were mainly involved in the axon, postsynapse, presynapse, neuron projection development, and pathways of multiple neurodegenerative diseases. Genes in the yellow module (Figures 5B, D) were mainly involved in the positive regulation of macrophage activation, integrin binding, side of membrane, and cellular response to hepatocyte growth factor stimulus. The results of GO and KEGG pathway enrichment analyses with regard to the green module are shown in Supplementary Figures S3A, B.

3.5. Identification of hub genes

In the present study, because we found there was an ideal overlap in the blue module with the top 30 hub DEGs, the yellow module was significantly positively associated with the DLB group, and we finally chose blue and yellow modules for further study. The scattered plots of blue and yellow modules (Supplementary Figures S4A, B) present significantly positive correlations (P < 0.01) between PDD and DLB. We identified 815 and 3 hub genes in the blue and yellow modules, respectively (Supplementary Table S2). Protein interactions among the 1,864 DEGs were predicted using the STRING-DB tool. The top 30 hub genes in DEGs were evaluated by the maximal clique centrality method with the Cytohubba plugin. The network of the top 30 hub genes and expanded DEGs included 234 nodes and 878 edges, visualized by Cytoscape software (Figure 6A). We intersected the hub genes of the blue module and the top 30 hub genes in DEGs (Figures 6B, C), and we identified seven overlapping hub genes. There was no overlap between the top 30 hub genes in DEGs and the hub genes of the yellow module. As shown in Table 1, the information about these seven overlapping hub genes included in the blue module (*SNAP25, 163 GRIN2A, GABRG2, GABRA1, GRIA1, SLC17A6,* and *SYN1*) is mentioned in more detail.

4. Discussion

The significantly enriched entries for GO and KEGG enrichment analyses demonstrated that the 1,864 DEGs

10.3389/fneur.2023.1029370

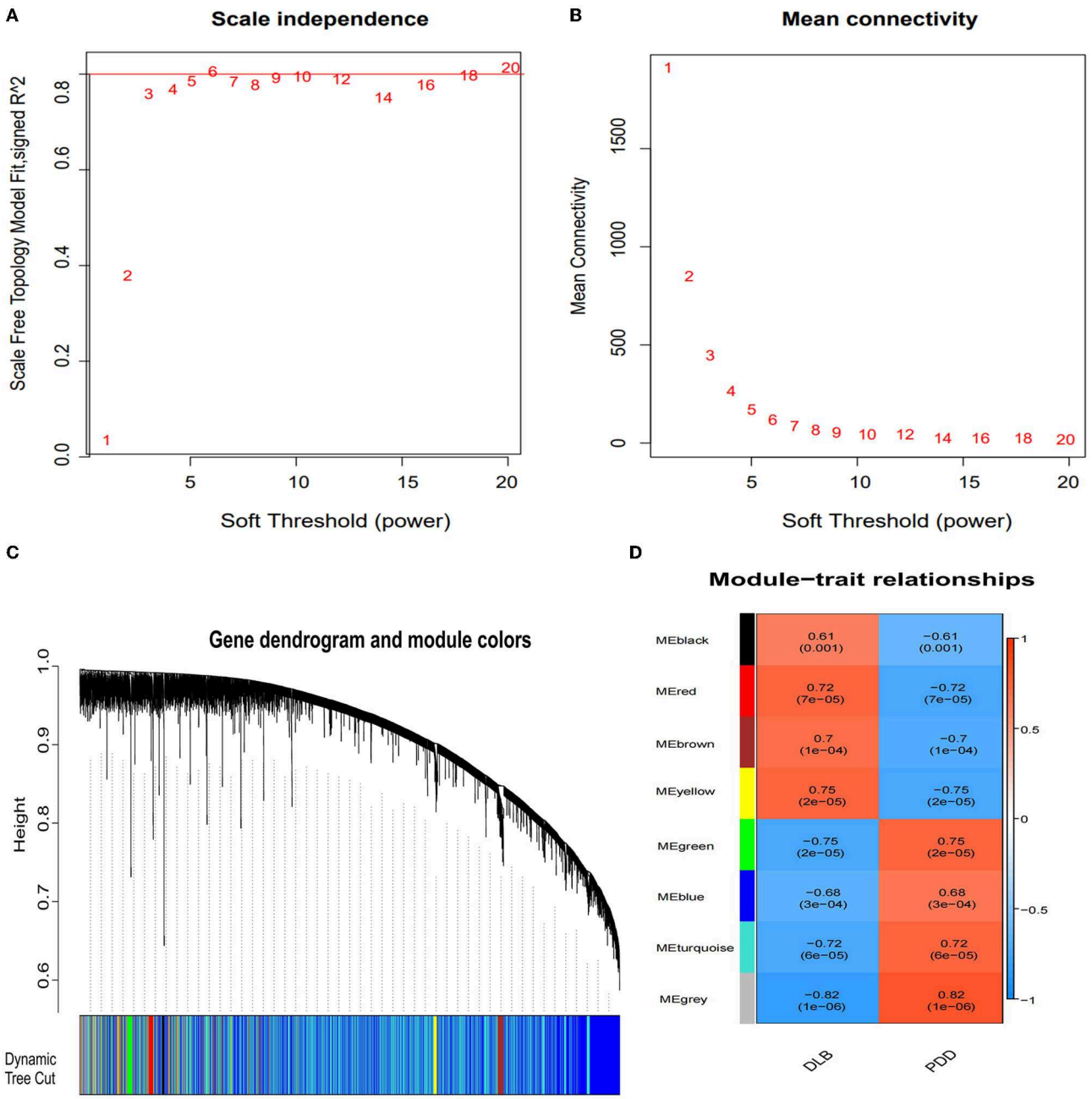

FIGURE 4
Identification of the gene modules related to Parkinson's disease dementia (PDD) and Dementia with Lewy bodies (DLB) by weighted gene co-expression network analysis (WGCNA). **(A)** Determination of the soft threshold in the WGCNA algorithm. The approximate scale-free fit index can be attained at the soft-thresholding power of 6. **(B)** Mean connectivity of various soft-thresholding powers. **(C)** Clustering dendrograms showing eight modules that contain a group of highly connected genes. Each designated color represents a certain gene module. Diverse colors reflect corresponding modules, and the gray module represents genes that are not assigned to each network. **(D)** The heatmap of the relationship between each gene module and each subtype of LBD. The red color represents a positive correlation, while the blue color represents a negative correlation. Each cell contains the corresponding correlation and *P*-value.

mainly enriched the functions of vesicles and synapses in neurodegenerative diseases. This study supports the mechanistic role of disturbed vesicle trafficking in neurodegenerative diseases (23). Positron emission computed tomography-based study suggests that the loss of synaptic density contributes to dysfunction and cognitive decline in patients with LBD (4). Presynaptic and postsynaptic proteins modulate axonal/dendritic growth and remodeling, thus representing likely key players in the synaptic dysfunction in neurodegenerative diseases (5). Synaptic disruption is a key pathophysiological mechanism leading to neurodegeneration (24). DLB and PDD differ in terms of not only the time of onset of cognitive deficits but also variability in affected functions (2). Patients with DLB present more severe and widespread cognitive dysfunction than those with PDD,

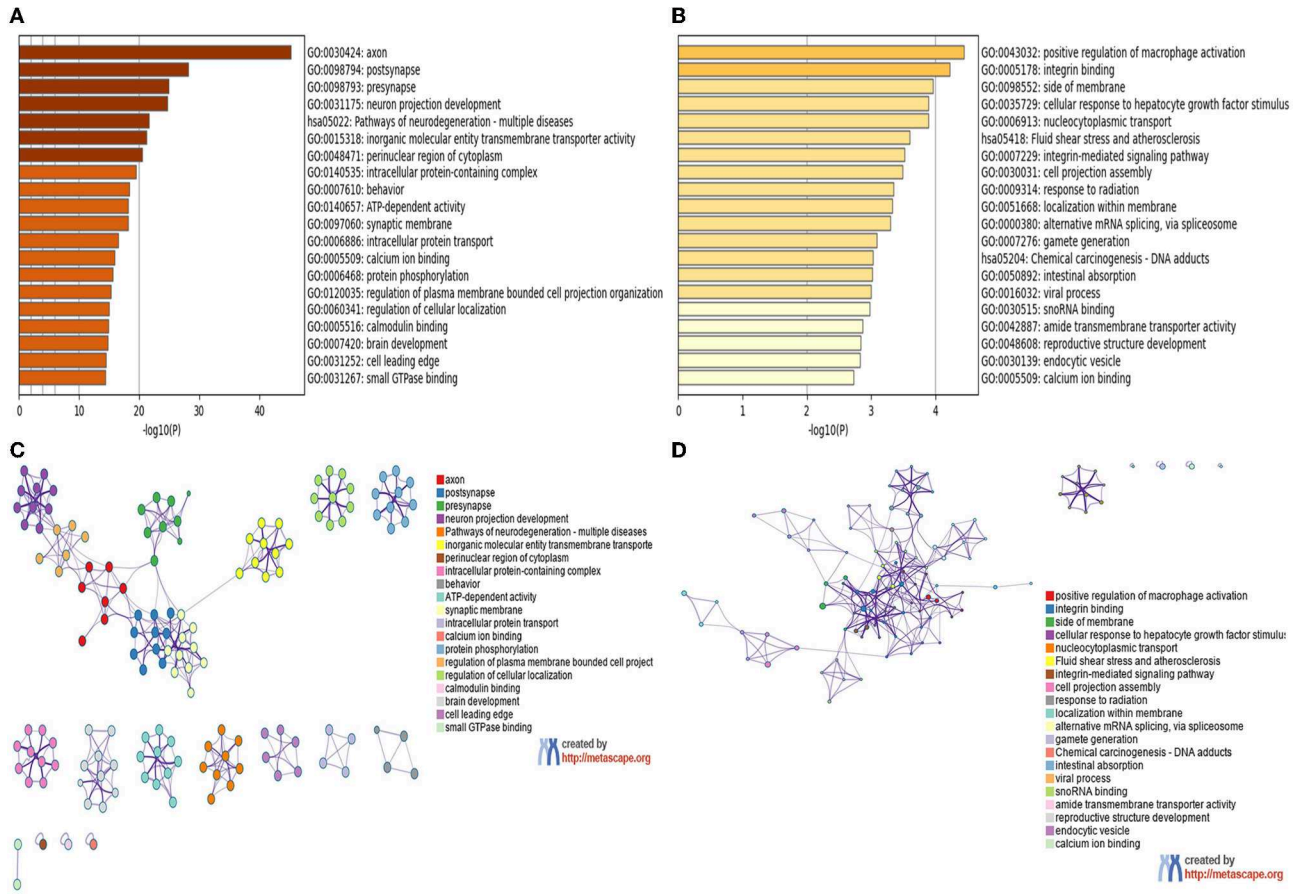

FIGURE 5
GO and KEGG enrichment analyses of module genes recognized by the WGCNA analysis. **(A)** Blue module. **(B)** Yellow module, bar plots colored by *p*-values. **(C)** Blue module. **(D)** Yellow module, Networks colored by genes.

particularly in attentive and visuospatial domains, executive functions, constructional tasks (25, 26), and episodic verbal memory (27). Hence, the Mini-Mental State Examination score is lower in patients with DLB than in those with PDD (28). The percentage of patients with DLB who fail to finish the Montreal Cognitive Assessment subitem analysis on the Digit Span Forward was higher than that of patients with PDD, possibly because the former is associated with a more severe attentive deficit than the latter (2). This may explain the enrichment of DEGs.

Due to acting in contrast to each other, DLB and PDD have opposite correlations to enriched pathways as shown in Figure 3. The GSEA data suggested that glycerolipid metabolism and viral myocarditis were positively correlated with PDD. Lipid metabolic dysregulation is involved in the pathogenesis of PDD; α-synuclein may induce dementia in patients with PD possibly through lipid metabolism (29). Coxsackievirus B3 is considered the dominant etiological agent of viral myocarditis. Coxsackievirus B3 infection can induce α-synuclein-associated inclusion body formation in neurons, which might act as a trigger for PD. Transgenic mice that express α-synuclein showed enhanced Coxsackievirus B3 replication and exhibited dopaminergic neuronal death in the substantia nigra (30). A B-cell receptor signaling pathway and one carbon pool by folate signaling pathways were positively correlated with the DLB subset. Accumulating evidence suggests the involvement of immune mediators in DLB (31, 32). Immunization of mice with different B-cell epitopes of human α-synuclein vaccines produced high titers of anti-human α-synuclein antibodies that bound to Lewy bodies and Lewy neurites in the brain tissue of patients with DLB and induced robust helper T-cell expression. Immunotherapeutic approaches that reduce α-synuclein deposits may provide therapeutic benefits for patients with DLB (33). Folate is an essential factor involved in nucleotide synthesis, one-carbon metabolism, and DNA methylation, which have been linked to cognitive impairment and dementia (34). Homocysteine is a central metabolite formed as an intermediate product of one-carbon metabolism, following transmethylation (35). Elevated plasma total homocysteine levels were independently associated with DLB (34).

To further investigate the relationship between co-expressed genes and different LBD subtypes, we performed WGCNA. The results of enrichment for the blue module included axon, postsynapse, presynapse, and neuron projection development. Axonal and synaptic pathology is an important feature of LBD (36). During the early prodromal phase of PD, synaptic alterations happen before cell death, and these alterations are linked to the synaptic accumulation of toxic α-synuclein, specifically in the presynaptic terminals, which affects neurotransmitter release (37).

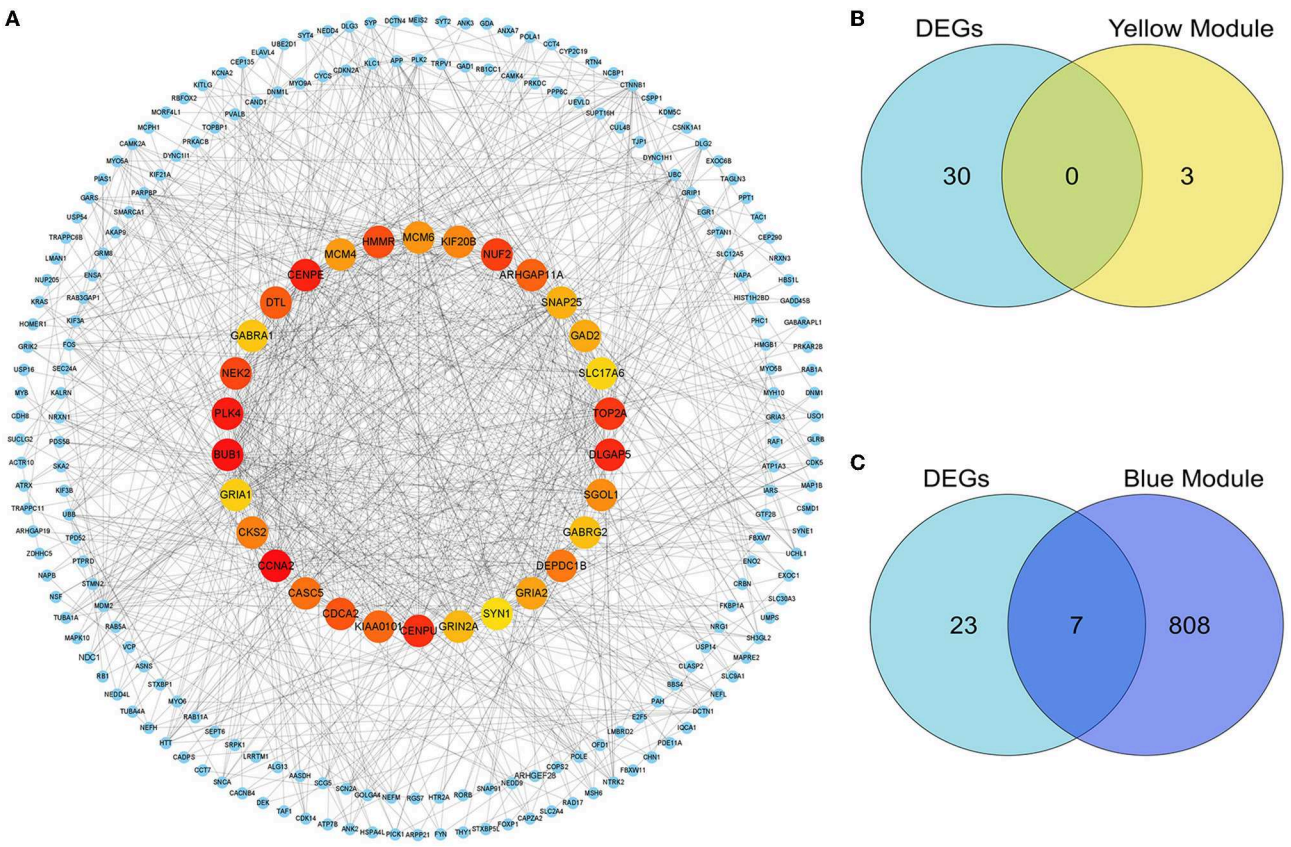

FIGURE 6
Identification of the hub genes and key genes. The PPI network of the DEGs. **(A)** The top 30 hub genes among DEGs were confirmed with the Cytohubba plugin. The colors of the nodes reflect the degree of connectivity, the darker the yellow color, the more obvious the connectivity is. The key genes are defined as the hub genes identified by both the DEG-PPI network and the WGCNA method. **(B)** The hub genes in DEGs and the yellow module are shown using a Venn diagram. No key genes were identified. **(C)** The hub genes in DEGs and the blue module are shown using a Venn diagram. Seven key genes were identified.

Generalized synaptic degeneration and loss of synaptic density and connectivity may contribute to dysfunction and cognitive decline in patients with neurodegenerative diseases (4, 5, 38). Reduced expression of synaptic proteins could be an index of the degree of synaptic degeneration in the central nervous system (38). Synaptic proteins reliably discriminated PDD and DLB from controls with high sensitivity and specificity (39). The particular synaptic proteins have an important predictive and discriminative molecular fingerprint in neurodegenerative diseases and could be a potential target for early disease intervention (39). The results of the enrichment for the yellow module included positive regulation of macrophage activation and integrin binding. α-synuclein expressed in neurons is released into the extracellular space and taken up by macrophages and microglia; α-synuclein fibrils are considered to be formed from monomers in macrophages and to spread to neurons to induce α-synuclein aggregation in PD model (40). Our data support the difference among axonal and synaptic, inflammation, and neurodegeneration-multiple diseases.

After taking the intersection of the top 30 hub genes of DEGs and the hub genes in blue modules, seven key genes were identified, including *SNAP25, GRIN2A, GABRG2, GABRA1, GRIA1, SLC17A6,* and *SYN1*. *SNAP25* and *SYN1* as presynaptic proteins are markers of functional synapses (38, 41, 42). *SYN1* is a phosphoprotein that coats the cytoplasmic side of synaptic vesicles and regulates their trafficking within nerve terminals. Inhibition or knockout of *SYN1* can reduce the density of excitatory and inhibitory synapses and impair both glutamatergic and GABAergic synaptic transmission (43). *SNAP25* is a key adhesion molecule for vesicle docking, trafficking, fusion of membranes, and exocytosis, and it has also been implicated in axonal outgrowth and neurite elongation (5). It has been suggested that *SNAP25* could be an effective and accessible biomarker reflecting synaptic integrity and degeneration in the brain (38, 44). In previous studies, *SNAP25* levels were negatively correlated with cognitive functions (38), and *SNAP25* expression was low in patients with PDD and DLB; however, the decrease was more pronounced in the DLB patient group (45), which is consistent with our study so that *SNAP25* is a known gene that is more relevant to LBD (44). The *GRIN2A* gene encodes a member of the glutamate-gated ion channel protein family. *GRIN2A* was found to play important roles not only in synaptic plasticity but also in learning and memory (46), and spatial or discrimination learning impairments have been observed in mice with *GRIN2A* subunit knockout (47, 48). Studies have also shown that the suppression of *GRIN2A* expression impairs

TABLE 1 The information on seven key genes.

Symbols	Full name	logFC	*P*-value	Change	MM	GS	Module
SNAP25	synaptosome associated protein 25	1.37	0.02310	UP	0.916355	0.431507	Blue
GRIN2A	glutamate ionotropic receptor NMDA type subunit 2A	1.46	0.01190	UP	0.938563	0.472282	Blue
GABRG2	gamma-aminobutyric acid type A receptor subunit gamma2	1.63	0.00386	UP	0.937568	0.532672	Blue
GABRA1	gamma-aminobutyric acid type A receptor subunit alpha1	2.12	0.00895	UP	0.922775	0.487116	Blue
GRIA1	glutamate ionotropic receptor AMPA type subunit 1	1.02	0.00722	UP	0.806288	0.505067	Blue
SLC17A6	solute carrier family 17 member 6	1.82	0.00997	UP	0.864285	0.481604	Blue
SYN1	synapsin I	1.09	0.04010	UP	0.876074	0.394251	Blue

Seven key genes were obtained from the intersection of 30 identified genes in 1,864 differentially expressed genes and 815 hub genes in the blue module. The seven key genes were upregulated in the Parkinson's disease dementia group.

the learning of complex motor skills (49). Dendritic branch pruning along with maturation is accompanied by an elevation in *GRIN2A* levels (50). *GRIN2A* deletion was shown to decrease the total dendritic length and dendritic complexity in the dentate gyrus neurons of the hippocampus located in the inner granular zone (51).

GRIA1 is a subunit in the α-amino-3-hydroxy-5-methylisoxazole-4-propionic acid subtype of ionotropic glutamate receptors, which is a primary receptor that mediates excitatory synaptic transmission at glutamatergic synapses in the central nervous system and plays key roles in synaptic plasticity, neuronal development, and neurological diseases (52). The α-amino-3-hydroxy-5-methylisoxazole-4-propionic acid subtype of ionotropic glutamate receptors mediates most of the fast postsynaptic responses at glutamatergic synapses (53). Synaptic plasticity relies on the normal integration of glutamate receptors at the postsynaptic density (54). The increased translation of *GRIA1* facilitates certain forms of hippocampus-dependent synaptic plasticity and memory (55–57). GO biological process enrichment analysis showed that *SNAP25, GRIN2A, GRIA1,* and *SYN1* were significantly enriched in learning and memory in our study, further suggesting that they participate in the neurobiological basis of pathogenesis by affecting synapse function. KEGG enrichment analysis of DEGs showed that *SNAP25* and *SLC17A6* were enriched in the synaptic vesicle cycle in our study. *SLC17A6* is responsible for the uploading of glutamate into presynaptic vesicles, while *SLC17A6* is utilized by a majority of cortical and subcortical glutamatergic excitatory neurons (58, 59). Kashani et al. observed that *SLC17A6* downregulation was correlated with the degree of cognitive impairment in Brodmann area 9 in patients with Alzheimer's disease (60); the lower the decline in *SLC17A6* expression, the greater the degree of cognitive impairment. Studies suggest that patients with DLB present more severe and widespread cognitive dysfunction than those with PDD (25–27). Consistent with the conclusions of our study, *GRIA1, GRIN2A,* and *SLC17A6* expressions were more upregulated in patients with PDD than in those with DLB, further genetically explaining the cognitive dysfunction is graver in patients with DLB than in those with PDD. The *GABRA1* and *GABRG2* genes encode subunits of the γ-aminobutyric acid (GABA) type A receptor family (61). *GABRA1* was found to be significantly more downregulated in the postmortem frontal cortices of patients with DLB than in those with neuropathological examination normal control (62). Similarly, *GABRG2* expression was found to be significantly low in symptomatic mouse models of tauopathy (63). Both play an important role in the maintenance of normal synaptic function. RNA-sequencing analysis of mutation of *GABRA1* in zebrafish larval brains identified a marked downregulation of genes encoding inhibitory synaptic components as well as proteins involved in axon guidance. Immunocytochemical analysis revealed a marked decrease in the accumulation of GABA synaptic markers; consistently, transgene *GABRG2* mutation resulted in postsynaptic and presynaptic defects (64, 65). *GABRG2* was found to be associated with suicidal behavior and major depressive disorder (66). Studies indicated that low brain levels of GABA may be related to schizophrenia and psychosis (67–69). Fluctuations in core clinical features of DLB are typically delirium-like, occurring as spontaneous alterations in cognition, attention, and arousal (70), which is different from PDD; similarly, in our study, *GABRA1* and *GABRG2* genes were downregulated in DLB.

These findings suggest the potential roles of *SNAP25, GRIN2A, GABRG2, GABRA1, GRIA1, SLC17A6,* and *SYN1* as biomarkers to distinguish PDD from DLB. The function of the seven hub genes participated in the neurobiological basis of pathogenesis by affecting synaptic function and the GABAergic/glutamatergic neurotransmitters. GO enrichment analysis showed that *SNAP25 was* the core gene participating in the neurobiological basis of pathogenesis by affecting synapse function in our study; KEGG enrichment analysis of DEGs showed that *SNAP25* was enriched in the synaptic vesicle cycle. *SNAP25* may be a more significant gene distinguishing between PDD and DLB by the affected synaptic vesicle cycle. In addition, *GRIN2A, GABRG2, GABRA1, GRIA1,* and *SYN1* are involved in regulated GABAergic/glutamatergic functions. Hence, synaptic transmission impairment and GABAergic/glutamatergic dysfunction may be the more outstanding difference between PDD and DLB.

5. Supplementary content

We also constructed sets of gene maps based on the online resource OMIM.org (https://omim.org/) (71) associated with DLB and PDD, compared the two lists of gene maps with the top 30 hub genes in DEGs and hub genes in the blue module, respectively, the results suggested that the three lists had no intersection. There were 15 (*GDAP1, ATP1A1, DNAJC6, SNCA, TUBA4A, VCP, GYG1, TRIM2, BMPR2, NEFL, C9orf72, DHX16, FIG4,* and *COPA*) overlap hub genes with the blue module and gene map in

PDD (Supplementary Figure S5A; Supplementary Table S3), there were four (*CAMTA1, EXOC6B, ATP6V1B1,* and *SFPQ*) overlap hub genes with the blue module and gene map in DLB (Supplementary Figure S5B; Supplementary Table S4).

Data availability statement

The original contributions presented in the study are included in the article/Supplementary material, further inquiries can be directed to the corresponding author.

Ethics statement

Ethical review and approval was not required for the study on human participants in accordance with the local legislation and institutional requirements. Written informed consent from the patients/participants or patients/participants' legal guardian/next of kin was not required to participate in this study in accordance with the national legislation and the institutional requirements.

Author contributions

J-jC was the senior author of the report. JX made the material preparation and the first draft of the manuscript. All authors contributed to the study's conception, design, read, and approved the final manuscript.

Funding

This study was supported by the Jilin Science and Technology Department Project (nos. 20200602045ZP and 20200201451JC).

Acknowledgments

We sincerely thank Dr. Tan MG and colleagues for sharing their data in the GEO database. We would like to thank Editage (www.editage.cn) for English language editing.

Conflict of interest

The authors declare that the research was conducted in the absence of any commercial or financial relationships that could be construed as a potential conflict of interest.

Publisher's note

All claims expressed in this article are solely those of the authors and do not necessarily represent those of their affiliated organizations, or those of the publisher, the editors and the reviewers. Any product that may be evaluated in this article, or claim that may be made by its manufacturer, is not guaranteed or endorsed by the publisher.

Supplementary material

The Supplementary Material for this article can be found online at: https://www.frontiersin.org/articles/10.3389/fneur.2023.1029370/full#supplementary-material

References

1. Walker Z, Possin KL, Boeve BF, Aarsland D. Lewy body dementias. *Lancet.* (2015) 386:1683–97. doi: 10.1016/S0140-6736(15)00462-6

2. Martini A, Weis L, Schifano R, Pistonesi F, Fiorenzato E, Antonini A, et al. Differences in cognitive profiles between Lewy body and Parkinson's disease dementia. *J Neural Transm.* (2020) 127:323–30. doi: 10.1007/s00702-019-02129-2

3. Jellinger KA. Dementia with Lewy bodies and Parkinson's disease-dementia: current concepts and controversies. *J Neural Transm (Vienna).* (2018) 125:615–50. doi: 10.1007/s00702-017-1821-9

4. Andersen KB, Hansen AK, Damholdt MF, Horsager J, Skjaerbaek C, Gottrup H, et al. Reduced synaptic density in patients with lewy body dementia: an [11 C]UCB-J PET imaging study. *Mov Disord.* (2021) 36:2057–65. doi: 10.1002/mds.28617

5. Mazzucchi S, Palermo G, Campese N, Galgani A, Della Vecchia A, Vergallo A, et al. The role of synaptic biomarkers in the spectrum of neurodegenerative diseases. *Expert Rev Proteomics.* (2020) 17:543–59. doi: 10.1080/14789450.2020.1831388

6. Overk CR, Masliah, E. Pathogenesis of synaptic degeneration in Alzheimer's disease and Lewy body disease. *Biochem Pharmacol.* (2014) 88:508–16. doi: 10.1016/j.bcp.2014.01.015

7. Zhan SS, Beyreuther K, Schmitt HP. Quantitative assessment of the synaptophysin immuno-reactivity of the cortical neuropil in various neurodegenerative disorders with dementia. *Dementia.* (1993) 4:66–74. doi: 10.1159/000107299

8. Taylor JP, McKeith IG, Burn DJ, Boeve BF, Weintraub D, Bamford C, et al. New evidence on the management of Lewy body dementia. *Lancet Neurol.* (2020) 19:157–69. doi: 10.1016/S1474-4422(19)30153-X

9. Low C, Lee JH, Lim F, Lee C, Ballard C, Francis PT, et al. Isoform-specific upregulation of FynT kinase expression is associated with tauopathy and glial activation in Alzheimer's disease and Lewy body dementias. *Brain Pathol.* (2021) 31:253–66. doi: 10.1111/bpa.12917

10. Rajkumar AP, Bidkhori G, Shoaie S, Clarke E, Morrin H, Hye A, et al. Postmortem cortical transcriptomics of lewy body dementia reveal mitochondrial dysfunction and lack of neuroinflammation. *Am J Geriatr Psychiatry.* (2019) 28:75–86. doi: 10.1016/j.jagp.06, 007.

11. Quan W, Li J, Jin X, Liu L, Zhang Q, Qin Y, et al. Identification of potential core genes in parkinson's disease using bioinformatics analysis. *Parkinsons Dis.* (2021) 1690341. doi: 10.1155./2021/1690341

12. Chai YL, Chong JR, Weng J, Howlett D, Halsey A, Lee JH, et al. Lysosomal cathepsin D is upregulated in Alzheimer's disease neocortex and may be a marker for neurofibrillary degeneration. *Brain Pathol.* (2019) 29:63–74. doi: 10.1111/bpa.12631

13. Xia P, Chen J, Bai X, Li M, Wang L, Lu Z, et al. Key gene network related to primary ciliary dyskinesia in hippocampus of patients with Alzheimer's disease revealed by weighted gene co-expression network analysis. *BMC Neurol.* (2022) 22:198. doi: 10.1186/s12883-022-02724-z

14. Zhou Y, Zhou B, Pache L, Chang M, Khodabakhshi AH, Tanaseichuk O, et al. Metascape provides a biologist-oriented resource for the analysis of systems-level datasets. *Nat Commun.* (2019) 10:1523. doi: 10.1038/s41467- 019-09234-6

15. Yang X, Li L, Xu C, Pi M, Wang C, Zhang Y, et al. Analysis of the different characteristics between omental preadipocytes and differentiated white adipocytes using bioinformatics methods. *Adipocyte.* (23945) 11:227–38. doi: 10.1080/2162022, 2063471.

16. Subramanian A, Tamayo P, Mootha VK, Mukherjee S, Ebert BL, Gillette MA, et al. Gene set enrichment analysis: a knowledge-based approach for interpreting genome-wide expression profiles. *Proc Natl Acad Sci.* (2005) 102:15545–50. doi: 10.1073/pnas.0506580102

17. Langfelder P, Horvath S. WGCNA: an R package for weighted correlation network analysis. *BMC Bioinform.* (2008) 9:559. doi: 10.1186/1471-2105-9-559

18. Guo Z, Zhang Y, Ming Z, Hao Z, Duan P. Identification of key genes in severe burns by using weighted gene coexpression network analysis. *Comput Math Methods Med.* (2022) 2022:5220403. doi: 10.1155/2022/5220403

19. Zhang R, Chen Y, He J, Gou HY, Zhu YL, Zhu YM, et al. WGCNA combined with GSVA to explore biomarkers of refractory neocortical epilepsy IBRO. *Neurosci Rep.* (2022) 13:314–21. doi: 10.1016/j.ibneur.09010

20. Chen G, Chen D, Feng Y, Wu W, Gao J, Chang C, et al. Identification of key signaling pathways and genes in eosinophilic asthma and neutrophilic asthma by weighted gene co-expression network analysis. *Front Mol Biosci.* (2022) 9:805570. doi: 10.3389/fmolb.2022.805570

21. Szklarczyk D, Gable AL, Nastou KC, Lyon D, Kirsch R, Pyysalo S, et al. The STRING database in 2021: customizable protein-protein networks, and functional characterization of user-uploaded gene/measurement sets. *Nucleic Acids Res.* (2021) 49:D605–12. doi: 10.1093/nar/gkaa1074

22. Yu G, Wang LG, Han Y, He QY. Cluster profiler: an R package for comparing biological themes among gene clusters. *OMICS.* (2012) 16:284–7. doi: 10.1089/omi.2011.0118

23. Grochowska MM, Carreras Mascaro A, Boumeester V, Natale D, Breedveld GJ, Geut H, et al. LRP10 interacts with SORL1 in the intracellular vesicle trafficking pathway in non-neuronal brain cells and localises to Lewy bodies in Parkinson's disease and dementia with Lewy bodies. *Acta Neuropathol.* (2021) 142:117–37. doi: 10.1007/s00401-021-02313-3

24. Jellinger KA, Korczyn AD. Are dementia with Lewy bodies and Parkinson's disease dementia the same disease?. *BMC Med.* (2018) 16:1016. doi: 10.1186./s12916-018-1016-8

25. Petrova M, Mehrabian-Spasova S, Aarsland D, Raycheva M, Traykov L. Clinical and neuropsychological differences between mild Parkinson's disease dementia and dementia with lewy bodies. *Dement Geriatr Cogn Dis Extra.* (2015) 5:212–20. doi: 10.1159/000375363

26. Takemoto M, Sato K, Hatanaka N, Yamashita T, Ohta Y, Hishikawa N, et al. Different clinical and neuroimaging characteristics in early stage parkinson's disease with dementia and dementia with Lewy bodies. *J Alzheimers Dis.* (2016) 52:205–11. doi: 10.3233/JAD-150952

27. Park KW, Kim HS, Cheon SM, Cha JK, Kim SH, Kim JW, et al. Dementia with Lewy bodies versus Alzheimer's disease and parkinson's disease dementia: a comparison of cognitive profiles. *J Clin Neurol.* (2011) 7:19–24. doi: 10.3988/jcn.71.19

28. Hansen D, Ling H, Lashley T, Foley JA, Strand C, Eid TM, et al. Novel clinicopathological characteristics differentiate dementia with Lewy bodies from Parkinson's disease dementia. *Neuropathol Appl Neurobiol.* (2021) 47:143–56. doi: 10.1111/nan.12648

29. Dong MX, Wei YD, Hu L. Lipid metabolic dysregulation is involved in Parkinson's disease dementia. *Metab Brain Dis.* (2021) 36:463–70. doi: 10.1007/s11011-020-00665-5

30. Park SJ, Jin U, Park SM. Interaction between coxsackievirus B3 infection and α-synuclein in models of Parkinson's disease. *PLoS Pathog.* (2021) 17:e1010018. doi: 10.1371/journal.ppat.1010018

31. Surendranathan A, Rowe JB, O'Brien JT. Neuroinflammation in Lewy body dementia Parkinsonism. *Relat Disord.* (2015) 21:1398–406. doi: 10.1016/j.parkreldis.10009

32. Krot M, Rolls A. Autoimmunity in neurodegeneration. *Science.* (2021) 374:823–4. doi: 10.1126/science.abm4739

33. Ghochikyan A, Petrushina I, Davtyan H, Hovakimyan A, Saing T, Davtyan A, et al. Immunogenicity of epitope vaccines targeting different B cell antigenic determinants of human α-synuclein: feasibility study. *Neurosci Lett.* (2013) 560:86–91. doi: 10.1016/j.neulet.12028

34. Zhang G, Liu S, Chen Z, Shi Z, Hu W, Ma L, et al. Association of elevated plasma total homocysteine with dementia with Lewy bodies: a case-control study. *Front Aging Neurosci.* (2021) 13:724990. doi: 10.3389/fnagi.202 1.724990

35. Kalecký K, Ashcraft P, Bottiglieri T. One-carbon metabolism in Alzheimer's disease and Parkinson's disease brain tissue. *Nutrients.* (2022) 14:599. doi: 10.3390/nu14030599

36. Xing H, Lim YA, Chong JR, Lee JH, Aarsland D, Ballard CG, et al. Increased phosphorylation of collapsin response mediator protein-2 at Thr514 correlates with β-amyloid burden and synaptic deficits in Lewy body dementias. *Mol Brain.* (2016) 9:84. doi: 10.1186/s13041-016-0264-9

37. Cardinale A, Calabrese V, Iure de, Picconi A. Alpha-synuclein as a prominent actor in the inflammatory synaptopathy of Parkinson's disease. *Int J Mol Sci.* (2021) 22:6517. doi: 10.3390/ijms22126517

38. Agliardi C, Guerini FR, Zanzottera M, Bianchi A, Nemni R, Clerici M, et al. SNAP-25 in serum is carried by exosomes of neuronal origin and is a potential biomarker of Alzheimer's disease. *Mol Neurobiol.* (2019) 56:5792–8. doi: 10.1007/s12035-019-1501-x

39. Bereczki E, Branca RM, Francis PT, Pereira JB, Baek JH, Hortobágyi T, et al. Synaptic markers of cognitive decline in neurodegenerative diseases: a proteomic approach. *Brain.* (2018) 141:582–95. doi: 10.1093/brain/awx352

40. Moriya S, Hanazono M, Fukuhara T, Iwase K, Hattori N, Takiguchi M, et al. A53T. mutant α-synuclein fibrils formed in macrophage are spread to neurons. *Cell Mol Life Sci.* (2022) 79:234. doi: 10.1007/s00018-022-04263-9

41. VanGuilder HD, Farley JA, Yan H, Van Kirk CA, Mitschelen M, Sonntag WE, et al. Hippocampal dysregulation of synaptic plasticity-associated proteins with age-related cognitive decline. *Neurobiol Dis.* (2011) 43:201–12. doi: 10.1016/j.nbd.03012

42. Taniguchi K, Yamamoto F, Amano A, Tamaoka A, Sanjo N, Yokota T, et al. Amyloid-β oligomers interact with NMDA receptors containing GluN2B subunits and metabotropic glutamate receptor 1 in primary cortical neurons: Relevance to the synapse pathology of Alzheimer's disease. *Neurosci Res.* (2022) 180:90–8. doi: 10.1016/j.neures.03001

43. Rocchi A, Sacchetti S, De Fusco A, Giovedi S, Parisi B, Cesca F, et al. Autoantibodies to synapsin I sequestrate synapsin I and alter synaptic function. *Cell Death Dis.* (2019) 10:64. doi: 10.1038/s41419-019-2106-z

44. Agliardi C, Meloni M, Guerini FR, Zanzottera M, Bolognesi E, Baglio F, et al. Oligomeric α-Syn and SNARE complex proteins in peripheral extracellular vesicles of neural origin are biomarkers for Parkinson's disease. *Neurobiol Dis.* (2020) 148:105185. doi: 10.1016/j.nbd.2020.105185

45. Bereczki E, Francis PT, Howlett D, Pereira JB, Höglund K, Bogstedt A, et al. (2016). *Synaptic proteins predict cognitive decline in Alzheimer's disease and Lewy body dementia Alzheimers Dement.* (2016) 12:1149–58. doi: 10.1016/j.jalz.04, 005.

46. Sun Y, Cheng X, Zhang L, Hu J, Chen Y, Zhan L, et al. The functional and molecular properties, physiological functions, and pathophysiological roles of GluN2A in the central nervous system. *Mol Neurobiol.* (2017) 54:1008–21. doi: 10.1007/s12035-016-9715-7

47. Sakimura K, Kutsuwada T, Ito I, Manabe T, Takayama C, Kushiya E, et al. Reduced hippocampal LTP and spatial learning in mice lacking NMDA receptor epsilon 1 subunit. *Nature.* (1995) 373:151–5. doi: 10.1038/373151a0

48. Brigman JL, Feyder M, Saksida LM, Bussey TJ, Mishina M, Holmes A, et al. Impaired discrimination learning in mice lacking the NMDA receptor NR2A subunit. *Learn Mem.* (2008) 15:50–4. doi: 10.1101/lm.777308

49. Lemay-Clermont J, Robitaille C, Auberson YP, Bureau G, Cyr M. Blockade of NMDA receptors 2A subunit in the dorsal striatum impairs the learning of a complex motor skill. *Behav Neurosci.* (2011) 125:714–23. doi: 10.1037/a0025213

50. Bustos FJ, Varela-Nallar L, Campos M, Henriquez B, Phillips M, Opazo C, et al. PSD95 suppresses dendritic arbor development in mature hippocampal neurons by occluding the clustering of NR2B-NMDA receptors. *PLoS ONE.* (2014) 9:e94037. doi: 10.1371/journal.pone.0094037

51. Kannangara TS, Bostrom CA, Ratzlaff A, Thompson L, Cater RM, Gil-Mohapel J, et al. Deletion of the NMDA receptor GluN2A subunit significantly decreases dendritic growth in maturing dentate granule neurons. *PLoS ONE.* (2014) 9:e103155. doi: 10.1371/journal.pone.0103155

52. Ge Y, Wang YT. GluA1-homomeric AMPA receptor in synaptic plasticity and neurological diseases. *Neuropharmacology.* (2021) 197:108708. doi: 10.1016/j.neuropharm.2021.108708

53. Wang GJ, Kang L, Kim JE, Maro GS, Xu XZ, Shen K, et al. GRLD-1 regulates cell-wide abundance of glutamate receptor through post-transcriptional regulation. *Nat Neurosci.* (2010) 13:1489–95. doi: 10.1038/nn.2667

54. Gong Y, Lippa CF. Review: disruption of the postsynaptic density in Alzheimer's disease and other neurodegenerative dementias. *Am J Alzheimers Dis Other Demen.* (2010) 25:547–55. doi: 10.1177/1533317510382893

55. Pavlopoulos E, Trifilieff P, Chevaleyre V, Fioriti L, Zairis S, Pagano A, et al. Neuralized1 activates CPEB3: a function for nonproteolytic ubiquitin in synaptic plasticity and memory storage. *Cell.* (2011) 147:1369–83. doi: 10.1016/j.cell.09056

56. Quadri Z, Johnson N, Zamudio F, Miller A, Peters M, Smeltzer S, et al. Overexpression of human wtTDP-43 causes impairment in hippocampal plasticity and behavioral deficits in CAMKII-tTa transgenic mouse model. *Mol Cell Neurosci.* (2020) 102:103418. doi: 10.1016/j.mcn.2019.103418

57. Yeung JH, Calvo-Flores Guzmán B, Palpagama TH, Ethiraj J, Zhai Y, Tate WP, et al. Amyloid-beta1–42 induced glutamatergic receptor and transporter expression changes in the mouse hippocampus. *J Neurochem.* (2020) 155:62–80. doi: 10.1111/jnc.15099

58. Kashani A, Betancur C, Giros B, Hirsch E, El Mestikawy S. Altered expression of vesicular glutamate transporters VGLUT1 and VGLUT2 in Parkinson disease. *Neurobiol Aging.* (2006) 28:568–78. doi: 10.1016/j.neurobiolaging.02010

59. Poirel O, Mella S, Videau C, Ramet L, Davoli MA, Herzog E, et al. Moderate decline in select synaptic markers in the prefrontal cortex (BA9) of patients with Alzheimer's disease at various cognitive stages. *Sci Rep*. (2018) 8:938. doi: 10.1038/s41598-018-19154-y

60. Kashani A, Lepicard E, Poirel O, Videau C, David JP, Fallet-Bianco C, et al. Loss of VGLUT1 and VGLUT2 in the prefrontal cortex is correlated with cognitive decline in Alzheimer disease. *Neurobiol Aging.* (2007) 29:1619–30. doi: 10.1016/j.neurobiolaging.04010

61. Steudle F, Rehman S, Bampali K, Simeone X, Rona Z, Hauser E, et al. A novel de novo variant of GABRA1 causes increased sensitivity for GABA *in vitro*. *Sci Rep.* (2020) 10:2379. doi: 10.1038/s41598-020-59323-6

62. Santpere G, Garcia-Esparcia P, Andres-Benito P, Lorente-Galdos B, Navarro A, Ferrer I, et al. Transcriptional network analysis in frontal cortex in Lewy body diseases with focus on dementia with Lewy bodies. *Brain Pathol.* (2018) 28:315–33. doi: 10.1111/bpa.12511

63. Jiang S, Wen N, Li Z, Dube U, Del Aguila J, Budde J, et al. Integrative system biology analyses of CRISPR-edited iPSC-derived neurons and human brains reveal deficiencies of presynaptic signaling in FTLD and PSP. *Transl Psychiatry.* (2018) 8:265. doi: 10.1038/s41398-018-0319-z

64. Samarut É, Swaminathan A, Riché R, Liao M, Hassan-Abdi R, Renault S, et al. γ-aminobutyric acid receptor alpha 1 subunit loss of function causes genetic generalized epilepsy by impairing inhibitory network neurodevelopment. *Epilepsia.* (2018) 59:2061–74. doi: 10.1111/epi.14576

65. Zhou J, Liang W, Wang J, Chen J, Liu D, Wang X, et al. An epileptic encephalopathy associated GABRG2 missense mutation leads to pre- and postsynaptic defects in zebrafish. *Hum Mol Genet*. (2021) 3:ddab338. doi: 10.1093./hmg/ddab338

66. Yin H, Pantazatos SP, Galfalvy H, Huang YY, Rosoklija GB, Dwork AJ, et al. A pilot integrative genomics study of GABA and glutamate neurotransmitter systems in suicide, suicidal behavior, and major depressive disorder. *Am J Med Genet B Neuropsychiatr Genet.* (2016) 171:414–26. doi: 10.1002/ajmg.b.32423

67. Blum BP, Mann JJ. The GABAergic system in schizophrenia. *Int J Neuropsychopharmacol.* (2002) 5:159–79. doi: 10.1017/S1461145702002894

68. Hoftman GD, Volk DW, Bazmi HH, Li S, Sampson AR, Lewis DA, et al. Altered cortical expression of GABA-related genes in schizophrenia: illness progression vs developmental disturbance. *Schizophr Bulletin.* (2015) 41:180–91. doi: 10.1093/schbul/sbt178

69. Quiñones GM, Mayeli A, Yushmanov VE, Hetherington HP, Ferrarelli F. Reduced GABA/glutamate in the thalamus of individuals at clinical high risk for psychosis. *Neuropsychopharmacology.* (2021) 46:1133–9. doi: 10.1038/s41386-020-00920-4

70. McKeith IG, Boeve BF, Dickson DW, Halliday G, Taylor JP, Weintraub D, et al. Diagnosis and management of dementia with Lewy bodies: Fourth consensus report of the DLB Consortium. *Neurology.* (2017) 89:88–100. doi: 10.1212/WNL.0000000000004058

71. Amberger JS, Bocchini CA, Scott AF, Hamosh A. OMIM.org: leveraging knowledge across phenotype-gene relationships. *Nucleic Acids Res.* (2019) 47:D1038–43. doi: 10.1093/nar/gky1151

Frontiers in Neurology

Explores neurological illness to improve patient care

The third most-cited clinical neurology journal explores the diagnosis, causes, treatment, and public health aspects of neurological illnesses. Its ultimate aim is to inform improvements in patient care.

Discover the latest Research Topics

See more →

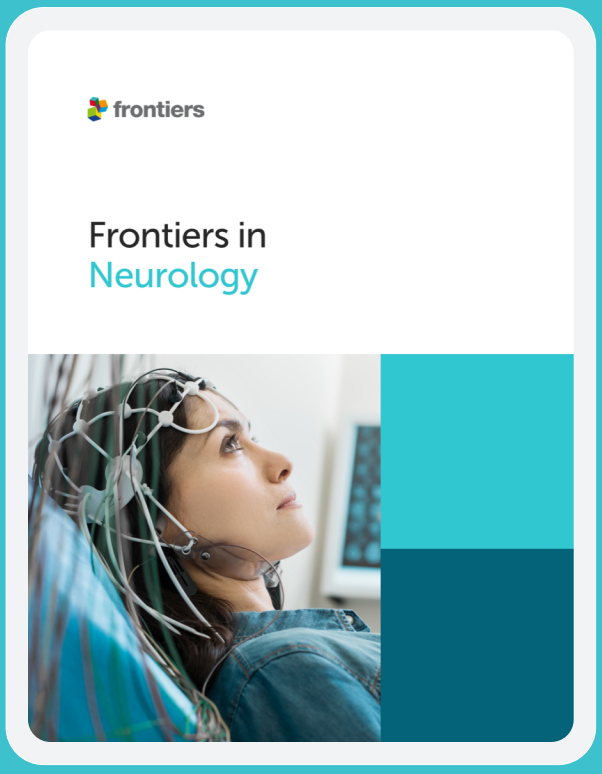

Frontiers

Avenue du Tribunal-Fédéral 34
1005 Lausanne, Switzerland
frontiersin.org

Contact us

+41 (0)21 510 17 00
frontiersin.org/about/contact